Cell Contact Dependent Events Involving CD151 in Atherosclerosis and Atherothrombosis

A thesis submitted in fulfilment of the requirements for the degree of Doctor of Philosophy

Kamaliah Hafilah Saiful Rijal

Masters of Laboratory Medicine

School of Medical Sciences

College of Science Engineering and Health

RMIT University

September 2014

Declaration

I certify that except where due acknowledgment has been made, the work is that of the author alone; the work has not been submitted previously, in whole or in part, to qualify for any other academic award; the content of the thesis is the result of work which has been carried out since the official commencement date of the approved research programme.

Signed:

Kamaliah Saiful-Rijal

S3177753

Date:

To My Grandmother, Nenek Sarina Yin Morsidi

Acknowledgements

*Alhamdullilah (*All praise is due to Allah SWT)

First and foremost, I wish to thank my parents, my siblings and nieces, my grandparents, who have stood by me through all my tribulations, moments of pique, impatience and absences throughout the fourteen years I have been in Melbourne, which have brought me to this day.

Next I would like to thank my supervisor, Professor Denise E. Jackson, who has guided me along my way as I grew as a scientist. Her support, experience and reminders that "it is all coming along together", helped me throughout my candidature.

To my colleagues who quickly became like brothers to me in the Thrombosis and Vascular Disease Laboratory, Mohammed Makkawi, Musaed AlShahrani and Naif AlHawiti, thank you for always being incredibly supportive and present in figuring out 'what next?!' to do. Thank you Dr Fatemeh Moheimani for keeping me positive and providing so much help in the earlier half of my candidature. To Eunice Yang, Jana Yip, I thank you both for your vast experience and the techniques you have taught me that provided me with some hope of beginning and completing experiments. Your experience and help is greatly missed in the Thrombosis and Vascular Disease Laboratory.

The entire Haematology Department has contributed to this thesis in so many ways, Thank you. I wish to also thank the Histology Department, especially my Secondary Supervisor Associate Professor Janine Danks for your guidance and access to the Histology laboratories.

I must thank my friends and family in Brunei and scattered around the globe. My best friend Izzat, I thank you for your constant faith in me. I have missed you all very much.

Last but certainly not least, I would like to thank the Government of His Majesty Sultan Haji Hassanal Bolkiah Mui'zzaddin Waddaulah for my Scholarship and granting me a chance to further my education in Melbourne.

Table of Contents

List of Figures

List of Tables

List of non-standard abbreviations

-/-	Knockout
α	Alpha
β	Beta
ϒ	Gamma
μM	Micromolar
ADP	Adenosine-5'-diphosphate
AEC	Animal ethics committee
AMI	Acute myocardial infarction
ApoE KO	Apolipoprotein E knockout
$ApoE^{-/-}$	Apolipoprotein E knockout
ApoE	Apolipoprotein E
ATP	Adenosine-5'-triphosphate
BSA	Bovine serum albumin
CAD	Coronary artery disease
cAMP	3'-5'-cyclic adenosine monophosphate
CD151	Tetraspanin CD151
$CD151^{-/-}$	CD151 homozygote knockout
COX	Cyclooygenase
CRP	C reactive protein
CVD	Coronary vascular disease
FcR ϒ	Fc receptor ϒ
$FeCl_3$	Ferric chloride
GAPDH	Glyceraldehyde 3-phosphate dehydrogenase
GP	Glycoproteins
GPI_a-II_a	Glycoprotein I_aII_a
GP-Ib-IX-V	Glycoprotein Ib-IX-V complex
GP IIb-IIIa	Glycoprotein IIb-IIIa
GP VI	Glycoprotein VI
GPCR	G-protein coupled receptor
HDL	High density lipoprotein
IL	Interleukin
IVM	Intravital microscopy
IP3	Inositol 1,4,5, triphosphate
LDL	Low density lipoproteins
LPA	Leukocyte platelet aggregates

LTA	Light transmission aggregometry
MFI	Mean fluorescence intensity
Min	Minute
mm	Milimeter
MPA	Monocyte platelet aggregate
NO	Nitric oxide
NOS	Nitrix oxide synthase
PAI-1	Plasminogen activator inhibitor-1
PAR	Protease activated receptors
PBS	Phosphate buffered saline
PCR	Polymerase chain reaction
PECAM-1	Platelet endothelial cell adhesion molecule-1
PG	Prostaglandin
PGI_2	Prostacyclin
PKC	Protein Kinase C
PPP	Platelet poor plasma
PRP	Platelet rich plasma
RPM	Revolutions per minute
Sec	Seconds
SMC	Smooth muscle cells
TEMs	Tetraspanin enriched microdomains
TF	Tissue factor
TP	Thromboxane A_2 receptor alpha isoform
TRAP	Thrombin receptor activating peptide
TSSC6	Tumour suppressing subchromosomal transferable fragment cDNA
TxA_2	Thromboxane A2
µ	Micro
VLDL	Very low density lipoprotein
v/v	Volume per volume
vWF	Von Willebrand factor
WBA	Whole blood aggregation
WCC	White cell count
WT	Wild type
w/v	Weight per volume

Abstract

Ischaemic heart disease is consistently the number one ranking cause of death in Australia, as well as the western world. Platelets are central in normal haemostasis to arrest bleeding following trauma and under pathological conditions of atherosclerotic plaque rupture and arterial thrombosis. The development of platelet thrombi leads to the clinical sequela of cardiovascular disease (CVD) which in 2011 accounted for 31% of all deaths in Australia.(1) Ischaemic heart disease specifically accounted for 14.65% of all deaths nationwide in 2011.(2)

Numerous factors are implicated in increasing the thrombogenic potential of ruptured plaques including the role of increased blood shear rates in narrowed blood vessels and the increased responsiveness of platelet activation. CD151 is a tetraspanin amongst several found on platelets. This tetraspanin is a promising target in anti-platelet therapies as it acts in conjunction with cognate receptors particularly integrin $\alpha_{IIb}\beta_3$ in the regulation of platelet thrombus formation *in vivo*. Tetraspanins constitute a conserved family of four transmembrane protein domains with the characteristic ability to associate laterally with other membrane proteins in forming tetraspanin enriched microdomains. These microdomains play critical roles in various functions such as fusion, trafficking and adhesion.(3) The functional and physical associations between CD151 and integrin $\alpha_{IIb}\beta_3$ in murine platelets emphasises the criticial involvement of CD151 in modulating outside-in $\alpha_{IIb}\beta_3$ signalling pathways.(4) Although studies have been done on CD151, none have specifically examined the effects of CD151 absence in an atherosclerosis setting. Tetraspanin CD151 was first identified in platelets and endothelial cells by using monoclonal antibodies against human acute myeloid leukaemia cells.(5) It has since been identified in numerous other cell types.(6, 7)

We developed a novel $ApoE^{-/-}.CD151^{-/-}$ model by crossing the $ApoE^{-/-}$ genotype with the $CD151^{-/-}$ genotype. CD151 has not been studied in the context of atherosclerosis and through this model, which we developed for the first time, *in vivo* and *in vitro* studies were able to be performed. As the absence of CD151 has been reported to impart a protective effect on thrombotic complications, we first characterised the $ApoE^{-/-}.CD151^{-/-}$ model, comparing it to the $ApoE^{-/-}$ gold standard model for atherosclerosis and examined the mendelian inheritance profiles, haematological and lipid parameters and cardiovascular risk factors such as body weight, age, body mass index and glucose levels. Apart from

significant differences in expected and generated Mendelian inheritance profiles and a raised total cholesterol level in the $ApoE^{-/-}$ we did not observe any other indication, from these parameters at least, that the $ApoE^{-/-}.CD151^{-/-}$ model has an influence on atherosclerosis and a decrease in cardiovascular risk factors (Chapter 3).

Histology and immunohistochemistry studies have also been performed on the novel $ApoE^{-/-}.CD151^{-/-}$ mouse model versus the $ApoE^{-/-}$ mouse. Preliminary findings indicate a significantly reduced plaque burden in the $ApoE^{-/-}.CD151^{-/-}$ mouse compared to the $ApoE^{-/-}$ mouse through haematoxylin and eosin staining of the aortic valve cusps (Chapter 4). Plaque composition on the contrary does not appear to be influenced by the absence of CD151 in atherosclerosis. This was determined through immunohistochemical staining for F4/80 pan macrophage markers, smooth muscle actin, type 1 collagen and CD151 for CD151 expression (Chapter 5).

Through *in vivo* studies, we showed the existence of a defect with $ApoE^{-/-}.CD151^{-/-}$ platelets having prolonged times to occlusion upon $FeCl_3$ induced vascular injury of the carotid arteries and also reduced thrombus formation as compared to $ApoE^{-/-}$ platelets. *In vivo* tail bleeding assays similarly suggested a defect of unstable haemostasis as bleeding times, volume of blood lost and rebleeds were significantly increased in the $ApoE^{-/-}.CD151^{-/-}$ model. These findings are consistent with what has been discussed in the literature. We also reported conflicting findings as platelet aggregation responses appeared unchanged between the $ApoE^{-/-}$ and $ApoE^{-/-}.CD151^{-/-}$ strains which implies that CD151 absence had no protective effect on agonist induced platelet aggregation. Furthermore, we saw a similar pattern in our *in vivo* studies of the mesenteric arterioles whereby, thrombus area, volume and stability mirrored that of $CD151^{+/+}$ findings from previous studies. This highlighted limitations to our study as $ApoE^{-/-}$ mice are atherogenic and accumulate fats more readily than wild-type mice. We must take into account that not only the presence of excess fat can potentially have an influence in the mesenteric injury model but also that CD151 is polygenic in nature where its involvement in the development and progression of atherosclerosis is unclear. *In vivo* studies in other vascular beds such as the cremaster arterioles where fat presence is lower, would be of benefit to confirm our findings (Chapter 6).

We have contributed further to the understanding of tetraspanin CD151 in platelet thrombus formation models *in vivo* and also its influence on plaque burden in atherosclerosis. We have particularly identified the potential of CD151 as an anti-thrombotic target for the development of novel anti thrombotics for cardiovascular diseases and cerebrovascular ischaemic diseases. Our findings will need to be elucidated further by the inclusion of *in vivo* studies on other vascular beds in a mouse model.

1 CHAPTER 1: LITERATURE REVIEW

1.1 Cardiovascular Disease overview

The physiological processes of haemostasis are mediated primarily by the activation of platelets in conjunction with the coagulation cascade. Whilst platelets are essential in endothelium repair or wound healing, platelets too can result in a cascade of unfavourable thrombotic events eventuating in myocardial infarction and ischaemic stroke.(8) In Australia, 31% of all deaths were caused by cardiovascular disease and 14.6% of registered deaths in 2011 were caused by ischaemic heart disease which continues to be a leading cause of death.(1,8) We have seen a steady decline in deaths caused by ischaemic heart disease since 2000 with the proportions of deaths decreasing to 14.6% or 21,513 deaths from 19.5% and 26,063 deaths.(2) The economic burden is an estimated six billion dollars per year for both treatment and prevention of ischaemic heart disease.(9) Anti-platelet drug use has risen substantially over the late 1990s, with aspirin being the most frequently prescribed drug. Additionally, this was not including over the counter non-prescribed purchases. Likewise, anti-coagulant drugs have increased steadily in their use over the 1990s.(9)

Where patients have underlying disease states falling under the category of acute coronary syndromes, specifically ischaemic stroke or transient ischaemic attack and peripheral artery disease (PAD), the likelihood of thrombosis occurring is increased. Permanent damage may occur to vascular beds and diseased vessels due to ischaemia and occlusion in vessels from uncontrolled thrombus formation. There are numerous factors leading to this, one being increased platelet activation and shear due to narrowing of vessels following the rupture of atherosclerotic plaques or erosion of endothelial cells. An interplay of several pathways and mechanisms are involved in the formation of platelet thrombi and overall haemostatic control.(8)

1.2 Platelet overview and ultrastructure

Platelets are formed from nucleated megakaryocytes (30 – 100 μm) in the bone marrow. Maturation of the megakaryocytes involves the development and extension of proplatelet elongations into blood vessels and eventually the release of platelets into the blood.(8-10) Throughout this process, the platelets develop characteristic systems, forming its complex structure. The two main systems developed are firstly, the open canalicular system (OCS) which is formed by surface membrane invaginations and secondly, the dense tubular system (DTS) which is formed of a closed network of residual endoplasmic reticulum of the megakaryocyte.(10,11) The DTS acts a reservoir for calcium storage and binding sites as well as for enzymes involved in prostaglandin synthesis. The DTS contains large amounts of amorphous materials and is distinct from the OCS system.(12,13) In addition to calcium, the DTS also stores adenylate cyclase (cAMPase) which are both key regulators involved in platelet activation.(14) The OCS on the other hand is a network of membrane channel microtubules which runs throughout the platelet. It acts as a conduit for α-granule release during platelet activation and provides an increased membrane surface area from the envaginated channels.(12,15)

Platelets are anuclear, terminally differentiated and measure between 2.0 μm to 5.0 μm in diameter. They circulate within the blood stream for approximately 8-10 days.(8,16-19) Thrombopoietin (TPO) is an important regulator of platelet production. Its production is modulated either as a result of interleukin 6 stimulation to the parenchymal or sinusoidal endothelial cells, or by the proximal convoluted tubule cells within the kidney.(20,21) Platelets contain secretory organelles, glycogen as well as lipid substrates which assist in coagulation. Under resting physiological conditions, circulating Prostaglandin I_2 and nitric oxide contributes in preventing platelet activation.(22) When activated the platelet cytoskeleton undergoes changes from a resting discoid shape to that of a spherical shape mediated by an actin-dependant process.(22) The cytoskeleton is imperative for both maintaining the platelet structure at rest and to facilitate this shape change which occurs upon activation.(22)

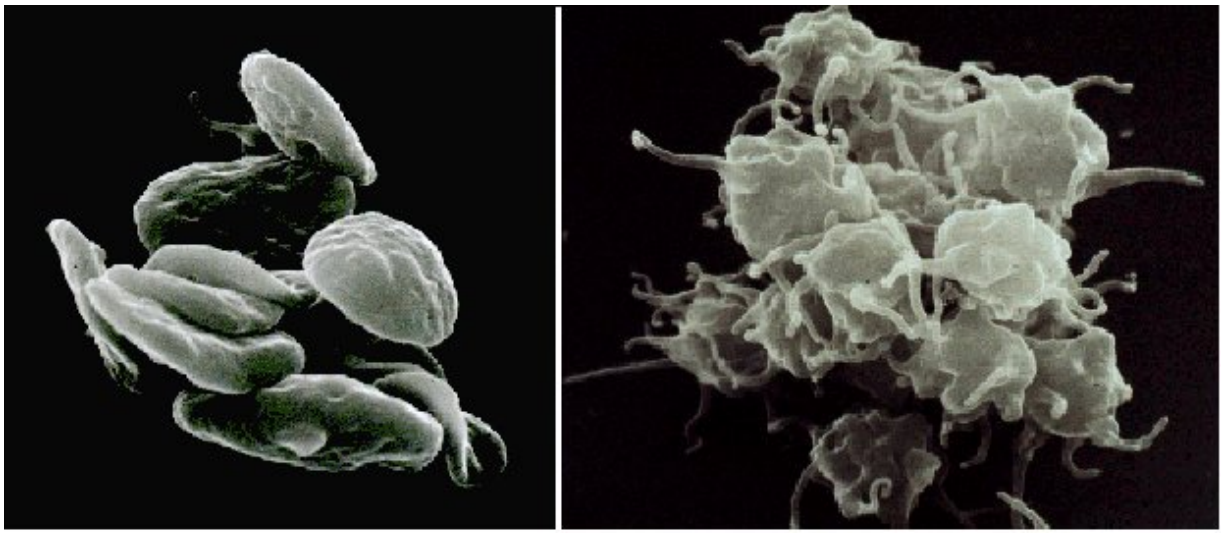

Figure 1.1: Left: Resting platelets are smooth and disc shaped. Right: Activated platelets, seen with protruding pseudopodia.(23)

The formation of a platelet-thrombus plug occurs in three main steps comprising of an initiation phase, extension phase and a stabilisation phase.(18,24), Platelet activation and aggregation is initiated when injury is caused to the subendothelium of blood vessels exposing collagen, which then triggers the capture of flowing platelets by the initial tethering of von Willebrand factor (vWF). Consequently this mediates the binding of Glycoprotein (GP) Ib-IX-V complexes on platelet surfaces with vWF and GPVI with exposed collagen.(8) Platelet adhesion is mediated with formation of these adhesion signaling complexes and ultimately the development of thrombi at the site of injury.(25)

1.2.1 Platelet granule contents

Platelets contain three main secretory organelles which are: α-granules, dense granules and lysosomes.(10,15) Granule content is abundant in platelets and imperative in platelet adhesion, activation and consequently thrombus formation.(26) These organelles are highly specific, from their secretion of adhesion molecules, to release of agonists and influence of pathways which alter the conformational structures of platelet receptors.(26)

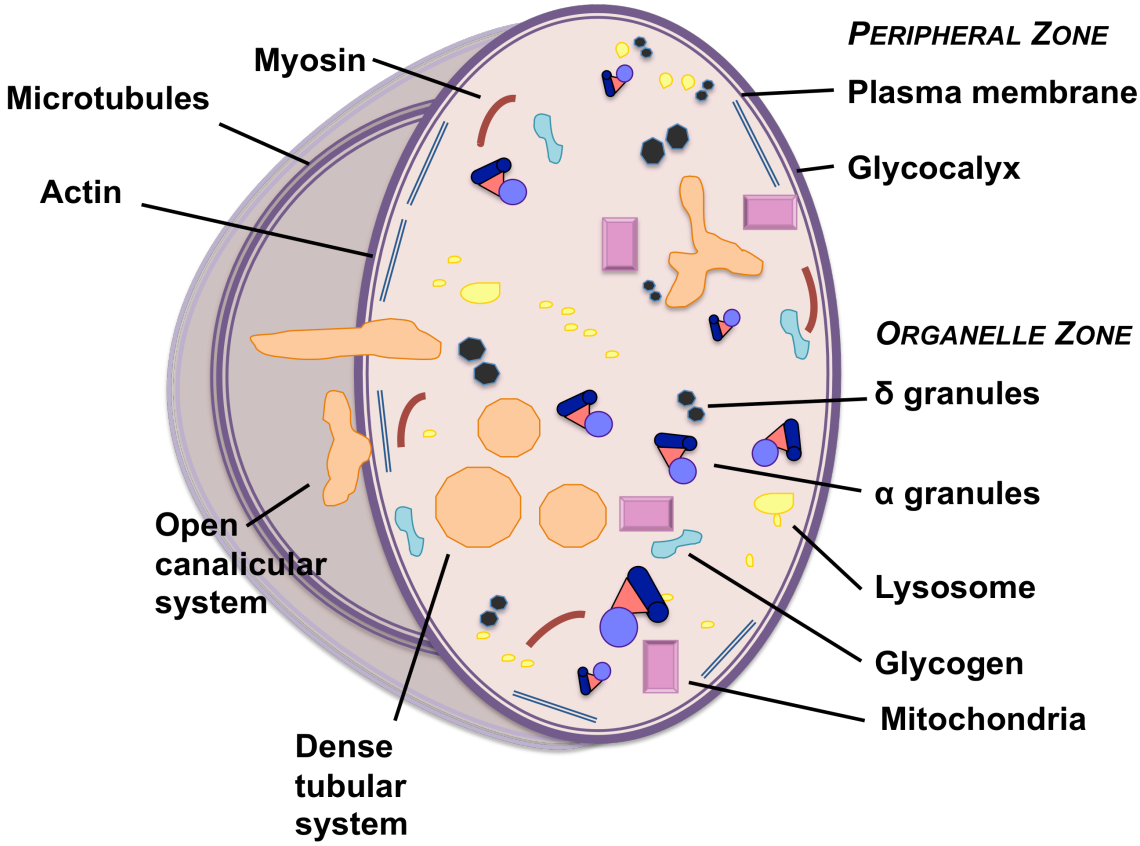

Figure 1.2: Platelets Granules. Platelets contain numerous mediators involved in the regulation of haemostasis and thrombosis, chemotaxis, vasomotor functions, cell growth and inflammation. These include: α-granules, δ granules, lysosomes (λ granules), mitochondria and glycogen. The plasma membrane is composed of a phospholipid bilayer and contains tunnel invaginations which forms the complex canalicular system. The dense tubular system is a storage site for calcium and enzymes involved in platelet activation.(28,29,40,47)

1.2.1.1 Alpha granules

Platelet α-granules are the most abundant type of secretory organelle found within platelets.(27,28) Each platelet contains approximately 50 – 80 α-granules, measuring 200 – 500 nm in diameter.(15,29) Alpha granules contain a range of membrane bound proteins that are expressed both on plasma membranes at rest as well as on platelet surfaces and proteins which have been secreted extracellularly.(30) However for some proteins, for instance P-selectin and CD109, expression of these proteins on platelet surfaces are only observed following activation.(31) These proteins include integral membrane proteins, coagulants, anti-coagulants, fibrinolytic proteins, adhesion proteins, chemokines, growth factors (TGFβ), angiogenic factors as well as inhibitors and microbicidal proteins.(32,33) Chemokines such as CXCL4 and CXCL7 are platelet mediators which influence inflammation and are one of the more highly expressed proteins found in platelets.(34) CXCL4 in particular has been implicated in both early and late atherosclerosis as studies have demonstrated its presence in atherosclerotic plaque lesions in the carotid arties which correlates with severity of atherosclerosis.(35)

Platelet to platelet interactions and platelet to endothelial interactions are mediated by adhesive proteins such as fibrinogen and vWF secreted from α-granules. The vWF found in α-granules amounts to approximately 20% of total vWF protein.(30) In platelet adhesion, α-granule contents such as GPIb-IX-V, integrin $\alpha_{IIb}\beta_{3,}$ and GPVI are expressed on plasma membranes following activation.(36) Fibrinogen, which is the ligand for integrin $\alpha_{IIb}\beta_3$, is also contained within the α-granules and when released cross links with activated platelets for the formation of a stable thrombus.(37) Alpha granules also contribute to coagulation with the release of factors and cofactors which are involved in the regulation of primary and secondary haemostasis. Upon platelet activation, coagulation factors such as factor V, XI and XIII are secreted which are important in the coagulation cascade and crosslinking of the fibrin clot.(30)

1.2.1.2 Dense granules

Dense granules are fewer by about ten fold compared to α-granules in platelets with there being only 3-8 dense granules per platelet. They are also smaller at 150 nm with a much smaller surface area coverage. Dense granules like α-granules are also formed in megakaryocytes.(38) These granules are lysosome-related organelles derived from endosomal compartments. Vesicle formation is mediated by AP-3 and by large protein complexes throughout its maturity.(30) Dense granules as especially important in

haemostasis and thrombosis with their ability to amplify initial platelet activation and subsequently thrombus growth. Platelet dense granules contain high concentrations of nucleotides such as ADP, ATP, cations such as calcium, magnesium, potassium, phosphates and bioactive amines.(38,39) Upon platelet activation, calcium and ATP platelet dense granules are released for protein kinase C phosphorylation, which are required for platelet aggregation.(40) ADP and serotonin release from the platelet dense granules propagates the activation pathways through a positive feedback mechanism. Although a weak agonist, ADP is capable of stimulating platelet shape change, reversible and secondary aggregation and ultimately is important in platelet function. ADP amplifies platelet responses which have been induced by other platelet agonists and contributes to stable platelet aggregates.(41,42) Studies have also identified dense granule contents being involved in atherosclerosis and atherothrombosis. Human atherosclerotic plaque lesions displayed the presence of 14-3-3zeta, which is secreted by activated platelets however it was absent in healthy normal aortic tissue.(43) Studies have also shown that mice with defective dense granule secretion and lacking HSP3 were protected from atherosclerosis as they were found to demonstrate reduced atherosclerotic plaque lesions.(44)

1.2.1.3 Lysosomes

Lysosomes are found in small numbers in platelets.(45,46) Platelet lysosomes contain glycosidases, proteases and cationic proteins with bactericidal capabilities. Lysosome membranes also contain integral membrane proteins and are suggested to be required for calcium regulation in cells, especially platelets.(47,48)

1.3 Coagulation

Upon injury caused to the subendothelial wall of blood vessels, coagulation is also initiated and occurs simultaneously with platelet recruitment and activation with the exposure of blood to tissue factor.(49,50) This is followed by thrombin production through the coagulation pathways: intrinsic, extrinsic and common pathways where coagulation factors are converted to their active forms. The extrinsic pathway is initiated with the abundant expression of tissue factor on subendothelial cells as well as the collagen platelet derived polyphosphates which subsequently triggers the intrinsic pathway involving factor XII pathway.(51-53) Factor V and factor VIII activation is mediated by thrombin, which further promotes the production of thrombin and eventually the production of fibrin and formation of a platelet plug or clot. The fibrin fibres present at platelet surfaces stabilises and strengthens the thrombus and later mediates the platelet dependent retraction of clots.(54,55) The fibrin web is capable also of capturing free flowing erythrocytes and leucocytes which may contribute further in vessel occlusion. Inactivation or degradation of FV and FVIII on the other hand is regulated via a negative feedback mechanism mediated by activated protein C (APC) and its cofactor protein S when thrombin is generated in excess. Activation of protein C in solution is catalysed by thrombin and is enhanced with binding to endothelial cell protein C receptor (EPCR). With binding of APC to EPCR, protease-activated receptor-1 (PAR-1) signalling is initiated. APC is also involved in the activation of endothelial cells through outside-in signalling. This in turn leads to intracellular G protein activation and cellular responses such as anti-apoptosis and anti-inflammation functions.(56) Until recently, interactions between protein C and APC with human platelets were vaguely defined. Studies have suggested the role of protein C and APC in the promotion of cell signalling with binding to either ApoER2 and GPIbα. The binding of platelets with immobilised protein C or APC induces intracellular signalling at a rapid rate and the subsequent activation of platelets. For this to occur ApoER2 and GPIbα are required. White et al. (57) demonstrated that with the presence of soluble recombinant apolipoprotein E receptor 2' (ApoER2') and receptor-associated protein (RAP), platelet adhesion to either APC or protein C is inhibited. Platelet adhesion as well as glycoprotein 1bα dependent aggregation, was also found to be supported by protein C.(57)

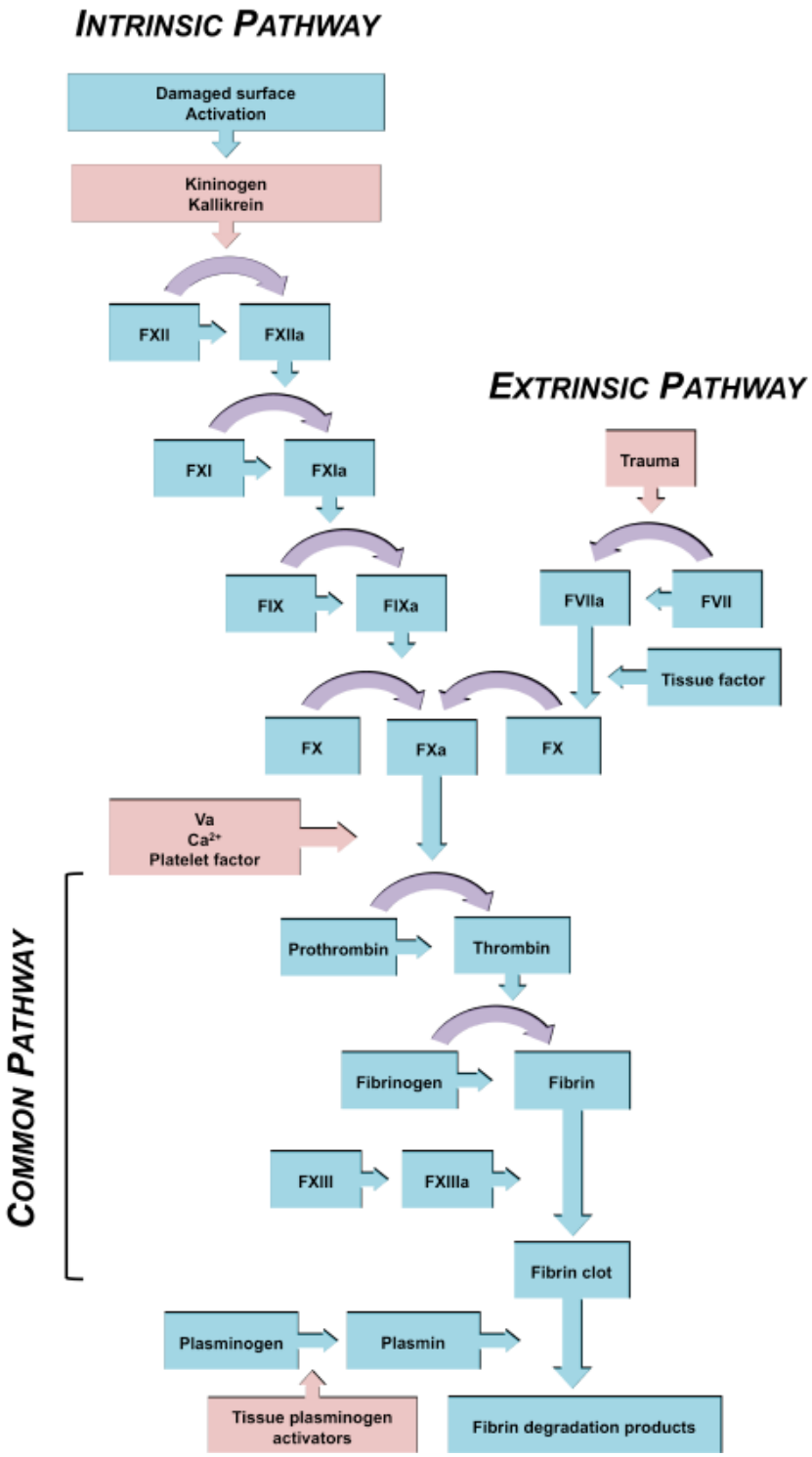

Figure 1.3: The coagulation cascade is initiated by either tissue factor exposure at the site of trauma (*Extrinsic Pathway*) or by activation of factor XII by activation of damaged negatively charged surfaces (*Intrinsic Pathway*). The extrinsic and intrinsic pathways converge at the *Common Pathway* for thrombin formation, through the conversion of prothrombin to thrombin by the prothrombinase complex, FXa and FVa. Thrombus formation occurs as fibrinogen cleaves thrombin and aggregation of platelets occur. FXIII stabilises the fibrin clot which is later followed by plasmin mediated fibrinolysis resulting in the production of fibrin degradation products and clot dissolution. Plasminogen conversion to plasmin occurs by tissue type plasminogen activator (tPA), whilst inhibition of tPA is regulated by plasminogen activator inhibitor 1. The coactivation of plasminogen by fibrin is also inhibited by the thrombin activatable fibrinolysis inhibitor, which cleaves the c-teminal lysine residues of fibrin.(51,52)

1.3.1 Coagulation: extrinsic pathway

The key step to beginning the extrinsic pathway is the exposure and expression of tissue factor at the site of vascular injury which acts as a potent trigger for the initiation of the *in vivo* coagulation cascade.(58) Tissue factor binds to and activates factor VII which is a soluble clotting factor. FVII, like factors X, IX, protein C and prothrombin are vitamin K-dependent proteins containing a γ-glutamyl carboxyl acid Gla residue at the N terminal, necessary for normal functioning of the molecule with calcium ions, activators, substrates and phospholipid surfaces.(59) It is estimated that approximately 1% of total factor VII circulates in factor VIIa form. The exposure of tissue factor results in the formation of TF:VII inactive complex as well as TF:VIIa active complex. Other factors such as factor IXa, Xa, XIIa and thrombin are capable of activating factor VII.(60, 61) The TF:VIIa formed complex activates factor IX through proteolysis, and is capable of activating factor X directly *in vitro*.(62) In the presence of activated factor VIII, activated factor IX may also activate factor X. Formation of the tenase complex is integral for activation of factor X. In humans, deficiencies in factor VIII or IX is associated with haemophilia A and B and the corresponding haemorrhagic symptoms which manifest.(63) Studies have shown that trace amounts of factor Xa has the ability to activate prothrombin bound to integrin $\alpha_{IIb}\beta_3$ consequently producing localised thrombin.(49) Recent studies have also suggested that in atherosclerotic disease the rupture of vulnerable plaques exposing prothrombotic material particularly tissue factor is a rapid activator of the coaguation cascade. Factor XIIa dependent amplification comes second where a delay in the activation of FXIIa may be attributed by plaque contents such as collagen, nucleic acids and polyphosphates and thus proposing FXIIa as a potential anti-coagulant target.(64)

1.3.2 Coagulation: intrinsic pathway

The intrinsic pathway is initiated when factor XII comes in contact with negatively charged surfaces, resulting in activation of factor XII. A series of events occur following the binding of factor XII heavy chains to negative surfaces. These include an increase in the concentration of local enzymes, autoactivation, factor XI, factor XIIa dependent prekallikrein and high molecular weight kininogen (HK). Factor XIa is a dimeric serine protease which then activates factor IX.(65) HK is cleaved by kallikrein and results in the release of bradykinin. Activation of factor XII can also by triggered by kallikrein. The intrinsic pathway also functions through a negative feedback process as the light chain of HK is cleaved by factor XIa which releases the factor from activated surfaces.(66) The intrinsic pathway was

previously thought to be insignificant however recent studies have shown that mice with Factor XII deletions have a greater propensity to developing unstable thrombi.(67,68)

1.3.3 Coagulation: common pathway

The common pathway is where the extrinsic and intrinsic pathways converge for the generation of thrombin. Factor Xa converts prothrombin (FII) to thrombin (FIIa) by cleaving off the N terminal Gla portion of prothrombin. Conversion of FII to FII also results in the cleavage of fibrinogen to form fibrin following fibrin polymerisation and the formation of the fibrin clot.(69) Thrombin generation can increase more than 300,000 fold as a result of prothrombinase complex interaction on prothrombin, and interacts with fibrinogen, factor V, VIII, XI, platelet receptors and proteins S and C in the formation of a haemostatic plug or fibrin clot.(69) Activation of factors V, VII, VIII and XI by thrombin enhances thrombin formation. Thrombin production can be controlled by conversion of protein C to activated protein C by thrombomodulin and consequently inhibiting factors Va and VIIIa.(70)

1.3.4 Coagulation: fibrinolysis

Clot formation and dissolution is a highly regulated process ensuring blood loss is controlled and balanced against controlled thrombus formation to avoid occlusion of blood flow. Plasminogen activator inhibitors are produced during thrombus formation allowing fibrin formation to continue until the site of vascular injury is repaired. Plasminogen activator inhibitor-1 protects against excessive fibrinolysis. Once repaired, endothelial cells release tissue plasminogen activators such as tissue type plasminogen activator (tPA) or urokinase-like plasminogen activator (uPA) which then converts plasminogen to plasmin.(71) Fibrin degradation products such as D-dimers are produced as plasmin mediated fibrinolysis progresses and clot lysis occurs. These act as markers of thrombotic activity.(72) Factors Va, VIIIa, protein C and S are also inactivated in plasmin presence. Fibrinolysis is also regulated by α2 anti-plasmin which degrades circulating plasmin ensuring fibrinolysis of the thrombus is limited.(73)

1.4 Membrane surface proteins

Certain Glycoproteins (GP), form adhesion signaling complexes on platelet plasma membranes. These complexes are crucial for initiating signaling events and consequently platelet activation.(25)

1.4.1 GPIb-IX-V complex

Platelet GPIb-IX-V is a leucine rich repeat glycoprotein, which binds not exclusively just to vWF but also α-thrombin, coagulation factors and adhesive proteins.(74) As mentioned, GPIb-IX-V binds with vWF to form complexes on the platelet plasma membrane and contributes towards the adhesion of platelets in the blood.(25) Platelets in the circulation express GPIb-IX-V on their surface, and is suggested to be a major adhesion receptor amongst other receptors.(75) The GP-Ib-IX-V complex is composed of 4 polypeptide genes: GPIb*α,* GPIb*β,* GPIX, GPV*,* that in a mature megakaryocyte is arranged in a 2:2:2:1 stoichiometry. These polypeptides associate very closely with one another seeing its role in the biosynthesis of platelet receptors. Of these peptides, GPV appears to be the least associated with the complex seeing no genetic defects of the GPV gene has been reported as far in Bernard Soulier Syndrome (BSS) cases.(25) BSS occurs with dysfunction or deficiency to the GPIb-IX-V complex and results in a severe bleeding diathesis. According to studies, the GPIb-IX complex is required for transport or trafficking of the complex to the platelet plasma membrane. Recent studies show that GPIbα and GPIbβ interact at transmembrane (TM) domains. Disulfides formed between GPIbα and the 2 GPIbβ subunits are suggested to occur with assistance from the TM-TM interactions. These interactions cause the membrane-proximal Cys residues to come together closer and encourage the formation of the disulfide bonds. (25,48)

Under conditions of high shear, GPIbα is of critical importance for platelet adhesion. Both platelet tethering and adhesion is hindered in wild type mice, which have had the GPIbα binding site for vWF blocked.(76) Stoll et al. (77) blocked this binding site in an arterial thrombosis model of wild type mice through the use of antibody p0p/B Fab fragments. The authors reported prolonged tail bleeding times but no spontaneous haemorrhage. GPIbα is also reported to be involved in the pathogenesis of focal ischaemic stroke in mice. (76) In humans the risk of ischaemic stroke is increased where allelic variants of GPIbα are present.(76)

1.4.2 Collagen receptors $\alpha_2\beta_1$ GPVI/FcR γ-chain complex

The subendothelial collagen exposed as a result of vascular injury, actions as a potent agonist for the eventual formation of thrombus and platelet adhesion.(78) As an agonist, collagen has the capabilities to induce the secretion of granules, shape change and platelet aggregation. Two collagen receptors are found in human platelets, namely integrin $\alpha_2\beta_1$ and the GPVI/FcR γ-chain complex. At the site of injury and under shear stress, $\alpha_2\beta_1$ serves as a better receptor in platelet-collagen interactions in ensuring stable platelet adhesion. The GPVI/FcR γ-chain complex meanwhile is associated with platelet activation.(79) Marjoram et al. (79) reported findings indicating the interplay of $\alpha_2\beta_1$ with other platelet receptors for ADP, TXA_2 and thrombin. A mechanism involving platelet priming of $\alpha_2\beta_1$ by first initiating suboptimal stimulation of platelet G_q-linked G protein coupled receptors (GPCRs) resulted in more efficient adhesion of platelets to collagen.(79) GPVI on the other hand is an activating receptor which on binding with collagen initiates a signaling cascade and consequently platelet activation. The absence or inhibition of GPVI is found to prevent the formation of arterial thrombi, both in humans and mouse platelets.(80) In contrast to $\alpha_2\beta_1$, GPVI binds to collagen at lower affinity. GPVI is composed of two Immunoglobulin like extracellular domains, a mucin-like core, transmembrane domain region and a cytoplasmic short tail. This latter feature allows for the binding of Fyn and Lyn Src kinases to the 51-aa tail of GPVI as well as complexing constitutively with FcR γ-chain dimer. This association of FcR γ-chain dimer with GPVI is mediated primarily by arginine found in the transmembrane region of GPVI. (18,74) The FcR γ-chain dimer acts as a signal-transducing subunit for the GPVI receptor being an immunoreceptor tyrosine-based activation motif (ITAM).(18,74) The Src kinases, Fyn and Lyn phosphorylates the ITAM sequence when GPVI cross links with its ligands. Syk then undergoes autophosphorylation and activation on binding with the tyrosine phosphorylated ITAM sequence. Consequently a signalling cascade involving the effector proteins phospholipase (PL) Cγ2, PI3 kinase and adaptors, SLP76 and phosphorylated LAT forms a signalosome scaffold. Inositol 1,4,5 triphosphate (IP_3) and 1,2 diaglycerol (DAG) are secondary messengers formed by PLCγ2. Together protein kinase (PK) C is activated and cytosolic calcium concentrations increased.(8,18,74)

1.5 Integrins

Integrins are cell adhesion receptors with a central role in promoting cell membrane bidirectional signaling.(81) These receptors act also in enabling anchorage dependent cell events, given the constant exposure to haemodynamic forces of the vasculature.(81) Integrins are composed of a heterodimeric complex consisting of non-covalent bound α and β subunits. Twenty-four distinct integrin heterodimers are said to be formed through the combination of 18α and 8β known subunits. For each heterodimer, a large extracellular domain (approximately 80 to 150 kDa structures) is present and bound to it are proteins from the extracellular environment. Furthermore, a single transmembrane domain comprising of approximately 25 to 29 amino acid residues and a short cytoplasmic tail of 10 to 70 amino acid residues is contained within each subunit of an integrin.(82) The transmission of bidirectional signaling across the cell membrane is achievable due to the structural features of integrins. The intracellular cytoplasmic domains are capable of anchoring cytoskeletal proteins, whilst the extracellular domains are able to bind with a range of ligands. This subsequently forms a link between the interior and exterior components of the cell and ultimately bidirectional signaling.(82)

Integrins possess the ability to intracellulary transduce signals after ligand binding. This mechanism of signaling is referred to as outside-in signaling. For instance, in the vasculature, integrins are observed to associate with the ECM and transduce outside in signaling which is crucial for adhesion, proliferation and migration of endothelial cells.(81) Integrins also can undergo conformational changes from a low to high affinity ligand binding state.(81,82) This latter mechanism of integrin signaling is referred to as inside-out signaling. (81,82)

1.5.1 Integrin $\alpha_2\beta_1$

Integrin $\alpha_2\beta_1$ is expressed at approximately 2000 to 4000 copies per platelet and makes for the second most expressed platelet integrin. Binding of $\alpha_2\beta_1$ with triple helical peptides occurs at a high affinity. These peptides contain a GFO-GER or collagen derived hexapeptide sequence.(83) With injury to the vasculature, platelets possess the capabilities of directly binding to the collagen exposed as a result of injury. This is possible via $\alpha_2\beta_1$ and GPVI receptors. Integrin $\alpha_2\beta_1$ in particular undergoes a conformational change to an active state with platelet activation and subsequently an increased affinity for binding with collagen.

Furthermore, in its active conformation and association with collagen, $\alpha_2\beta_1$ promotes several events. Firstly, GPVI induced signaling to PLCγ2 activation, integrin activation, as well as Ca^{2+} release and secretion. Both human and mouse platelet *ex vivo* flow studies have been carried out also and revealed that platelet activation in some platelets was induced by GPVI prior to $\alpha_2\beta_1$ binding. The other remaining platelets however were observed to bind with $\alpha_2\beta_1$ before displaying stable adhesion.(83)

1.5.2 Integrin $\alpha_{IIb}\beta_3$

Intergrin $\alpha_{IIb}\beta_3$, a type 1 transmembrane receptor plays a critical role in haemostatic maintenance. This integrin is converted to a high affinity state change where it binds to its natural ligand, fibrinogen. Similarly with $\alpha_2\beta_1$, this activation step is linked to GPIb-IX-V signalling. When activated, $\alpha_{IIb}\beta_3$ assists in platelet spreading, adhesion, capture of more platelets to the growing thrombus and ultimately stopping bleeding.(8,48)

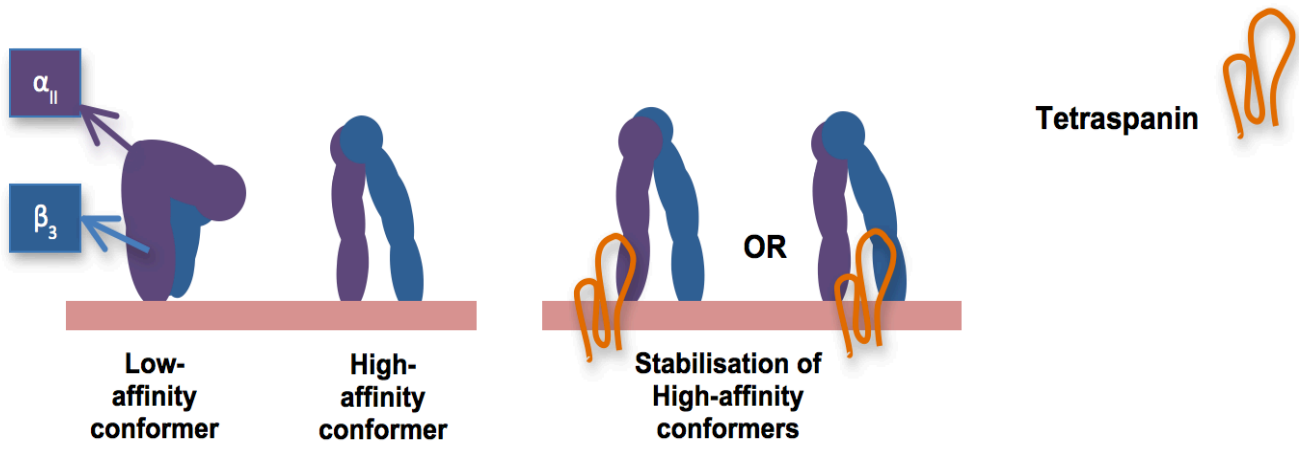

Figure 1.4. Integrin $\alpha_{IIb}\beta_3$ in a low affinity conformation versus high affinity conformation schematic model and stabilisation of the integrin by tetraspanin association. In a low affinity state, the integrin is bent down and when activated the integrin is in a straight position. Tetraspanin association with the integrin during the high affinity conformer phase will result in stabilisation of the complex and consequently allowing the complex to engage with other molecules.

The integrin $\alpha_{IIb}\beta_3$ binds to its soluble ligand, fibrinogen via a conformational change mediated by agonists from a bent or low affinity state to that of an extended or active high affinity state.(8,48) Integrin $\alpha_{IIb}\beta_3$ is expressed on the surface membranes of resting platelets at approximately 800,000 copies per cell (84) in platelets and megakaryocytes and is formed by the α_{IIb} and β_3 subunits within the endoplasmic reticulum.(85) The α_{IIb} subunit is cleaved into light and heavy chains by post-translational processing occurring in the golgi complex. The rapid conversion to its active conformation is said to occur with the binding of the FERM (4.1/ezrin/radixin/moesin) domain of the cytoskeletal protein talin-1 to the β_3 cytoplasmic tail.(86) Delivery of talin-1 to β_3 also occurs through the low molecular weight GTP binding protein Rap-1 and RIAM (Rap1-GTP interacting adapter molecule) which links platelet agonist-stimulated Rap-1 activaton to $\alpha_{IIb}\beta_3$ activation. Recent advances by Choi et al. (87) have identified a new structural model of integrin $\alpha_{IIb}\beta_{3.}$ By isolating purified intact inactive integrin $\alpha_{IIb}\beta_3$ and performing 3D reconstruction, the authors found that instead of the domain head bent downwards towards the membrane bilayer, they observed a upwards orientation of the domain head and confirmed this by using antibody-based epitope mapping which has also been discovered in studies examining cryo-electron microscopy models of intact integrin $\alpha_{IIb}\beta_3$.(88) Another interesting finding was that the legs of integrin $\alpha_{IIb}\beta_3$ were coiled and not straight as previously demonstrated. Despite these new discoveries, Choi et al. (87) noted that these discoveries were made in the absence of extracellular ligands and intracellular regulators and as such requires further examination to observe if the integrin maintains this proposed new conformation when binding to fibrinogen, talin and/or kindin.(87)

Integrin $\alpha_{IIb}\beta_3$ is critical for haemostasis and is the most highly expressed integrin in platelets amongst the integrins. Integrin $\alpha_{IIb}\beta_3$ is imperative in mediating the aggregation, adhesion and spreading of platelets, as well as in clot retraction through post ligand binding signaling at the site of injury.(8) Thrombin, Thromboxane (TxA_2), ADP and epinephrine are platelet agonists which are crucial for platelet plug extension. These agonists respectively bring rise to numerous events contributing to amplification of platelet activation and ultimately extension and growth of the platelet plug/thrombus. (8,74) A series of signaling events occurs on activation of $\alpha_{IIb}\beta_3$ specifically inside-out signaling that occurs through agonist-induced activation of the integrin and outside-in signaling.(8) Binding of vWF to the extracellular domain of GPIb initiates intracellular signalling leading to calcium immobilisation.(18) The regulation of the inside-out integrin $\alpha_{IIb}\beta_3$ pathway is observed to be regulated by charge related interactions involving the α and β subunit cytosplasmic tails. Studies have shown that deletions or mutagenesis to the proximal areas of these

cytoplasmic dails leads to nonreversible activation of integrin $\alpha_{IIb}\beta_3$.(89,90) Activation may also be mediated by the binding of GPVI with collagen and integrin $\alpha_2\beta_1$, resulting in the generation of soluble agonists such as thrombin and ADP which acts on integrin $\alpha_{IIb}\beta_3$. Outside-in integrin $\alpha_{IIb}\beta_3$ signalling is characterised by the binding of $\alpha_{IIb}\beta_3$ to its ligands. Fibrinogen occupied $\alpha_{IIb}\beta_3$ binding induces integrin clustering and consequently the reorganisation of the platelet cytoskeleton. Platelet aggregation, spreading and clot retraction are post occupancy events which follow.(4)

Recent studies have demonstrated binding of kindlin-3 to integrin $\alpha_{IIb}\beta_3$ is involved in activation of the integrin as well as integrin $\alpha_{IIb}\beta_3$ dependent responses of platelets and thus may be necessary for arterial thrombus formation.(91) Impaired integrin $\alpha_{IIb}\beta_3$ mediated platelet aggregation is observed *in vivo* to be impaired when kindlin-3 expres sion is defective, as the protein is known to be important in integrin function.(91) Activation of integrin $\alpha_{IIb}\beta_3$ in platelets and irreversible binding to fibrinogen has also recently been identified to occur in response to ADAP, a haematopoietic restricted adapter protein.(92) Integrin $\alpha_{IIb}\beta_3$ is a unique ligand binding integrin whereby it is able to complex with tetraspanins and as such improve its stability when it its active conformation.(93) Genetic defects affecting the quantitative or qualitative expression or dysfunction of $\alpha_{IIb}\beta_3$ in turn causes Glanzmann's thrombasthenia (GT). This disorder is characterized by severe bleeding, due to the defective aggregation of platelets, defective fibrinogen binding and retraction of fibrin clots which highlights the important of $\alpha_{IIb}\beta_3$ for the maintenance of haemostasis.(81,94)

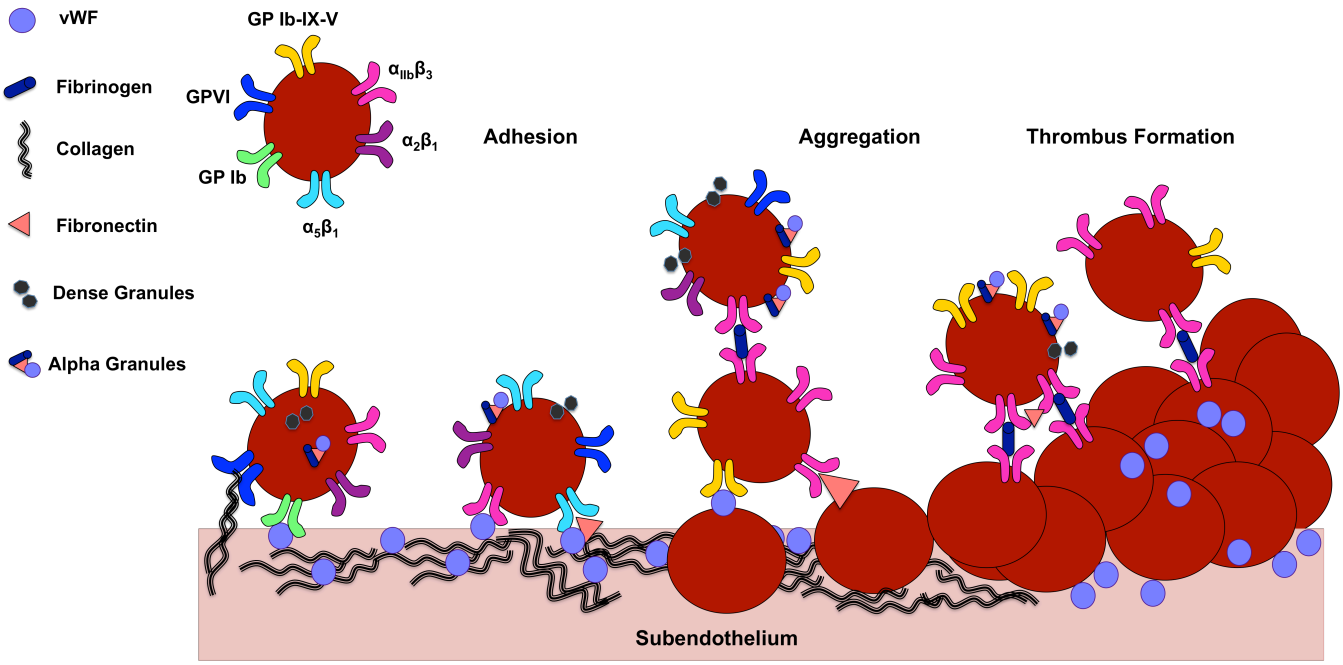

Figure 1.5. Platelet activation and aggregation. Platelets are drawn to the site of injury where the subendothelium is exposed, and interacts with GP Ib and GP Ib-IX-V complexes with collagen bound vWF. Following platelet adhesion, integrin $\alpha_{IIb}\beta_3$ activation interacts with fibirnogen, vWF and fibronectin which in turn maintains stable platelet aggregates, promoting thrombus growth. Agonists such as ADP, TXA_2 and thrombin are released from the platelet alpha and dense granules amplifying platelet activation through their respective receptors.(4)

1.6 Tetraspanins

Tetraspanins are transmembrane proteins involved in the regulation of cell morphology, fusion, signalling and cell migration. These proteins possess four transmembrane domains conserved amino acids, a conserved CCG motif, and two cysteine residues.(95,96) EC1 or the short extracellular loop hosts 13-31 of the 200-350 amino acids in tetraspanins whilst EC2 or large extracellular loop has 69-132 amino acids with a constant and variable region. The constant region is split into three α helices A, B and E.(97,98) Structurally, tetraspanins are demonstrated to have rod-shaped structures that are compacted together. These structures project from the plasma membrane at a height of approximately 5 nm. Tetraspanin clustering and modification, as well as the formation of tetraspanin microdomains is influenced by palmitoylation of the membrane proximal cysteine residues and additional N-linked sugars to the structure.

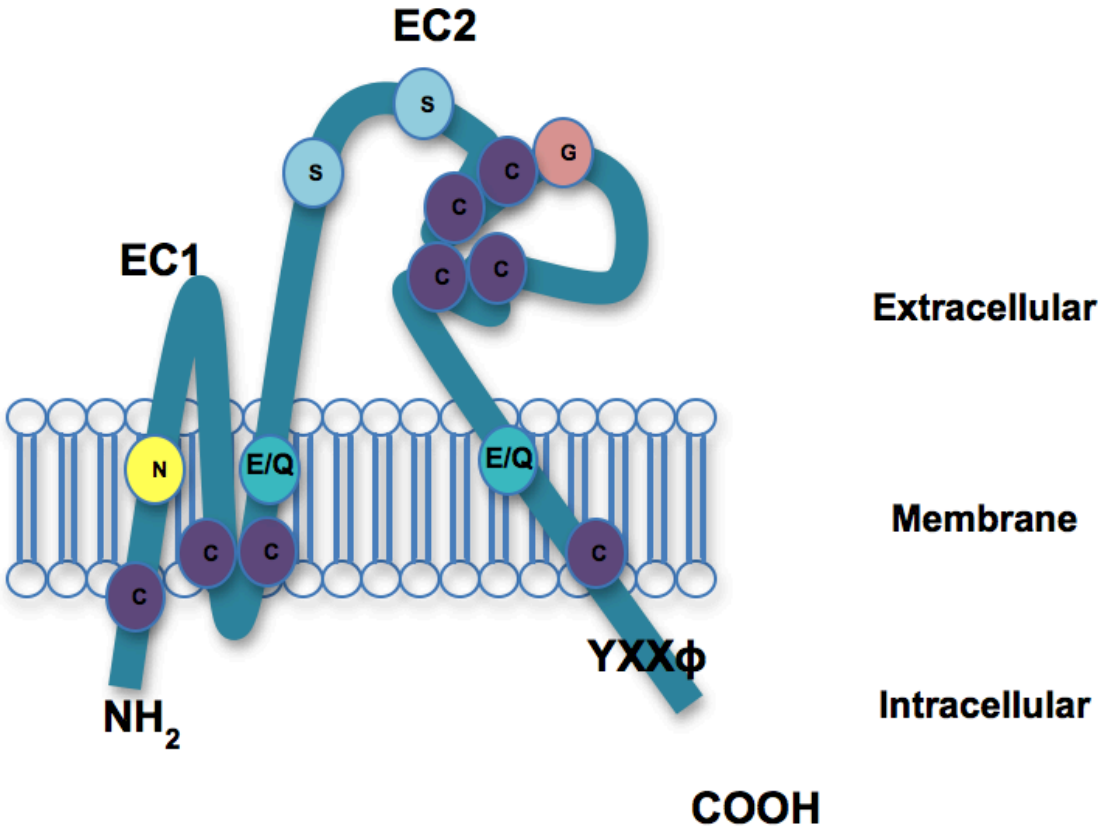

Figure 1.6. Common structural model of a tetraspanin. Tetraspanins possess four transmembrane domains, two extracellular loops (labeled EC1 and EC2) and also contain highly conserved cysteine amino acid residues.

Tetraspanins are known to form multimolecular membrane complexes into tetraspanin enriched microdomains (TEMs). TEMs are also formed through signalling and major histocompatibility antigen complexes and growth factors.(8,97,99,100) Recent data confirms the presence of TEMs in platelets in association with membrane receptors, both integrin and non-integrin.(101) Also, interactions between tetraspanins with gangliosides and other tetraspanins are suggested to occur in *cis*.(100) Studies have also shown links between integrins and tetraspanins. Cell adhesion to specific laminins, are mediated via this association being integrin dependent.

The tetraspanins CD151, CD81, CD82, C0/029 and CD9 in both *in vitro* and *in vivo* studies are shown to moderate cancer cell motility.(102) Until recently, several other tetraspanins have been identified in platelets and currently include the following platelet tetraspanins, namely CD9 (Tspan29), Tspan32 (TSSC6, PHEMX), CD63 (Tspan30), Tspan9 (NET-5), Tspan33 (Penumbra), Tspan14 (DC-TM4F2), Tspan15 (NET-7), Tspan2, Tspan18 (Neurospanin) and CD151 (Tspan24).(103)

1.6.1 Tetraspanin CD151 (Tspan24)

CD151 is a 254 amino acid protein with a structure specific to that of a tetraspanin.(98,103, 104) CD151, like CD9, CD63, CD81, CD82, and A15/Talla1 are palmitoylated. CD151 palmitoylation in particular requires intracellular membrane proximal cysteines. Palmitoylation of CD9, CD63, and CD151 specifically is imperative seeing its involvement in stabilising tetraspanin-tetraspanin associations. Studies have revealed impairments in heterophilic tetraspanin interactions where mutations to the CD9 and CD151 palmitoylation sites have occurred. It has been shown also that a common impairment in the aggregation of platelets and formation of thrombi at sites of vascular injury occurs with an inhibition in palmitoylation of platelets. Studies suggest both CD151 N and C termini are intracellular.(105) It has a N-glycosylation site in the EC2 loop and also shown to be palmitoylated on cysteine residues.(106, 107) The C-terminal (SLKLEHY) cytoplasmic domain bears a YRSL sequence referred to as a YXX endocytosis motif. This motif is imperative in promoting internalisation of CD151. This in turn modulates the endocytosis of related integrins and consequently integrin-dependent cell migration. Hemler (99,100) demonstrated that mutations caused to this motif disrupts and decreases CD151 internalisation and cell migration, therefore suggesting that cell motility is regulated through integrin trafficking.(99,100) Because CD151 is unable to autophosphorylate it is proposed that signalling molecule/cytoskeletal protein recruitment is mediated by 'phosphorylation or nonphosphorylation events'.(100) CD151 is expressed quite predominantly in endothelial, epithelial (cell to cell junctions), Schwann cells, smooth and cardiac muscles, platelets and megakaryocytes as well as the immune system.(96,100,101) The tetraspanin is typically located on cell surfaces and in contact with basement membranes.(108)

In humans, the CD151 gene is found on chromosome 11p15.5. The gene is comprised of 8 exons. Of this, the exons 2 to 8 are found to encode for CD151 polypeptide.(99,106) Ashman observed CD151 to demonstrate double bands appearing in the region of 28 to 32 kDa.(5) In platelets, studies have reported varying data in the expression of CD151.(5) Whilst several studies has reported CD151 to be expressed at levels as high as approximately 10,000 copies per platelet, a study has also shown CD151 being expressed at approximately 1,000 copies per platelet only. It is proposed that perhaps the type of mAb used is important on whether it detects CD151 alone or in combination with other receptors including integrin $\alpha_{IIb}\beta_3$.(8)

In in vitro and *in vivo* platelet related studies, CD151 is suggested to be involved in regulating platelet function. CD151 is noted to be crucial in the regulation of laminin binding

proteins, especially in organising the integrins $\alpha_3\beta_1$, $\alpha_6\beta_1$ and $\alpha_6\beta_4$ into TEMs.(102) The association of CD151 with integrin $\alpha_3\beta_1$ in particular has been shown to stabilise the activated conformation of integrin $\alpha_3\beta_1$ with laminin and thus increasing its binding activity.(103)

In addition, the integrin $\alpha_{IIb}\beta_3$ through recent studies is also reported to be closely linked with CD151 and TSSC6, and important in mediating cell adhesion strengthening in platelets as well as in regulating integrin $\alpha_{IIb}\beta_3$ outside-in signalling.(8) Integrin $\alpha_{IIb}\beta_3$ outside-in signalling occurs with binding of fibrinogen resulting in integrin cross-linking. With this, signalling molecules and the platelet proteins undergo tyrosine phosphorylation and ultimately resulting in cytoskeletal reorganisation, aggregation of platelets and cell adhesion. Note that CD151 and TSSC6 however does not mediate inside-out integrin $\alpha_{IIb}\beta_3$ signalling through agonist induced activation such as with Tyrosine kinase pathways or G-coupled receptors. Like CD151 and TSSC6, CD9 has also been found to show a constitutive association with the integrin $\alpha_{IIb}\beta_3$.(4, 109) The findings of Roberts et al. (111) and Ashman (5) are supportive of CD151 and this tetraspanins involvement in platelet function.(5,110) In using 14A2.H1, a monoclonal antibody (mAb) against CD151 and ADP as an agonist, the authors were able to demonstrate platelet activation and aggregation occurring in a Fc receptor dependent manner.(5,110) Signalling mediated by Fcγ receptor II α (FcγRIIα) is thus suggestive to be influenced by CD151 involvement. More recently, platelet activation occurring independent of the Fc receptors was identified where the mAb 11B1.G4 was used.(4) The degree of this association between CD151 and $\alpha_{IIb}\beta_3$ is said to be of a first level direct interaction out of a classification of 3 levels. Lau et al. (4) supported this with their findings in which the interaction showed stability and was resistant to Triton X-100.(4)

Associations between CD151 and signalling molecules have also been documented. Both phosphatidylinositol 4-kinase and PKC are observed to associate with CD151 on cytosolic surfaces and therefore providing a link between integrins and signalling molecules.(93,109) Studies have indicated that these associations may be co-immunoprecipitated.(4) In addition, the expression of protein tyrosine phosphatase μ is reported to be regulated by CD151 as well as recruitment of this protein at cell-cell junctions.(111) CD151 appears to have a regulatory role on Ras and in inhibiting activation of Ras that is mediated through adhesion dependent pathways.(112) CD151 is seen to be influential also in GTPase activity particularly in the activation of Cdc42 and RhoA.(113,114) Recent findings have identified CD151 involvement in non-tumorigenic HB2 mammary epithelial cells in activating

extracellular signal regulated kinases 1 and 2 or Erk1/2 and also protein kinase B (Akt) signalling. Research has also shown Erk 1/2 involvement in cell proliferation.(115) Erk1/2 is one of four mitogen-activated protein kinase (MAPK) members. Prior to the immediate pathway leading to activation of Erk1/2, vWF binding with GP1b-IX-V and the subsequent activation of $\alpha_{IIb}\beta_3$ in platelets occurs first.(116) Activation of Erk1/2 then is initiated by MAP/Erk kinase 1 (MEK 1) and MAP/Erk 2 (MEK2). MEK1/2 are part of the MAPK kinase (MAPKK) family. MEK activation occurs by phosphorylation with Raf kinase of which protein kinase activity foremost requires activation by Ras.(117) Consequently, with activation and phosphorylation of MEK1/2, the Thr-Glu-Tyr (TEY) sequence components, threonine and tyrosine residues are then phosphorylated and thus Erk1/2 activation.(115)

CD151 involvement in Erk 1/2 is suggested to occur upstream of the activation events as an absence of CD151 is observed to disrupt signalling of both Erk1/2 and Akt pathways.(118) Studies utilizing rat fibroblasts showed decreased Ras activation (adhesion dependent) with CD151 expression. As Erk1/2 and Akt activation in cells occurs downstream of the Ras signalling pathway, these were both affected and therefore failed to be activated with CD151 expression. Focal adhesion kinase (FAK) and c-Src on the other hand did not appear to be attenuated with CD151 expression. The importance of the C-terminal domain of CD151 is further demonstrated here with the use of mutant CD151 produced, showing its imperativeness in the negative regulation of Ras activity.(112) In addition, studies have reported also of the influence of calcium and calmodulin interactions in Erk pathways, as with modulating the activity of Src kinases and Ras activity. It was established also that with calmodulin inhibitors, Erk pathways were observed to be disrupted.(119)

Apart from cell motility, studies have also mentioned of CD151 involvement in cancer and metastasis regulation. Data shows an inhibition in the migration of endothelial cells for wound healing, neutrophil chemotactic motility and cancer cell phagokinetic motility when anti-CD151 antibodies are used.(120) Studies have also observed treatment with anti-CD151 antibodies and reported a decrease in the invasiveness and spread of specific cancer cells. On the other hand where over expression of the tetraspanin is observed, metastasis is more aggressive.(120-122) Studies indicate also the importance of CD151 in vasculogenesis and angiogenesis regulation. *In vitro* Matrigel assay studies reveal CD151 influence in regulating the formation of EC cables. In addition, pathological angiogenesis is found to be defective in CD151 knockout mice.(123)

Mutations and the resultant diseases in both human and mouse CD151 have been identified. In humans, where CD151 does not have an integrin binding domain intact, patients are seen to suffer from the diseases: end stage hereditary nephritis and pretibial epidermolysis bullosa.(8) This mutation is rare and occurs in only approximately 8% of the population, specifically individuals of Indian Jewish heritage.(8,124) The mutation occurs at position 140 where an in-frame stop codon causes truncation and loss of the integrin binding domain. In mice, mutations in CD151 leads to diseases and symptoms different to that identified in humans.(8)

In vitro studies have revealed that initial ligand binding is not affected by CD151. Integrin-dependent adhesion strengthening and post ligand binding events however are shown to be influenced by CD151.(125) Data involving mice studies demonstrate laminin binding integrins in CD151 knockout mice *in vivo* to function normally despite the altered phenotype. Haemostasis however is unstable with this phenotype. Platelet aggregation is abnormal with prolonged bleeding times, increased blood loss and occurrence of rebleeds. Notably, CD151 deletion has not been found to affect $\alpha_{IIb}\beta_3$ integrin inside-out signalling. However, $\alpha_{IIb}\beta_3$ outside-in signalling is impaired in $CD151^{-/-}$ platelets. Furthermore, recent findings have identified that *in vivo* regulation of thrombus formation requires platelet CD151.(4) Thrombi is unstable and smaller in $CD151^{-/-}$ and $CD151^{+/-}$ mice in comparison to $CD151^{+/+}$ mice, observed through laser induced injury to cremaster muscle arterioles. In a similar pattern, $CD151^{-/-}$ and $CD151^{+/-}$ mice versus $CD151^{+/+}$ mice were seen to have prolonged times in reaching 95% of vessel occlusion. For this latter experiment, the authors employed the Folt $FeCl_3$ induced carotid injury model. Collectively, this demonstrates the importance of tetraspanin-integrin $\alpha_{IIb}\beta_3$ complexes in regulating the formation of platelet thrombi and effective platelet adhesion.(111)

In human platelets, the integrin $\alpha_{IIb}\beta_3$ is observed to associate with only a smaller non-glycosylated section of CD151 whilst $\alpha_6\beta_1$ and $\alpha_3\beta_1$ are capable of associating with glycosylated CD151.(83) The lateral associations of CD151 with integrin $\alpha_6\beta_1$ is particularly influential in the integrins role in outside-in signalling.(112) Cell morphology regulation and migration are influenced by the complexes formed between $\alpha_6\beta_1$ and $\alpha_3\beta_1$, and CD151.(113, 114,125) This regulation is achieved by mediating cytoplasmic signalling(126) and adhesion. (113,114,125) Studies have suggested also of the role CD151 has in $\alpha_3\beta_1$ glycosylation and trafficking regulation.(99, 116)

The CD151 and $\alpha_3\beta_1$ complex compared to other integrin and tetraspanin complexes is observed to exhibit a greater level of stoichiometry and stability. This is seen with the resistance of the complex to triton X-100 detergent and interaction being present when immunoprecipitated and specificity with the $QRD^{194-196}$ binding sequence.(102,117) In addition, with direct covalent cross linking, this complex also shows high levels of proximity.(102) The integrin $\alpha_3\beta_1$ is not found to be present in cells or tissues where CD151 association is also absent. Studies have identified the regions in the CD151 extracellular loop ($QRD^{194-196}$) and α_3 extracellular domain to be the sites most important in forming more stable associations.(127) In contrast, the interactions between CD151 with $\alpha_6\beta_1$ and $\alpha_6\beta_4$ are less stable than compared to $\alpha_3\beta_1$. Integrin $\alpha_3\beta_1$ in contrast to other integrins is also seen to demonstrate greater PtdIns 4-kinase activity. With CD151 immunodepletion, this activity is observed to decrease. This association between CD151 and $\alpha_3\beta_1$ is reported to be localised in the integrins extracellular domain.(5) Also, Lammerding et al. (122) found adhesion strengthening mediated by integrins and cell spreading which are both dependent on α_6 to be reduced where the CD151 and α_6 complex is affected.(122) This is supported by findings in which the C-terminal of CD151 is specifically observed to be vital for these functions to occur and ultimately form on matrigel experiments.(112)

CD151 involvement in platelet function is important as evidenced by its involvement in the regulation and organisation of laminin binding proteins into tetraspanin enriched microdomains.(102) In addition, cytoskeletal reorganisation, platelet aggregation and cell adhesion is mediated by outside-in signalling through the constitutive association of CD151 with integrin $\alpha_{IIb}\beta_3$.(5,110) *In vitro* studies have reported abnormalities in platelet aggregation as a result of platelet CD151 deficiency. The formation of thrombi *in vivo* was also noted to be affected by the absence of CD151 in platelets.(4) In the context of atherosclerosis in humans, CD151 expression and distribution is poorly understood. Human *in vitro* studies demonstrated increased protein expression and distribution of CD151 in atherosclerotic tissues suggesting the involvement of CD151 in atherosclerosis disease progression.(128) Although the literature shows that *in vitro* studies of CD151 in platelets have been well studied, its involvement in the physiological setting of atherosclerosis is lacking.

1.7 PECAM-1

In humans, Platelet endothelial cell adhesion molecule-1 (PECAM-1) is found on activation responses by sending inhibitory dephosphorylating signals to platelets and immune cells via the Immunoreceptor tyrosine-based activatory motifs (ITAM)-dependent pathways.(129,130) The regulation of cell signalling therefore is crucial between the negative regulation of ITAM receptors with ITIM-containing receptors as it is necessary for producing the appropriate responses and required cellular activities. The structure of PECAM-1 is composed of an intracellular region with two tyrosine (Y663 and Y686) ITIMs, 1 transmembrane domain and 6 Ig domains in the extracellular domain. On a molecular level, the extracellular Ig domains in PECAM-1 are suggested to be involved in both homophilic and heterophilic interactions with ligands located on adjacent cells. Intracellular signalling molecules interact with PECAM-1 non-convalently for transduction of the extracellular signals to occur. This is due to the inability of PECAM-1 to elicit intrinsic enzymatic activities. Outside-in signalling events are induced with PECAM-1 engagement which is followed by tyrosine phosphorylation, protein-tyrosine phosphatase (PTP) activation and recruitment. Cell adhesion is then disrupted following Inside-out signalling and selective dephosphorylation. In contrast, It has not been established as far whether the cytoplasmic signalling and cytoskeleton molecules such as Ƴ-catenin, β-catenin, PLC-Ƴ1 and PI3-kinase interacts directly PECAM-1 as would PTP, despite the associations observed. The two tyrosines Y663 and Y686 in the intracellular region of PECAM-1 are common sites for Src homology 2 (SH2) domains. The tyrosines subsequently undergo phosphorylation in response to stimuli. Both Src family kinases and Csk related kinases are suggested to be involved in phosphorylation. Studies have shown that phosphorylation still occurs where Src kinase inhibitors have been used thus suggesting Csk kinase involvement.(129) PECAM-1 is known to mediate several functions and has a role in the negative regulation of platelet activation and immune cells. It is involved also in cell-cell contact formation and stabilisation. This occurs at the lateral junctions of endothelial cells where it is most abundantly expressed.(129)

In platelets, PECAM-1 acts as a key negative regulator where the collagen GPVI/FcR γ-chain and ITAM signalling pathways are concerned.(129, 130) PECAM-1 knockout mouse studies have shown that PECAM-1 negatively regulates receptor antigen complexes on B cells, mast cells and FcRI-mediated signalling. Thrombi formation was also increase in a study by Jackson kson which observed thrombus formation on immobilised collagen, under flow conditions in human models. This was determined through a dose-dependent experiment with human PECAM-1-Ig chimera over control IgG. Mice studies also revealed

that wild type mice formed smaller thrombi compared to PECAM-1 knockout mice.(131) Additionally PECAM-1 is known to mediate and maintain the vascular permeability barrier whilst also playing an imperative role in the transmigration of leukocytes with PECAM-1 specifically modulating monocyte and neutrophil migration.(129,132,133) PECAM-1 has been observed to be a regulator in angiogenesis and phagocytosis of apoptotic cells. Studies have shown also of PECAM-1 and its role in ECM adhesion and cell motility, cellular cytoskeleton assembly and integrin activities. With this, recent research is suggestive of PECAM-1 in being linked to intracellular signal complexes formation with the molecule functioning as a scaffolding protein.(129) Recent studies have demonstrated a constitutive association between PECAM-1 and Calmodulin (CaM). This interaction is one of several PECAM-1 interactions found to occur independent of the ITIM region. The association between PECAM-1 and CaM requires the sequence located in the intracellular region of PECAM-1, ^{599}RKAKAK^{604}. (129,130)

1.8 Mechanisms of stable thrombus formation in mice

The temporal and spatial formation of a platelet thrombus has been shown through *in vivo* murine studies to be a dynamic and complex process. The interplay of platelets and platelet activation and aggregation, vWF, collagen, fibrinogen and fibronectin, intracellular calcium mobilisation, release of secondary mediators, ADP and TxA_2 are all involved in this process. The translocation of platelets and adhesion through platelet adhesive receptor-ligand interactions to the exposed endothelium occurs as part of the initial stages of thrombus formation. The accumulation of platelets occurs at this site followed by shedding of the thrombus and embolisation downstream.(134-137) Occlusion of the vessel occurs with growth of the thrombus in due course, as a result of recurring plaque injuries and thrombus formation. The stability of the thrombus is also influenced by numerous factors, in particular, the signalling events of integrin $\alpha_{IIb}\beta_3$, platelet adhesive ligand interactions, platelet adhesion, Src family kinases, protein tyrosine phosophatase PTP1B, secondary wave mediators and receptors: $P2Y_{12}$, ADP and TxA_2.(138) *In vivo* studies have also reported the involvement of the following receptors in thrombus stability: Semaphorin 4D, CD40L and Gas6.(134,139)

1.9 Atherosclerosis

Atherosclerosis is a chronic inflammatory disorder involving the complex interactions of plasma lipoproteins, monocytes, vascular endothelial and smooth muscle cells, lymphocytes, platelets, lipids, genetics and the haemodynamics of arterial blood flow.(140-142) It is characterised by the narrowing of blood vessels caused by growth and presence of atherosclerotic plaque lesions, also referred to as atheromas or fibro-fatty plaques.(143) The rupture or erosion of an atherosclerotic plaque lesion leads to atherothrombosis, termed as the formation of a thrombus, following these events. Subsequently, occurring in conjunction with the accumulation of lipids, an occlusive thrombus/thrombi develops as the intima of the coronary and carotid arteries thickens progressively and ultimately resulting in myocardial infarction and stroke. (64,140) In Australia, 14.6% of deaths in 2011 were caused by ischaemic heart diseases and has continuously been the number one cause of death since 2000.(2)

Platelets have an integral role in the onset and development of atherosclerosis, and is associated with the inflammation processes and atherogenesis of this disorder.(144) Platelet adhesive interactions with leukocytes and the endothelium subsequently leads to the recruitment of leukocytes to the vascular wall, migration of mononuclear cells and foam cell formation. (140,145,146) The interaction of platelets with leukocytes and endothelial cells initiates a localised inflammatory response which is contributed by cytokine, chemokine, proinflammatory molecule and modulators such as CD40L (CD154) release, accelerating the formation of early atherosclerotic lesions.(146) The release of platelet derived growth factor from platelets also contributes to plaque angiogenesis as it stimulates smooth muscle proliferation.(147) The contribution of platelets in atherosclerosis and plaque development is further evidenced by studies in which ApoE knockout mice platelets were observed to adhere to arterial intimas prior to the detection of atherosclerotic lesions. Platelets in the circulation were also observed to have secreted proinflammatory chemokines and formed platelet-monocyte aggregates.(148-150) These studies also showed that genetic deletion of the α_{IIb} subunit of integrin $\alpha_{IIb}\beta_3$ resulted in a decrease in lesion development.(148-150) Furthermore, *in vivo* studies using intravital microscopy models showed that platelets adhered to arterial walls even in the absence of endothelial cell disruption.(145,151) These *in vivo* and *in vitro* findings support the theories of platelet involvement in the onset and development of atherogenesis and atherosclerosis disease in mice.(144-146) This also reiterates the importance of examining platelet signalling pathways and tetraspanins such as CD151 for the prevention and management of atherosclerosis through targeted therapies.

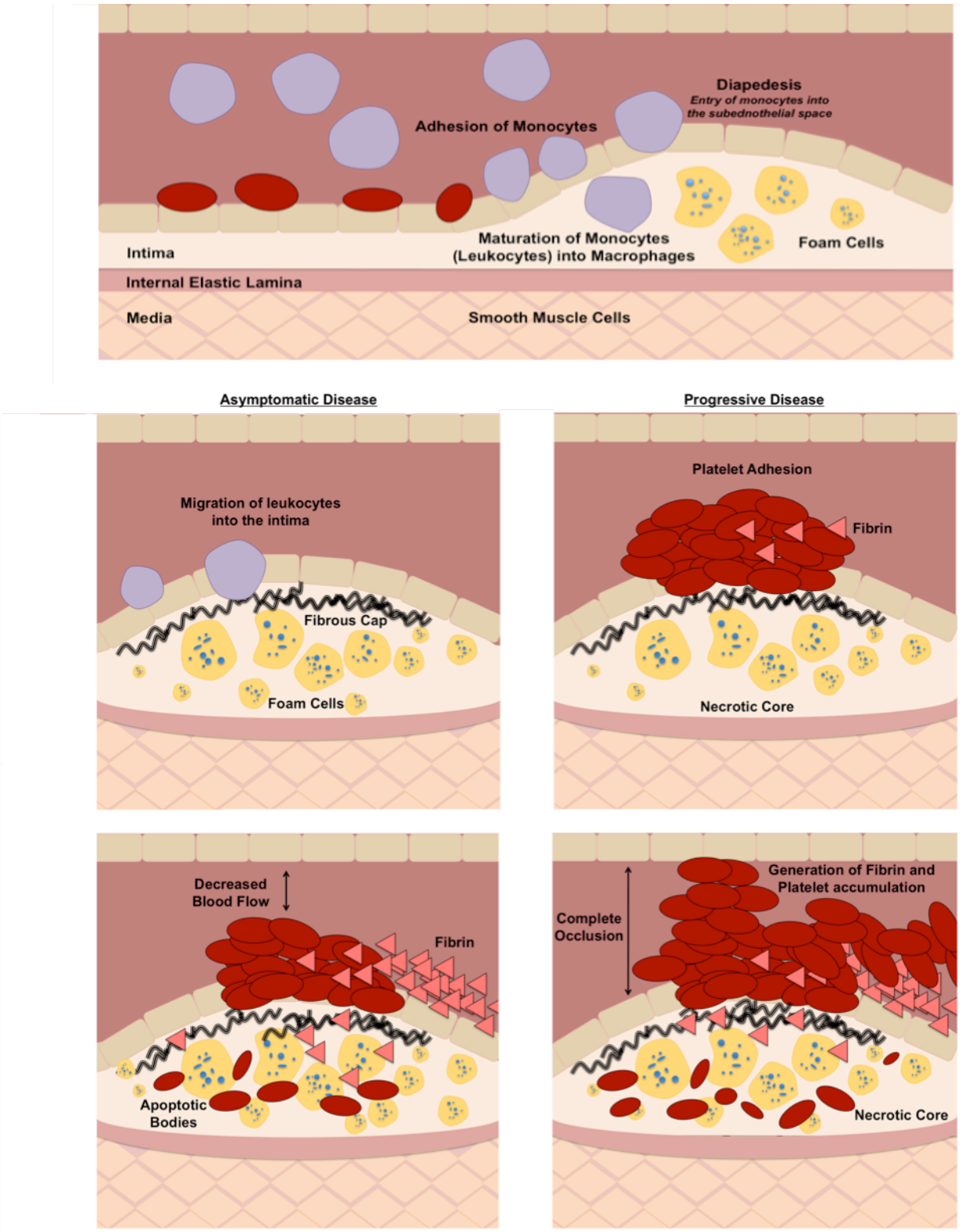

Figure 1.7. Progression of atherosclerotic lesions in arterial thrombosis. The development of atherosclerotic lesions is preceded by leukocyte to platelet and leukocyte to endothelial interactions. In asymptomatic disease, proatherogenic leukocytes and foam cells are recruited throughout progression of atherosclerosis which stabilises the plaque. The collagen rich fibrous cap developed also improves plaque stability. As atherosclerosis progresses, the lipid core becomes necrotic and the fibrous cap begins to thin. This unstabilises the plaque and renders it vulnerable to rupture. Exposure of the thrombogenic contents following plaque rupture results in rapid platelet accumulation and generation of fibrin. The repetitive cycles of injury and thrombus formation leads to progression of the atherosclerotic lesion and gradual narrowing of the lumen causing a stenosis and eventually a myocardial infarction, or ischaemic stroke.(146)

1.9.1 Thrombotic complications in atherosclerosis

Arterial thrombosis occurs mostly in the coronary circulation and involves the exposure of thrombogenic components of an unstable atherosclerotic plaque to the blood.(152-155) Previous studies have identified the primary involvement of platelet rich thrombi in plaque development and consequently also the increased risk of an acute coronary event occurring. Most atherosclerotic lesions develop slowly and rarely cause life threatening thrombosis.(146) Studies have shown that in some individuals (postmortem) atherosclerosis was reversed spontaneously. Thrombi which had formed on disrupted plaques appeared small and non occlusive, suggesting an asymptomatic coronary disease condition.(154, 156-158) In unstable coronary lesions on the other hand, the risk of suffering an acute coronary event is increased as compared to asymptomatic conditions and progresses rapidly over a matter of months.(154,156,159) Platelets also appear to be more reactive to platelet agonists such as ADP, thrombin and collagen in atherosclerotic patients. Studies also show an increase in their adhesion to the endothelium and secretion of other proinflammatory proteins such as chemokines and cytokines.(160) These inflammatory responses accelerates the progression of atherosclerosis and subsequent risk of acute coronary syndromes.(161)

1.9.2 Tetraspanins in atherosclerosis

Studies have reported of the involvement of tetraspanins in the pathogenesis of atherosclerosis and atherothrombosis. Platelets have also been implicated in the progression of disease not just in the late stages but also in the early stages of atheroma or atherosclerotic plaque lesion formation.(162) Tetraspanin CD63 has been shown to be associated with atherosclerosis disease. CD63 is highly expressed in platelets and localised predominantly to the lysosomes and dense granules, and is expressed together with P-selectin upon platelet activation on platelet surfaces.(123,163) According to Cha et al. (164) whole blood flow cytometry analysis revealed the expression of CD63 and P-selectin was elevated and persisted up to 90 days after atherosclerotic ischaemic stroke events. CD63 and P-selectin expression has also been shown to be elevated in the acute phase on an ischaemic stroke by Zeller and colleagues.(165) It was suggested that the hyperactivation of platelets in atherosclerotic ischaemic stroke may persist for long periods and assist in proposing renewed anti platelet agents for the management of atherosclerosis disease.(164) Furthermore, the use of statins have been demonstrated to be helpful in regulating atherosclerotic ischaemic stroke which saw a reduction in CD63 expression.(166) Platelet derived microparticle (PMP) subpopulations have also been studied in atherosclerosis

disease as it is associated with raised levels of platelet activation and been observed to circulate in higher concentrations in atherosclerosis. It has been reported that PMP subpopulations exposes CD63 and P-selectin, and thus act as a more reliable marker of platelet activation rather than overall PMP numbers.(167) Similarly, CD81 like CD63 is conserved as part of a syntenic group in that their chromosomal order is preserved between the mouse and human species.(106) CD81 is broadly expressed and influences cellular function in the nervous and immune systems.(168-172) Endothelial CD81 has been shown in human arteries to be upregulated in early human atheromas. The authors proposed that CD81 may play an integral role in early atherosclerotic plaque formation by enhancing monocyte adhesion involving intercellular adhesion molecule 1 (ICAM-1) and vascular cell adhesion molecule 1 (VCAM-1).(173) Recently, another group also identified CD81 as a valuable marker of early atherosclerotic plaque presence. They performed *in vitro* studies using ultraonic imaging on murine bend.3 cells and inducing oxidative stress with phenazine methosulfate. The results demonstrated that epithelial CD81 expression was upregulated in the presence of oxidative stress which corrected with the administration of anti-CD181 antibodies.(174) Another tetraspanin said to be involved in the pathogenesis of atherosclerosis is CD9. Tetraspanin CD9 was first identified by its reactivity with BA-1 monoclonal antibody raised against the leukaemia cell line, NALM-6.(175,176) CD9 is expressed on numerous cells including eosinophils, basophils, macrophages, fibroblasts, neuronal cells, oocytes, smooth muscle cells epithelial cells and various cancers.(177-179) Expression of CD9 was demonstrated and localised to the human aortas and coronary arteries, especially in atherosclerotic plaque lesions through immunohistochemical studies.(180) The proliferation of smooth muscle cells in the intima of arteries is a key event in plaque formation and was proposed by Nishida et al. (180) to be associated with CD9 expression. *In vitro* studies of cultured smooth muscle cells showed high expression of CD9 and was also associated with vascular smooth muscle cell proliferation.(181) The authors also identified that an increase in CD9 expression in the proliferative phenotype was double that of the contractile phenotype, and also found that CD81, was upregulated likewise.(181) Double immunofluorescence studies displayed the co-localisation of CD9 with CD36 on human platelets prior to solubilisation. CD36 is a scavenger receptor involved in the formation of foam cells through the phagocytosis of oxidised low density lipoprotein (LDL) by macrophages in atherosclerosis.(182) According to Miao et al. (182) CD9 may be involved in mediating the biological functions of CD36 as their findings showed associations between the proteins.

1.10 Apolipoprotein E

Apolipoprotein E (ApoE) is an important glycoprotein required for the metabolism and transport of lipids. ApoE has been noted also to have a protective role on atherosclerosis and is a component of all lipoproteins with the exception of LDL.(183-188) ApoE acts on the lipid metabolism pathway and is associated with hepatic uptake as well as the breakdown of lipoproteins via LDL receptors (LDL-R) and LDL like receptor proteins in the liver. These proteins act also in clearing chylomicron remnants, reverse cholesterol transport (RCT), hepatic very low-density lipoprotein (VLDL) stimulation, as well as in enzyme activation.(184-189) Recent studies have demonstrated the particular importance of ApoE in RCT *in vivo* where deletion of ApoE caused a decrease in macrophage RCT by 30%.(184) The anti-atherogenic effects of ApoE extends into LDL oxidation inhibition, endothelial and smooth muscle cell proliferation, platelet aggregation and inhibition of T-lymphocyte proliferation and activation.(183)

1.10.1 Apolipoprotein E structure

ApoE is a 299 amino acid protein and is found on the 5' end of a 50kb gene cluster on chromosome 19 in humans.(190,191) ApoE has two functional heparin binding domains. The N terminal contains the ApoE receptor binding regions at residues 136 – 150 whilst the C terminal at residues 244 - 272 contains highly lipophilic binding regions which inserts into lipoprotein surfaces.(191-194) ApoE exists as three isoforms: ApoE2 (Cysteine 112 and Cysteine 158), ApoE3 (Cysteine 112 and Arginine 158) and ApoE4 (Arginine 112 and Arginine 158).(195, 196)

1.10.2 Apolipoprotein E mouse model

The ApoE knockout mouse model was first developed in 1992 and since then has allowed scientists to observe the progression of atherosclerosis.(185) Mice possess a natural resistance to atherosclerosis, an attribute likely to be a result of plasma cholesterol ester transfer protein absence. Approximately 85% or 85 mg/dL of total serum cholesterol circulates as HDL which is understood to have an atheroprotective effect. This shift in plasma lipid profile differs to that of humans significantly.(185) Through genetic manipulation and disruption of ApoE, this natural resistance is challenged and thus allowing us to study

atherosclerosis in a murine model. The differences in lipid profiles and cholesterol metabolism between murine and humans presents some limitations however is still widely acknowledged to be a gold standard murine model atherosclerosis studies.(185)

When comparing between C57BL/6 wild type mice and ApoE knockout mice, the latter maintains a normal heart rate as well as blood pressure, however the aortic and mitral flow velocities and pulse velocities are elevated in ApoE knockout mice. Furthermore, when fed a standard chow diet, the ApoE knockout mouse exhibits cholesterol levels of up to approximately five times more than wild type with hypercholesterolaemia ranging around 400 mg/dl.(185) Heterozygous knockout mice on the contrary were observed to exhibit comparable cholesterol levels to wild type control mice.(183)

Studies have shown that in $ApoE^{-/-}$ mice atherosclerotic lesions develop at a greater rate than in normal mice. Even on a normal mouse diet, $ApoE^{-/-}$ mice compared to normal mice are seen to demonstrate abnormalities in lipid metabolism with data showing the accumulation of foam cells on aortic walls at approximately 3 months which then by 8 months develop into atherosclerotic lesions and vessel occlusion. CD151 on the other hand is important in thrombus formation as $CD151^{-/-}$ arterioles develop smaller thrombi that are less stable and have a tendency to embolise.(127) $CD151^{-/-}$ mice have prolonged bleeding times, increased blood loss and occurrence of rebleeds, indicating unstable haemostasis.(197)

As discussed, CD151 a tetraspanin superfamily member is required for the regulation of thrombus formation and growth *in vivo.* Also, particularly in cell adhesion strengthening and acting as a structural scaffold. Factors such as platelet and ligand interactions, as well as integrin signalling events involving $\alpha_{IIb}\beta_3$ are influential in the stability of thrombi formed. As with signalling events, Src family kinases, Eph kinases and PTP1B are also involved; as are the following agonists: ADP, TXA_2, P_2Y_{12} receptors. Research also indicates the involvement of Gas6 and CD40L in platelet signalling. PECAM-1 on the contrary plays a crucial role in inducing outside in signalling events with engagement of PECAM-1.(197) Therefore, PECAM-1 is highly influential on the stability of thrombi formed given its role in inducing outside in signal transduction, and the phosphorylation events which follow together with the activation and recruitment of relevant signalling molecules. Prolonged tail bleeding

times have been demonstrated in studies observing PECAM-1 deficient mice.(131) This was reported by irradiating mice followed by reconstitution with either PECAM-1 or wild type platelets and observing for a correction in bleeding time which required presence of endothelial PECAM-1.(131)

Additionally, in a disease setting, atherosclerosis is polygenic in nature involving the contribution of an altered lipid metabolism, multiple cell types, inflammation, development of atherosclerotic lesions and plaque formation. CD151 is broadly expressed in multiple cell types and has never been studied in the context of atherosclerosis. Using a proatherogenic mouse model ApoE$^{-/-}$ crossed with CD151$^{-/-}$ mouse strain will give investigators an indication of whether cell surface contact receptors play an important role in regulating atherothrombosis and plaque stability. Previous findings determined by the Jackson laboratory have shown that at least in platelets, CD151 is important for the growth and stability of platelet thrombi formed *in vivo*.(4,197) Absence of CD151 may confer some resistance in the setting of a proatherogenic mouse model of ApoE$^{-/-}$.CD151$^{-/-}$ in the development of atherothrombosis and plaque stability. These findings will elucidate the extent of CD151 deficiency in atherosclerosis and identify potential targets for the development of anti-thrombotic therapies.

1.11 Summary and aims

Platelets are paramount in the regulation of haemostasis. Platelets are anucleate fragments of megakaryocytes found only in mammals and are involved in a range of processes such as inflammation, host defense, coagulation, malignancies and wound healing. Its diverse abilities to adapt to different physiological situations emphasises its importance in haemostasis. Defects to platelet functioning and the subsequent impact on coagulation, platelet aggregation and activation can pose serious implications to patient health. Bleeding and thrombotic events which manifest as ischaemic heart disease continues to be the leading cause of death in Australia as reported in the latest statistics released in 2013.(2) Studies on tetraspanins and in particular CD151 have examined the effects of deficiencies on platelet function. CD151 regulates the function of integrin $\alpha_{IIb}\beta_3$ and therefore the formation of a haemostatic plug to suspend bleeding. Whilst conclusions have been made in the literature on the effects of CD151 absence and the outcomes expected, none of these studies have examined the effects of CD151 deficiency specifically in atherosclerosis. Plaque rupture and the sequential development of thrombi leads to vessel occlusion and potentially a myocardial infarction or stroke. Based on the literature, we hypothesise that CD151 deficiency may confer resistance in an atherosclerotic setting by using a novel ApoE$^{-/-}$.CD151$^{-/-}$ model for the investigation of atherothrombosis and plaque stability. In order to address this hypothesis, the following aims were projected:

1. Develop and characterise the ApoE$^{-/-}$.CD151$^{-/-}$ genotype. This is a novel model in which the specific CD151 gene knockout mouse crossed with an ApoE knockout mouse permitted the *in vivo* study of the absence of CD151 in atherosclerosis. ApoE$^{-/-}$ mice were used as a control as this model has been established to be a gold standard for experimental atherosclerosis studies. Chapter 3 of this thesis documents the development of the novel strain as well as haematological, lipid, glucose and weight profiles.

2. To examine plaque burden between the ApoE$^{-/-}$ and ApoE$^{-/-}$.CD151$^{-/-}$ model. CD151 is expressed not only in platelets but also in endothelial, cell to cell junctions in epithelial cells, Schwann cells, smooth and cardiac muscles, and the immune system.(96, 100, 101) The tetraspanin is typically located on cell surfaces and in contact with basement membranes.(108) Histology studies were used to asses the impact CD151 deficiency on atherosclerotic plaques and their development in Chapter 4 and 5.

3. To examine plaque composition between the ApoE$^{-/-}$ and ApoE$^{-/-}$.CD151$^{-/-}$ model. Immunonhistochemical studies were used to assess the role of smooth muscle actin type I collagen and macrophages.

4. To investigate whether platelet activation, aggregation and the formation of thrombi is affected *in vivo* and *in vitro* in CD151 deficiency in atherosclerosis compared to the literature where it has been examined in a non-atherosclerotic setting. Chapter 6 discusses the investigation of different vascular beds subjected to injury and the observation of platelet recruitment *in vivo*. Thrombotic events and thrombus formation in response to these injuries were investigated in an atherosclerotic setting with the use of the ApoE$^{-/-}$.CD151$^{-/-}$ model. *In vitro* studies on the other hand examined platelet aggregation and adhesion responses to agonists.

2 CHAPTER 2: METHODS

2.1 Mice and development of the ApoE$^{-/-}$.CD151$^{-/-}$ strain

ApoE$^{-/-}$ C57BL/6 background mice were purchased from the Animal Resources Centre (ARC, Perth, WA). CD151$^{-/-}$ (C57BL/6 background) mice were originally generated by A.Prof Mark Wright and Professor Leonie Ashman as previously described.(102) Both ApoE$^{-/-}$ and CD151$^{-/-}$ strains were generated using C57BL/6 genetic embryos. ApoE$^{-/-}$ and CD151$^{-/-}$ mice were crossed to generate the ApoE$^{-/-}$.CD151$^{-/-}$ strain. All mice were housed in a pathogen-free and barrier protected facility room in the RMIT Animal House Facility under protocols approved by the RMIT Animal Ethics Committee (AEC). The age and sex matched mice were given free access to food and water throughout experiments and fed a standard chow diet comprising of 65% carbohydrate, 15% fat, 20% protein (NIH-31 Chow diet; Ziegler Brothers, Gardner, PA) for 16 weeks. All experimental procedures were approved by the RMIT AEC – AEC Number 0927 and 1332. The mouse genotypes were confirmed by polymerase chain reaction (PCR) screening of mouse tail genomic deoxyribonucleic acid (DNA).

2.1.1 Genotyping of ApoE$^{-/-}$ and ApoE$^{-/-}$.CD151$^{-/-}$ mice

2.1.1.1 Isolation of mouse genomic DNA

Mouse tail tissue clippings from 3 week old pups were taken for the isolation of mouse genomic DNA. The 'DNeasy' protocol for rodent tails was used and is as detailed in the DNeasy tissue kit handbook from Qiagen Pty. Ltd. (Clifton Hill, Victoria). All materials used for the protocol were purchased from Qiagen Pty. Ltd. (Clifton Hill, Victoria).

2.1.1.2 PCR protocol

For ApoE PCRs, PCR products were prepared using ApoE primers only whereas for ApoE.CD151 genomic DNA, PCR products were prepared using both CD151 and ApoE primers.

For CD151, three primers were used to genotype mouse tail DNA from the tail clippings of the pups. Firstly as the forward primer (FP) for wild type mice, CD151 primer 1 (5' GCTCCATGTTCCGTACACT 3'). Secondly, for the common reverse primer (RP) for both wild

type and CD151 knockout, CD151 primer 2 (5' CAGCTTAGGACCTCTTCTCA 3'). Finally, as the forward primer which is specific for $CD151^{-/-}$ located on the 5' of the PGK-Neo cassette, CD151 primer 4 (5' ATGATAACCCACCATGTGTC 3'). PCR products for wild type and $CD151^{-/-}$ yield 400 base pair (bp) products.

Preparation of the PCR master mix was made according to the number of genomic DNAs prepared. For each tail clipping, a mix was prepared containing 1 x PCR Taq Gold Buffer (Perkin Elmer, Boston, MA), 0.09 mM $MgCl_2$ (Perkin Elmer, Boston, MA), 2.5 mM dNTPs (Progen Industries Ltd., Richlands BC, Qld), 1.25 mM each of forward and reverse primers (KO allele: CD151 2, CD151 4; WT allele: CD151 1, CD151 2), 0.2 U/µl of Taq Gold DNA polymerase (Perkin Elmer, Boston, MA), and made to a final volume of 25 µl. The PCR master mix was aliquoted in 25 µl aliquots and to each tube, 1 µl of each genomic DNA pre diluted 1:20 Milli-Q water was added.

For ApoE, three primers were used to genotype mouse tail DNA from the tail clippings obtained. These were: ApoE 180 (5' GCCTAGCCGAGGGAGAGCCG 3') as the FP, ApoE 181 (5' TGTGACTTGGGAGCTCTGCAG 3') as the RP and ApoE 182 (5' GCC GCC CCG ACT GCA TCT 3') also as the reverse primer. When the WT allele is present, the ApoE 180 and 181 primer pair yields a 155 bp product and when the KO allele is present, the ApoE 180 and 182 primer pair yields a 245 bp product.

The ApoE master mix was prepared with 1x PCR Taq Gold Buffer (Perkin Elmer, Boston, MA), 2 mM $MgCl_2$ (Perkin Elmer, Boston, MA), 0.2 mM dNTPs (Progen Industries Ltd., Richlands BC, Qld), 0.5 µM each ApoE forward and reverse primers, 0.3 U/µl Taq Gold DNA polymerase (Perkin Elmer, Boston, MA), and was made up to a final volume of 10 µl. The PCR master mix was aliquoted in 10 µl aliquots and to each tube, 2 µl of each genomic DNA was added.

The DNA amplification process for both ApoE and CD151 PCR products were treated similarly. DNA amplification was performed under these cycling conditions on a C1000 Touch™ Thermal Cycler (Bio-rad Laboratories, Budapest, Hungary), as follows. The starting temperature was set to 94 °C for 15 min followed by 35 cycles of denaturation at 94 °C for 1 min, annealing was set at 55 °C for 1 min and extension at 72 °C for 30 sec.

2.1.1.3 GAPDH PCR control

Glyceraldehyde 3-phosphate dehydrogenase (GAPDH) is commonly used as a control in PCR to determine the integrity of genomic DNA. GAPDH is not only a crucial enzyme involved in glycolysis but is also known to be a housekeeping gene as its expression is inherent and required for cell survival.(198)

The two primers used to confirm the presence and integrity of genomic DNA from the tail clippings obtained were: GAPDH 5'TCACCACCATGGAGAAGGC as the FP and GAPDH 5' GCTTAAGCAGTTGGTGGTGCA as the RP. Where DNA is present, the primer pair yields a 200 bp product.

The GAPDH master mix was prepared with 1x PCR Taq Gold Buffer (Perkin Elmer, Boston, MA), 1.0 mM $MgCl_2$ (Perkin Elmer, Boston, MA), 0.1 mM dNTPs (Progen Industries Ltd., Richlands BC, Qld), 0.4 µM each of GAPDH forward and reverse primers (Sigma Aldrich, St. Louis, MO), 0.06 U/µl Taq Gold DNA polymerase (Perkin Elmer, Boston, MA), and was made up to a final volume of 10 µl with milli-Q water. The PCR master mix was aliquoted in 10 µl aliquots and to each tube, 1 µl of each genomic DNA was added. The DNA amplification process was performed as per ApoE and CD151 PCR products with a C1000 Touch™ Thermal Cycler (Bio-rad Laboratories, Budapest, Hungary) at a starting temperature of 94 °C for 15 min followed by 35 cycles of denaturation at 94 °C for 1 min. Annealing was set at 55 °C for 1 min and extension at 72 °C for 30 sec.

2.1.1.4 Agarose gel electrophoresis

Electrophoresis of PCR products was performed using a 2% (w/v) agarose Tris-Acetic Acid-EDTA (TAE) gel, pH 8.5. The gel solution was prepared with 1x Gel Red Nucleic Acid stain (Invitrogen, Camarillo, CA). Once the gel had set, it was submerged in 1x TAE buffer pH 8.5. Prepared PCR products were mixed with DNA loading buffer (Geneworks, Thebarton, South Australia) in a 7 µl to 3 µl ratio. In the first well on the gel (from left), 4 µl of 2 log ladder NEB marker was loaded as a DNA marker standard. On each gel, known $CD151^{+/-}$ or $ApoE^{+/-}$ heterozygous, $CD151^{-/-}$ or $ApoE^{-/-}$ homozygous, WT DNA were loaded as controls. A milli-Q water lane was also loaded as a blank and non-DNA control for contamination. Electrophoresis was carried out at 120V and run until the dye migrated approximately three quarters down the

gel. The Gel Red Nucleic Acid stain when bound to DNA, will fluoresce at an excitation maximum of 280 nm and 502 nm and at an emission maximum of 530 nm. The Biorad Molecular Imager Gel Doc™ XR+ system was used to visualise DNA and Infinity Capture Software Version 12.6 for Windows to capture and print the PCR images.

2.1.2 Body weights

The body weights of ApoE$^{-/-}$ and ApoE$^{-/-}$:CD151$^{-/-}$ mice were documented from 5 weeks of age to 16 weeks of age. Body weights were measured with scales in the RMIT Animal Facility. At 16 weeks, mice were issued for experiments.

2.1.3 Body mass index

Body Mass Index (BMI) of ApoE$^{-/-}$ and ApoE$^{-/-}$.CD151$^{-/-}$ mice were calculated at 16 weeks on the day of experimentation. BMI is reported as an arbitrary unit (AU) and is measured by the formula: weight of mouse (g) / length from mouse nose to anus $(mm)^2$. BMI is a gross measurement of weight adjusted for height in humans or in our study, for the body length of mice. This measurement is incapable of differentiating between over weightedness due to lean or fat mass, and is used in the human population to provide a quick measurement for the assessment of obesity.

2.1.4 Full blood examination

ApoE$^{-/-}$ and ApoE$^{-/-}$.CD151$^{-/-}$ mice at 16 weeks were anaesthesised by inhalation with 2% (v/v) isoflurane (vaporised) with 3 litres/min oxygen. An Isotec 3 machine was used to carry out the anaesthesia. Blood for full blood examination (FBE) was drawn via cardiac puncture with a 1 ml syringe and a 26 gauge needle. Whole blood was transferred from the syringe into a potassium ethylene-diaminetetraacetic acid (EDTA) 1.3 ml capacity microtube (Sarstedt, Nümbrecht, Germany). After cardiac puncture, mice were sacrificed via cervical dislocation. A Cell Dyn Emerald analyser was used to run the blood samples for acquiring full blood examination parameters. At all times, Cell Dyn controls (high, normal and low ranges) were run to ensure the analyser was performing optimally and recording true results. Note, the mice had free access to food (Section 2.1) and water with no restrictions.

2.1.5 Non-fasting blood glucose

Random blood glucose (mmol/L) was measured from mouse whole blood. A drop of blood drawn from each ApoE$^{-/-}$ and ApoE$^{-/-}$.CD151$^{-/-}$ mice (Section 2.1.4) was reserved for non-fasting blood glucose testing with an Accu-Chek® Advantage meter and Accu-Chek® Comfort Care test strips (Roche Diagnostics, Indianapolis, IN). Results are verified by control tests carried out with the use of Accu-Chek® comfort curve control solutions.

2.1.6 Lipid profiling

Blood samples for random non-fasting/no diet controlled lipid profiles were collected from the same syringe of blood drawn via cardiac puncture for FBE, as described in section 2.1.4. However, instead of transferring all the blood drawn into a paediatric EDTA tube, approximately 100 µl of blood for lipid profiling was transferred into a lithium heparin 1.3 ml capacity microtube (Sarstedt, Nümbrecht, Germany). Lithium heparin was used as an anticoagulant as it is known to have minimal interference in water shifts, chelation and has low concentrations of cations.(199) Plasma samples were obtained by centrifugation of the whole blood samples for 10 minutes at 1960 xg without brake in a Beckman Coulter Allegra X-12R centrifuge. The plasma samples were then transferred to eppendorf tubes and stored in a - 80 °C freezer for batch analysis. A Dimension XL (Dade Behring, Deerfield, Illinois) biochemistry analyser was used to obtain the lipid profiles. To ensure the accuracy of results, controls and calibrators specific for the Dimension XL analyser were run and made sure to be within the expected control result ranges. All controls and calibrators used were produced and purchased from Dade Behring (Dade Behring Inc, Deerfield, Illinois).

2.1.7 Organ weights and lengths

ApoE$^{-/-}$ and ApoE$^{-/-}$:CD151$^{-/-}$ mice were anaesthesised by inhalation with 2% (v/v) isoflurane (vaporised), 3 litres/min oxygen with an Isotec 3 machine. After cervical dislocation, a dissection was made to expose the heart and other internal organs. A 1 ml syringe with a 25 gauge needle of phosphate buffered saline (PBS) pH 7.4 (8 g NaCl, 0.2 g, KCl, 1.44 g Na_2HPO_4, 0.24 g KH_2PO_4, bring to 1 L milli-Q water, pH adjusted to pH 7.4 with concentrated HCl) was infused into the left ventricle. PBS pH 7.4 was flushed through the heart gently to remove blood cells from the heart and aorta. The heart was removed with the aortic arch intact. Where possible, the arch of the aorta down to the ascending aorta was also kept intact and removed together. Fat and irrelevant tissues attached to the aorta were

trimmed off carefully under a Prism Optical microscope (Scitech, Preston, Victoria). The brachiocephalic, left common carotid and left subclavian arteries on the aortic arch were also kept intact and fat trimmed around these areas. The heart and attached aorta was measured for length with a ruler and weighed. Following this the heart and aorta was immediately fixed in 10% (v/v) buffered formalin (disodium hydrogen orthophosphate 203.7g, sodium dihydrogen orthophosphate 88.5 g, formaldehyde 2.5L and Milli-Q H_2O 22.5L) at room temperature for 48 hours. The kidneys, lungs and liver were also collected, measured for length and weight and subsequently fixed in 10% (v/v) buffered formalin as above.

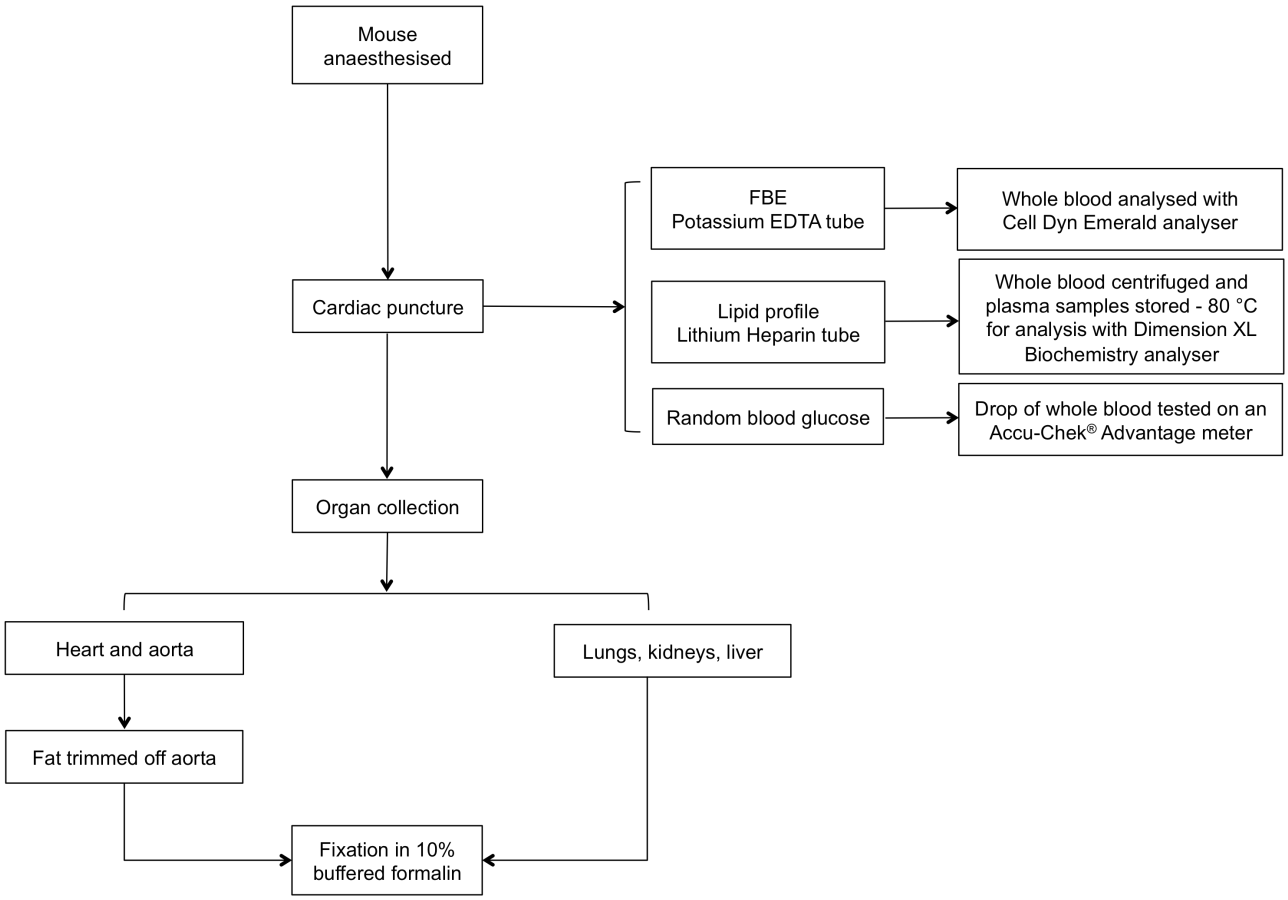

Figure 2.1. Outline of blood collection for FBE, random blood glucose, lipid profiling and collection of organs, beginning from time of anaesthesia.

2.1.8 Tissue sectioning and staining

The heart, kidneys, lungs and liver were collected from ApoE$^{-/-}$ and ApoE$^{-/-}$. CD151$^{-/-}$ mice as described in Section 2.1.7. The organs were maintained in 10% (v/v) buffered formalin solution for 48 hours for adequate fixation. The heart of each mouse was cut transversely caudal to the atria after fixation as shown below (Figure 2.2). This image also illustrates the area of the heart, which was sectioned and studied.

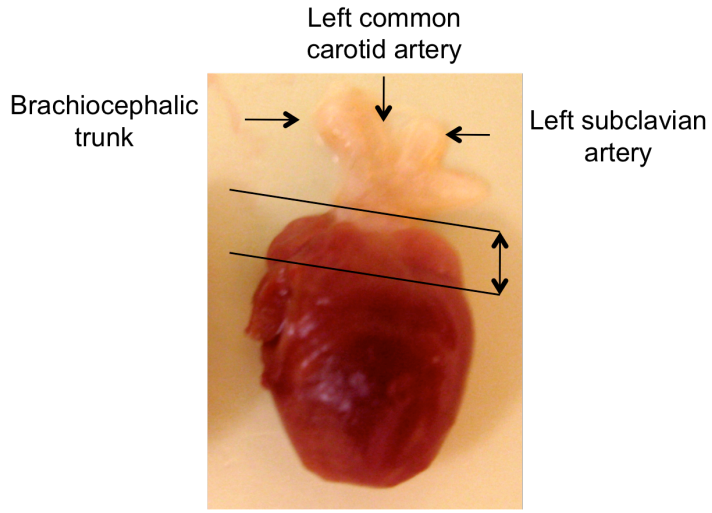

Figure 2.2. Representative image of a heart and aorta isolated from ApoE$^{-/-}$ and ApoE$^{-/-}$.CD151$^{-/-}$ mice. The image shows fat and surrounding tissues have been removed and trimmed from the aorta. The area between the two lines illustrates the area in which atherosclerotic lesions were examined.

After isolating this area, the hearts were placed in individual cassettes. Other organ tissues such as the liver, kidneys and lungs were also trimmed of fat if necessary and cut into small sections for tissue processing. These organs were placed in individually labelled cassettes as well. Each individual cassette was labelled with the animal ID and date of collection of organs. Tissue processing was performed using a Leica ASP200 S (Leica Biosystems, Wetzlar, Germany) fully enclosed tissue processor. A pre-programmed rodent schedule for processing was used. This runs in six hour schedules or can be prolonged to an overnight schedule. The tissues were sectioned beginning from the transverse cut in 5 µm serial sections with a Leica MM2235 microtome (Leica biosystems, Wetzlar, Germany) and stained with Haematoxylin and eosin, Verhoeff's Van Gieson to identify elastic fibres and Masson's trichrome for the identification of collagen and differentiating it from smooth muscle. These sections were sectioned onto uncoated glass slides. Sections were also made on Superfrost® plus positively charged microscope slides (Thermo Fisher Scientific Inc.,

Waltham, MA) for immunohistochemistry (IHC) type 1 collagen, smooth muscle actin, macrophage F4/80 and CD151 H80 staining.

2.1.8.1 Haematoxylin and eosin

All organs collected and processed were stained for H & E. Tissue sections were dewaxed and hydrated through xylene, graded alcohols and tap water. Nuclear staining was performed in Mayer's haematoxylin [haematoxylin (1.0 g), sodium iodate (0.2 g), potassium aluminium sulphate (50.0 g), choral hydrate (50.0 g), citric acid (1.0 g), distilled water (1 l)] for approximately 2.5 min then rinsed in tap water briefly, followed by several dips in Scott's tap water [potassium bicarbonate (2.0 g), magnesium sulphate (20.0 g), distilled water (1 l)], then rinsed in tap water thoroughly for approximately 2 min. Tissue sections were examined at this stage to ensure sharp staining of the nuclei. Where a stronger stain was required, the steps beginning from staining with the Mayer's haematoxylin was repeated. The subsequent steps involved counterstaining with 1% (w/v) aqueous eosin [eosin Y (10.0 g), acetic acid (1 ml/g), distilled water (1 litre)] for 2 min followed by a brief rinse in tap water. Finally the tissues were dehydrated through increasing concentrations of alcohol culminating with xylene, mounted with DPX [Lustrex (80 mg), xylol (280 ml) and dibutyl phosphate (40 ml)] and coverslipped.

2.1.8.2 Masson's trichrome for collagen

For Masson's trichrome staining the Hall's modification was used.(200) This method has been shown to be reliable for formalin fixed paraffin tissues and requires an essential step involving a mordanting step with Bouin's solution that has been brought to 60°C. Only aortic cusp sections were examined with Masson's trichrome staining for both $ApoE^{-/-}$ and $ApoE^{-/-}$. $CD151^{-/-}$ mice. Tissue sections were dewaxed and hydrated through xylene, graded alcohols and tap water. Tissues were then treated in Bouin's fixative solution for 30 min at 60°C, followed by a brief rinse in water and stained with Weigert's iron haematoxylin for 10 min [haematoxylin (5.0 g), absolute ethanol (500 ml), ferric chloride (30% (w/v) aqueous) (20 ml), distilled water (500 ml), concentrated hydrochloric acid (5 ml)]. A brief rinse in water was followed with differentiation of nuclei in 0.5% (v/v) acid alcohol (0.5 ml of hydrochloric acid in 100 ml of 70% ethanol) and a 1 min wash in water. Staining with 1% (w/v) brilliant crocein in 1% (v/v) phosphotungstic acid was done for 10 min, rinsed with 1% (v/v) phosphotungstic

acid then stained in 0.5% (w/v) aniline blue in 1% (v/v) acetic acid for 10 min. A last wash in 1% (v/v) acetic acid for 1 min was performed then finally tissues were dehydrated in alcohol, xylene, mounted with DPX [Lustrex (80 mg), xylol (280 ml) and dibutyl phosphate (40 ml)] and coverslipped.

2.1.8.3 Verhoeff's Van Gieson for elastic fibers

Only aortic cusp sections were examined with Verhoeff's Van Gieson staining for both $ApoE^{-/-}$ and $ApoE^{-/-}$. $CD151^{-/-}$ mice. Tissue sections were dewaxed and hydrated similar to other staining methods mentioned above. Tissues were stained with a solution composed of 5% (w/v) alcoholic haematoxylin (20 ml), 10% (w/v) aqueous ferric chloride (8 ml) and Lugol's iodine solution (7 ml) for 15 min. This solution was freshly prepared for each staining batch. Tissues were then briefly rinsed in water with excess water wiped from the slide gently with a tissue. Sections were differentiated in 2% (w/v) aqueous ferric chloride for a few seconds. The reaction was stopped by rinsing briefly in tap water then 3 – 4 quick dips in 95% (v/v) ethanol and rinsed in water again. Counterstaining was carried out with Van Gieson's stain [picric acid saturated aqueous (93 ml), acid fuchsin (7 ml)] for 5 min where sections were then blotted with Grade 1 Whatman paper (GE Healthcare Life Sciences, Buckinghamshire, England). Tissues were dehydrated in alcohol, xylene, mounted with DPX [Lustrex (80 mg), xylol (280 ml) and dibutyl phosphate (40 ml)] and coverslipped.

2.1.8.4 Immunohistochemical staining: anti type I collagen

Immunohistochemical (IHC) staining was performed with a Dako autostainer plus automated system. Sections were stained with anti type I collagen polyclonal rabbit antibody (Rockland Immunochemicals Inc, Gilbertsville, PA). Firstly, tissues underwent antigen retrieval in a 97°C tank for 10 min in DAKO flex low pH 6 retrieval solution (Agilent Technologies, Glostrup, Denmark). This solution also deparaffinises the paraffin fixed section. The slides were moved to the DAKO autostainer plus where they were rinsed with 0.05 M Tris-HCL 0.05% (v/v) Tween 20 [10 x Tris HCL Tween 20, 0.5M Tris base, 0.5% (v/v) Tween 20, pH 7.6. Trizma base (61 g), distilled water (1 l), adjusted to pH 7.6 with concentrated HCl] (Tris-HCL wash buffer) and incubated for 30 min in 1% (v/v) triton X solution to permeabilise the tissues. Slides were washed again with Tris-HCL wash buffer followed by a blocking step for background and unspecific staining with a peroxidase blocking solution [30% (v/v) H_2O_2 (10 ml), 1X PBS (90 ml)] for 10 mins followed by another washing step. This was followed by a 0.4 % (w/v) casein protein block (Tris-HCL Wash buffer (100 ml), skim milk powder (4 g)] for 30 mins, a wash step to remove the protein block, and incubation with the primary antibody

for 30 mins being the anti type I collagen rabbit polyclonal antibody at a 1/200 dilution to reveal the presence of collagen in the aortic valve cusp. After rinsing with Tris-HCL wash buffer the sections were stained for 30 min with a secondary peroxidase conjugated affini-pure goat anti rabbit antibody at a dilution of 1/800 (Jackson ImmunoResearch Laboratories Inc., Westgrove, PA). The tissues were washed again with Tris-HCL wash buffer and incubated for 5 min with 3,3' diaminobenzidine (DAB substrate) solution. After the final rinse with Tris-HCL wash buffer, slides were counterstained in Mayer's haematoxylin as detailed in section 2.1.8.1, mounted with DPX and coverslipped.

2.1.8.5 Immunohistochemical staining: smooth muscle cell actin

IHC staining of the aortic valve cusp of ApoE$^{-/-}$ and ApoE$^{-/-}$.CD151$^{-/-}$ mice was performed to the same protocol as for anti type I collagen. Note, to stain specifically for smooth muscle cell actin (SMC α), an anti-alpha Smooth muscle actin rabbit polyclonal antibody (Abcam, Cambridge, UK) was used as the primary antibody at a dilution of 1/200 and with a peroxidase conjugated affini-pure goat anti-rabbit antibody at a dilution of 1/800 (Jackson ImmunoResearch Laboratories Inc., Westgrove, PA).

2.1.8.6 Immunohistochemical staining: CD151 H80

Likewise to the above IHC methods, the staining protocol was similar with the exception of antibodies used. In this case, a CD151 H80 rabbit polyclonal antibody (Santa Cruz Biotechnology Inc., Dallas, Texas) was used at a dilution of 1/800. A peroxidase conjugated affini-pure goat anti rabbit secondary antibody was also used at a dilution of 1/800 (Jackson Immunoresearch laboratories, PA, USA).

2.1.8.7 F4/80 pan macrophage marker (MAC)

Pan macrophage staining in the aortic valve cusps of ApoE$^{-/-}$ and ApoE$^{-/-}$. CD151$^{-/-}$ mice was performed to the same protocol as above. For this specific staining, an anti-mouse F4/80 Antigen PE antibody (Ebioscience, San Diego, CA) was used at a dilution of 1/400 and for the secondary antibody, a peroxidase goat anti-rat IgG secondary at a dilution of 1/2000 (Invitrogen, Camarillo, CA).

2.1.9 Quantification of plaque burden

Haematoxylin and Eosin stained sections were examined for plaque burden and presence in the aortic valve cusps of ApoE$^{-/-}$ and ApoE$^{-/-}$. CD151$^{-/-}$ mice. This was measured consistently at the level in which the aortic valve leaflets were visible. Sections were imaged using a Leica DMD108 microscope (Leica Microsystems, Wetzlar, Germany) with a 4x and 10x objective and camera. The Leica imaging system was used to digitally measure the aortic area, which is expressed as the aortic cross sectional area. The percentage of the aortic valve cusp area that shows evidence of plaque formation was calculated by also using the Leica DMD 108 imaging system program function to outline the plaque and dividing the plaque area by the aortic valve cusp area (Figure 2.3). Measurements were performed in a blinded mode with mice specimens labeled independently and decoded on conclusion of analysis.

2.1.10 Quantification of positive staining in IHC

Quantification of positive staining for Immunohistochemical stains was determined by a positive pixel count algorithm v9.1 (Aperio Technologies Inc, CA, USA). Slides were firstly scanned with an Olympus BX 41 microscope with a 4x and 10 x objective and an Olympus DP70 camera (Olympus Optical Co. Ltd, Tokyo, Japan). Digital Image files were opened in the Image Scope (Aperio Technologies Inc, CA, USA) program then analysed with the algorithm. The algorithm quantifies the amount of a specific stain found present on the scanned image by counting the number and intensity sum and categorises the intensities into weak, positive and strong intensity range. Negatively stained pixels which did not fall within the positive intensity ranges were also counted to allow for quantification of positive stained pixels in proportion to total stained pixels on the scanned image. Staining was quantified on only the areas which were occupied by a plaque by selecting the plaque areas with the measurement and selection tool.

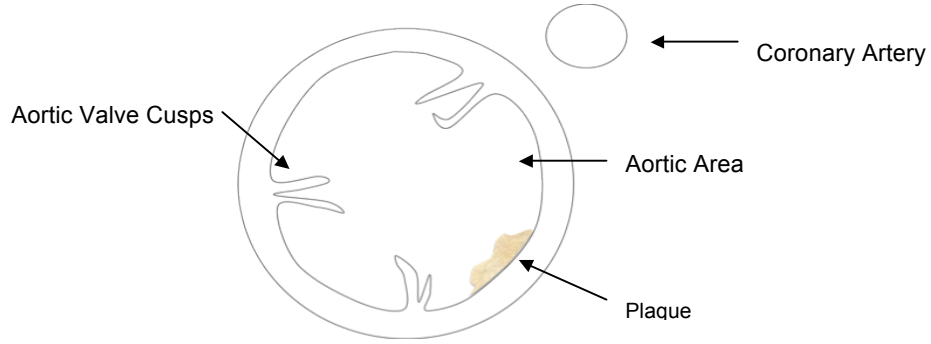

Figure 2.3 Schema of a cross section of an aorta at the level in which the aortic valve cusps are visible and coronary artery is in view. This area was selected for plaque burden measurements with H & E staining, as well as examination of plaque burden via immunohistochemical staining.

2.1.11 Intraperitoneal anaesthesia administration for dissection experiments

The anesthesia is administered interperitoneally with a 26 gauge needle, with a combination of Ketamine (200 mg/kg 20:1 w/v) (Ketalar, Pfizer, New Zealand) and Xylazil (10 mg/kg 1:1 w/v) (Ilium, Xylazil 1001: Troy Laboratories Pty Ltd, Smithfield, NSW). A pedal reflex test is performed by pinching the front and hind paws gently with forceps to determine if the mouse is anesthesised sufficiently. If the mouse does not withdraw its paw or respond by flinching, dissection of the mouse can begin.

2.1.12 Ferric chloride ($FeCl_3$) induced carotid artery injury

Ferric Chloride ($FeCl_3$) induced carotid artery injury experiments were performed on $ApoE^{-/-}$ and $ApoE^{-/-}$. $CD151^{-/-}$ mice of 4 to 6 weeks in age. Experiments were done in pairs where one strain, for instance an $ApoE^{-/-}$ mouse would be anesthesised and subjected to experimentation, then culled prior to beginning another experiment with an $ApoE^{-/-}.CD151^{-/-}$ mouse. The order in which mice were experimented on was randomised.

Once the mouse is sufficiently anesthesised as per Section 2.1.11, a straight line cut incision is made along the throat with a pair of scissors, followed by a blunt dissection made to expose the trachea. Connective tissue is removed gently to avoid damage to the surrounding jugular vein and vagus nerve whilst locating the artery. The carotid artery is found approximately 2 mm laterally and posterior to the trachea. Once isolated, a piece of suture thread is placed under the artery and another on the furthest end of the exposed carotid artery to support and elevate it throughout the experiment.

A Moor instruments laser doppler perfusion monitor and probe (Moor Instruments, UK) is used to monitor the blood flow in the carotid artery. The Doppler flow probe is placed gently near the artery with the red laser visible and aimed on the middle of the artery. A baseline reading of 1000 AU on the monitor indicates that 100% blood flow rate is present. Blood flow is recorded beginning at 1000 AU. A standardised 4 mm x 1 mm strip of Whatman filter paper (Grade 1, Whatman) infused in 20% (w/v) $FeCl_3$ (Sigma Aldrich, St. Louis, MO) for 3 seconds is placed carefully on the carotid artery without disrupting the laser placement for 4 minutes to induce $FeCl_3$ injury then removed. The carotid artery was then washed with saline gently to remove any residual $FeCl_3$. Blood flow recording is continuous throughout this time

and is stopped after the monitor displays a reading of below 50 AU which is equivalent or greater than 95 % vessel occlusion. The blood flow trace is saved for later analysis. To conclude the procedure, the mouse is sacrificed via cervical dislocation. The time to occlusion is determined by measuring the time from removal of the $FeCl_3$ filter paper to when only 5% or less blood flow remained.

2.1.13 Cardiac puncture blood collection

$ApoE^{-/-}$ and $ApoE^{-/-}.CD151^{-/-}$ mice were subject to anaesthesia by inhalation of 2% (v/v) isoflurane (vaporised) with 3 litres/min oxygen (BOC gases, Preston, Victoria). An Isotec 3 machine was used to carry out the anaesthesia. Blood for *in vitro* collagen adhesion and platelet aggregation experiments were drawn via cardiac puncture with a 1 ml syringe and a 26 gauge needle. Whole blood was transferred from the syringe into a tube containing 100 µl 3.2 % (w/v) trisodium citrate and mixed by inverting gently.

2.1.14 *In vitro* flow shear rate

An Ibidi three channel µ-slide III (0.1 × 1.0 × 45 mm, IBIDI, Martinsried, Germany) flow chamber was coated with 500 µg/mL type 1 fibrillar chrono-par collagen (Nycomed, Konstanz, Germany) and incubated at 37 °C for 60 min. Whole blood samples were collected from $ApoE^{-/-}$ and $ApoE^{-/-}.CD151^{-/-}$ mice through cardiac puncture as per Section 2.1.13. Platelet counts were obtainined by diluting whole blood 1:10 in Ringers citrate buffer (RCD) pH 6.5 (108 mM NaCl, 38 mM KCl, 1.7 mM $NaHCO_3$, 21.2 mM sodium citrate, 27.8 mM glucose and 1.1 mM $MgCl_2 \cdot 6\,H2O$, pH adjusted to pH 6.5), then normalise platelet counts across both strains to 100 x 10^9L in RCD pH 7.4 (108 mM NaCl, 38 mM KCl, 1.7 mM $NaHCO_3$, 21.2 mM sodium citrate, 27.8 mM glucose and 1.1 mM $MgCl_2 \cdot 6\,H2O$, with pH adjusted to 7.4). The blood was then incubated with 0.05% (w/v) rhodamine (Sigma Aldrich, St. Louis, MO) at 37 °C for 30 min away from direct light. A Harvard Apparatus PHD 2200 standard syringe pump (Harvard Apparatus, Boston, MA) was used to induce a wall shear rate of 1800^{-1} seconds, at an infusion rate of 168.65 on the device. Only one microslide was coated and examined at a time. The microslide was examined with a Zeiss Axiovert 135 microscope (Zeiss, Oberkochen, Germany), Zeiss Axiocam Mrm camera and corresponding analysis and recording program, Axiovision Rel version 4.6 software. Real-time images were captured in 1 min cycles for 6 cycles at the time of perfusion. Thrombus area, thrombus height and thrombus volume were determined using Z-stack analysis image obtained through the deconvolution process in the Axiovision Rel version 4.6 software.

2.1.15 Ferric chloride-induced vascular injury and intravital microscopy (IVM)

$ApoE^{-/-}$ and $ApoE^{-/-}.CD151^{-/-}$ mice were anesthesised as per section 2.1.11. Once sufficiently anesthesised a dissection was made to either right or left side of the mouse neck to locate the jugular vein and insert a cannula (0.61 mm x 0.28 mm, Microtube extrusions, Sydney, NSW). Two silk suture threads (Fine Science Tools, BC, Canada) were placed under the jugular vein to raise and support the vein and cannula. This allowed for direct infusion of 0.05 % (w/v) rhodamine dye as well as anaesthetic into the mouse circulatory system. The mesentery was then located and exposed by creating a midline abdominal incision. The internal organs were undisturbed and intestines untangled on the microscope board to expose the arterioles. Mesenteric arterioles of 80-100 µm diameter were identified under the microscope with a 20 x objective under bright field light settings. Once isolated, the arteriole was subjected to 7.5 % (w/v) $FeCl_3$-induced injury by soaking a 1 mm x 4 mm strip of Whatman filter paper for 3 seconds in the $FeCl_3$ solution and gently placing this strip on the arteriole for 4 minutes. Rhodamine dye was infused into the animal through the cannula inserted into the jugular vein. From bright field light the microscope settings were changed to a rhodamine channel to view platelets fluorescing in the artery on the monitor. Images were recorded on an Axiovision Rel version 4.6 software using a Zeiss Axiovert 135 microscope (Zeiss, Oberkochen, Germany) and Zeiss Axiocam Mrm camera. The Axiovision software recorded z-stack real time images through time lapse analysis over 5 cycles for 2 minutes each for analysis of thrombus formation upon $FeCl_3$ induced injury. This was performed for each arteriole isolated. Anesthesia was infused into the animals circulatory system through the cannula inserted into the jugular vein to ensure the mouse is adequately anesthesised throughout the experiment. Pedal reflex checks were performed on the mouse's paws to ensure the mouse is anaesthesised sufficiently. At the conclusion of the procedure, the mouse was sacrificed via cervical dislocation. Parameters including vessel length and diameter were documented whilst parameters such as thrombus area, thrombus height, thrombus volume, vessel volume, percentage of vessel occlusion and stability score were determined through the deconvolution process in the Axiovision Rel version 4.6 software.

2.1.16 Z-Stack analysis and acquiring parameters analysed from IVM images

Deconvolusion of rendered Z-stack images was performed using the Axiovision Rel version 4.6 software. This produced 3D images of the thrombus present. The thrombus was calculated from the front view above the vessel as well as the length of the vessel and its radius to obtain the volume of the vessel. Side profile views of the 3D image acquired was used to determine the height of the thrombus.

The thrombus height (μm) was calculated from the average of the highest and lowest point of the thrombus, while thrombus area (μm^2) was calculated by outlining the thrombus or thrombi recorded. The volume of the thrombus was calculated by multiplying the height and area together. The percentage of vessel occluded by thrombus was calculated by dividing the thrombus volume by the volume of the vessel (π x radius of vessel^2 x length of vessel) multiplied by 100. The stability score is an arbitrary unit of clot stability which is representative of the stability of thrombus growth over a given time. This was calculated by the average of the percentage of vessel that was occupied by the thrombus over 2 min (at time points 6 min and 8 min). The stability score is categorised according to the percentage of vessel occlusion as follows: 0-10 % = **1**, 11-20 % = **2**, 21-30 % = **3**, 31-40 % = **4**, 41-50 % = **5**, 51-60 % = **6**, 61-70 % = **7**, 71-80 % = **8**, 81-90 % = **9**, 91-100 % = **10**.

2.1.17 Platelet aggregation

ApoE$^{-/-}$ and ApoE$^{-/-}$.CD151$^{-/-}$ mice were subjected to the procedure as described in section 2.1.13 for the collection of whole blood through cardiac puncture. Following blood collection, the tubes were centrifuged in a Beckman Coulter Allegra X-12R centrifuge (Beckman Coulter, USA) at 190 xg for 10 min at room temperature without brake to obtain platelet rich plasma (PRP). After separation, the PRP layer was gently isolated into a new tube. Platelet counts were obtained by diluting 1:10 of the PRP in RCD Buffer pH 6.5 (108 mM NaCl, 38 mM KCl, 1.7 mM $NaHCO_3$, 21.2 mM sodium citrate, 27.8 mM glucose and 1.1 mM $MgCl_2 \cdot 6\,H2O$, pH adjusted to 6.5) and analysed with a Cell Dyn Emerald haematology analyser (Abbott Laboratories, Abbott Park, Illinois). The platelet count for both ApoE$^{-/-}$ and ApoE$^{-/-}$.CD151$^{-/-}$ mice was normalised to 100 x 10^9L in RCD Buffer pH 7.4 (108 mM NaCl, 38 mM KCl, 1.7 mM $NaHCO_3$, 21.2 mM sodium citrate, 27.8 mM glucose and 1.1 mM $MgCl_2 \cdot 6\,H2O$, with pH adjusted to 7.4). The remaining blood was centrifugated at 930 xg for 10 min room temperature, without brake to obtain platelet poor plasma (PPP) which will act

as a murine baseline for platelet aggregation testing. The PPP was diluted 1:2 in RCD pH 7.4.

A Chronolog 4-channel platelet aggregometer (Chrono-log Corp, Havertown, PA) was used for light transmission platelet aggregation. PRP aggregation was performed by aliquoting 250 µl of prepared PRP from each $ApoE^{-/-}$ and $ApoE^{-/-}.CD151^{-/-}$ mice into glass cuvettes, with a magnetic stirring flea in each for constant stirring at 1000 RPM. To each glass cuvette, 100 µg/ml of fibrinogen and 1 mM $CaCl_2$ was added and incubated for 5 minutes at 37°C in the aggregometer, appropriately labeled as $ApoE^{-/-}$ or $ApoE^{-/-}.CD151^{-/-}$ PRP. The baseline was set using the prepared PPP prior to stimulation with agonists for the initiation of platelet aggregation. For each agonist, a cuvette containing the prepared $ApoE^{-/-}$ PRP was analysed as trace 1 versus $ApoE^{-/-}.CD151^{-/-}$ PRP as trace 2. The following agonists were used independently for stimulation of platelets in sequential tests: lyophilised ADP (5 µM and 10 µM; Chrono-Log Corp, Havertown, PA), protease-activated receptor 4 (PAR-4) (200 µM and 300 µM; H-Ala-Tyr-Pro-Gly-Lys-Phe-NH_2 (AYPGKF-NH_2; GL Chemicals, China), type 1 fibrillar collagen (3.75 µg/ml and 7.50 µg/ml; Chrono-Log Corp, Havertown, PA), CRP (0.625 µg/ml and 1.25 µg/ml; CC Peptide Gly-Cys-Hyp-(Gly-Pro-Hyp)$_{10}$-Gly-Cys-Hyp-Gly-NH_2 (M_r: 3294), Cross linked with 1.5 M SPDP (3-(2-pyridyldithio)propionic acid N-hydroxysuccinimide ester; Sigma P3415). Platelet aggregation was monitored and recorded over a 10 minute period to obtain the maximal aggregation amplitude.

2.1.18 *In Vivo* tail bleeding assay

In vivo tail bleeding assays were conducted on $ApoE^{-/-}$ and $ApoE^{-/-}.CD151^{-/-}$ mice of age 6 – 8 weeks to examine haemostasis. The mice were subjected to anaesthesia via inhalation with 2% (v/v) isoflurane (vaporised) with 3 litres/min oxygen. An Isotec 3 machine was used to carry out the anaesthesia. A 2 mm diameter, by 1 cm section of tail tip was selected and excised with a scalpel blade. The volume of blood lost was measured by allowing blood droplets from the tail to fall into an eppendorf tube filled with 100 µl of 3.2 % (w/v) trisodium citrate, followed by a calculation subtracting the 100 µl of 3.2 % (w/v) trisodium citrate to obtain the final volume of blood lost. The bleeding time was measured from when blood first appeared at the tip of the tail to cessation of bleeding. If bleeding was found to restart within 1 minute, this was recorded as a rebleed and plotted as a percentage of the group tested which showed a positive rebleed result.

2.1.19 Results analysis

GraphPad Prism version 6.0 (GraphPad Software, Inc. La Jolla, CA) was used to perform all statistical analysis. All values are expressed as mean ± standard error of the mean (SEM). Haematological parameters, body weights, organ lengths and weights, and random blood glucose results, maximal platelet aggregation, time to 95% vessel occlusion, blood volume lost, time to cessation of bleeding, haemostasis instability, thrombus parameters, plaque lesion areas, % pixel positive staining were calculated as mean ± standard error of the mean (SEM) in $ApoE^{-/-}$ vs $ApoE^{-/-}.CD151^{-/-}$ groups. Mean ± SEM between $ApoE^{-/-}$ vs $ApoE^{-/-}.CD151^{-/-}$ groups were compared statistically using a students two tailed unpaired t-test. When comparing more than two groups, the ANOVA test was used.. Statistical significance was reported when the p value was < 0.05.

3 CHAPTER 3: DEVELOPMENT AND CHARACTERISATION OF THE ApoE$^{-/-}$.CD151$^{-/-}$ STRAIN

3.1 Introduction

The role of CD151 in atherosclerosis *in vivo* has to date not been examined. As such, ApoE$^{-/-}$.CD151$^{-/-}$ mice were generated by cross breeding CD151$^{-/-}$ mice with ApoE$^{-/-}$ mice. Being a novel mouse line, the development and characterisation of the ApoE$^{-/-}$.CD151$^{-/-}$ strain had not been reported previously.

The CD151 protein is linked to vascular morphogenesis, hemidesmosome formation, cancer metastasis, neurite outgrowth, cell migration, wound healing, immune responses, integrin trafficking and haemostasis.(4,6,102,119,175,197,201) CD151 is ubiquitous and present in endothelial cells, smooth muscle, megakaryocytes, cardiac muscle, immune system, epithelia and platelets.(5) In platelets, CD151 has been shown to have functional importance in the positive regulation of platelet function both *in vivo* and *in vitro*. Recent findings have determined the absence of platelet CD151 *in vivo* results in smaller and thrombi that are less stable and tend to embolise. Orlowski et al.(197) also identified platelet CD151 as a regulator of thrombus growth and stability *in vivo*.(197)

Little is known of the involvement of CD151 specifically in atherosclerosis and plaque stability in this diseased setting. Yang et al. (128) investigated CD151 protein expression and distribution of the tetraspanin in atherosclerotic tissues in humans. The authors reported a significantly increased level of CD151 protein expression in atherosclerotic arteries compared to normal healthy arteries through western blotting analysis.(128) Histological studies further suggested CD151 involvement in atherosclerosis development as atherosclerotic arteries stained more intensely for CD151 than healthy arteries.(128)

The mouse model of atherosclerosis was introduced in the mid 1980s. It has since seen many developments from using inbred mice to genetically engineered mice that are more widely accepted in atherosclerosis research for mimicking human disease.(202) Findings have shown the C57BL/6 WT mouse strain to have a genetic predisposition to atherosclerosis and thus used commonly for atherosclerosis studies. Genetically modified mice used in atherosclerosis studies are also often back crossed onto the C57BL/6 WT

strain. The ApoE$^{-/-}$ atherosclerosis model is capable of developing spontaneous and diet induced atherosclerotic lesions which resembles many of the features observed in humans. With this, the mouse model has gained in popularity and is the most used mammalian model for the study of atherosclerosis today.(203)

ApoE is understood to have multiple functions. Its role predominantly is in the regulation of lipoprotein metabolism and maintaining homeostasis of plasma cholesterols. ApoE has, since, its discovery in 1973 by Shore and Shore, been identified as a major component in plasma lipoproteins.(204) Low Density Lipoprotein Receptor (LDL-R) recognition sites are found in the amino terminal region of the ApoE protein where upon binding with lipids causes a conformational change in the amino terminus. The amino acids 165-169 forms a helix resulting in an increase in positive electrostatic potential and consequently rendering a higher binding affinity of ApoE with the LDL-R on parenchymal liver cells for the uptake and degradation of lipoproteins.(205-207) Secondary mechanisms of lipoprotein regulation and transport is also maintained through the attachment of ApoE to LDL related receptor proteins (LRP) and heparan sulphate proteoglycans (HSPG) for chylomicron clearance. Studies have also reported the activation of enzymes associated with lipoprotein metabolism, direct stimulation of triglyceride and hepatic Very Low Density Lipoprotein (VLDL) production and reverse cholesterol transport capabilities by ApoE. (188, 208-210) Its role in atherosclerosis is reported by numerous studies performed on humans and animals. In humans, decreased expression or absence of the ApoE glycoprotein is shown to be associated with atherosclerosis and a raised lipoprotein profile.(211,212) Schaefer et al. (211) and Ghiselli et al. (212) demonstrated that the condition Type III hyperlipoproteinaemia is associated with and manifests in individuals with homozygous familial ApoE deficiency. This condition is a rare autosomal recessive condition of which defect is suggested to be caused by the inability to synthesise ApoE and an accumulation of lipoprotein constituents in the LDL and VDL regions. In homozygotes, Schaefer et al. observed significantly elevated LDL and VLDL cholesterol whilst heterozygotes develop mild hyperlipidaemia. Menopause and aging is also proposed to have an influence on expression of hyperlipidaemia.

Similarly, animal studies of ApoE$^{-/-}$ mice report significantly raised cholesterol levels caused primarily by impaired clearance of low density lipoproteins in comparison to wild type mice.(213,214) Even on a low fat or chow diet, ApoE$^{-/-}$ mice develop complex atherosclerotic lesions as a consequence of lipoprotein accumulation.(213,215) The involvement of ApoE in atherosclerosis is further supported by its potential anti-atherogenic roles evidenced in studies reporting a reduction in atherosclerosis progression with the reconstitution of ApoE

through synthetic ApoE peptide injections and also via increasing the expression of ApoE genes in $ApoE^{-/-}$ mice.(216,217)

In humans, circulating lipoproteins in hypercholesterolaemic patients are suggested to influence platelet function and the abnormalities associated in atherosclerosis.(218,219) LDL, VLDL and oxidised LDL are atherogenic lipoproteins with which contain apolipoprotein B-100, and have been observed to increase platelet aggregation and activation in patients with raised cholesterol levels.(220,221) A similar situation is observed in mice where dyslipidaemia precedes atherosclerosis disease and the development of atherosclerotic lesions.(203)

Cross breeding the $ApoE^{-/-}$ (C57BL/6 WT background) proatherogenic mouse model with a $CD151^{-/-}$ mouse strain will give insight into the effects of the absence of CD151 (C57BL/6 WT background) in an atherosclerotic setting. Our observations will give an indication as to the involvement of cell surface contact receptors in the regulation of atherogenesis and atherothrombosis. Normal reference ranges on the haematological parameters and lipid profiles of $ApoE^{-/-}.CD151^{-/-}$ are not available. In addition, Mendelian ratios and development of the strain have not been documented. Whilst Whitman et al. (203) found $ApoE^{-/-}$ mice to breed efficiently and produce acceptable litter sizes, and $CD151^{-/-}$ mice to breed similarly, the Mendelian inheritance frequencies of $ApoE^{-/-}.CD151^{-/-}$ strain has not been studied.(203) It is not known whether any developmental problems, mortality or morbidity is affected. Given these lines of evidence, establishing mouse lipid and haematological parameters of this novel $ApoE^{-/-}.CD151^{-/-}$ mouse strain and developmental characteristics holds great value for investigating the hypothesis and presumed protective effect of knocking out the CD151 gene in an atherosclerosis setting.

3.2 Results

3.2.1 Development of the ApoE$^{-/-}$.CD151$^{-/-}$ strain

Previous studies have demonstrated that the tetraspanin family member, CD151 is important in modulating the function of platelet integrin $\alpha_{IIb}\beta_3$ and is also associated functionally and or physically with GPVI.(4,109) CD151 is thus required for the regulation of thrombus growth and stability and this has been supported by *in vivo* studies.(197,222) It is not known whether cell surface contact receptors such as CD151 play an important role in regulating atherogenesis and atherothrombosis. Therefore to investigate this, the proatherogenic ApoE$^{-/-}$ model was intercrossed with the CD151$^{-/-}$ mouse strain to examine if CD151 has any influence in atherosclerosis. As this was the first reported ApoE$^{-/-}$.CD151$^{-/-}$ generated, how the strain was developed from genotyping the strain, to the mendelian inheritance frequencies, measurement of haematological parameters, lipid profiling and body weights was investigated.

Heterozygote matings sired ApoE$^{-/-}$.CD151$^{+/-}$ and ApoE$^{-/-}$.CD151$^{-/-}$ offspring. The first ApoE$^{-/-}$.CD151$^{-/-}$ breeders generated through these crosses were two females (51 B and 120 D) and one male (110 E) (Figure 3.1).

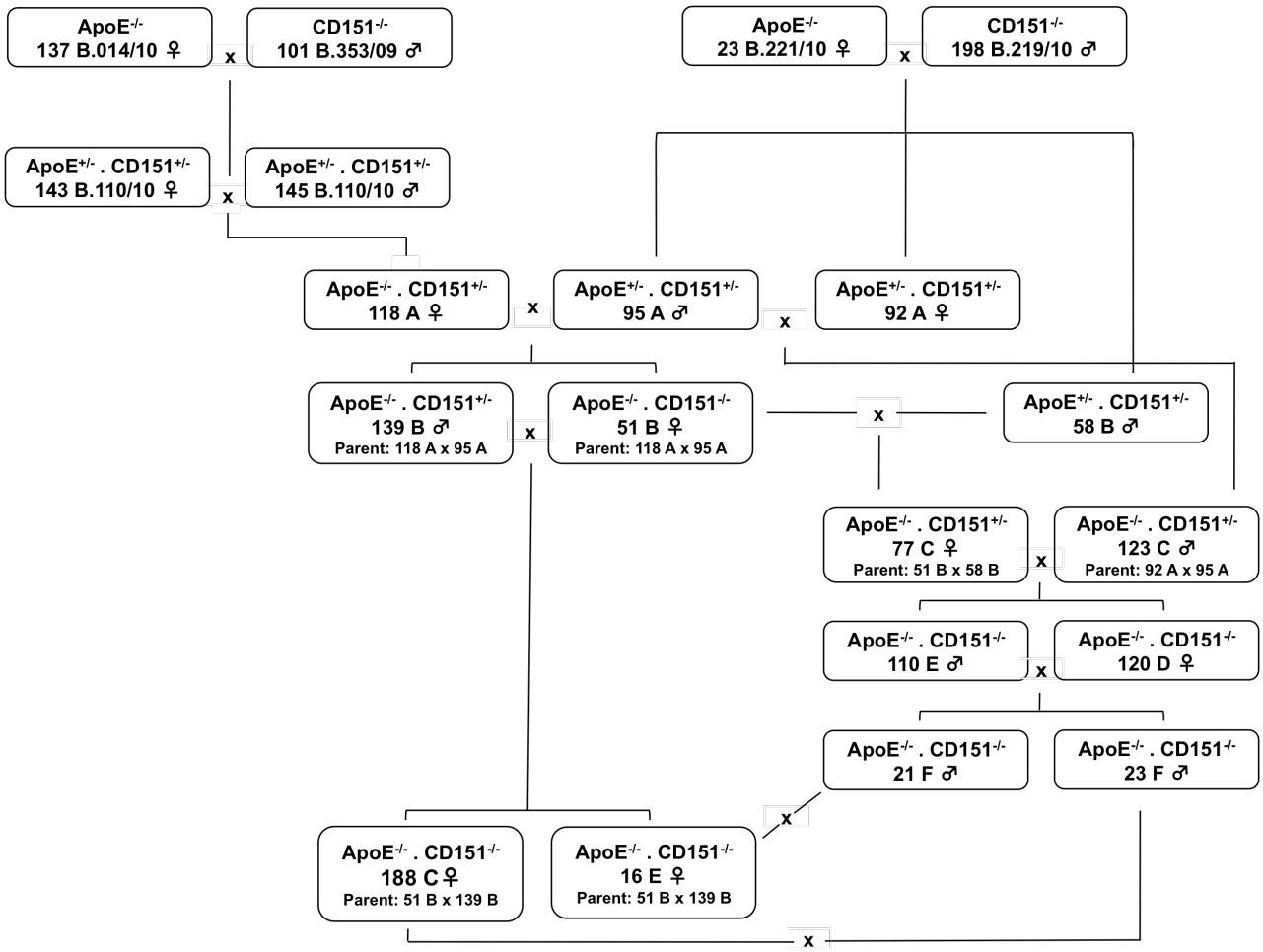

Figure 3.1. Development of the ApoE$^{-/-}$ and the ApoE$^{-/-}$.CD151$^{-/-}$ strain. ApoE$^{-/-}$ and CD151$^{-/-}$ mice were crossed producing litters of ApoE$^{+/-}$. CD151$^{+/-}$ mice. The first ApoE$^{-/-}$.CD151$^{-/-}$ breeders were obtained through the crossing of Mouse 118 A with 95 A to give 51 B (ApoE$^{-/-}$.CD151$^{-/-}$). Animals 77 C and 123 C were crossed producing another two ApoE$^{-/-}$.CD151$^{-/-}$, animal(s) 110 E and 120 D.

Genotyping of the ApoE$^{-/-}$.CD151$^{-/-}$ was carried out to confirm both ApoE and CD151 proteins had been knocked out. Glyceraldehyde-3-phosphate dehydrogenase (GAPDH) was used as a control to confirm the integrity of isolated genomic DNA. This was important to ensure that the relevant proteins were lacking in the mice. Visualisation of a 245 bp product on an ApoE PCR, in the absence of a 155 bp wild-type product confirms the ApoE protein has been knocked out. Figure 3.2 (a) demonstrates this with 188C and 16E being ApoE$^{-/-}$ mice. As CD151 wild-type and knockout allele yields a similar 400 bp product, two separate 2% (w/v) agarose gels were run with primers specific for the wild-type or CD151 knockout allele. Figure 3.2 (b) and (c) demonstrates that the CD151 gene has been knocked out in animals 188 C and 16E, which subsequently concludes that both these animals are ApoE$^{-/-}$.CD151$^{-/-}$ mice. A glyceraldehyde-3-phosphate dehydrogenase (GAPDH) PCR was run as an internal control to validate these results and the integrity of mouse genomic DNA where bands of 200 bp were produced and visible on the PCR.

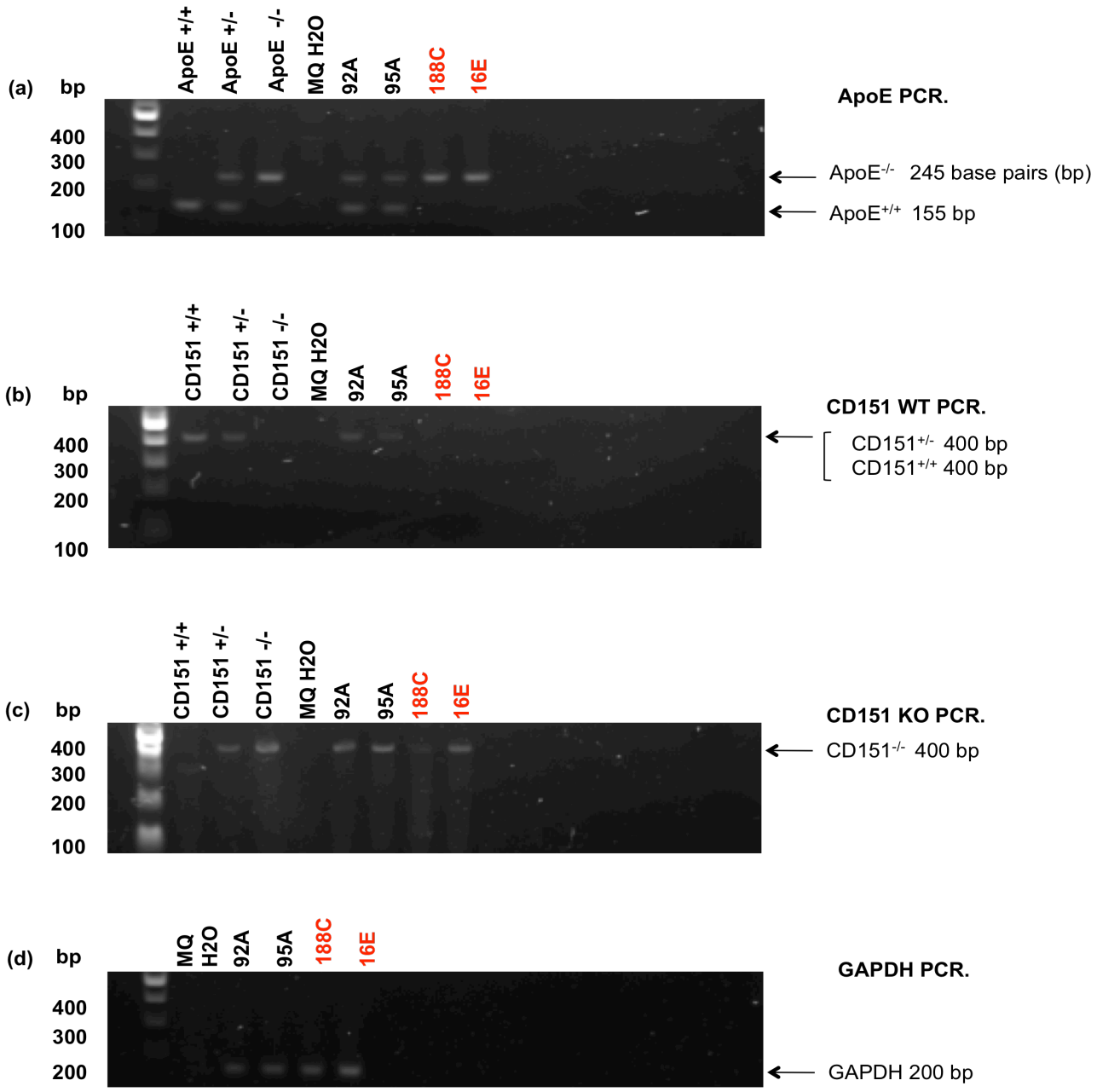

Figure 3.2. Representative PCR to determine the ApoE$^{-/-}$.CD151$^{-/-}$ mouse strain. Analytical gels showing amplified PCR products of mouse (a) ApoE$^{-/-}$ fragment (245 bp); (b) CD151$^{+/-}$ (400 bp); (c) CD151$^{-/-}$ (400 bp) and (d) GAPDH (200 bp) respectively. PCR products were electrophoresed on Gel Red nucleic acid stained 2% (w/v) agarose gel. (a) Lane 1: 2 NEB 2-log ladder marker, Lane 2: WT mouse DNA control, Lane 3: Heterozygous ApoE$^{+/-}$ DNA control, Lane 4: Homozygous ApoE$^{-/-}$ DNA control, Lane 5: Milli-Q H_2O control, Lanes 6-7: ApoE$^{+/+}$ offspring DNA, Lanes 8-9: ApoE$^{-/-}$. (b) Lane 1: 2 NEB 2-log ladder marker, Lane 2: WT mouse DNA control, Lane 3: Heterozygous ApoE$^{+/-}$ DNA control, Lane 4: Homozygous ApoE$^{-/-}$ DNA control, Lane 5: Milli-Q H_2O control, Lanes 6-7: ApoE$^{+/-}$ offspring DNA, Lanes 8-9: ApoE$^{-/-}$ offspring DNA. (b) Lane 1: 2 NEB 2-log ladder marker, Lane 2: WT mouse DNA control, Lane 3: Heterozygous CD151$^{+/-}$ DNA control, Lane 4:Homozygous ApoE$^{-/-}$ DNA control, Lane 5: Milli-Q H_2O control, Lanes 6-7: CD151$^{+/-}$ offspring DNA, Lanes 8-9: CD151$^{-/-}$ offspring DNA. (c) Lane 1: 2 NEB 2-log ladder marker, Lane 2: WT mouse DNA control, Lane 3: Heterozygous CD151$^{+/-}$ DNA control, Lane 4:Homozygous ApoE$^{-/-}$ DNA control, Lane 5: Milli-Q H_2O control, Lanes 6-9: CD151$^{+/-}$ offspring DNA. (d) Lane 1: 2 NEB 2-log ladder marker, Lane 2: Milli-Q H_2O control, Lanes 6-9: GAPDH gene of offspring DNA. (a)-(d) Animals 188C and 16E are ApoE$^{-/-}$.CD151$^{-/-}$ and is confirmed with the GAPDH PCR which acts as a housekeeping gene and an internal control for integrity of mouse genomic DNA. Bp, Base pairs.

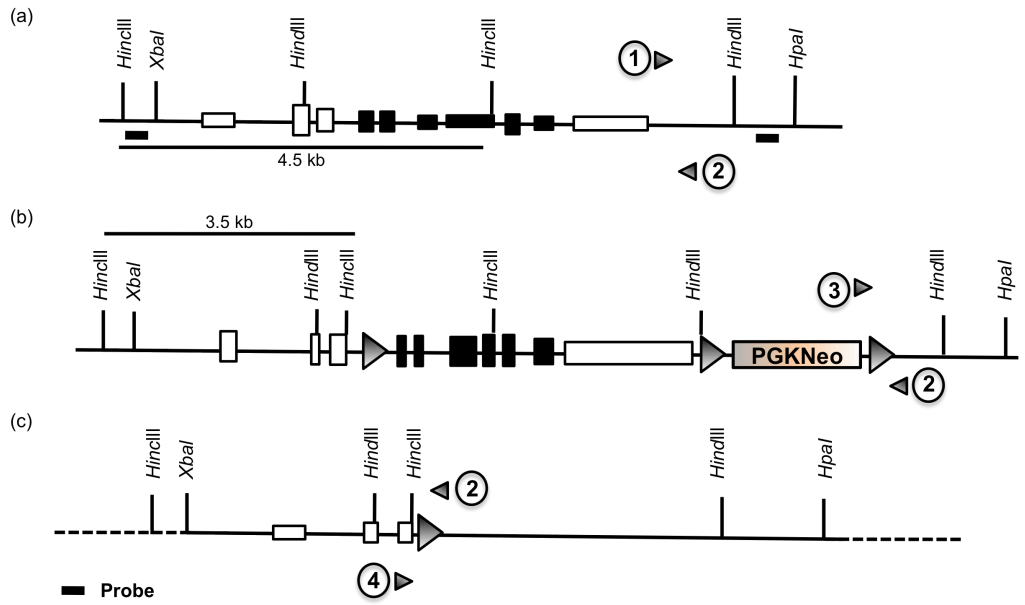

Figure 3.3. CD151 primer design. (a) Wild-type CD151 locus. (b) Restriction maps are shown for the targeting vector. (c) Mutated CD151 locus after Cre-mediated recombination. Coding exons are illustrated as shaded boxes, and noncoding exons are shown as open boxes. *loxP* sites are indicated by triangles. Primer 1, 3 and 4 are all forward primers. These forward primers complemented the common reverse primer shown as primer 2 in the figure above to distinguish between wild-type, targeted or floxed and deleted alleles. The common reverse primer (5-CAGCTTAGGACCTCTTCTCA) is homologous to the sequence downstream of exon 7. Primer 1 (5-GCTCCATGTTCCTGTACACT) is used to detect the wild-type alleles and is homologous to the sequence in exon 7, whilst primer 3 (5-GCCTCTGTTCCACATACACT) is used to detect the targeted or floxed alleles as is homologous to the the sequence in the neomycin cassettee. Lastly primer 4 (5-ATGATAACCCACCATGTGTC) targets the deleted alleles and is homologous to the sequence in exon 1b. PCR products for wild type and CD151$^{-/-}$ yields a 400 base pair (bp) product.

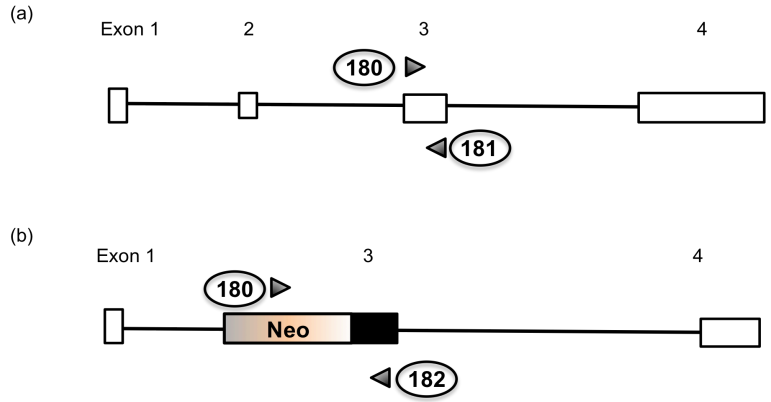

Figure 3.4. ApoE primer design. (a) Wild-type ApoE locus. (b) Insertion of the neomycin cassette (neo) disrupts the gene sequence replacing exons 2 and a portion of exon 3. Part of exon 3 (illustrated as a shaded box in (b)) and the neo cassette is amplified and yields either a knockout allele of 245 bp or a wild type allele of 155 bp. ApoE 180 is the sense or common forward primer with sequence 5-GCC TAG CCG AGG GAG AGC CG-3 which in conjunction with reverse primer ApoE 181 (5'-TGT GAC TTG GGA GCT CTG CAG C) yields a 155 bp PCR wild type product. Whilst primer ApoE 180 in conjunction with reverse primer ApoE 182 (5'-GCC GCC CCG ACT GCA TCT) yields a 245 bp PCR knockout product.

3.2.2 Mendelian inheritance frequencies

The Mendelian inheritance frequencies for ApoE$^{-/-}$ mice was as expected. No obvious signs of developmental problems, mortality or morbidity was observed in this strain. However, as shown in Table 3.1 (a), the mice lacking the CD151 protein showed a marked reduction in the percentage generated. The expected percentage of CD151$^{-/-}$ mice is approximately three fold than what was actually achieved. This is reflected also in the number of mice where 10 were expected but only 3 CD151$^{-/-}$ mice were achieved as shown in Table 3.1(b). This carried over to when CD151$^{+/-}$ mice were crossed with ApoE$^{-/-}$ mice and the percentage of animals obtained were half than what was expected (Table 3.1 (c)). Table 3.1 (d) shows the number of mice expected and the actual number of mice achieved through heterozygous breeding of CD151$^{+/-}$ mice on ApoE$^{-/-}$. Both the percentage and number of CD151$^{-/-}$ mice on ApoE$^{-/-}$ achieved was half of what was expected.

Table 3.1: Mendelian inheritance frequencies

(a)

Heterozygous breeding (Percentage)			
	+/+	**+/-**	**-/-**
ApoE	15.8%	52.6%	31.6%
Expected	25.0%	50.0%	25.0%
CD151	23.7%	68.4%	7.9%
Expected	25.0%	50.0%	25.0%

(b)

Heterozygous breeding (Number of Mice)			
	+/+	**+/-**	**-/-**
ApoE	6	20	12
Expected	10	19	10
CD151	9	26	3
Expected	10	19	10

(c)

Heterozygous breeding of CD151$^{+/-}$ on ApoE$^{-/-}$ (Percentage)			
	+/+	**+/-**	**-/-**
CD151	17.6%	70.6%	11.8%
Expected	25.0%	50.0%	25.0%

(d)

Heterozygous breeding of CD151$^{+/-}$ on ApoE$^{-/-}$ (Number of Mice)			
	+/+	**+/-**	**-/-**
CD151	3	12	2
Expected	4	19	4

The ratios of expected and actual percentage and percentage achieved of heterozygous ApoE and CD151 breeding is shown in table 3.1(a). Table 3.1(b) shows the numbers of mice obtained through heterozygous pairings, whilst table 3.1(c) and 3.1(d) shows the ratio of percentages and numbers achieved through heterozygous breeding of CD151$^{+/-}$ mice on ApoE$^{-/-}$.

3.2.3 Body weights of ApoE$^{-/-}$ compared to ApoE$^{-/-}$.CD151$^{-/-}$ mice

Body weights were recorded every week from 5 weeks of age to the day of experiment at 16 weeks of age. A population of n=17 mice from each strain was compared at each progressing week (Figure 3.5) and analysed for statistical difference via an unpaired Student's t-test. A steady increase in body weight is observed as the mice progressed in age however no significant differences (P > 0.05; NS) were seen throughout the testing period between the different strains of mice. No statistically significant differences were observed between the body weights of ApoE$^{-/-}$ and ApoE$^{-/-}$.CD151$^{-/-}$ mice (Table 3.2).

Table 3.2: Body weight of ApoE$^{-/-}$ versus ApoE$^{-/-}$.CD151$^{-/-}$ mouse strains

Age (weeks)	ApoE$^{-/-}$ ± SEM (n= 17) (grams)	ApoE$^{-/-}$.CD151$^{-/-}$ ± SEM (n= 17) (grams)	P Value (P < 0.05)
5	20.50 ± 0.50	19.33 ± 1.09	NS
6	22.03 ± 0.29	21.67 ± 0.93	NS
7	23.83 ± 1.30	23.00 ± 0.29	NS
8	24.33 ± 1.30	23.83 ± 0.44	NS
9	24.67 ± 1.30	24.67 ± 0.33	NS
10	26.00 ± 1.44	25.33 ± 0.44	NS
11	27.67 ± 1.64	25.83 ± 0.44	NS
12	29.67 ± 1.83	26.67 ± 0.44	NS
13	30.33 ± 1.67	26.67 ± 0.67	NS
14	31.00 ± 1.76	27.73 ± 0.73	NS
15	31.50 ± 1.76	28.50 ± 0.76	NS
16	32.17 ± 1.59	29.17 ± 0.93	NS

The mouse body weight ± SEM over a 16 week period on a chow fed diet shows no significant difference between strains as P values are greater than 0.05 at every stage. NS, Not Significant, unpaired Student's t-test.

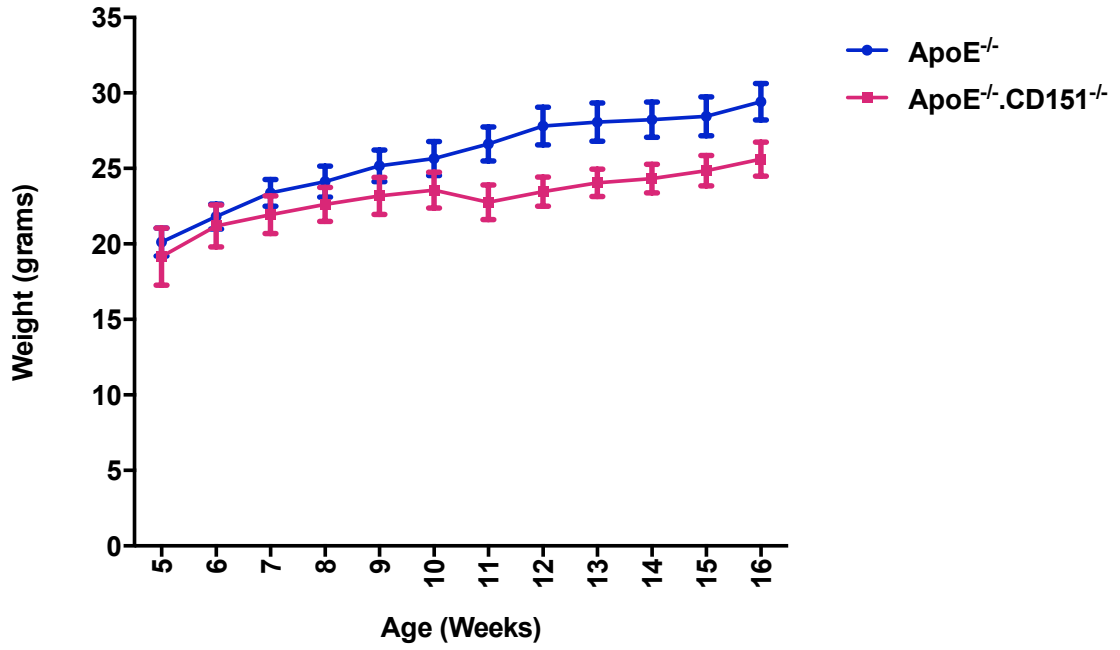

Figure 3.5. Body weight of ApoE$^{-/-}$ versus ApoE$^{-/-}$.CD151$^{-/-}$ mouse strains on a chow fed diet for 16 weeks. The graph of mouse body weight ± SEM over a 16 week period on a chow fed diet shows no significant difference between strains as P values are greater than 0.05 at every stage. N=17 in each group, unpaired Student's t-test.

3.2.4 Body mass index

Body Mass Index was calculated using the body weights in Section 3.2.3. For each animal, the weight (g) was divided by the length (mm) of the mouse from nose to anus squared. BMI is reported as an arbitrary unit and is a general measurement for assessing obesity.

ApoE$^{-/-}$ mice are reported to have lower body weights and are leaner than wild type mice.(223,224) A near identical BMI profile between the ApoE$^{-/-}$ mouse and ApoE$^{-/-}$.CD151$^{-/-}$ strain suggests that the absence of CD151 has not had an effect on adipogenesis and ApoE mediated VLDL uptake.(225) No statistical difference was observed between ApoE$^{-/-}$ and ApoE$^{-/-}$.CD151$^{-/-}$ mice BMI as calculated by a unpaired Student's t-test (n=17 in each group $P > 0.05$).

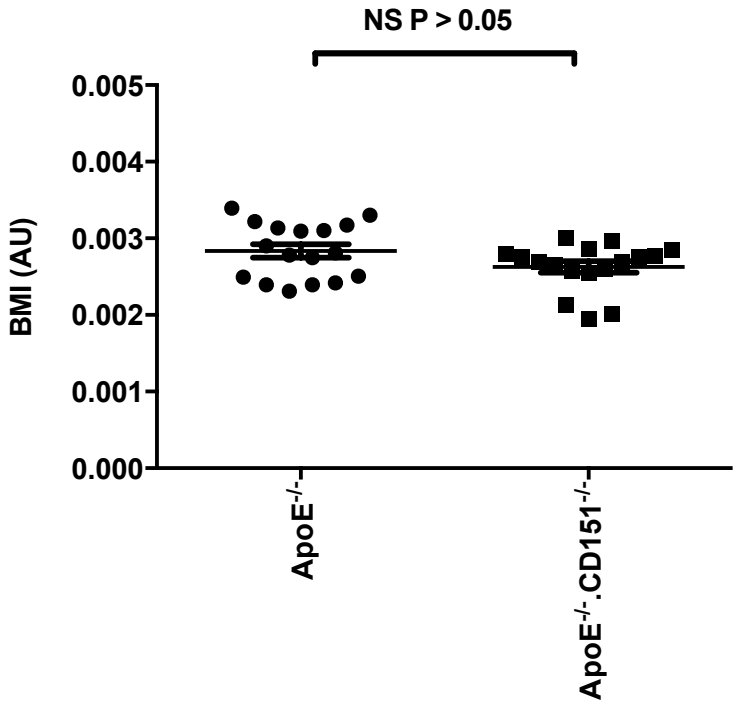

Figure 3.6. Body mass index (BMI) of ApoE$^{-/-}$ versus ApoE$^{-/-}$.CD151$^{-/-}$ mouse strains on a chow fed diet for 16 weeks. BMI is measured as weight in grams divided by length in mm squared and reported as an arbitrary unit (AU). The P value (P<0.05) is greater than 0.05 and shows no significant difference in BMI between of ApoE$^{-/-}$ versus ApoE$^{-/-}$.CD151$^{-/-}$ mouse strains. N=17 in each group. NS, Not Significant, unpaired Student's t-test.

3.2.5 Haematological parameters ApoE$^{-/-}$ compared to ApoE$^{-/-}$.CD151$^{-/-}$ mice

The absence of CD151 in atherosclerosis and its compounding effect on haematological parameters have not been tested as such full blood examinations were performed on ApoE$^{-/-}$ and ApoE$^{-/-}$.CD151$^{-/-}$ mouse strains (n=10). Results from our laboratory for C57BL/6 WT mice were provided (n=6) of which was comparable with no significant differences to reference ranges established by the University of Arizona, Animal Pathology Services (226) Only the platelet count between ApoE$^{-/-}$ and ApoE$^{-/-}$.CD151$^{-/-}$ showed a remarkable difference with a statistical significance of P < 0.0001 (n=10 per group). However, when referred to the University of Arizona mouse wild-type reference ranges, mouse platelet counts are observed to range from 592 x 10^9/L to 2972 x 10^9/L.(226) All other haematological parameters in the ApoE$^{-/-}$ and ApoE$^{-/-}$.CD151$^{-/-}$ mice appeared normal with no statistical difference observed compared to the C57BL/6 WT reference ranges.

Table 3.3: Haematological parameters of C57BL/6 versus ApoE$^{-/-}$ versus ApoE$^{-/-}$.CD151$^{-/-}$ mice

Haematological parameters	C57BL/6 WT ± SEM n=10	ApoE$^{-/-}$ ± SEM n=10	ApoE$^{-/-}$.CD151$^{-/-}$ ± SEM n=10	P Value < 0.05
WBC x 10^{9}/L	6.20 ± 1.03	4.78 ± 0.97	4.90 ± 1.08	NS
RBC x 10^{12}/L	9.07 + 0.22	8.87 ± 0.23	8.59 ± 0.09	NS
HGB g/L	132.33 ± 3.08	138.33 ± 3.53	122 ± 3.00	NS
PCV L/L	0.44 ± 0.01	0.47 ± 0.01	0.42 ± 0.01	NS
MCV fl	48 ± 0.6	52 ± 1.9	49 ± 1.5	NS
MCH pg	14.6 ± 0.2	15.3 ± 0.5	14.0 ± 0.3	NS
MCHC x 10^{3}/L	302 ± 3.4	297 ± 1.8	288 ± 5.5	NS
RDW %	13.3 ± 0.2	13.3 ± 0.3	13.7 ± 1.0	NS
PLT x10^{9}/L	726.67 ± 23.10	785.33 ± 111.49 ***	1124.67 ± 14.86 ***	P < 0.001
WBC/Neut x10^{9}/L	0.56 ± 0.18	0.33 ± 0.09	0.99 ± 0.10	NS
WBC/Lymph x10^{9}/L	5.47 ± 0.89	3.69 ± 0.83	4.88 ± 0.32	NS
WBC/Mono x10^{9}/L	0.17 ± 0.07	0.21 ± 0.07	0.47 ± 0.12	NS

Table 3.3 shows the haematological parameters of C57BL/6 versus ApoE$^{-/-}$ versus ApoE$^{-/-}$.CD151$^{-/-}$ mouse strains on a chow fed diet for 16 weeks. Platelet count in ApoE$^{-/-}$.CD151$^{-/-}$ mice is significantly higher than compared to C57BL/6 wild type mice, and compared to ApoE$^{-/-}$ mice with a P value of < 0.001. There is no significant difference reported in the remaining haematological parameters between ApoE$^{-/-}$ versus ApoE$^{-/-}$.CD151$^{-/-}$ mouse strains and are comparable to the C57BL/6 WT strain. The P value for each parameter is greater than 0.05 , n=10 tested in each group, unpaired Student's t-test.

3.2.6 Non-fasting blood glucose testing

Blood glucose testing was performed as described in Section 2.1.5 for ApoE$^{-/-}$ and ApoE$^{-/-}$.CD151$^{-/-}$ mouse strains. Statistical analysis with a Student's unpaired t-test revealed no significant difference in random glucose results between strains (P > 0.05; n=17 in each group) (Figure 3.7). Reference values for C57BL/6 wild type mice were sourced from an article by Fernandez et al.(227). The mice in their study were tested at 16 weeks of age, fasted for 5 hours and blood collected through submandibular venipuncture. Apart from the age of mice at time of testing (16 weeks), other conditions were not consistent between their study and ours. Their findings however were very similar to what we reported with their

C57BL/6 WT blood glucose reported at 225.7 ± 26.5 mg/dL. In our study, the ApoE$^{-/-}$ mouse had a blood glucose of 227.5 ± 10.9 mg/dL, whilst the ApoE$^{-/-}$. CD151$^{-/-}$ reported a blood glucose reading of 238.5 ± 8.5 mg/dL. Results from the current study were converted from mmol/L to mg/dL for a fair comparison by multiplying mean ± SEM in mmol/L by 18 to obtain values in mg/dL. Note that the authors cautioned on the various methods of blood retrieval and the outcome on biochemistry analysis. Factors such as animal handling, restraining, mode of anaesthesia, level of invasiveness and subsequent discomfort will influence results.(227) Perhaps a closer comparison is an article by Moghadasian et al.(228) which compared ApoE$^{-/-}$ and C57BL/6 wild type mice between 10 – 12 weeks old, fed ad libitum with a glucose (mmol/l) reading at 15.2 ± 0.2 mmo/L in C57BL/6 WT and at 13.4 ± 1.1 mmol/L in ApoE$^{-/-}$ mice.(228)

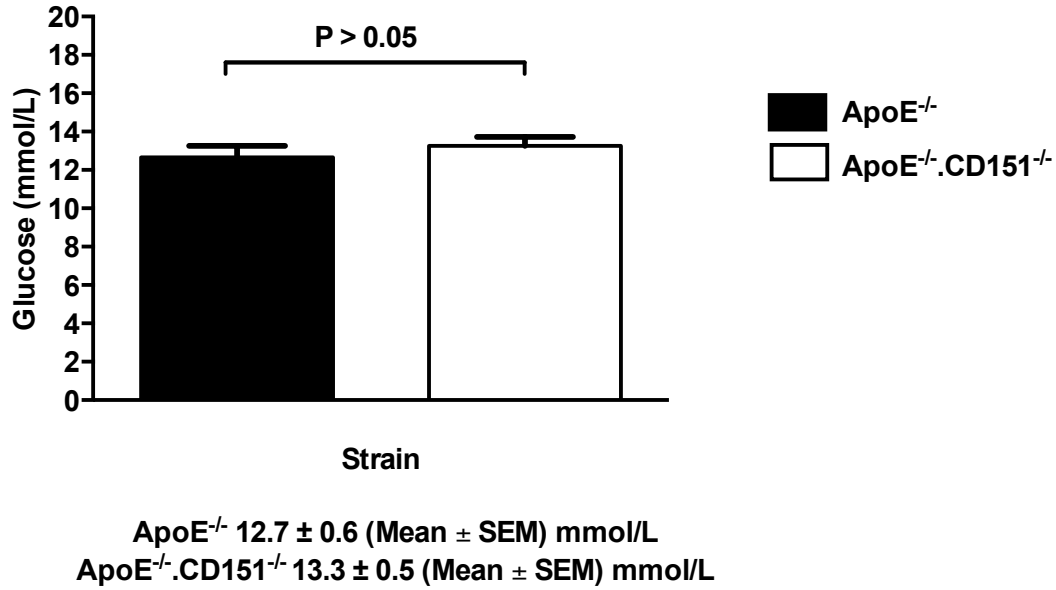

Figure 3.7. Random non-fasting blood glucose measurement of ApoE$^{-/-}$ versus ApoE$^{-/-}$.CD151$^{-/-}$ mouse strains on a chow fed diet at 16 weeks of age. Graph of mouse random blood glucose is taken at time of cardiac puncture. Mice were sacrificed via cervical dislocation after collection of blood samples. No significant difference in blood glucose is observed between ApoE$^{-/-}$ and ApoE$^{-/-}$.CD151$^{-/-}$ mouse strains. N=17 in each group, unpaired Student's t-test.

3.2.7 Lipid profiling of ApoE$^{-/-}$ compared to ApoE$^{-/-}$.CD151$^{-/-}$ mice

Data on the lipid profiles of ApoE$^{-/-}$ and ApoE$^{-/-}$.CD151$^{-/-}$ mice are shown in Figures 3.8 (a) to (d). Figure 3.8 (a) shows the ApoE$^{-/-}$.CD151$^{-/-}$ total cholesterol being significantly lower than the ApoE$^{-/-}$ mice. This was analysed with an unpaired Student's t test, which reported the difference of a P value of < 0.05. The total cholesterol in the ApoE$^{-/-}$ mouse at 131.7 ± 6.8 mg/dL (7.3 ± 0.4 mmol/L) however, is less than half of the expected estimated cholesterol

levels which in previous murine studies are reported to be around 400-500 mg/dL even when fed a normal chow diet, ad libitum. Additionally, it is also known that wild type mice carry their cholesterol predominantly as HDL with figures approximating 80-85 mg/dL.(225,229) Note however that studies have consistently shown HDL levels to be approximately 8 mg/dl in ApoE$^{-/-}$ mice.(230) The current results are significantly different from previous ApoE$^{-/-}$ mice results and reflect HDL levels of that of wild-type mice instead of an ApoE$^{-/-}$ HDL cholesterol profile. Figure 3.8 (b) shows that ApoE$^{-/-}$ had 82.4 ± 2.5 mg/dL (4.6 ± 0.1 mmol/L) HDL levels similar to previous findings on wild type mice but not ApoE$^{-/-}$ mice. ApoE$^{-/-}$.CD151$^{-/-}$ however displayed significantly lower HDL at 63.6 ± 3.1 mg/dL (3.5 ± 0.2 mmol/L) (unpaired Student's t-test, $P < 0.0005$) which is suggestive of alterations to lipid metabolism in the absence of CD151. The triglycerides and LDL levels results between the strains were not statistically different. LDL was calculated using the formula(231): LDL= Total Cholesterol – HDL Cholesterol – (Triglycerides/5).

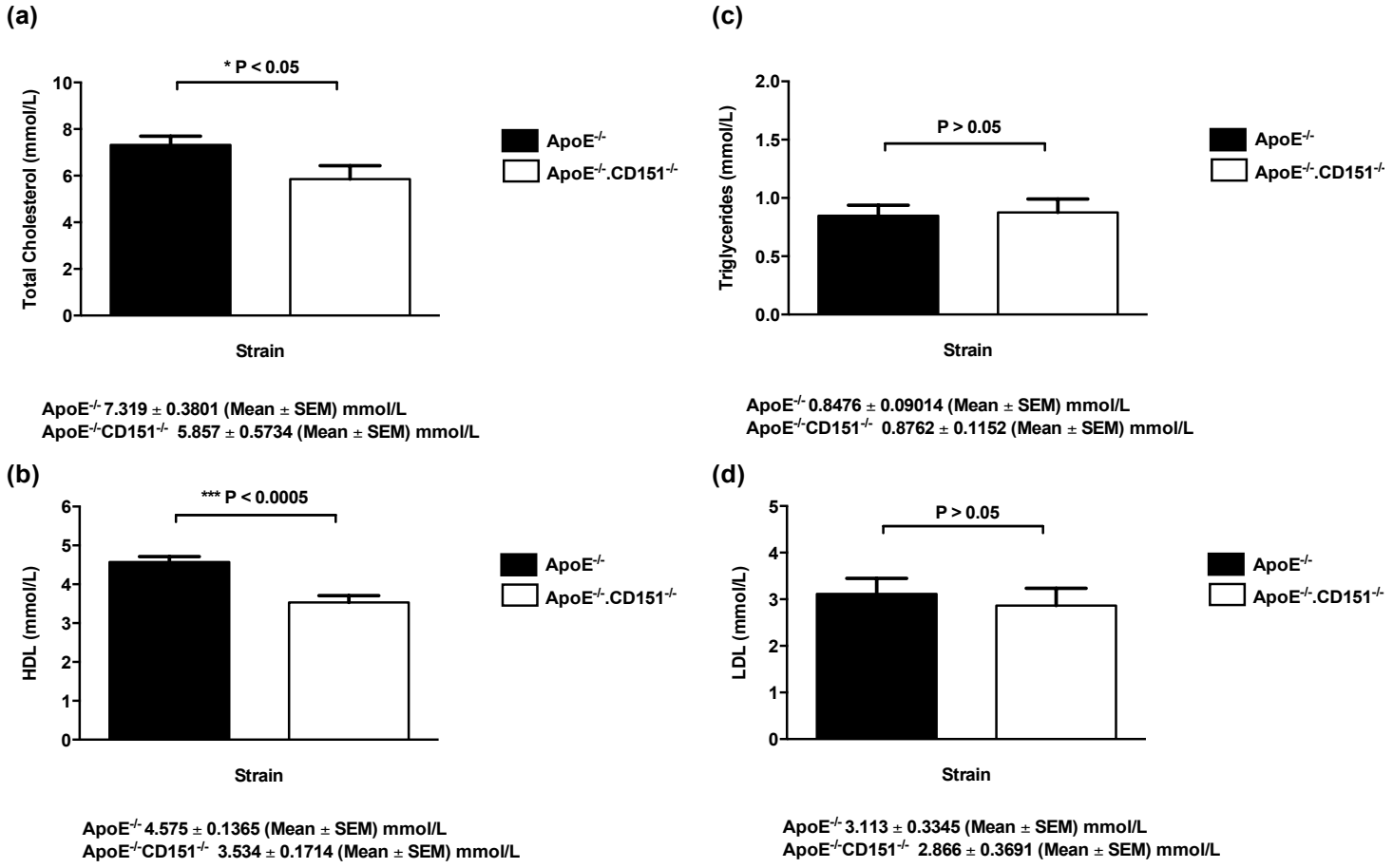

Figure 3.8 (a) – (d): Random non fasting lipid profiles of ApoE$^{-/-}$ versus ApoE$^{-/-}$.CD151$^{-/-}$ mice on a chow fed diet for 16 weeks. (a) and (b) Total Cholesterol (mmol/L) (n=21) and High Density Lipoprotein (HDL) cholesterol (mmol/L) (n=15) is significantly higher in ApoE$^{-/-}$. (c) and (d) No significant difference in Triglycerides (mmol/L) (n=21) and Low Density Lipoprotein cholesterol (LDL) (mmol/L) (n=17) is observed between ApoE$^{-/-}$ and ApoE$^{-/-}$.CD151$^{-/-}$ mouse strains. An unpaired Student's t-test was used to determine statistical significance.

3.2.8 Cardiovascular risk factors of ApoE$^{-/-}$ compared to ApoE$^{-/-}$.CD151$^{-/-}$ mice

Atherosclerosis is widely known to lead to unfavourable CVD events. The weight, length, BMI and glucose levels of ApoE$^{-/-}$ and ApoE$^{-/-}$.CD151$^{-/-}$ mice were summarised together to identify if any significant quantitative changes are present in the ApoE$^{-/-}$.CD151$^{-/-}$mice compared to the ApoE$^{-/-}$ mouse strain. The P values for each parameter was greater than 0.05 and thus presenting no significant differences.

Table 3.4: CVD Risk Factors between ApoE$^{-/-}$ and ApoE$^{-/-}$.CD151$^{-/-}$ mice

Parameter	ApoE$^{-/-}$ n=17	ApoE$^{-/-}$.CD151$^{-/-}$ n=17	P Value < 0.05
Weight (g) ± SEM	28.18 ± 1.11	25.89 ± 0.94	NS
Length (mm) ± SEM	99.51 ± 0.52	99.12 ± 0.65	NS
BMI (AU) ± SEM	0.0028 ± 0.00	0.0026 ± 0.00	NS
Glucose (mmol/L) ± SEM	12.65 ± 0.60	13.25 ± 0.47	NS

Table 3.4 displays a summary of the CVD risk factors for ApoE$^{-/-}$ and ApoE$^{-/-}$.CD151$^{-/-}$ mice. No significant difference is reported as P values were greater than 0.05 for all parameters (unpaired Student's t-test). Mouse length is measured from nose to anus in mm. Body Mass Index (BMI) is measured as weight in grams divided by length in mm squared. Glucose is measured with a Accu-Chek® Advantage meter and Accu-Chek® Comfort Care test strips (Roche Diagnostics, Indianapolis, USA).

3.2.9 Organ weights and lengths of ApoE$^{-/-}$ compared to ApoE$^{-/-}$.CD151$^{-/-}$ mice

The heart, lungs, kidneys and liver of ApoE$^{-/-}$ and ApoE$^{-/-}$.CD151$^{-/-}$ mice were macroscopically observed for any morphological changes in overall appearance, size and weight. Figure 3.9 shows a representative image of organs derived from ApoE$^{-/-}$ versus ApoE$^{-/-}$.CD151$^{-/-}$ mice. Despite a visually larger ApoE$^{-/-}$.CD151$^{-/-}$ lung and liver compared to that of ApoE$^{-/-}$ (Figure 3.10 (c) and (d)), Figure 3.9 shows various organ weights, revealing no significant difference between mouse strains ($P > 0.05$, unpaired Student's t-test).

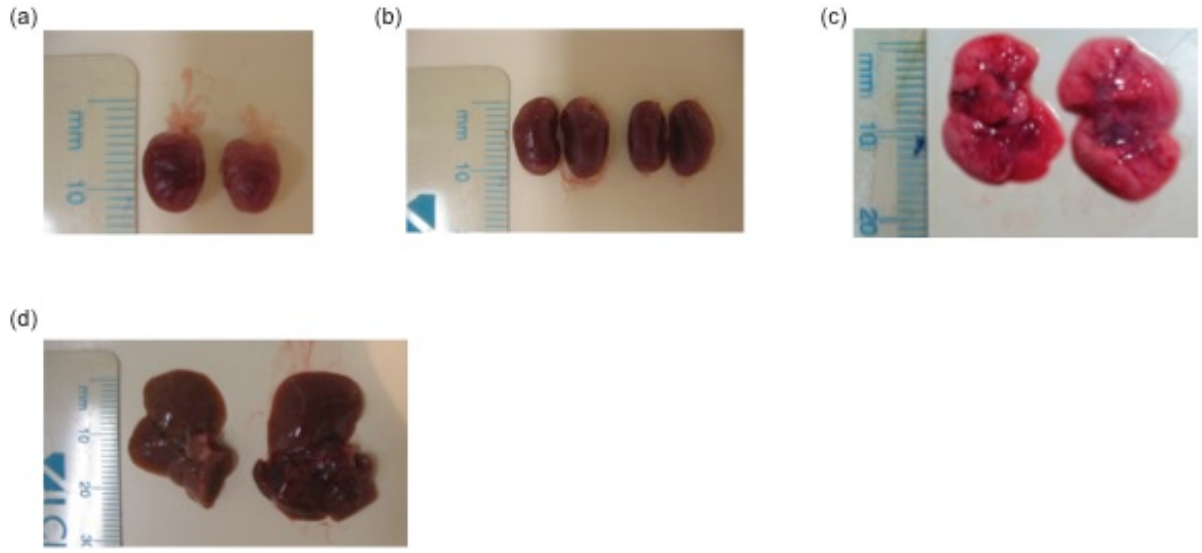

Figure 3.9 Images of organs from ApoE$^{-/-}$ and ApoE$^{-/-}$.CD151$^{-/-}$ strains, harvested for histology. Organs from Left to Right are from, ApoE$^{-/-}$ and ApoE$^{-/-}$.CD151$^{-/-}$. A. Heart with aortic arch attached. B. Kidneys. C. Lungs. D. Liver lobes: Media, Right, Left and Caudate. Organs were harvested in 10% (v/v) Neutral Buffered Formalin for 48 hours followed by processing with a rodent schedule on a Leica automated tissue processor.

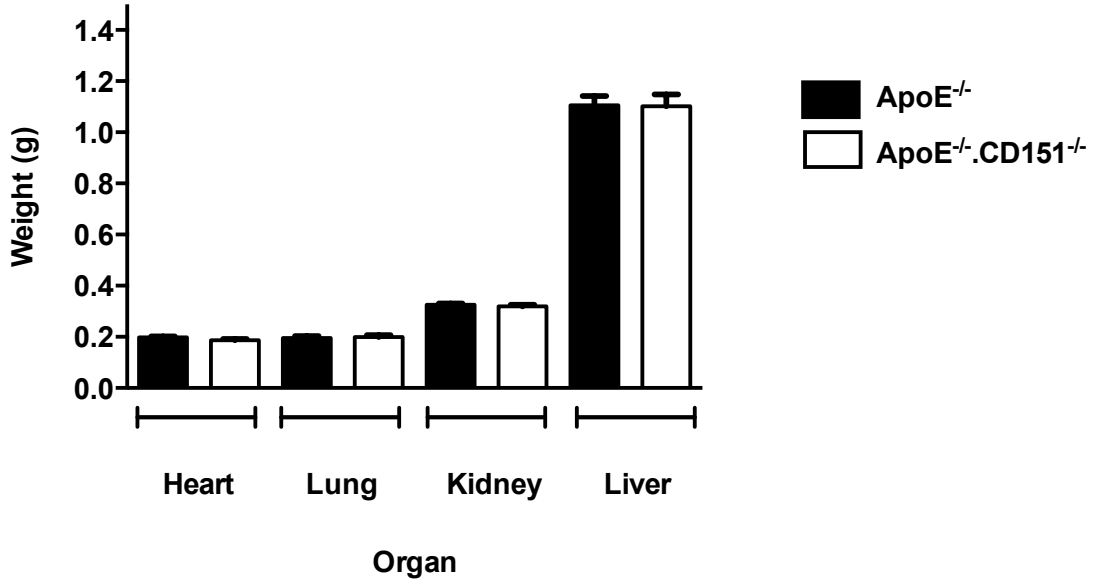

Figure 3.10. Organ weights of ApoE$^{-/-}$ vs ApoE$^{-/-}$.CD151$^{-/-}$ mouse strains on a chow fed diet for 16 weeks (n=17 in each group). Graph of organ weight ± SEM over a 16 week period on a chow fed diet. No significant difference is observed between heart, lung, kidney and liver between ApoE$^{-/-}$ vs ApoE$^{-/-}$.CD151$^{-/-}$ mouse strains (unpaired Student's t-test).

At 16 weeks, ApoE$^{-/-}$ is observed to have a heart weight of 0.19 ± 0.01 g (Figure 3.9). Although the mice in our study are much younger, ApoE$^{-/-}$ heart weights in a previous study at 13 months, had a heart weight of 0.19 ± 0.01 g. This study also noted that heart weights in ApoE$^{-/-}$ mice were 23% higher than heart weights of wild-type mice.(232) This serves as a helpful guide in suggesting that the heart weights between ApoE$^{-/-}$ and ApoE$^{-/-}$.CD151$^{-/-}$ mice are unchanged in the absence of CD151 and is increased when compared to wild-type mice.

ApoE$^{-/-}$ mice kidney weights in our study were 0.33 ± 0.01 g and ApoE$^{-/-}$.CD151$^{-/-}$, 0.34 ± 0.01 g, no statistically significant difference was recorded between the strains in an unpaired Student's t-test. These results were similar to a study which involved observing the weight of ApoE$^{-/-}$ mice at 20 weeks. They reported a left kidney weight of 0.16 ± 0.003 g and right kidney weight of 0.16 ± 0.002 g. Whilst we did not discriminate between the left and right kidneys, their study did. Though, when added together (left and right kidneys), the overall weight of the kidney is 0.32 g and similar to what was documented in our observations.(233)

The liver and lung weights of ApoE$^{-/-}$ mice have not reported in previous literature. Our study will thus provide a useful guide for other researchers should they need a means of comparison for liver and lung weights of ApoE$^{-/-}$ mice. Throughout our observations of lung, liver, heart and kidney weights of ApoE$^{-/-}$ and ApoE$^{-/-}$.CD151$^{-/-}$ mice, no statistical significance in weights for each organ were observed between the strains ($P > 0.05$, unpaired Student's t-test).

3.3 Discussion

The literature on ApoE and its absence in the murine model *in vivo*, *in vitro* and in humans is comprehensive. Tetraspanin CD151 has also been studied however not to the same extent as ApoE especially in an atherosclerotic setting in either animal models or humans. The $ApoE^{-/-}$ proatherogenic model crossed with a mouse lacking the CD151 gene provides a means of investigating the absence of CD151 and its implication on atherothrombosis and atherogenesis. This is of upmost importance given that the latest statistics from the Australian Bureau of Statistics (ABS) reported ischaemic heart disease as the leading underlying cause of death in Australia in 2011. Ischaemic heart disease accounted for 21,513 deaths in 2011 though this figure has seen a steady decline since 2000.(2) This persists as a worldwide concern as cardiovascular disease is the leading cause of death.

One of the more notable results deduced from characterisation of the $ApoE^{-/-}.CD151^{-/-}$ is the significant reduction in the expected Mendelian inheritance frequencies. This proved to be a great challenge throughout the study as litter sizes were small and few mice would survive past the weaning stages. The percentage of $CD151^{-/-}$ generated through heterozygous breeding was only 7.9% which is approximately three fold less than the expected Mendelian inheritance frequency of 25% (Table 3.1 (a)). This is reflected also in the number of mice obtained through heterozygous pairings where 10 were expected but only 3 $CD151^{-/-}$ mice were generated, as shown on Table 3.1(b). Heterozygous breeding of $CD151^{+/-}$ mice on $ApoE^{-/-}$ also shows a reduction in the actual Mendelian Inheritance frequency achieved as opposed to the expected percentage. This was nearly halved as only 11.8% of $ApoE^{-/-}.CD151^{-/-}$ were generated and is also observed in Table 3.1(d) where the 2 $ApoE^{-/-}.CD151^{-/-}$ mice were generated compared to the 4 animals expected.

Additional throughout the study numerous $ApoE^{-/-}.CD151^{-/-}$ mice were culled before meeting the age suitable for experimentation due to malocclusion in accordance with ethical guidelines and regulations. This is a common condition in rodents in which maxillary and mandibular teeth are not aligned causing the incisors to overgrow.(234) Other isolated incidents requiring culling also included culling of a female breeder due to a pup stuck in her birth canal, whilst another presented with a rectal prolapse. Environmental factors were also noted to have an influence over the breeding patterns of mice. The area in which the mice were housed was subjected to echoing noises and vibrations due to strong winds. These

factors have been associated with stress in the female mice breeders subsequently leading them to eat their pups.

Physically, the ApoE$^{-/-}$.CD151$^{-/-}$ mice did not show any signs of malformation throughout its lifespan in the RAF and at time of experimentation. Their body weights were comparable with no distinguishable difference to the ApoE$^{-/-}$ control strain (Figure 3.5). Previous studies indicate ApoE$^{-/-}$ in having leaner bodies and a lower body weight to wild type C57BL/6 mice.(223,224,235,236) Despite also lacking the CD151 protein, the ApoE$^{-/-}$.CD151$^{-/-}$ model appears to share similar body weight parameters to the ApoE$^{-/-}$ model suggesting body weight and lean mass to be uninfluenced by the absence of the tetraspanin in this atherosclerotic setting. Furthermore, deletion of CD151 has not corrected body weights of ApoE$^{-/-}$.CD151$^{-/-}$ mice and not reverted to a C57BL/6 WT mose body weight profile which as discussed is reported to be higher than ApoE$^{-/-}$.

Body weights of CD151$^{-/-}$ mice have been observed in studies investigating kidney renal disease. Its presence is ubiquitous in endothelial, epithelial (cell to cell junctions), Schwann cells, smooth and cardiac muscles, platelets and megakaryocytes as well as the immune system.(6,96,100,101,237) In epithelial cells in particular, the integrins $\alpha_3\beta_1$ and $\alpha_6\beta_4$ are expressed predominantly in the basolateral compartments.

The interaction and high stoichiometry of CD151 and integrin $\alpha_3\beta_1$ for example is reported to provide stability to $\alpha_3\beta_1$ and laminin in its active conformation.(103,125) The extracellular matrix and the intracellular cytoskeleton are linked together by αβ heterodimeric cell surface proteins such as $\alpha_3\beta_1$. Human studies have demonstrated the importance of maintaining the CD151:$\alpha_3\beta_1$ association, as well as the CD151:$\alpha_6\beta_4$ associated heterodimers. A condition of junctional epidermolysis bullosa is found to occur in human patients lacking a functional $\alpha_6\beta_4$ heterodimer, with detachment of the epidermis occurring in the absence of β_4.(238,239) In the case of α_3, skin blistering is observed to occur as a result of basement membrane ruptures. Mice lacking the α_3 subunit suffer abnormalities in their lung and kidney epithelia and do not survive long after birth.(240,241) Renal failure and glomerulosclerosis is observed to also occur when the complex organisation of the renal glomerulus is affected with the absence of α_3. The literature also reports early indications of kidney dysfunction being observed in CD151$^{-/-}$ mice before reaching 3 weeks of age as mice were found to

develop proteinuria and were culled before 36 weeks of age due to substantial loss of body weight. The authors did not state the exact age at which body weight declined and may likely, if compared to Figure 3.5 have occurred after 16 weeks of age as our study showed a steady and parallel increase in body weight between the ApoE$^{-/-}$ mice and the ApoE$^{-/-}$.CD151$^{-/-}$ mice up to this age. It is not definitive if a decline can be predicted in the ApoE$^{-/-}$.CD151$^{-/-}$ strain given that our study extends only to 16 weeks. Their study also found the extent of renal damage to be variable between CD151$^{-/-}$ litters and ranged from being mild to severe. Perhaps in litters where renal damage is severe, the ApoE$^{-/-}$.CD151$^{-/-}$ strain might struggle to thrive with reduced body weights due to the weight profiles of the ApoE$^{-/-}$ strain which show mice have leaner and lower body weights and the CD151$^{-/-}$ mice which are culled due to renal abnormalities leading to severe weight loss. In contrast however, a study by Wright et al. (102) characterised mice lacking the CD151 protein and found them to be "normal, healthy and fertile".(102) The authors did predict a possible occurrence of neonatal lethality for the reasons discussed above but did not encounter any difficulties with breeding and developing the strain. This is further supported by a more recent article which reported the CD151$^{-/-}$ mouse strain to develop normally without any obvious deficiencies in their vascular development, tissues or organs, with specific attention towards the liver, heart, lungs and kidneys. They concluded that the CD151 was not associated with vascular development as this was their study aim.(242) The inconsistent findings in the literature on the development and survival of CD151$^{-/-}$ mice could well be contributed by the varied severity of renal damage between litters found in previous studies as well as being highly dependent on the genetic background of mice examined.

In contrast, the literature on ApoE$^{-/-}$ development is consistent with the current findings as shown in Table 3.1 where the percentage and number of mice generated through ApoE heterozygous breeding was comparable to the expected values. No obvious signs of developmental problems, mortality or morbidity was observed in this strain. This is consistent with findings by Whitman (203) where he states ApoE$^{-/-}$ on a C57BL/6 WT background breeds well and generates a reasonable litter.(203) Other scientists however also do note that the reduction in body weight of ApoE$^{-/-}$ mice and possibly ApoE$^{-/-}$.CD151$^{-/-}$ could be due to a disruption in the delivery of liver derived very low density lipoprotein to adipocytes. ApoE interaction with the VLDL receptor promotes triglycerides hydrolysis by lipoprotein lipase. It is already well established that VLDL null mice are protected from obesity. Perhaps the reduction in body weight in ApoE mice may be accounted partly by the absence of ApoE in this reaction.(243,244)

Whilst cholesterol transport and metabolism are relatable between mice and humans, lipid profiles however present differently between the species. In humans, the risk of atherosclerosis and associated cardiovascular events are attributed by the low HDL to LDL ratios.(245) It is known that humans predominantly carry their plasma cholesterol in the LDL form as opposed to wild-type mice, which carry their plasma cholesterol mostly in HDL fractions at approximately 80 mg/dl.(246) In $ApoE^{-/-}$ mice, the predominant lipoprotein fractions found are VLDL/LDL with HDL lipoprotein fractions approximating 8 mg/dl only.(230) Mice lacking the ApoE gene even on a normal chow diet, ad libitum are found to have total cholesterol ranges exceeding 400 mg/dl.(247,248) This study imparts novel insights into the lipid profiles of $CD151^{-/-}$ mice in an atherosclerotic diseased setting with generation of the $ApoE^{-/-}.CD151^{-/-}$ mouse line. Plasma samples of $ApoE^{-/-}.CD151^{-/-}$ mice were obtained at 16 weeks of age and compared to the $ApoE^{-/-}$ mouse strain. Our findings show that $ApoE^{-/-}.CD151^{-/-}$ mice total cholesterol is significantly lower compared to $ApoE^{-/-}$ mice ($P < 0.05$ n=21) (Figure 3.8). Meanwhile we also found that $ApoE^{-/-}$ mice total cholesterol at 131.7 ± 6.8 mg/dL (7.3 ± 0.4 mmol/L) is less than half of the expected ranges for cholesterol levels compared to previous literature. It appears just based on total cholesterol levels that the mice bred in the current study did not present a greater propensity to developing dyslipidaemia as expected when referred to the literature. Furthermore the HDL profile of $ApoE^{-/-}$ mice (82.35 ± 2.46 mg/dL) in the current study also varied against expected HDL profiles of the $ApoE^{-/-}$ mice found in the literature, where the current HDL levels resembled more closely to a wild-type HDL lipoprotein profile ranging from 80-85 mg/dL instead.(225,229) Previous studies conducted on $ApoE^{-/-}$ mice consistently report HDL fractions to be in the 8 mg/dl range.(230) Despite $ApoE^{-/-}.CD151^{-/-}$ HDL levels being significantly lower at 63.6 ± 3.1 mg/dL (3.5 ± 0.2 mmol/L) (unpaired Student's t-test, $P < 0.0005$) compared to $ApoE^{-/-}$ at 82.35 ± 2.46 mg/dL (4.575 ± 0.14 mmol/L), these findings were still greater than expected. Again compared to the literature, on a normal chow diet and ad libitum, triglycerides (15.3 ± 1.2 mg/dL) and LDL (56.0 131.7 ± 6.1 mg/dL) levels of $ApoE^{-/-}$ mice recorded in this study were also significantly lower. These inconsistencies with the literature suggests that variables such as fasting or non fasting blood collection, and specimen handling are likely to have an influence in total cholesterol, HDL, LDL and triglycerides profiles. With respect to total cholesterol, HDL and LDL, the absence of CD151 in an atherosclerotic setting as observed in the $ApoE^{-/-}.CD151^{-/-}$ mouse line saw a reduction in these parameters compared to the $ApoE^{-/-}$ mouse strain. Being a novel model, the influence of CD151 absence on atherosclerosis has not been studied and the findings of this thesis serves as a sole reference for lipid profiling in atherosclerotic mice deficient in CD151.

Recently Tani et. al (249) concluded that it is inaccurate to directly compare and extrapolate HDL results between ApoE$^{-/-}$ mice and humans. This is because ApoE is integral in the formation of HDL particles in the murine model, ApoE is not required for HDL formation in humans. They suggest this to be contributed by the lack of cholesteryl ester transfer proteins in mice. Thus although clearly the absence of CD151 has had an influence on the lipid profiles of the ApoE$^{-/-}$.CD151$^{-/-}$ with significantly lowered levels of HDL and total cholesterol compared to the ApoE$^{-/-}$ mouse strain, the former may not be reflective in a human atherosclerotic setting.

The haematological parameters and glucose levels of ApoE$^{-/-}$ and ApoE$^{-/-}$.CD151$^{-/-}$ were compared. These parameters were measured at time of experimentation (16 weeks of age) where the mice were fed ad libitum on a normal chow diet. Table 3.3 shows no significance between the red and white blood cell parameters of ApoE$^{-/-}$, ApoE$^{-/-}$.CD151$^{-/-}$ as well as wild-type C57BL/6 WT mice. Our findings did however report a significantly increased platelet count in the ApoE$^{-/-}$.CD151$^{-/-}$ mouse compared to ApoE$^{-/-}$ and wild-type C57BL/6 WT mice. We note however that platelet counts are known to be variable and as evidence is reported to range between 592 x 10^9/L to 2972 x 10^9/L in a wild-type C57BL/6 mouse.(226) These findings suggest that the absence of CD151 did not influence haematological production as measured by haematological parameters. Likewise with body weight, the absence of ApoE is reported to reduce some aspects of the metabolic syndrome including impaired glucose tolerance due to obesity. Glucose tolerance is unchanged in an ApoE mouse and this is seen in our study where the ApoE$^{-/-}$ and ApoE$^{-/-}$.CD151$^{-/-}$ mouse strains showed an unchanged glucose level between strains. CD151 absence does not seem to have impacted on this either however it is not possible to conclude also if CD151 absence may have possibly imparted a protective effect and improved insulin sensitivity like the absence of ApoE. Nonetheless, investigating this parameter is important as cardivovascular events as a result of atherosclerosis are significantly increased in patients with diabetes.

In a similar pattern, the organ weights between ApoE$^{-/-}$ and ApoE$^{-/-}$.CD151$^{-/-}$ mice were also observed to be unchanged with no significant differences in their weights when harvested and measured at 16 weeks. Again as our study is characterising this novel ApoE$^{-/-}$.CD151$^{-/-}$ mouse, our findings were compared to the ApoE$^{-/-}$ mouse which has been studied extensively. Compared to previous literature the ApoE$^{-/-}$ mice in our study displayed similar heart and kidney weights. Between the ApoE$^{-/-}$ and ApoE$^{-/-}$.CD151$^{-/-}$ mice, no differences

were seen in body organ weights. The literature however does not appear to have any data on liver and lung weights. This study has observed the weights of these organs in both ApoE$^{-/-}$ and ApoE$^{-/-}$.CD151$^{-/-}$ mice, and has not reported any significant differences (unpaired Student's t-test, $P > 0.05$, $n=17$) between the strains (Figure 3.10).

The summarised cardiovascular risk factors shown in Table 3.4 maintains that there is no significant increase in cardiovascular risk potential between ApoE$^{-/-}$ and ApoE$^{-/-}$.CD151$^{-/-}$ mice for risk factors such as weight, body mass index and glucose levels, whilst lipid profiling in Figure 3.8 indicates a reduction of total cholesterol in the ApoE$^{-/-}$.CD151$^{-/-}$ strain and consequently a reduction in HDL levels. These results are paramount as 5.6 million Australian adults are reported to have high total cholesterol levels.(250) The National health measures survey (NHMS) measured cholesterol levels and utilised these parameters as an indicator of cardiovascular disease.

3.4 Conclusion

Characterising the ApoE$^{-/-}$.CD151$^{-/-}$ strain allows us not only to investigate the role of CD151 in atherosclerosis and this may lead to strategies in the prevention and management of atherothrombosis and atherosclerosis, it also provides a baseline and foundation for this study to develop hypotheses and conclusions from the parameters collected. There are no significant distinguishable features observed in this section of the study between the ApoE$^{-/-}$ and ApoE$^{-/-}$.CD151$^{-/-}$ mouse strains. Altough statistically significant reductions in total cholesterol and LDLs were observed in the ApoE$^{-/-}$.CD151$^{-/-}$ genotype, as well as a raised platelet count in the ApoE$^{-/-}$.CD151$^{-/-}$ strain, we are however limited by elements of diet and age of the mice which may have a profound effect on these findings. This addresses our interest in the clinical sequela of disease in that we have observed key indicators of cardiovascular disease specifically lipid profiling and not found a clear cut answer on whether the absence of CD151 is protective in cardiovascular disease or not. (250) Indeed, haematological parameters, lipid profiles are not sufficient to investigate the protective effect of CD151 if any, and requires other investigations in the following chapters to be analysed cumulatively.

3.5 Limitations

As discussed, animal welfare is of high priority in that the age of the mice examined were maintained at a maximum of 16 weeks so as to avoid the formation of cutaneous xanthomas and skin lesions. It would be most ideal to investigate haematological, lipid and glucose parameters at multiple time points such as at 16 weeks and an extended time point for instance 32 weeks to permit the investigation of more advanced atherosclerosis and the influence of CD151 absence in advanced disease. The mice in this study were fed a chow diet ad libitum and were not subjected to fasting periods prior to blood draw for analysis of haematological, lipid and glucose parameters. Therefore, further investigation under fasting parameters are warranted.

4 CHAPTER 4: INVESTIGATING THE ROLE OF CD151 IN PLAQUE BURDEN USING AN APOE$^{-/-}$ MOUSE MODEL.

4.1 Introduction

The role of tetraspanin CD151 and the consequences of CD151 deficiency in atherosclerosis has not been determined. To date, *in vitro* and *in vivo* studies have investigated and been published on the influence of CD151 in various clinical conditions such as cancer metastases, pulmonary fibrosis, glomerulosclerosis, end stage renal disease, infectious diseases, wound healing as well as thrombus growth and stability.(107,119,121,197,251-256)

At the molecular level, CD151 is proposed to be involved in organising and modulating transmembrane protein function, which include laminin-binding integrins, proteases, hepatocyte growth factor receptors, epidermal growth factor receptors and transforming growth factor β receptors.(125,257-260) The laminin binding integrins $\alpha_3\beta_1$, $\alpha_6\beta_1$, $\alpha_6\beta_4$ complexes lateral associations with CD151 where the interaction of CD151 with α_3 and α_6 occurs in the extracellular loop region.(261,262) It was previously postulated that the absence of this interaction affects cell functions that are integrin dependent such as adhesion strengthening. Recently however, Kazarov et al. (258) and Zevian et al. (263) demonstrated that the CD151 formed complex with α_3 and α_6 is not critical for function though is found to enhance the tetraspanin integrin complex.(258, 263) Furthermore, Lau et al. (4) have also determined the role of CD151 in integrin $\alpha_{IIb}\beta_3$ fibrinogen binding protein function and its significance in the maintenance of haemostasis. Absence of CD151 was reported to result in *in vivo* bleeding defects and impaired outside in integrin $\alpha_{IIb}\beta_3$ signalling.(4,102)

Histological analyses on CD151 deficiency in mice have been studied in various animal models. This thesis investigates the effect of the absence of CD151 in the kidneys, lungs, liver and heart in an atherosclerotic setting and whether the phenotype associated with the absence of this tetraspanin observed in other animal models would present similarly in the ApoE$^{-/-}$.CD151$^{-/-}$ mouse model. The tissue architecture and organ morphology of ApoE$^{-/-}$

and ApoE$^{-/-}$.CD151$^{-/-}$ mice were examined with light microscopy to identify if the absence of CD151 has any influence in an atherosclerotic setting.

The high affinity associations and complexes formed between CD151 and integrins $\alpha_3\beta_1$, $\alpha_6\beta_1$, $\alpha_6\beta_4$ are paramount in the development, maintenance and function of kidney as well as skin epithelia.(240,241,264,265) Glomerulosclerosis is a condition in which the kidney glomerulus suffers scarring leading to end stage renal disease. Podocytes are visceral epithelial cells located in the glomerulus.(266) Interference in the attachment of podocytes to glomerular basement membranes is central to the development of glomerulosclerosis. Integrin $\alpha_3\beta_1$ is the most abundantly expressed laminin receptor integrin located on podocytes.(267) Podocyte loss is progressive and ultimately resulting in the death at 5 – 6 weeks of age in mice which lack the β_1 subunit.(268, 269) Deficiencies in either α3 or the β1 subunit results in proteinuria, a subsequent condition beginning with glomerulosclerosis. CD151 association with the $\alpha_3\beta_1$ integrin stabilises the attachment of podocytes to the glomerular basement membrane. This finding was validated by Sachs et al.(270) who found mice on a C57BL/6 WT background with a CD151 deficiency developing renal injury when subjected to severe hypertension. It should be noted that studies have also reported C57BL/6 WT mice to be amongst several which are resistant to renal disease, which may thus suggest the involvement of other genetic factors in the development of glomerulosclerosis.(242,270,271) The 'Friend Leukemia Virus Strain B' or better known FVB mouse model is susceptible to renal injury and was backcrossed with CD151 deficient mice to confirm and determine the influence of CD151 on glomerulosclerosis. Further to the phenotype demonstrated by C57BL/6 WT mice, the FVB mouse lacking CD151 also exhibited spontaneous glomerular injury.(272) Histological examinations of 12 week old mice kidneys were observed to display abnormal endothelium and bowmans capsules.(270) On the other hand, mice lacking CD151 of 6-8 weeks in age were compared to C57BL/6 WT mice by Wright et al. (102) and found to demonstrate normal morphology with no comparable difference between the mouse strains.(102)

Abnormalities in the lung architecture of CD151 deficient mice on a C57BL/6 WT background have recently been linked to the progression of idiopathic pulmonary fibrosis. According to Tsujino et al. (273), CD151 appears to be a valuable therapeutic target for fibrotic disease treatment.(273) The development of pulmonary fibrosis is understood to stem from the impediment to the normal functioning of alveolar epithelial cells and consequently resulting in the activation of alveolar epithelial cells and immune response.(274,275) Secretion of transforming growth hormone β_1 and profibrotic factors

stimulates excessive extracellular matrix and collagen deposition in lungs.(273) CD151 was found to be critical for epithelial integrity and was initially proposed to be linked to pulmonary fibrosis by the tetraspanins ability to form stable complexes with laminin binding proteins. Deficiencies in the β_1 subunit of integrins have similarly been observed in pulmonary fibrosis given its associations with CD151.(276,277) Analysis of lung architecture through histology studies display decreased CD151 expression in alveolar epithelial cells of human patients with pulmonary fibrosis. Also, CD151 mice on a C57BL/6 WT background aged 8-10 weeks were subjected to low dose bleomycin injury to enhance epithelial disintegrity and induce pulmonary fibrosis, both wild type and CD151 deficient mice showed increased lung fibrosis compared to saline controls.(273)

CD151 has also been implicated in numerous stages of cancer progression where studies on mouse lung endothelial cells have demonstrated the influence of CD151 on tumor growth and metastasis. The tetraspanin is suggested to act as a linker joining MT1 MMP and $\alpha_3\beta_1$ and regulating endothelial haemostasis at endothelial lateral junctions, thus acting as a positive regulator of tumor growth and metastasis.(278) CD151 influence on signalling pathways in cancer and endothelial cells have also suggested its integral role in angiogenesis. Although vascular development is unchanged in CD151 deficient mice, endothelial cell migration, invasion and spreading was found both *in vitro* and *in vivo* to have been affected. Deletion of CD151 was found to cause abnormalities in PKB/c-Akt, e-NOS, Rac and Cdc42 adhesion dependent activation.(242) Furthermore, a poor prognosis in lung carcinomas is associated with overexpression of CD151 and have in turn led to CD151 in being considered as an improved prognostic marker. According to Kwon et al. (279) increased expression of CD151 correlates well with non-small cell lung cancers and patients with lung adenocarcinomas and thus may be an improved prognostic marker. Studies have also shown in other cancers such endometrial cancers, CD151 expression is argued to be more a reliable prognostic marker than possibly histology studies.(280,281)

Liver phenotypes associated with diseased conditions as a consequence of CD151 deficiency have not been reported in the literature. Tsujino et al. (273) did report however of fibrotic changes occurring in the liver of CD151 deficient mice however in humans liver symptoms are very rarely observed in pulmonary fibrosis. In a transgenic adenocarcinoma mouse prostate model, mice lacking CD151 displayed a significant decrease on metastasis in the lung but not the liver.(282) The effect of CD151 absence in the liver remains unclear however given the numerous lines of evidence in the literature, physiological functions

relying on integrin-ligand interactions, signalling, integrin intracellular trafficking, and compartmentalisation will likely be affected by the absence of CD151.(107,252)

In addition to investigating the tissue architecture of organs, plaque development in ApoE$^{-/-}$ and ApoE$^{-/-}$.CD151$^{-/-}$ in the aortic valve cusps of 16 week old mice were also investigated in this chapter. Atherosclerotic plaque lesions were measured as a marker of plaque burden in ApoE$^{-/-}$ and ApoE$^{-/-}$.CD151$^{-/-}$ mice. Although the absence of CD151 has not been observed in the context of atherosclerosis, studies have shown to expect plaque development and the formation of foam cells in as early as approximately 10 to 15 weeks of age in ApoE$^{-/-}$ mice on a C57BL/6 WT background.(247,248,283) The progression of atherosclerosis and development of plaques occurs quicker in ApoE$^{-/-}$ western diet fed mice compared to chow fed mice.(283) Fibrous plaques begin appearing in ApoE$^{-/-}$ mice after 20 weeks and were reported to be smaller in lesion size compared to mice fed a chow diet.(283) Early fibrous plaques contain necrotic cores with foam cells enclosed by a fibrous cap composed of smooth muscle cells, elastic fibres and collagen. Nakashima et al. (244) also found foam cells to persist in chow fed mice up to 30 weeks of age.(248) Plaque lesions in the aortic valve cusps of 16 week old ApoE$^{-/-}$ and ApoE$^{-/-}$.CD151$^{-/-}$ chow fed mice were subjected to H & E staining, Van Giesons and Massons trichrome staining for the identification of plaques and comparison in plaque lesion area between the strains. Specialised staining allowed for identification of collagen deposition and smooth muscles in plaques as well staining of normal tissue architecture. We predicted that the types of lesions expected would be that of early to intermediate atherosclerotic plaque lesions as categorised according to Virmani et al. (284) atherosclerotic plaque classification guidelines.(284)

4.2 Results

4.2.1 Histopathology of lung sections between ApoE$^{-/-}$ and ApoE$^{-/-}$.CD151$^{-/-}$ mice

Despite the abundant expression of CD151 in lungs, its role in lung functioning in an atherosclerotic setting has not been determined. Studies have investigated CD151 deletion and its implication on lung function in C57BL/6 WT mice.(273) The presence of CD151 is found to be critical for the function of alveolar epithelial cells where a deficiency results in mesenchymal-like abnormalities and transforming growth factor-β activation which leads to pulmonary fibrosis.(274,275) CD151 is most abundantly expressed in the basolateral surfaces of endothelial and epithelial cells. The tetraspanin is required to maintain epithelial integrity and adhesion of alveolar epithelial cells to basement membranes and thus essential for lung structural development and maintenance.(285,286) *In vitro* and *in vivo* models of cancer have also found CD151 be a positive regulator of tumour progression in various types of tumours.(251,256) Intravasation and cell migration is augmented by CD151 and contributes to tumour metastasis.(287) CD151 has been associated with the retention of cancer cells in lung vascular beds and lung metastasis.(121,257) Transgenic adenocarcinoma of mouse prostate cancer models with a CD151 deficiency displayed significant impairments in the pulmonary metastasis formation.(282)

Histopathological studies were performed on lung sections of ApoE$^{-/-}$ and ApoE$^{-/-}$.CD151$^{-/-}$ mice. It is unknown if the absence of CD151 affects the lung architecture of ApoE$^{-/-}$ atherosclerotic mice and if in an atherosclerotic setting, CD151 deficient mice may display a similar phenotype to C57BL/6 WT mice lacking CD151. H & E staining was used to identify if any abnormalities were present in the morphology of the lung between the strains, and to characterise the lung morphology of ApoE$^{-/-}$ and ApoE$^{-/-}$.CD151$^{-/-}$ mice.

Lungs were harvested from 16 week old ApoE$^{-/-}$ and ApoE$^{-/-}$.CD151$^{-/-}$ mice. Cross sections stained with H & E were imaged with a Leica DMD108 microscope with a 4x and 10x objective and camera. This investigation did not find any abnormalities in lung morphology in the absence of CD151 between the strains (Figure 4.1), as the morphology of the alveoli appears normal in ApoE$^{-/-}$ and ApoE$^{-/-}$.CD151$^{-/-}$ mice (Figure 4.1 b and 4.1 d).

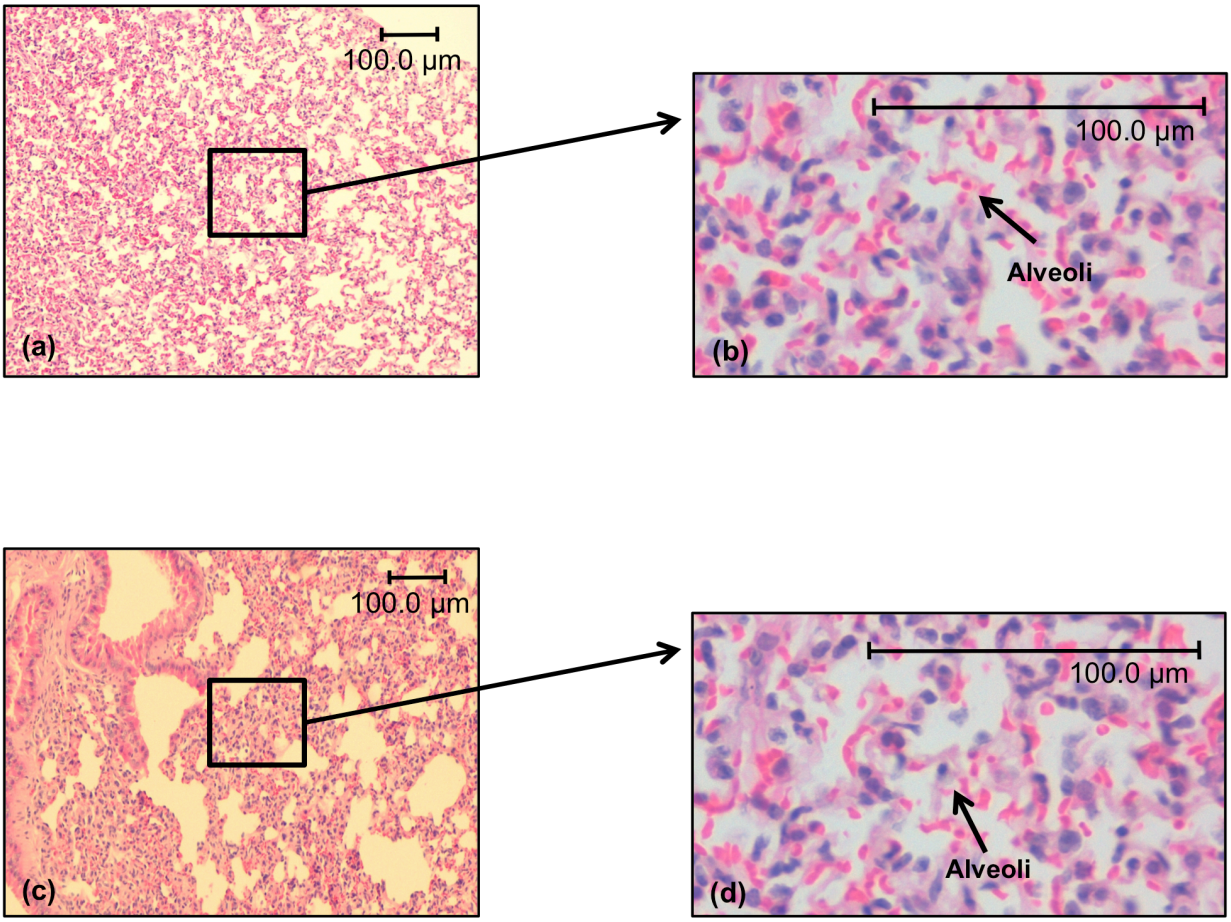

Figure 4.1. Histopathology of the lung from an ApoE$^{-/-}$ mouse. Representative images indicate that (a) Lungs show normal morphology (H&E), x10). (b) Alveoli appears normal (H&E, x40). Histopathology of the lung from an ApoE$^{-/-}$.CD151$^{-/-}$ mouse (c) shows normal morphology (H&E), x10). (d) Alveoli appears normal (H&E, x40). An N=17 was examined in each group.

4.2.2 Histopathology of liver sections between ApoE$^{-/-}$ and ApoE$^{-/-}$.CD151$^{-/-}$ mice

Liver cross sections of ApoE$^{-/-}$ and ApoE$^{-/-}$.CD151$^{-/-}$ mice were studied. It is unknown if the absence of CD151 affects the liver function and the morphology of the organ in ApoE$^{-/-}$ atherosclerotic mice. H & E staining was used to identify if any liver abnormalities were present between the strains, and to characterise the liver morphology of ApoE$^{-/-}$ and ApoE$^{-/-}$.CD151$^{-/-}$ mice.

Representative images of liver cross sections harvested at 16 weeks and stained with H & E are shown in Figure 4.2. Sections were imaged with a Leica DMD108 microscope with a 4x and 10x objective and camera. No abnormalities were observed in the liver of both ApoE$^{-/-}$ and ApoE$^{-/-}$.CD151$^{-/-}$ mice. The sinusoids, hepatocytes and binucleate hepatocytes appears normal and similar in both strains.

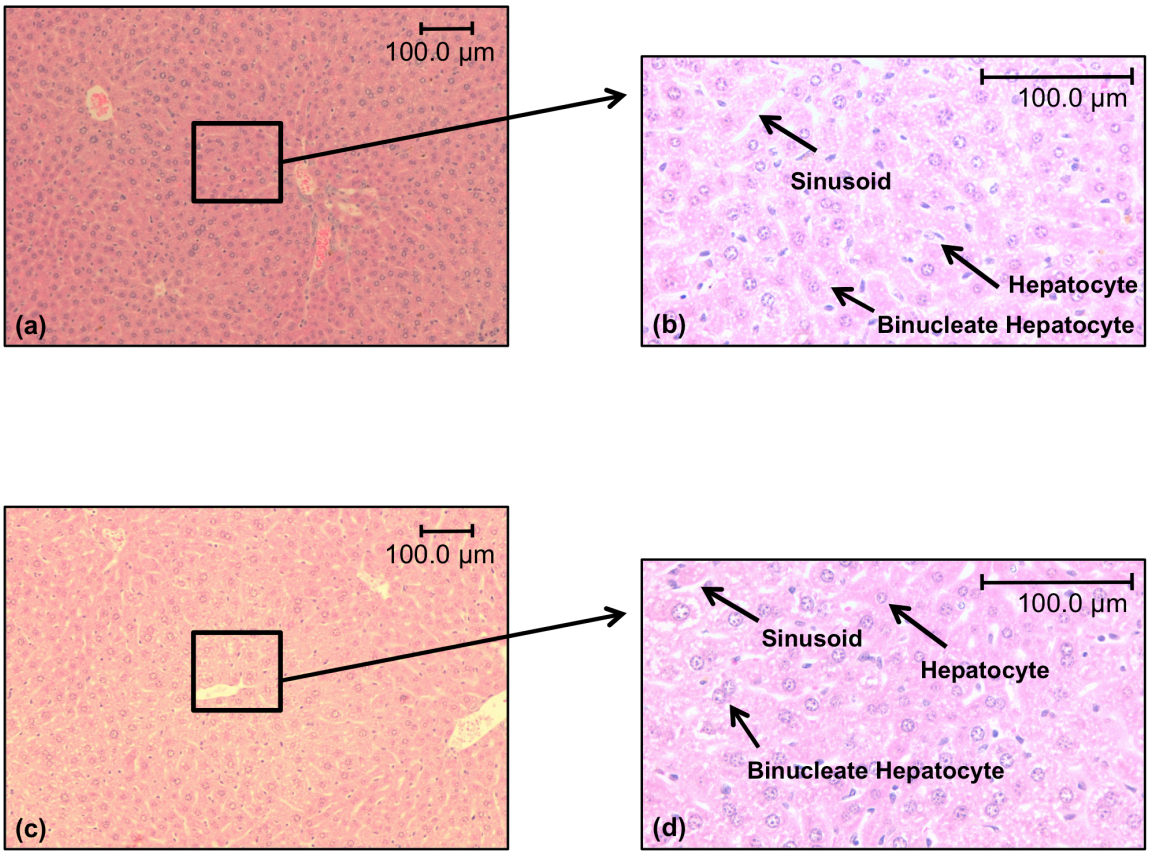

Figure 4.2. Histopathology of the liver from an ApoE$^{-/-}$ (a) and (b), and ApoE$^{-/-}$.CD151$^{-/-}$ (c) and (d) mouse. (a) and (c) Both livers shows normal morphology with sinusoids and hepatocytes visible (H&E, x10). (b) Hepatocyte and sinusoid appears normal (H&E, x40). Binucleate hepatocytes can be seen and are common both in mouse and human hepatocytes. An N=17 was examined in each group.

4.2.3 Histopathology of kidney sections between ApoE$^{-/-}$ and ApoE$^{-/-}$.CD151$^{-/-}$ mice

ApoE$^{-/-}$ and ApoE$^{-/-}$.CD151$^{-/-}$ mice kidneys were harvested at 16 weeks, cross sectioned and stained with H & E. The absence of CD151 in an atherosclerotic setting has not been studied, where its influence on kidney function and architecture are unknown. H & E staining was used to identify if any abnormalities were present in the morphology of the kidneys between the strains, and to characterise ApoE$^{-/-}$ and ApoE$^{-/-}$.CD151$^{-/-}$ mice kidney morphology through histopathological studies.

Representative images of kidney sections are shown in Figure 4.3 identifying no differences between ApoE$^{-/-}$ and ApoE$^{-/-}$.CD151$^{-/-}$ genotypes. The Bowmans capsule, glomerulus and epithelia appear normal (Figure 4.3 b and d). The absence of any abnormalities indicate the deletion of CD151 in an atherosclerotic setting has had no influence on kidney morphology.

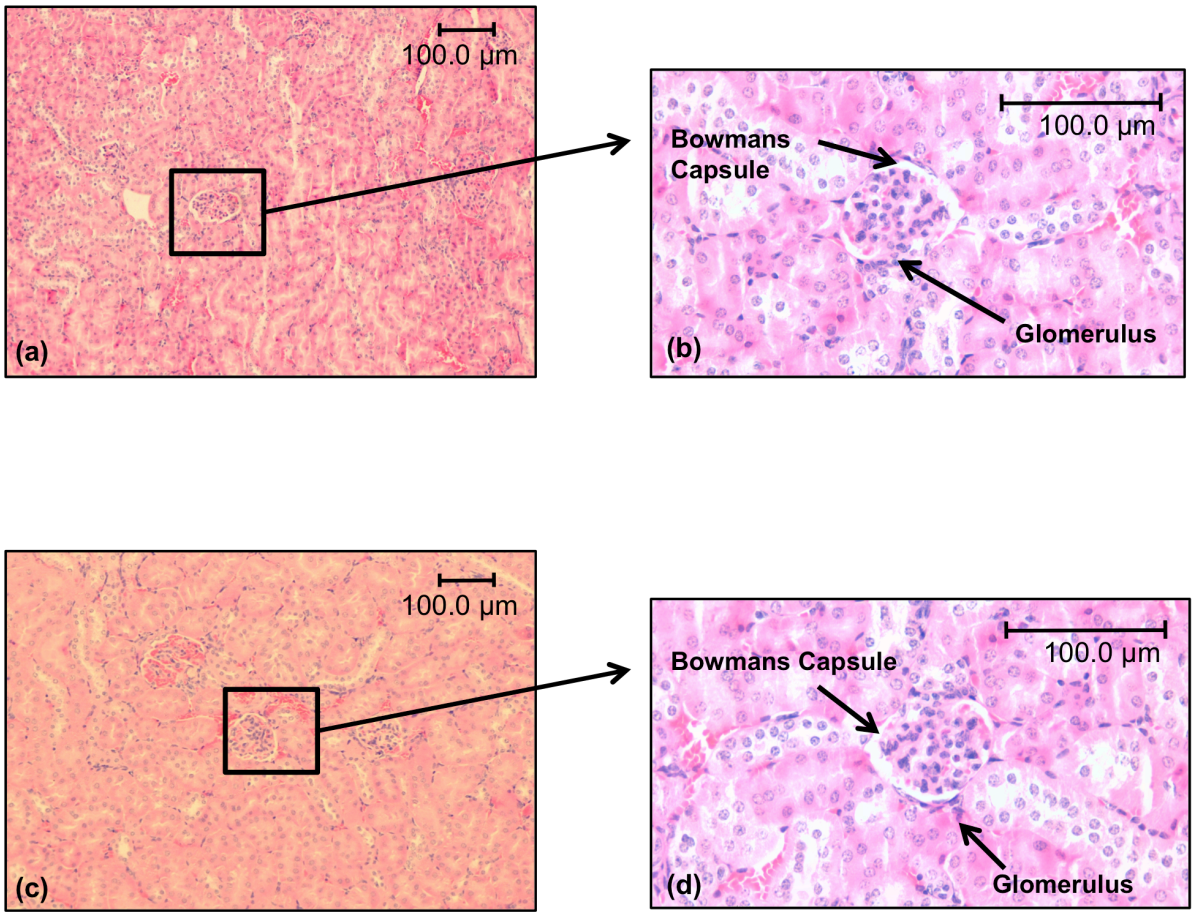

Figure 4.3. Histopathology of the kidney from an ApoE$^{-/-}$ (a) and (b), and ApoE$^{-/-}$.CD151$^{-/-}$ (c) and (d) mouse. (a) and (c) Kidneys show normal morphology (H&E, x10). Glomeruli and the flattened epithelial linings of the loops of Henle are also visible. (b) and (d) The glomerulus is surrounded by the Bowmans capsule (H&E, x40). The Bowmans capsule epithelium is squamous in a female mouse. An N=17 was examined in each group.

4.2.4 Identifying collagen presence in atherosclerotic plaques with Masson's trichrome staining

Specialised Masson's trichrome Staining was used to reveal the presence of collagen deposition in atherosclerotic plaques of 16 week old ApoE$^{-/-}$ and ApoE$^{-/-}$.CD151$^{-/-}$ mice. Plaques were restricted to those located in the aortic valve cusps of ApoE$^{-/-}$ and ApoE$^{-/-}$.CD151$^{-/-}$ mice. Representative microphotographs of atherosclerotic plaques in these mice showed collagen deposits and some cholesterol clefting present in both ApoE$^{-/-}$ and ApoE$^{-/-}$.CD151$^{-/-}$ mice. Qualitatively, the morphological characteristics of the plaques were indistinguishable between the mouse genotypes. The ApoE$^{-/-}$ mice genotype were observed to have more lesions present in their aortic valve cusps compared to ApoE$^{-/-}$.CD151$^{-/-}$ mice. Quantitative studies of lesion areas and overall plaque burden was performed on aortic valve cusp sections stained with H & E in subsequent studies. Until the current study, no previous reported studies have been found to have studied the absence of CD151 in atherosclerosis and its influence of collagen deposition in plaque development through the use of specialised stains such as the Massons trichrome Stain.

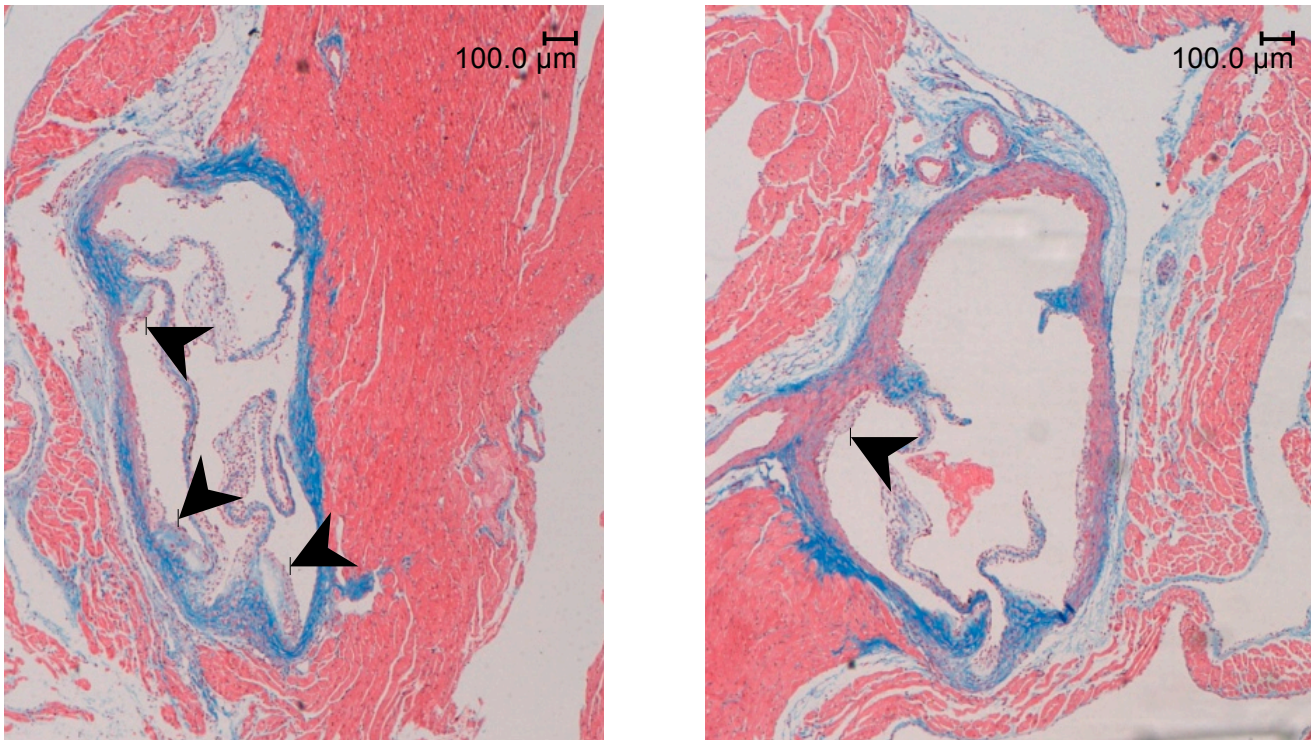

Figure 4.4. Aortic Valve Cusps (AVC) in ApoE$^{-/-}$ (Left), ApoE$^{-/-}$.CD151$^{-/-}$ (right) stained with Masson's trichrome for collagen. Black arrow heads identify lesion areas. Collagen is stained blue, nuclei is stained black and cytoplasm, muscle and erythrocytes are stained red. Light microscopy, original magnification 4x. An N=17 was examined in each group.

4.2.5 Identifying the presence of elastic fibres and collagen in atherosclerotic plaques with Verhoeff Van Giesons staining

The aortic valve cusps of ApoE$^{-/-}$ and ApoE$^{-/-}$.CD151$^{-/-}$ mice were stained with Verhoeff Van Gieson stain to identify the presence of elastic fibres and collagen in atherosclerotic plaques (Figure 4.5). No distinguishable differences in plaque morphology was observed between the ApoE$^{-/-}$ and ApoE$^{-/-}$.CD151$^{-/-}$ genotypes. Elastic fibres and nuclei stained blue-black and black whilst collagen is stained red. Studies were performed on 16 week old mice on a normal chow diet fed ad libitum.

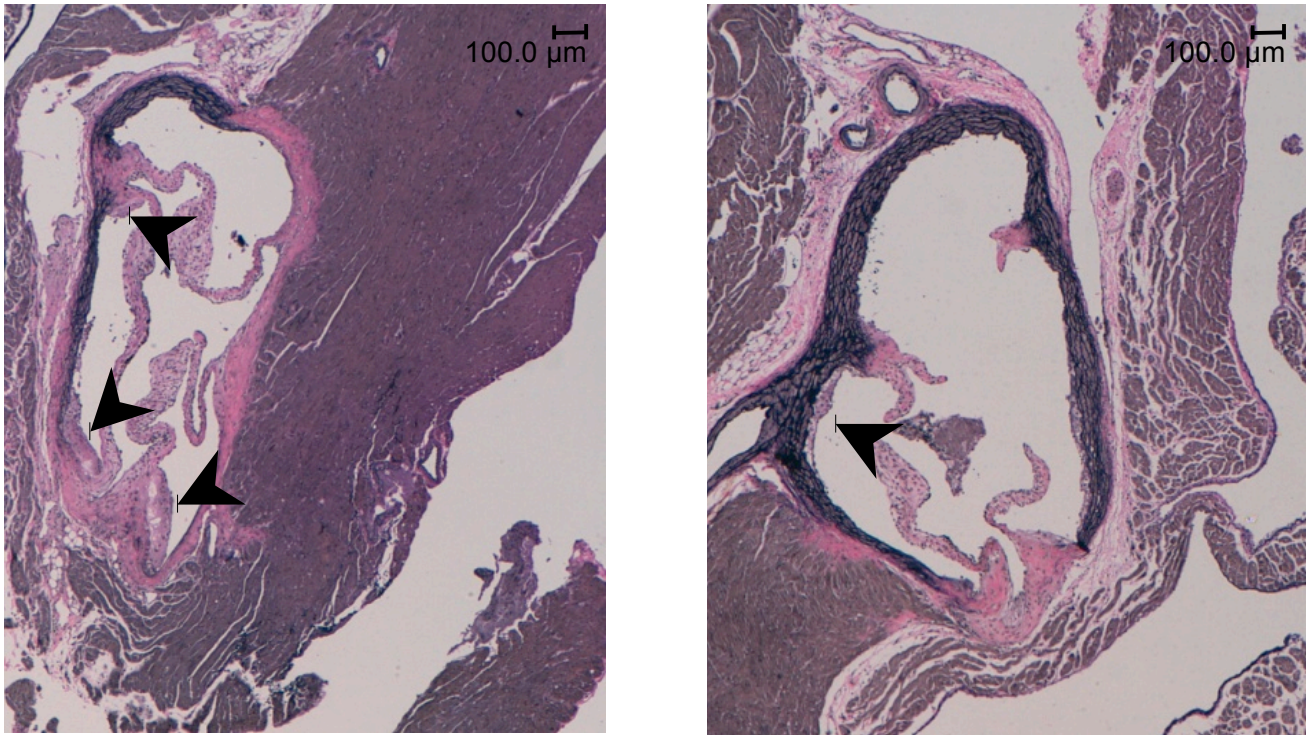

Figure 4.5. Aortic Valve Cusps (AVC) in ApoE$^{-/-}$ (Left), ApoE$^{-/-}$.CD151$^{-/-}$ (right) stained with Verhoeff Van Gieson for elastic fibres. Black arrow heads identify lesion areas. Elastic fibres and nuclei are stained a blue/black colour and collagen a red stain. Light microscopy, original magnification 4x. An N=17 was examined in each group.

4.2.6 Comparing plaque burden of ApoE$^{-/-}$ mice to ApoE$^{-/-}$.CD151$^{-/-}$ mice by quantifying atherosclerotic lesion areas in aortic valve cusps

Haematoxylin and eosin stained aortic valve cusp sections from ApoE$^{-/-}$ and ApoE$^{-/-}$.CD151$^{-/-}$ mice were measured to determine plaque burden and the influence of CD151 absence on atherosclerotic lesion development. Quantification was performed using the area measurement tool in the Leica DMD108 microscope imaging system. At 16 weeks, ApoE$^{-/-}$.CD151$^{-/-}$ mice showed significantly reduced atherosclerotic lesion areas compared to ApoE$^{-/-}$ mice (5266 μm^2 ± 1427 versus 34265 ± 2427, P < 0.0001 *** n=10) suggesting a delay in the development of atherosclerosis as demonstrated in the ApoE$^{-/-}$.CD151$^{-/-}$ model (Figure 4.7).

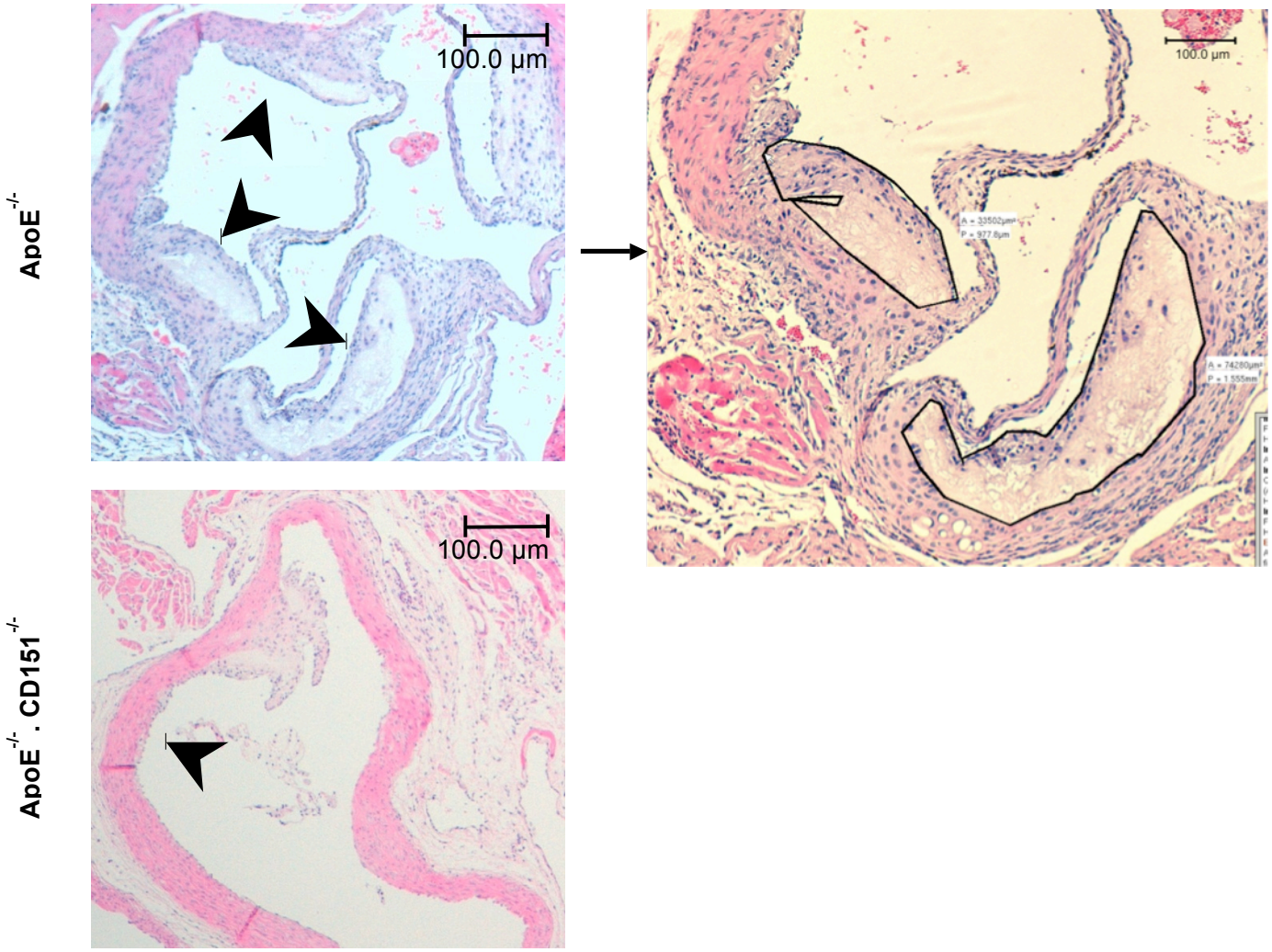

Figure 4.6. Representative images of ApoE$^{-/-}$ (female) and ApoE$^{-/-}$.CD151$^{-/-}$ (female) aortic valve cusp sections stained with H & E. Lesion areas are determined by measuring around lesions with measurement tools in the Leica DMD 108 microscope imaging system software. Black arrows indicate lesions measured and foam cells. Light microscopy, original magnification 4x. The representative image shown at a higher magnification shows an inset of the ApoE$^{-/-}$ panel and a mask identifying plaque boundaries. Light microscopy, original magnification 10 x .

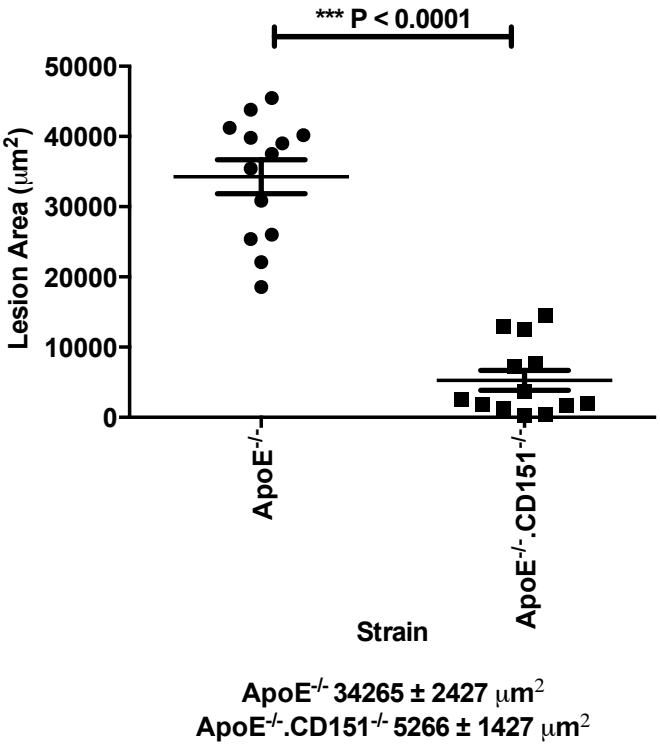

Figure 4.7. Plaque burden was quantified by measuring lesion area (μm^2) in the aortic valve cusps of 16 week old $ApoE^{-/-}$ and $ApoE^{-/-}.CD151^{-/-}$ mice. A significant reduction in plaque burden is observed in the $ApoE^{-/-}.CD151^{-/-}$ mouse genotype as compared to the $ApoE^{-/-}$ mouse. Each data point represents the average lesion area per mouse, (*** P < 0.0001, n=13, unpaired Student's t-test).

4.2.7 Sex differences in plaque burden between $ApoE^{-/-}$ and $ApoE^{-/-}.CD151^{-/-}$ mice

To investigate if sex difference has an influence on plaque burden and lesion development, plaque burden was quantified by measuring lesion areas present in the aortic valve cusps of $ApoE^{-/-}$ and $ApoE^{-/-}.CD151^{-/-}$ female and male mice. As shown in Figure 4.8, a sex difference is observed to be evident and also influential in atherosclerotic lesion development in the absence of CD151. CD151 is suggested to have a protective effect on plaque burden development in female mice as compared to male mice as observed by the marked reduction in plaque burden in the absence of CD151.

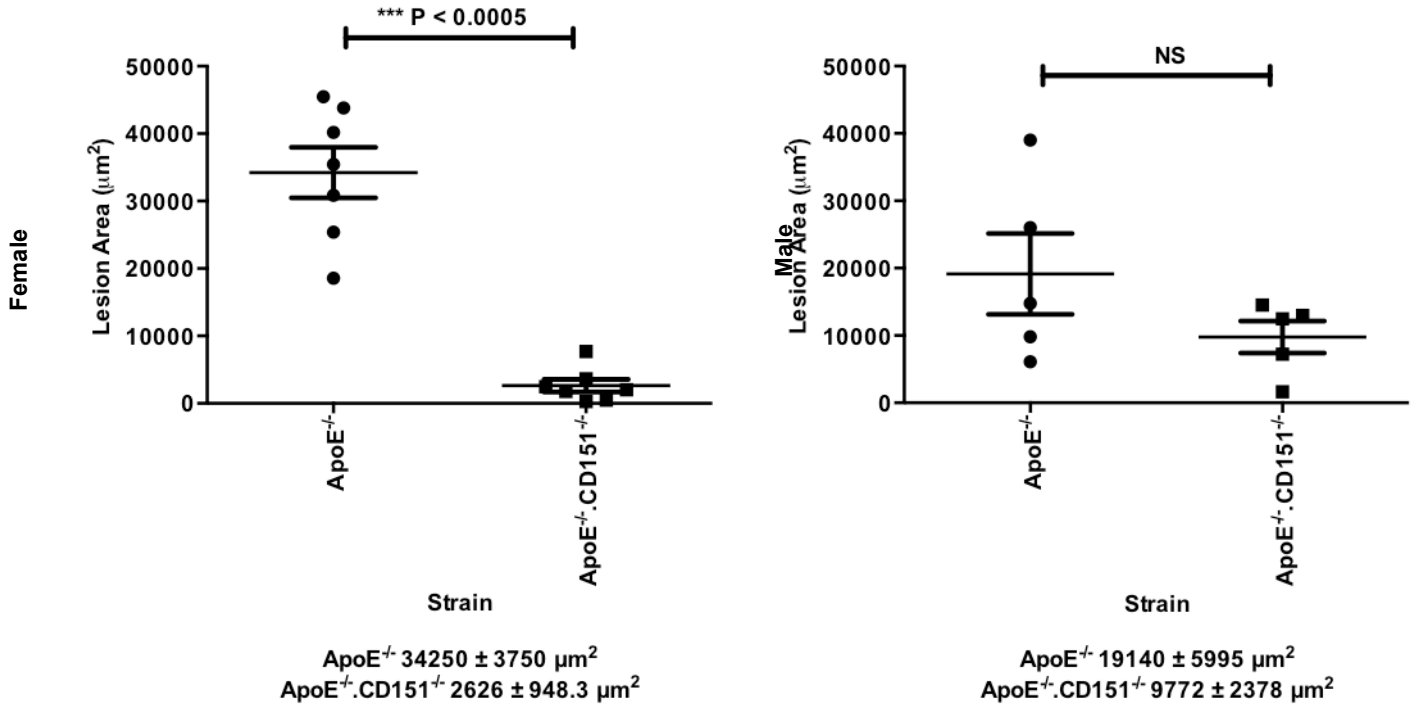

Figure 4.8. Sex difference appears to have an influence on plaque burden between ApoE$^{-/-}$ and ApoE$^{-/-}$.CD151$^{-/-}$ mice. Female ApoE$^{-/-}$.CD151$^{-/-}$ mice were found to have significantly lower plaque burden compared to female ApoE$^{-/-}$ mice. The absence of CD151 in an atherosclerotic setting does not have as much of a profound effect on male ApoE$^{-/-}$ mice. No statistically significant difference was reported between male ApoE$^{-/-}$ and ApoE$^{-/-}$.CD151$^{-/-}$ mice for lesion area and thus plaque burden. (female n=7; male n=5, unpaired Student's t-test).

4.3 Discussion

In order to explore the influence of which CD151 may have on atherosclerosis, it was important to study the implications of CD151 deficiency on the development of atherosclerotic plaque lesions. Aspects of plaque burden were studied in 16 week old $ApoE^{-/-}$ and $ApoE^{-/-}$. $CD151^{-/-}$ mice. These mice were fed a standard chow diet consisting of 65% carbohydrate, 15% fat and 20% protein. This study is formed on the hypothesis that CD151 confers a protective effect on atherosclerosis when CD151 is absent. The results indicate that $ApoE^{-/-}$.$CD151^{-/-}$ mice have a significantly decreased plaque burden compared to $ApoE^{-/-}$ mice.

Prior to the development of the $ApoE^{-/-}$ mouse model, the C57BL/6 mice was the sole murine atherosclerosis animal model available.(288,289) There are limitations however to this latter model in that the development of atherosclerosis and atherogenesis lacks consistency with the progression of the disease in humans. The atherosclerotic lesions which are formed in C57BL/6 WT models differ in their characteristics and composition when compared to human atherosclerosis. The $ApoE^{-/-}$ model develops not only hypercholesterolaemia but also forms several types of lesions thatare observed to present in aortic valve cusps as well as in the arterial tree, whereas lesions in the $ApoE^{-/-}$ model are more extensive varying from foam cells to fibrous plaques observed in more chronic and advanced atherosclerosis.(215, 290) On a normal chow diet, $ApoE^{-/-}$ mice are reported to begin displaying small nodule like lesions at 10 weeks of age. In C57BL/6 WT mice however, a diet consisting of 1.25% cholesterol, 10% - 15% saturated fats and 0.5% cholic acid is required to induce lesion development, and is physiologically irrelevant to human diets.(288,289)

Atherosclerotic plaque lesions in the aortic valve cusps were stained with H & E and measured for lesion area size as an indication of plaque burden. The results propose a protective effect of CD151 deficiency as the $ApoE^{-/-}$.$CD151^{-/-}$ group showed significantly lower plaque lesion areas (34265 ± 2427 μm^2 versus 5266 ± 1427 μm^2, $P < 0.0001$ *** n=10; Figure 4.6). A spread in the results was observed (Figure 4.7) and upon further analysis for sex differences, it appears that the female $ApoE^{-/-}$.$CD151^{-/-}$ group specifically were found to have a significantly reduced plaque burden (Figure 4.8). This protective effect of CD151 absence did not carry over in males, as the plaque burden in $ApoE^{-/-}$ and $ApoE^{-/-}$. $CD151^{-/-}$ groups did not show any statistically significant differences. Compared to the literature, the plaques found to predominantly develop in the $ApoE^{-/-}$ and $ApoE^{-/-}$.$CD151^{-/-}$ mice were early

and occasionally intermediate lesions. Necrotic cores formed were small and did not appear to be advanced in nature. Note that Nakashima et al. (248) reported well formed fibrous plaques to develop only after 20 weeks of age in mice fed a chow diet whereas mice fed western style diets may begin demonstrating formation of early fibrous plaques in as early as 15 weeks of age as lesion formation is known to be delayed in chow fed mice compared to high fat western diet fed mice.(248) Classification according to human atherosclerotic lesion classification by the American Heart Association places the plaques observed in ApoE$^{-/-}$ and ApoE$^{-/-}$.CD151$^{-/-}$ to also be early lesions varying from Type II to Type III lesions.(143,291)

In humans, gender predisposition to atherosclerosis is suggested to occur in males.(292) As monocyte derived macrophages are known to be integral in the introduction of early signs of atherosclerosis by the formation of fatty streaks, McCrohon et al. (292) hypothesised that increased expression of androgen receptors in males would result in a predisposition to atherosclerosis. Their data indicated that a dose related, as well as a receptor mediated, increase in human macrophage lipid accumulation occurred in males only.(292) On the contrary, a paper investigating published reviews of associations of ApoE genotype and coronary disease noted biases in findings due to small study populations. The authors reassessed published associations between lipid levels, coronary risk and ApoE genotypes which previously had suggested a link between ApoE genotypes and women.(293,294) Furthermore they established that such associations in relation to sex and atherosclerosis disease is not relevant.(293) Females however are reported to develop atherosclerosis and heart disease later in life compared to men, and is associated with the decrease in sex steroid hormones which occur in menopause.(295) A study examined the response of vascular neotintimal formation in males and females by using a cuff on the femoral artery. The results showed male mice respond more significantly than females in intimal growth.(296) Studies have also shown that disease prognosis specifically in acute or chronic coronary disease is reported to be worse in males than females.(297) Males and females are said to encounter similar levels of cardiac risk factors however the response to increased atherosclerotic risk burdens may be dependent on gender specific differences that may be influenced by hormones.(298-305) Studies in murine models have shown that administration of estrogen provides atheroprotective effects.(306) Interestingly, studies have also reported that female ApoE$^{-/-}$ mice develop larger lesions that males in the aortic sinus.(307) Minimal differences in plaque burden and distribution of lesions throughout the aorta have been noted between male and female ApoE$^{-/-}$ mice as well as LDL receptor deficient mice.(308) Atherosclerosis development has also been reported to show associations between gender and immunity. The extent of atherosclerosis in the inominate

arteries of male and female ApoE$^{-/-}$ mice are reported to be similar however in conditions in which immunity is compromised and deficiencies are present, atherosclerosis is reduced in ApoE$^{-/-}$ mice only.(309) In light of the literature, our findings suggest a protective role of CD151 absence in atherosclerosis, specifically in female mice. With this, it would be of interest to consider examining the influence of CD151 absence in mice of older ages and also to monitor reproductive hormones, and detectable immune deficiencies. Note that animal welfare and the monitoring of skin lesions is of upmost importance and may be limiting in the experimental period of future studies.

Representative images of H & E stained aortic valve cusps shown in Figure 4.6 illustrates the presence of early foam cell presence in ApoE$^{-/-}$ and ApoE$^{-/-}$.CD151$^{-/-}$ mice. Visually the ApoE$^{-/-}$. CD151$^{-/-}$ mice had fewer and smaller lesions present. In both ApoE$^{-/-}$ and ApoE$^{-/-}$. CD151$^{-/-}$ groups, the Masson's trichrome (Figure 4.4) specialised stain for collagen showed collagen staining (blue) being more dominant in the mass of the lesion and very minimally on the perimeter or cap of lesions, which showed some red staining indicative of muscle, erythrocyte and cytoplasm staining. Likewise when the Verhoeff Van Gieson stain was used, the lesions stained red for collagen, whilst around the perimeter of the lesion, staining was mostly blue/black which is suggestive of elastic fibre staining (Figure 4.5). These qualitative findings reveal that at 16 weeks, ApoE$^{-/-}$ and ApoE$^{-/-}$.CD151$^{-/-}$ have developed foam cells and are beginning to show formation of a fibrous cap and progressing from early to intermediate lesion development. As discussed prior, fibrous plaques are typically observed after 20 weeks where in comparison this study did not extend further than 16 weeks as a precaution against animal welfare issues of skin lesion development. Immunohistochemical studies staining specifically for anti type I collagen, macrophages and smooth muscle actin would assist further in confirming the type of cells found in the plaque and determine composition of plaques between ApoE$^{-/-}$ and ApoE$^{-/-}$.CD151$^{-/-}$ mice. These findings will follow in Chapter 5.

Furthermore, histology analysis on the morphology of representative kidney, lung, and liver sections stained with H&E showed normal morphology and organisation of structures in both ApoE$^{-/-}$ and ApoE$^{-/-}$. CD151$^{-/-}$ mouse groups. The loss of CD151 in the double knockout model did not bring about conditions which have been reported in the literature. Studies have shown that due to the high affinity associations of CD151 with integrins $\alpha_6\beta_4$ and $\alpha_3\beta_1$, deletion or mutations to any of the integrin chains namely α_6 or β_4 leads to neonatal death by a condition with phenotype similar to epidermolysis bullosa in humans.(265,310) These

patients which present with a syndrome referred to as Alport display symptoms of sensorineural deafness in addition to epidermolysis bullosa. Patients exhibiting these symptoms are recommended to be tested for assays pertaining to lung function and observation of fibrotic changes, if present.(124)

Basement membrane rupture occurring in kidneys and lung epithelia also leads to neonatal deaths in mice with an α_3 integrin deletion.(240) Absence of the β_1 unit in conjunction with α_3 absence are also observed to contribute to proteinuria and renal disease.(270) Similarly deficiencies in the β_1 subunit of integrins is observed in pulmonary fibrosis, given its associations with CD151.(276,277)

Sachs and colleagues (270) found in 12 week old CD151$^{-/-}$ mice on a similar C57BL/6 WT background to display a variability in the severity of renal pathology in mice lacking the CD151 tetraspanin in different litters. Through light microscopy the authors noted of interstitial fibrosis, some glomerulosclerosis occurring mildly and more extensive glomerulosclerosis and adhesions to the Bowman's capsule in mice that were more severely affected by the deficiency of CD151.(270) The current investigation did not detect any of these abnormalities and was unchanged between ApoE$^{-/-}$ and ApoE$^{-/-}$.CD151$^{-/-}$ mice, with structures staining and appearing normally. Parallels drawn from previous literature and the differences in genetic background of mice used to investigate the deficiency of CD151 in kidneys as well as other organs may be accountable for reasons as to why renal failure did not manifest in the ApoE$^{-/-}$ and ApoE$^{-/-}$.CD151$^{-/-}$ mouse groups.(102,242,270) FVB models have been used in the past to validate the involvement of CD151 in adhesion strengthening.(272) Nonetheless, the absence of CD151 was consistently shown to be imperative for normal renal function and especially in the adhesion of podocytes to glomerular basement membranes.(272)

Although no specific disease phenotypes have been associated with CD151 deficiency in the liver, CD151 absence has been implicated in cancer conditions whereby CD151 is involved in tumour progression and the migration and invasion of cancer cells which are associated with the lateral complexes formed between integrins $\alpha_6\beta_4$ and $\alpha_3\beta_1$, $\alpha_6\beta_1$ with CD151.(237,261,262) Histology analysis conducted for this thesis did not observe any differences between ApoE$^{-/-}$ and ApoE$^{-/-}$.CD151$^{-/-}$ mouse groups in the tissue architecture and morphology and thus in atherosclerosis, CD151 deficiency is unlikely to affect liver

function.(107) According to the literature increased CD151 expression has been shown to correlate with poor prognosis of various cancers, inclusive of liver tumours. (195,311)

Histology analysis of ApoE$^{-/-}$ and ApoE$^{-/-}$. CD151$^{-/-}$ lung tissue architecture and morphology in this study did not demonstrate any changes associated with CD151 deficiency in atherosclerosis disease. Prior to the investigations led by Tsujino et al. (311), CD151 had not been studied in the context of pulmonary fibrosis disease. The only other condition in which CD151 absence has been observed to result in disease is cancer where overexpression of CD151 correlated with lung carcinomas.(280) H & E staining of 30 week old CD151 (C57BL/6 WT background) deficient mouse lungs showed only slight changes to alveolar structures which the authors concluded to be insignificant. However through Azan staining, they reported an increase in the deposition of collagen in alveolar walls which together with microarray studies were proposed to be linked with the spontaneous development of pulmonary fibrosis.(273) To validate these findings, Tsujino et al. (273) performed electron microscopy studies which at 16 weeks of aged showed an increase in collagen deposition in alveolar walls and presence of hypertrophied alveolar epithelial cells. The basement membranes of the epithelial cells were also thicker than normal. On a similar C57BL/6 WT background but in conjunction with atherosclerotic disease and at approximately half the age, the ApoE$^{-/-}$ and ApoE$^{-/-}$.CD151$^{-/-}$ mouse groups investigated in this study did not appear to be affected by the absence of CD151 in tissue architecture, morphology as well as function.

In light of these findings CD151 was not observed to have impacted on the liver, kidneys and lungs of ApoE$^{-/-}$.CD151$^{-/-}$ mice with tissue architecture being comparable between ApoE$^{-/-}$ and ApoE$^{-/-}$.CD151$^{-/-}$ mouse groups. Being a novel strain, ApoE$^{-/-}$.CD151$^{-/-}$ mouse genetical data has not been studied and thus the Mendelian distribution demonstrated in this study does not have a point of reference to compare to. As discussed in Chapter 3.3, the Mendelian inheritance frequencies was altered with smaller litter sizes and survival in the ApoE$^{-/-}$.CD151$^{-/-}$ mouse group. Previous studies which had investigated conditions associated with the absence of CD151 resulting in abnormalities of lung and kidney were suspected and proposed to have an influence in this reduction in Mendelian inheritance frequencies, however was not demonstrated or observed to have manifested through visualisation of respective tissue architectures in the present study. Indeed, in studying the Mendel laws of inheritance, numerous factors beyond the scope of this thesis' study may be implicated and contributory to this survival bias and segregation. Meiotic Drive Elements

(MDs) are capable of cheating Mendel laws of inheritance through disrupting chromosome segregation during the process of meiosis. In the literature, non mendelian inheritance in mice have been reported to occur as a result of the mouse t haplotype in the house mouse, involving the interaction of different genes and ultlimately affecting population numbers.(312) Note also that previously documented mutations have been identified and shown to not alter CD151 function.(124)

4.4 Conclusion

Plaque burden was found to be significantly reduced in the $ApoE^{-/-}$ mouse group lacking CD151 ($ApoE^{-/-}.CD151^{-/-}$) compared to $ApoE^{-/-}$ mice. Histological analysis of organ morphologies and tissue structures did not display any abnormalities and were consistent between the strains with organ structures appearing unchanged in the absence of CD151.

4.5 Limitations

At 16 weeks, $ApoE^{-/-}.CD151^{-/-}$ mice showed significantly reduced plaque burden compared to $ApoE^{-/-}$ mice suggesting a positive protective effect of CD151 absence. The atherosclerotic lesion types observed at this age were early to intermediate plaque lesions. As the morphology of lesions transform over the progression of atherosclerosis disease, re-examining the parameters of plaque burden at an older age would greatly extend our understanding of the contribution CD151 absence and whether the protective effect seen at 16 weeks on atherosclerosis plaque burden extends in older age. To confirm the findings determined on the characterisation of organs in the absence of CD151 in atherosclerotic disease, organs should be harvested at an older age to examine for defects if any, to the epithelial membranes in particularly the kidneys and lungs. Finally, the gold standard of histology staining in atherosclerosis is Oil red O and Sudan black staining for lipids and thus warrant further studies to include these staining techniques for determining the presence of plaques lesions in the aortic valve cusps of $ApoE^{-/-}$ and $ApoE^{-/-}.CD151^{-/-}$ mice. Despite this, studies have been observed to assess plaque lesion areas and burden solely on H&E stained sections. Due to logistics, limited access to facilities and training, Oil Red O staining was not achievable and technique was unsatisfactory. H&E staining was found to provide in this instance, more accurate measurements of plaque lesions areas in the aortic valve cusps of mice studied.

5 CHAPTER 5: INVESTIGATING THE ROLE OF CD151 IN PLAQUE COMPOSITION USING AN APOE$^{-/-}$ MOUSE MODEL.

5.1 Introduction

Atherosclerosis is referred to as a chronic inflammatory disease characterised by the interaction of monocytes with adhesion molecules on endothelial surfaces.(313,314) These events of endothelium dysfunction are observed to precede the appearance of atherosclerotic plaques which is subsequently followed by a series of events involving the migration of lipoproteins, lymphocytes into the endothelial space, an increase in vascular permeability, proliferation of smooth muscle cells and progression to an increased proinflammatory state.(315,316) Vascular inflammation occurring in the early stages of atherosclerosis is associated with the influx of monocytes and leukocytes within the vessel wall.(317) Macrophages and dendritic cells are formed from the differentiation of monocytes and proceed to transforming into macrophage derived foam cells through the phagocytosis of lipoproteins.(318,319) Fatty streaks which present in the early phases of atherosclerosis are composed of these foam cells as well as VLDLs or LDLs.(320) The fibrous plaque is composed of foam cells, cholesterol crystals and cell debris which progressively form the necrotic core.(313,321)

The formation and progression of atherosclerotic plaques is polygenic in nature involving multiple cell types that express numerous cell adhesion molecules including CD151, a tetraspanin superfamily member. CD151 is localised to the intracellular vesicles and at cell-cell junctions in endothelial cells, at the cellular level.(7) As mentioned prior, CD151 associations with integrins are well known where complexes of this tetraspanin with specific integrins are shown to have the ability to mediate biological processes.(6, 261, 262, 322-324) These complexes include the stable associations of CD151 with laminin-binding integrins such as $\alpha_3\beta_1$, $\alpha_6\beta_1$, $\alpha_6\beta_4$, as well as $\alpha_7\beta_1$ (237,325,326) primarily in processes of cancer metastasis, cell to cell adhesion, cell to extracellular matrix adhesion strengthening and cell motility.(111,113,119,122,261,287,327,328) CD151 is expressed in endothelial cells, dendritic cells, smooth muscle cells, T lymphocytes, macrophages and platelets which are all involved in atherosclerotic plaque development and rupture.(6)

Despite showing increased CD151 expression in human atherosclerotic arteries as compared to healthy arteries, the influence of CD151 on atherosclerosis is still yet to be

elucidated.(128) CD151 is shown to be present in the medial layer and adventitial layer of vessel walls, including the endothelium.(123) A study has shown that in cultured human umbilicial vein cells, 66% of CD151 is located intracellularly. Endothelial cell CD151 meanwhile is concentrated at cell to cell junctions together with tetraspanins CD9 and CD81.(329) The interactions of CD151, CD9 and CD81 on endothelial cells are reported to be crucial for the adhesion of ICAM-1 and VCAM-1. In atherosclerosis, lesions develop and are localised in areas of which blood flow is disturbed and prone to inflammation.(330) ICAM-1 and VCAM-1 expression is increased at these areas in the course of plaque formation.(331-334) CD81 expression is upregulated in atherosclerotic lesions, especially in early stages of the disease as compared to advanced human atherosclerotic plaque lesions. Rohlena et al. (173) published on the suspected involvement of CD81 in early plaque formation. Their previous studies did not find an increased expression of CD151 or CD9 in an atherosclerotic setting in comparison to CD81.(335) Notwithstanding the varied and limited findings on CD151 in atherosclerosis, it is critical to investigate these findings particularly as atherosclerosis is influenced by a number of different cells, inclusive of platelets.(336) Disruption to the endothelium consequently results in platelet adhesion and leukocyte infiltration, occurring early in the development of atherosclerosis.(145) Inhibition of platelet adhesion has shown to decrease the accumulation of leukocytes and the subsequent reduction in atherosclerotic lesion development in $ApoE^{-/-}$ mice.(337) Barreiro et al. (338) have similarly reported the integral role of CD151 in the migration of lymphocytes and in maintaining stable adhesion of lymphocytes subjected to extravasation.(338)

According to recent *in vitro* and *in vivo* studies, CD151 has been shown to be a promoter of angiogenesis.(7,102,242,322) Studies utilising CD151 deficient animals have supported this finding, and reinforced the function of CD151 in vesicle trafficking.(339-342) Angiogenesis is reported through histology studies to be influential in the development of atherosclerotic plaque lesions, as the formation of new vessels within atherosclerotic plaques and arterial walls are associated in the pathogenesis of cardiovascular events.(343,344)

Whilst histologic analysis of the aortic valve cusps for quantification of plaque lesion areas are informative in determining plaque burden in $ApoE^{-/-}$ versus $ApoE^{-/-}$. $CD151^{-/-}$ mice (Chapter 4), immunohistochemical studies for the assessment of CD151 expression, F4/80 macrophages, type I collagen and smooth muscle actin are also important to investigate plaque composition. The influence of CD151 absence is unknown in the progression of atherosclerosis and plaque development. Investigating different markers allows for the

characterisation of cellular components associated with plaques at 16 weeks of age between the ApoE$^{-/-}$ and ApoE$^{-/-}$.CD151$^{-/-}$ mouse model and to support the hypothesis that CD151 absence confers a protective effect on atherosclerosis. Histopathological examination of plaque lesions with H & E staining in Chapter 4 (Representative images shown in Figure 4.6) showed that plaques formed were comparable to early and intermediate lesions of ApoE$^{-/-}$ on a C57BL/6 WT genetic background observed by Nakashima et al. (248) Classification of the atherosclerotic lesions according to the American Heart Association showed early lesions or Type II to Type III lesions. The latter lesion type, also known as intermediate lesion (preatheroma) was mostly observed in the ApoE$^{-/-}$.CD151$^{-/-}$ mouse group.(345)

5.2 Results

5.2.1 CD151 H80 expression in atherosclerotic plaques of ApoE$^{-/-}$ mice compared to ApoE$^{-/-}$.CD151$^{-/-}$ mice

CD151 expression was examined in ApoE$^{-/-}$ atherosclerotic plaque lesions formed in the aortic valve cusps of 16 week old mice. ApoE$^{-/-}$.CD151$^{-/-}$ plaque lesions were also examined to compare the affect of CD151 absence on the development of an atherosclerotic plaque and to confirm the presence of CD151 in atherosclerotic plaque lesions. Being a broadly expressed tetraspanin, CD151 is present not only on platelets but also on endothelial cells, smooth muscle, megakaryocytes, cardiac muscle, immune system and epithelia.(5) In platelets specifically, the absence of platelet CD151 *in vivo* results in smaller and thrombi that are more prone to embolisation and instability. Thrombus growth and stability *in vivo* has also been reported to be regulated by platelet CD151.(197)

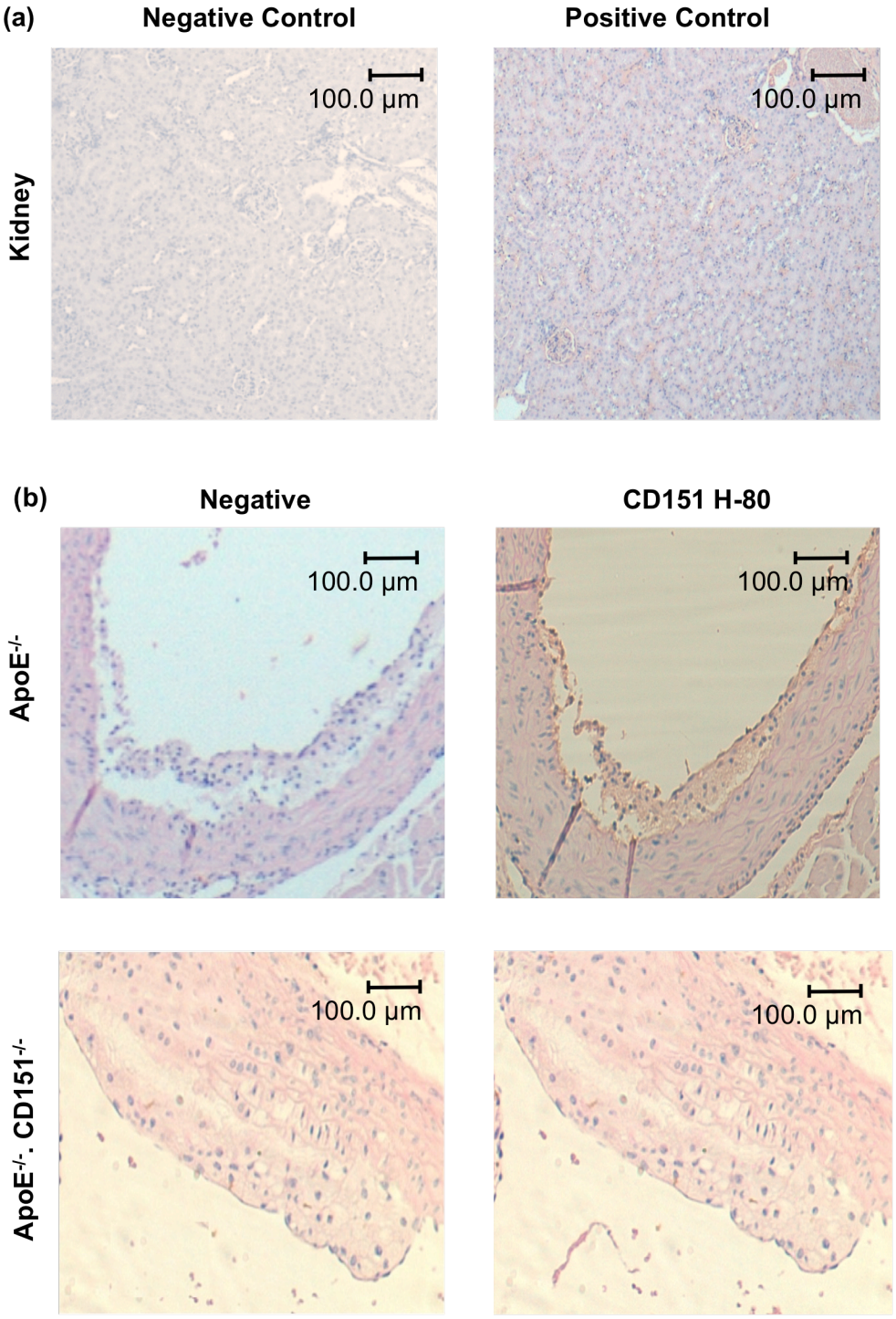

Figure 5.1. IHC staining of the aortic valve cusp of $ApoE^{-/-}$ and $ApoE^{-/-}$. $CD151^{-/-}$ mice was performed to stain for CD151 expression. (a) – (b) CD151 H80 rabbit polyclonal primary antibody was used at a dilution of 1/800, whilst a peroxidase conjugated affini-pure goat anti rabbit secondary antibody was used at a dilution of 1/800. Visualisation of the stain was carried out with DAB solution. (a) kidney tissue was subjected to the same staining protocols to serve as a positive control. CD151 expression is evident in $ApoE^{-/-}$ plaque lesions whilst $ApoE^{-/-}$. $CD151^{-/-}$ plaques lack any positive staining which is as expected.

Plaque composition was analysed and expression of CD151 quantified with the Aperio positive pixel algorithm v9.1. The results of this investigation are reported in Table 5.1 and Figure 5.1. ApoE$^{-/-}$ lesions were positive for CD151 with strong positive CD151 staining accounting for 5.7 ± 0.8 % of plaque lesions, 31.9 ± 5.5 % positive staining and 8.4 ± 3.9 % weak positive staining. ApoE$^{-/-}$.CD151$^{-/-}$ lacked positive staining with very minimal unspecific weak positive staining observed (3.4 ± 1.1 %) and negativity for 96.0 ± 1.3 % of the plaque lesion (Table 5.1 and Figure 5.2). These results confirm the presence and expression of CD151 in atherosclerotic plaque lesions in the ApoE$^{-/-}$ mouse model. Positive control kidney tissues validates these results together with the lack of positive staining of CD151 in atherosclerotic plaque lesions of ApoE$^{-/-}$.CD151$^{-/-}$ mice.

Table 5.1. CD151 stained in plaque lesions

	Stain (Mean ± SEM % pixel positive staining)			
Genotype	**Negative**	**Strong Positive**	**Positive**	**Weak Positive**
ApoE$^{-/-}$	51.943 ± 3.561 ***	5.671 ± 0.758 ***	31.880 ± 5.467 **	8.404 ± 3.875
ApoE$^{-/-}$.CD151$^{-/-}$	96.013 ± 1.299	0.308 ± 0.090	0.261 ± 0.130	3.418 ± 1.096

An unpaired Student's t-test shows statistical significance in negative, strong positive and positive staining in ApoE$^{-/-}$ compared to ApoE$^{-/-}$.CD151$^{-/-}$ CD151 expression in atherosclerotic plaque lesions (*** $P < 0.0005$, ** $P < 0.005$, n=10 in each group).

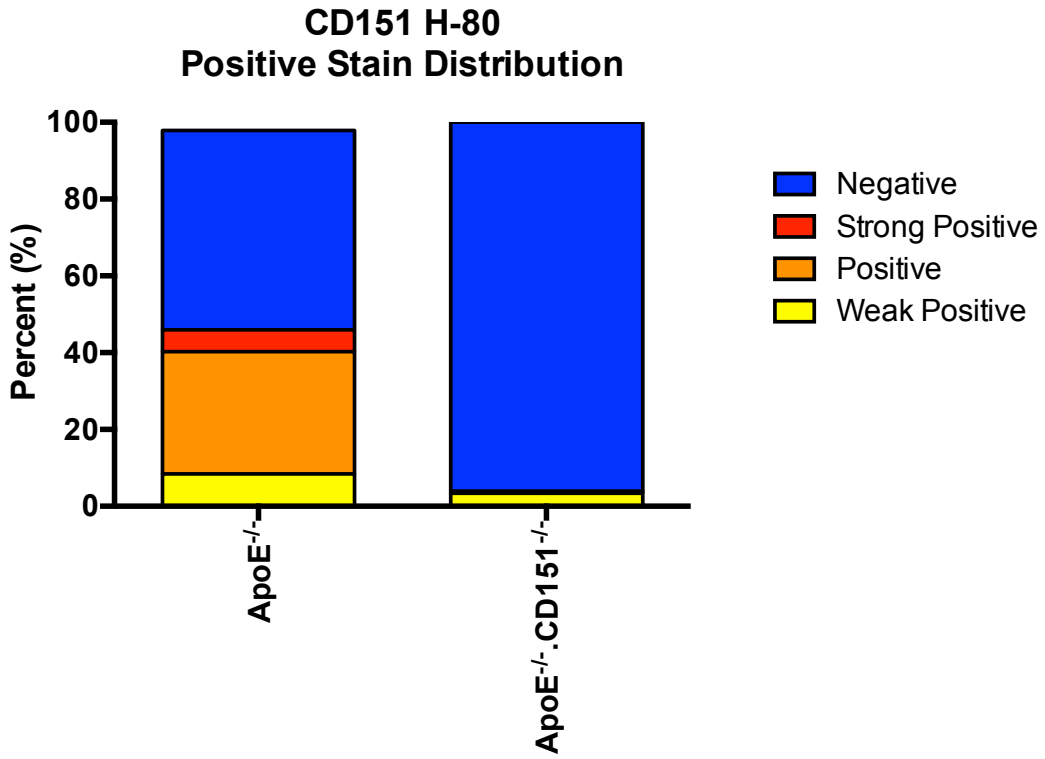

Figure 5.2. IHC studies for CD151 shows positive antibody staining at 5.7 ± 0.8 % in the ApoE$^{-/-}$ mouse strain. Positive and Weak positive staining was also observed (31.9 ± 5.5 % and 8.4 ± 3.9) confirming CD151 expression and presence in atherosclerotic plaque lesions in the aortic valve cusps of 16 week old ApoE$^{-/-}$mice. The ApoE$^{-/-}$. CD151$^{-/-}$ lacked positive staining with the plaque lesions showing 96.0 ± 1.3 % negativity or absence of any positive staining. The ApoE$^{-/-}$. CD151$^{-/-}$ plaque lesions showed 3.4 ± 1.1 % weak staining however this is attributed by unspecific weak staining.

5.2.2 Type 1 collagen immunohistochemical staining of plaques in the aortic valve cusps of ApoE$^{-/-}$ mice compared to ApoE$^{-/-}$.CD151$^{-/-}$ mice

IHC staining was performed to quantitate for type I collagen present on plaques. Collagen is important in maintaining atherosclerotic plaque stability. Whilst there are many types of collagen present in vessel walls, type I and type III are the most abundant.(346,347) As fibrillar collagen adds strength and elasticity to a plaque, an imbalance in the synthesis and degradation of collagen will influence vessel wall stability and the vulnerability and rupturing of plaques.(347-349)

Aortic valve cusp sections were stained with anti type I collagen antibody to detect collagen, followed by peroxidase conjugated affini-pure goat anti rabbit secondary antibody, with antibody staining visualised with DAB solution. Representative images (Figure 5.3) of 16 week old mice fed a normal chow diet ad libitum, demonstrates positive staining and presence of collagen in the test tissues. The atherosclerotic plaque lesions appeared to be early in type, with intimal thickening observed and foam cells present. In the early phases of atherosclerosis, plaque composition is typically unchanged and only seen to change after 17 weeks onwards as it progresses into the advanced phases of atherosclerosis.(350,351) Kidney tissues were used as a positive control.

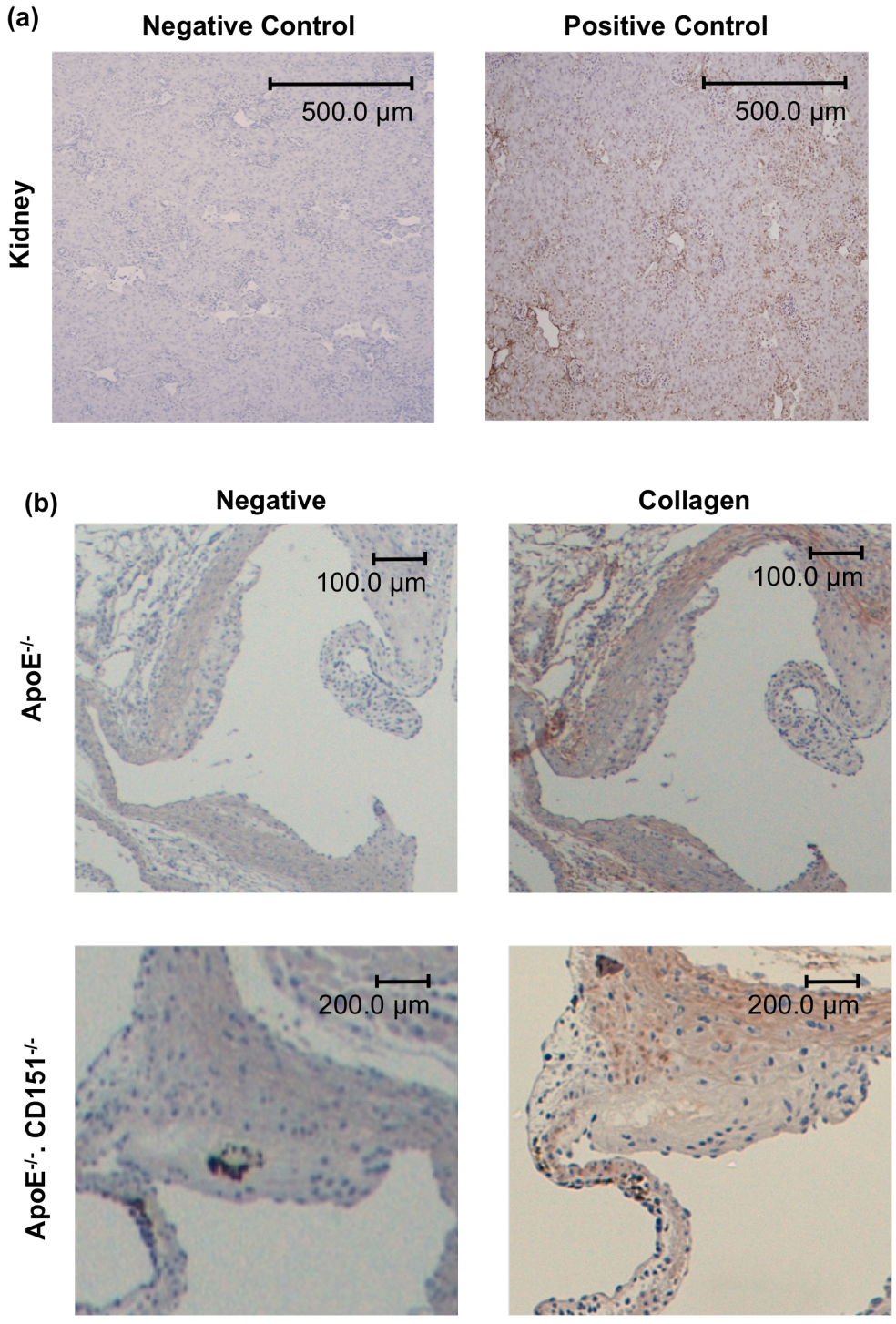

Figure 5.3. IHC staining of the aortic valve cusp of $ApoE^{-/-}$ and $ApoE^{-/-}$. $CD151^{-/-}$ mice was performed for detection of type 1 collagen. (a) Kidney sections were used as a positive control. (b) A primary anti type I collagen rabbit polyclonal antibody was used at a dilution of 1/200, followed by a peroxidase conjugated affini-pure goat anti rabbit secondary antibody at a dilution of 1/800. DAB was used for visualisation of the antibody stain. Light microscopy, original magnification 10 x.

The Aperio positive pixel count algorithm v9.1 was used to quantify positive collagen staining in ApoE$^{-/-}$ and ApoE$^{-/-}$.CD151$^{-/-}$ atherosclerotic plaque lesions. Positive staining was minimal with only 0.1 ± 0.1 % strong positive for ApoE$^{-/-}$ and 0.1 ± 0.04 for ApoE$^{-/-}$.CD151$^{-/-}$. ApoE$^{-/-}$ showed slightly higher weak positive staining at 19.4 ± 1.7 percent compared to ApoE$^{-/-}$.CD151$^{-/-}$ at 18.0 ± 1.6 % (Mean ± SEM, n=10 in each group).

Table 5.2. Percentage of type 1 collagen stained in lesions

	Stain (Mean ± SEM % pixel positive staining)			
Genotype	**Negative**	**Strong Positive**	**Positive**	**Weak Positive**
ApoE$^{-/-}$	80.131 ± 2.421	0.088 ± 0.067	2.233 ± 0.495	19.362 ± 1.691
ApoE$^{-/-}$.CD151$^{-/-}$	78.957 ± 1.918	0.079 ± 0.043	3.649 ± 0.556	17.980 ± 1.571

Table 5.2 does not show any statistical significance between all categories of positive and negative staining between ApoE$^{-/-}$ and ApoE$^{-/-}$.CD151$^{-/-}$ atherosclerotic plaque lesions. An unpaired Student's t-test was used to determine statistical significance. P values were greater than 0.05 for all categories of staining percentages between ApoE$^{-/-}$ and ApoE$^{-/-}$.CD151$^{-/-}$ genotypes (n=10 in each group).

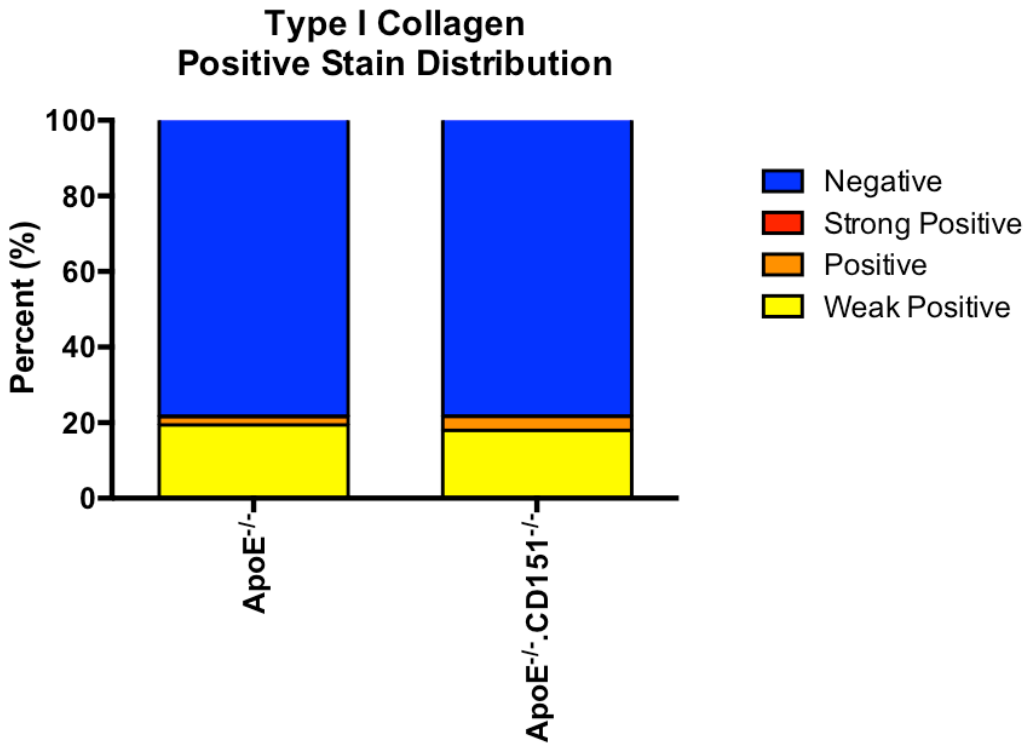

Figure 5.4. Positive stain distribution of Type 1 Collagen Immunohistochemical staining in 16 week old $ApoE^{-/-}$ and $ApoE^{-/-}.CD151^{-/-}$ mice. Positive and Strong positive staining is low with only weak positive staining of collagen present. The plaque has stained predominantly negative for collagen.

5.2.3 Smooth muscle actin immunohistochemical staining of plaques in the aortic valve cusps of ApoE$^{-/-}$ mice compared to ApoE$^{-/-}$.CD151$^{-/-}$ mice

Presence of smooth muscle cells in atherosclerotic plaque lesions was quantified in 16 week old ApoE$^{-/-}$ and ApoE$^{-/-}$.CD151$^{-/-}$ aortic valve cusps. SMCs are involved in the synthesis of collagen in plaques, migrating from the media to intima layer of vessel walls resulting in the subsequent increase of collagen synthesis.(352) Collagen is a key regulator of SMC proliferation suggesting its central involvement in atherosclerotic plaque lesion development. The absence of CD151 and its influence on plaque development has not been studied and as such the SMC content of atherosclerotic plaques in ApoE$^{-/-}$ and ApoE$^{-/-}$.CD151$^{-/-}$ were compared.

An anti-alpha SMC rabbit polyclonal antibody was used as the primary antibody (dilution 1:200), and a peroxidase conjugated affini-pure goat anti-rabbit antibody as the secondary antibody (dilution 1:800). Antibody staining was visualized with DAB solution and imaged with an Olympus BX 41 microscope and an Olympus DP70 camera, followed by quantification analysis with the Aperio positive pixel count algorithm v9.1 on atherosclerotic plaque lesions. Figure 5.5 (b) shows positive staining of SMC in atherosclerotic lesions in both ApoE$^{-/-}$ and ApoE$^{-/-}$.CD151$^{-/-}$ genotypes. The absence of CD151 has not influenced SMC composition in plaques as no statistically significant difference was observed between the genotypes in percent positive staining.

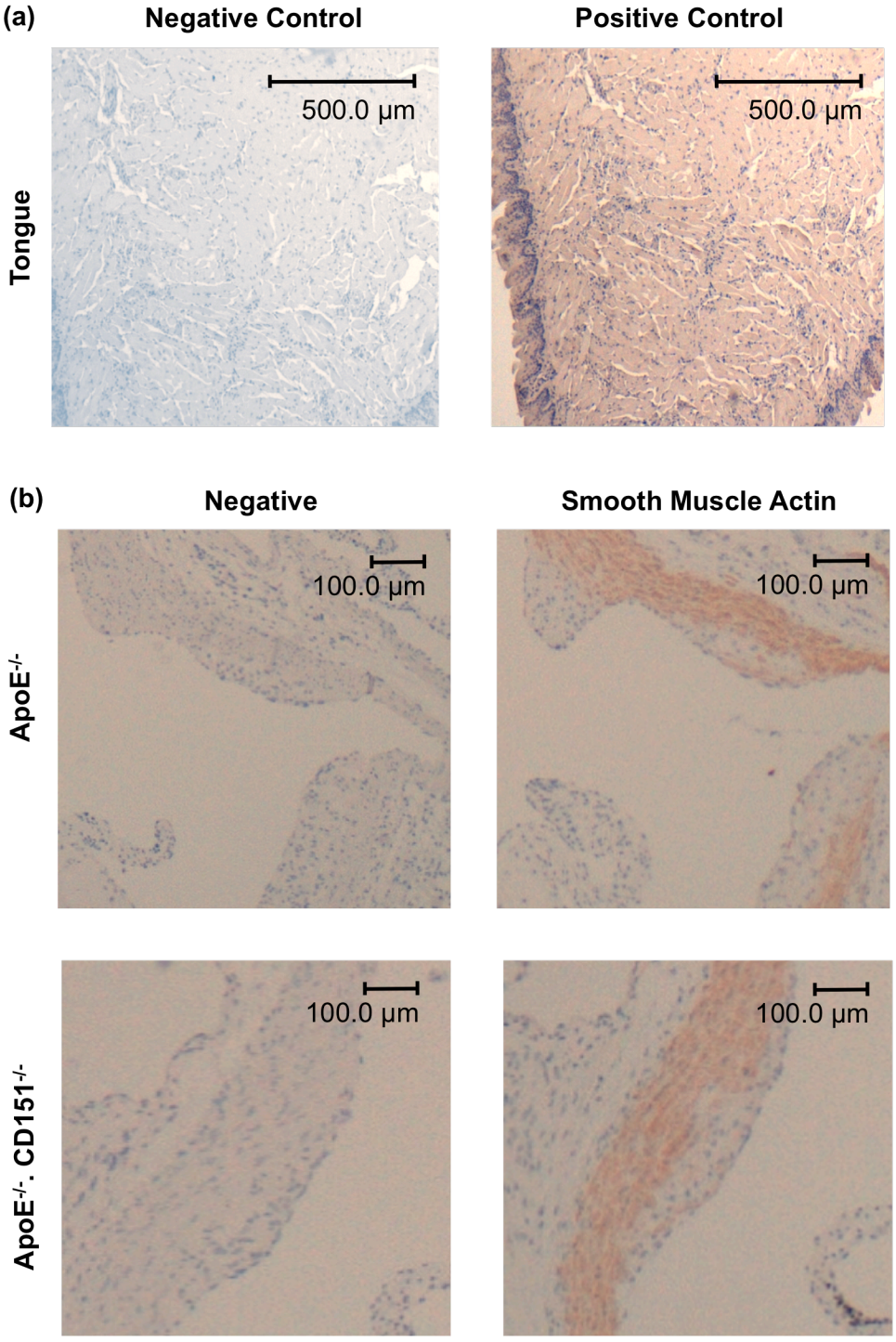

Figure 5.5. IHC staining of the aortic valve cusp of $ApoE^{-/-}$ and $ApoE^{-/-}$. $CD151^{-/-}$ mice was performed to stain for smooth muscle cell actin. (a) A tongue section was stained under the same conditions as $ApoE^{-/-}$ and $ApoE^{-/-}$. $CD151^{-/-}$ aortic valve cusps as a positive control. (b) Representative images of atherosclerotic plaque lesions stained with anti-alpha smooth muscle actin rabbit polyclonal antibody (primary antibody 1/200) and with a peroxidase conjugated affini-pure goat anti-rabbit antibody (secondary antibody 1/800). DAB was used to visualise antibody staining. Light microscopy, original magnification 10 x.

Quantified values for SMC positive pixel counts in ApoE$^{-/-}$ and ApoE$^{-/-}$.CD151$^{-/-}$ atherosclerotic plaque lesions are shown in Table 5.3. In ApoE$^{-/-}$ plaque lesions, only 36.0 ± 2.8 % of the plaque stained weak positive for SMCs, 8.1 ± 0.9 % for positive and 0.3 ± 0.1 % for strong positive, whereas ApoE$^{-/-}$.CD151$^{-/-}$ plaque lesions were found to stain 39.7 ± 4.2 % weak positive, 8.5 ± 0.9 % positive and 0.07 ± 0.03 % for strong positive staining. In both ApoE$^{-/-}$ and ApoE$^{-/-}$.CD151$^{-/-}$ mice tested, negative staining accounted for more than 50% of negative staining with no statistical significance observed between the genotypes for any positive or negative staining ($P > 0.05$, n=10 in each group, unpaired Student's t-test). These findings suggest that SMC content in atherosclerotic plaque lesions are unchanged between the different genotypes and has not been affected by the absence of CD151.

Table 5.3 Percentage of SMCs stained in lesions

	Stain (Mean ± SEM % pixel positive staining)			
Genotype	**Negative**	**Strong Positive**	**Positive**	**Weak Positive**
ApoE$^{-/-}$	55.618 ± 2.018	0.318 ± 0.117	8.101 ± 0.877	35.963 ± 2.849
ApoE$^{-/-}$.CD151$^{-/-}$	51.746 ± 4.851	0.068 ± 0.033	8.459 ± 0.903	39.727 ± 4.229

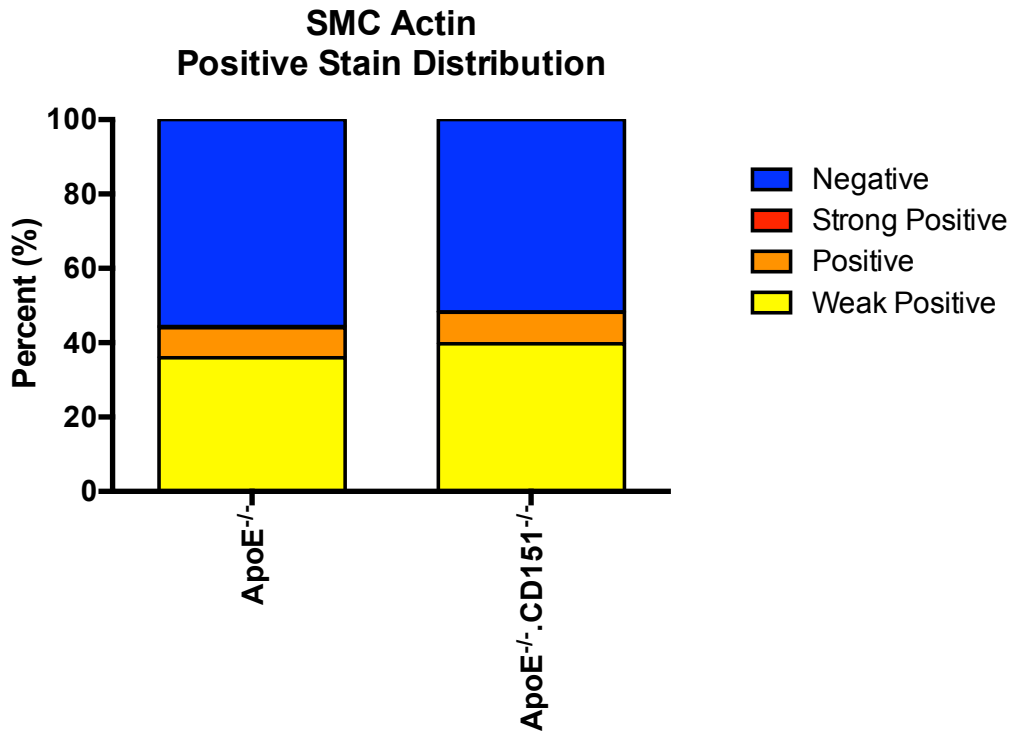

Figure 5.6. Atherosclerotic plaque lesions in 16 week old ApoE$^{-/-}$ and ApoE$^{-/-}$.CD151$^{-/-}$ mice stained weak positive and positive for SMCs. Negative staining amounted to 55.6 ± 2.0 % for ApoE$^{-/-}$ lesions and 51.7 ± 4.9 % ApoE$^{-/-}$.CD151$^{-/-}$ whilst in total approximately 40-50% of the atherosclerotic plaque lesion stained positive.

5.2.4 Macrophages F4/80 immunohistochemical staining of plaques in the aortic valve cusps of ApoE$^{-/-}$ mice compared to ApoE$^{-/-}$.CD151$^{-/-}$ mice

Macrophages are cells which have differentiated from monocytes into mononuclear phagocytes. The uptake of lipoproteins results in the transformation of these phagocytic cells into foam cells, which are essentially a class of macrophages. An impairment or imbalance to lipid metabolism influences the phenotype of macrophages, affecting the subsequent immune responses.(353) M2 macrophages are also known as alternatively activated macrophages and are reported to be dominant in earlier lesions as opposed to M1 macrophages which dominate in advanced plaques and atherosclerotic disease.(354-356)

Monocyte recruitment occurs as an inflammatory response to the accumulation of apolipoprotein B-containing lipoproteins in the subendothelium. Studies have shown that unstable atherosclerotic plaques are those which typically have thin fibrous caps and a substantial necrotic core with macrophages located close to the cap.(284357) Macrophages are inflammatory cells which are associated with collagen synthesis whereby the release of metalloproteinases results in collagen proteolysis and SMC apoptosis.(352) These metalloproteinases are often found in macrophages.(348) Deguchi et al. (358) suggested the vulnerability of a plaque to rupturing, may be associated with a disruption to collagen fibre organisation as a consequence of increased metalloproteinase expression.(358-362)

The characteristics and the composition of atherosclerotic plaque lesions in CD151 deficient mice are unknown. The study of ApoE$^{-/-}$.CD151$^{-/-}$ murine plaque lesions compared to ApoE$^{-/-}$ lesions and the contribution of macrophages to the development of atherosclerotic disease was investigated through immunohistochemical staining of lesions in the aortic valve cusps of 16 week old mice. Antibody staining was performed with a primary anti-mouse F4/80 antigen PE antibody at a dilution of 1/400 whilst a peroxidase goat anti-rat IgG secondary antibody was used at a dilution of 1/2000. Visualisation of the antibody stain was achieved with a DAB stain. Liver tissues were subjected to the same staining conditions to serve as a positive control and is shown in a representative image in Figure 5.7 (a). IHC antibody staining of ApoE$^{-/-}$ and ApoE$^{-/-}$.CD151$^{-/-}$ plaque lesions are shown in Figure 5.7 (b). Quantification of positive staining was performed by Aperio positive pixel count algorithm v9.1 on atherosclerotic plaque lesions.

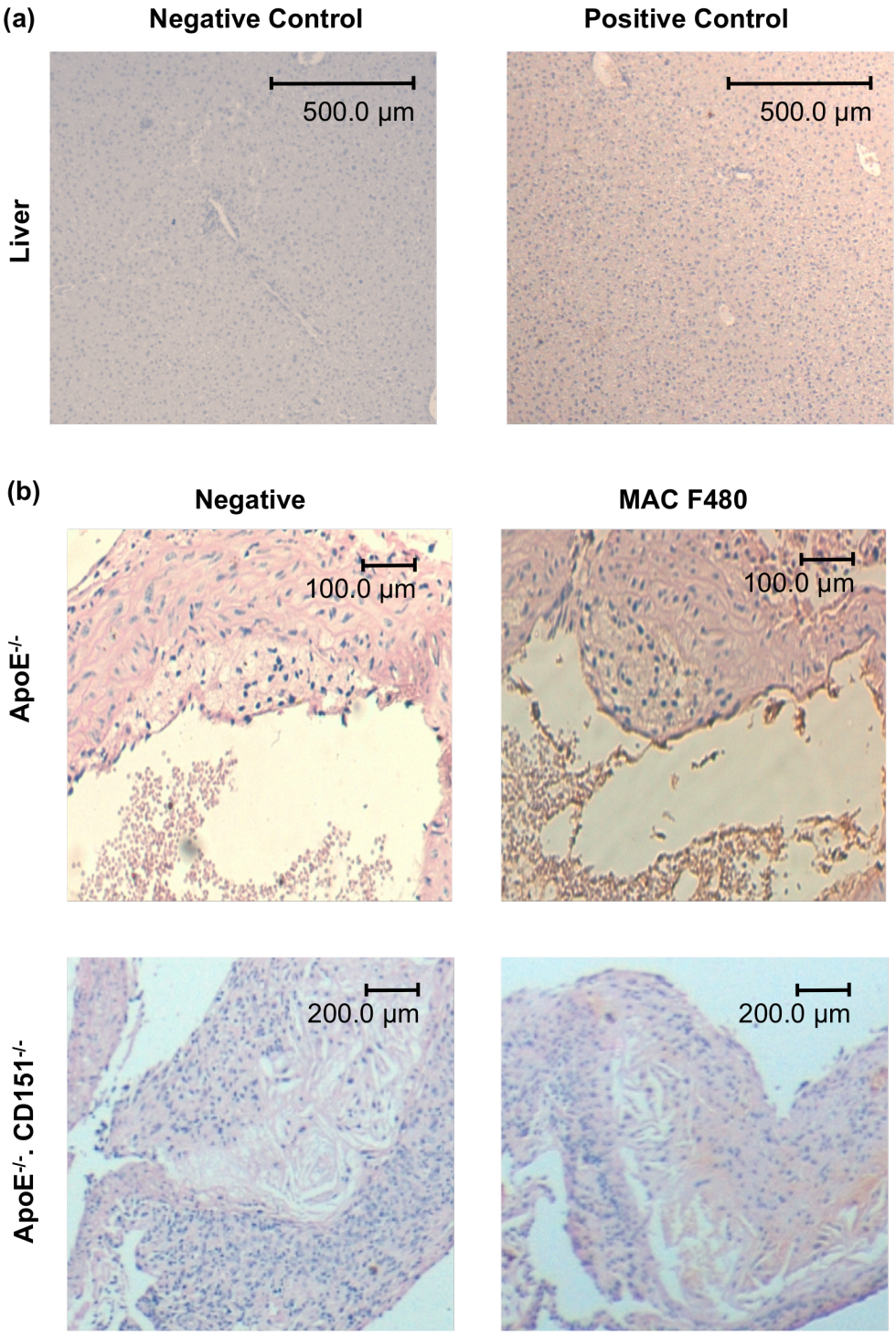

Figure 5.7. IHC macrophage staining of the aortic valve cusp of $ApoE^{-/-}$ and $ApoE^{-/-}$. $CD151^{-/-}$ mice was achieved with the use of a primary anti-mouse F4/80 macrophage antigen PE antibody (dilution 1/400) and a peroxidase goat anti-rat IgG secondary antibody (dilution 1/2000). (a) – (b) A representative image of a liver section is shown and was treated according to the same antibody staining protocol to act as a positive control. Stained $ApoE^{-/-}$ and $ApoE^{-/-}$. $CD151^{-/-}$ sections shows the presence of positive macrophage staining. Light microscopy, original magnification 10 x.

Positive macrophage staining in ApoE$^{-/-}$ and ApoE$^{-/-}$.CD151$^{-/-}$ was similar with no statistical significance (P > 0.05, n=10 in each group, Unpaired Student's t-test) observed between the strains. Table 5.4 shows only 0.03 ± 0.02 % strong positive staining occured in ApoE$^{-/-}$ and 0.03 ± 0.01 % in ApoE$^{-/-}$.CD151$^{-/-}$ when subjected to antibody staining. The plaque lesion stained predominantly negative with both strains approximately 80% negative. Figure 5.8 provides an illustration of the positive stain distribution with yellow or weak positive staining being the most dominant of the positive stain categories by both ApoE$^{-/-}$ and ApoE$^{-/-}$.CD151$^{-/-}$ mouse genotypes.

Table 5.4. Percentage of Macrophages stained in lesions

	Stain (Mean ± SEM % pixel positive staining)			
Genotype	**Negative**	**Strong Positive**	**Positive**	**Weak Positive**
ApoE$^{-/-}$	79.715 ± 2.464	0.025 ± 0.023	2.169 ± 0.664	18.085 ± 2.240
ApoE$^{-/-}$.CD151$^{-/-}$	80.663 ± 1.920	0.026 ± 0.008	2.848 ± 0.595	16.460 ± 1.330

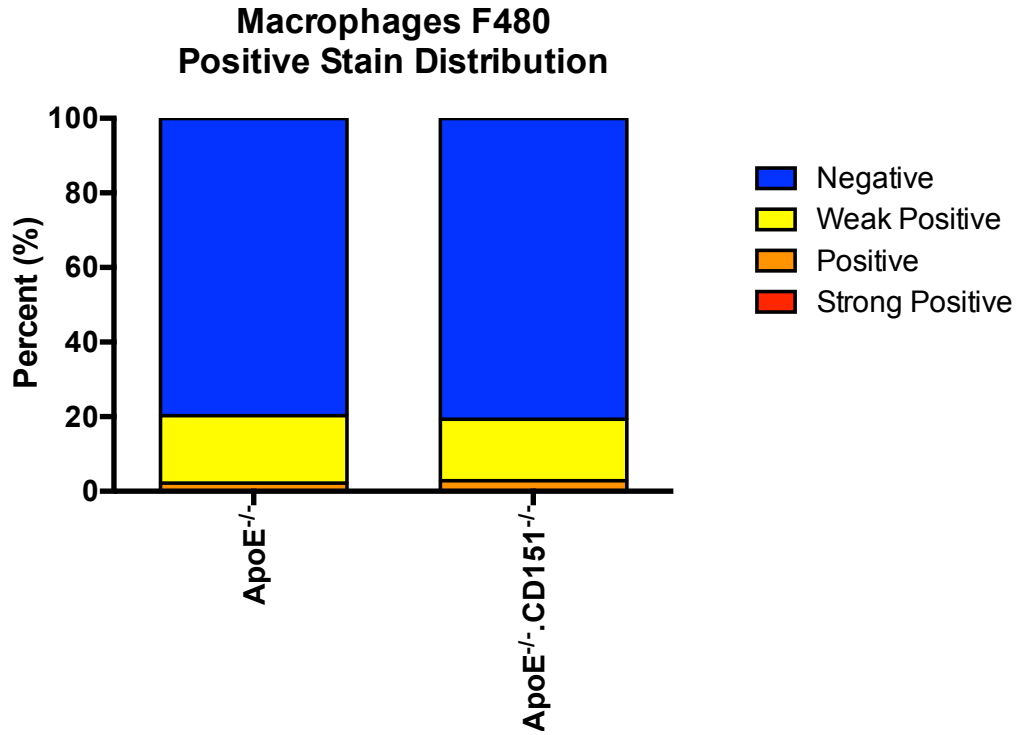

Figure 5.8. Atherosclerotic plaque lesions in 16 week old ApoE$^{-/-}$ and ApoE$^{-/-}$.CD151$^{-/-}$ mice stained 18.1 ± 2.2 % and 16.5 ± 1.3 % for weak positive macrophages, less than 3 % positive staining and less than 0.1% strong positive staining in both ApoE$^{-/-}$ and ApoE$^{-/-}$.CD151$^{-/-}$ plaque lesions. Lesions were negative for any positive staining or macrophages in 79.7 ± 2.5 % in ApoE$^{-/-}$ plaque lesions and 80.7 ± 1.9 % in ApoE$^{-/-}$.CD151$^{-/-}$ lesions.

5.3 Discussion

The influence of CD151 deficiency on atherosclerotic plaque development and composition during disease progression was studied in 16 week old ApoE$^{-/-}$ and ApoE$^{-/-}$.CD151$^{-/-}$ mice.

Although plaque burden appears to be significantly decreased in ApoE$^{-/-}$.CD151$^{-/-}$ compared to ApoE$^{-/-}$ mice, the composition of the plaques appear to be unchanged and unaffected by the lack of CD151 in atherosclerosis. Thus CD151 deficiency in atherosclerosis may provide resistance to the development of plaque lesions despite an insignificant transformation in plaque composition between the strains.

As ApoE$^{-/-}$ mice fed on an extended chow diet can develop skin lesions, the ApoE$^{-/-}$ and ApoE$^{-/-}$.CD151$^{-/-}$ mice were bred to 16 weeks only for histology studies to avoid animal welfare issues. When compared to the literature, studies have shown that on a normal chow diet, we would expect to observe early to intermediate lesions formed by the accumulation of early foam cells in the subendothelial layer of ApoE$^{-/-}$ plaque lesions from 10 – 15 weeks of age.(248) ApoE$^{-/-}$ mice on chow diets were only observed to begin displaying early fibrous plaques after 20 weeks of age. Nakashima et al.(248) noted that in ApoE$^{-/-}$ mice on the western type diet, early fibrous plaques developed after 15 weeks of age and atherogenesis was accelerated compared to mice on the chow diet. These mice presented with lesions containing necrotic cores and stable fibrous caps formed by SMCs, collagen and elastic fibres that were larger than lesions in chow fed mice.(248)

The ApoE$^{-/-}$ atherosclerosis murine model is a known and established gold standard that is frequently used for the study of atherosclerosis today.(185) CD151 on the other hand although studied extensively in metastasis, renal failure and recently platelet thrombus development and stability, its influence in atherosclerosis is unknown. As mentioned previously, a singular somewhat introductory study by Yang et al. (128) into the potential of CD151 as a therapeutic target for atherosclerosis disease, was carried out by scientists in China. They reported the significantly increased expression of CD151 in human atherosclerotic arteries compared to healthy arteries through histology studies. Western blotting studies conducted by this group also observed increased CD151 protein expression in atherosclerotic arteries which overall is suggestive of CD151 involvement in progression of this disease.(128) As briefly discussed earlier, increased CD151 expression has also

been observed to correlate with tumours of the lung, liver, breast, oesophagus, pangreas, colon, kidney, prostate and glioblastoma.(36,255,260,280,281,311,363-368)

The Aperio pixel positive algorithm v9.1 categorises positive staining into three categories being weak positive, positive and strong positive. Immunohistochemistry staining with antibodies against type I collagen, macrophages and smooth muscle actin in the plaques of $ApoE^{-/-}$ and $ApoE^{-/-}.CD151^{-/-}$ mice demonstrated predominantly weak positive staining collectively. These elements stained consistently between $ApoE^{-/-}$ and $ApoE^{-/-}.CD151^{-/-}$ mice with no significant difference observed in plaques in the absence of CD151 compared to the $ApoE^{-/-}$ group (unpaired Student's t-test, $P > 0.05$ n= 10). In reference to the literature, the $ApoE^{-/-}$ control in the current study was consistent in showing early plaques characterised by primarily the absence of large necrotic cores and well formed fibrous caps. Although mice fed a western type diet may at 15 weeks already begin demonstrating fibrous plaques, the $ApoE^{-/-}$ and $ApoE^{-/-}.CD151^{-/-}$ mice in this study were fed a chow diet ad libitum for 16 weeks which mirrored the types of lesions observed in the aortic valve cusps.(248)

Antibody staining against macrophages revealed 18.1 ± 2.2 % and 16.5 ± 1.3 % weak positive staining in $ApoE^{-/-}$ and $ApoE^{-/-}$. $CD151^{-/-}$ plaque lesions. Strong positive and positive staining was present but showed less than 3 % staining for macrophages (Table 5.4). The results demonstrated previously in Chapter 4 are not consistent with the amount of positive macrophage staining observed here. It was previously demonstrated that plaque lesion development in the $ApoE^{-/-}$ model was present however only minimal staining is observed through IHC studies as shown in Table 5.4 and Figure 5.8. The differences in lesion sizes is likely to be influenced by factors other than just macrophage composition. As the lesions observed in this study are those of early and intermediate types, it is acceptable to have observed very minimal changes in the macrophage distribution in the plaques. In the instance of advanced plaques, it is likely that macrophage staining would have been observed within the necrotic area of the lesion though studies have also reported higher macrophage presence in initial and intermediate plaque lesions as a result of infiltrated macrophage presence.(284,351,369) It is important to note also that Oil Red O staining would supplement the current results and assist in quantification of lesions. In addition, as a means of results validation, it would be recommendable to repeat IHC studies staining for F4/80. In having said that, we must take into consideration the altered Mendelian inheritance frequencies observed and restraints on mouse study population.(284,369) Similarly, the present study showed 36.0 ± 2.8 % and 39.7 ± 4.2% weak positive staining for

antibody staining against smooth muscle actin in the ApoE$^{-/-}$ and ApoE$^{-/-}$.CD151$^{-/-}$ mouse groups. Plaque composition was not altered and is characteristic of early and intermediate lesions evidenced by the weak staining of smooth muscle actin and lack of positive staining in the developing fibrous cap. Advanced lesions would demonstrate more fibrous smooth muscle cell presence in the perimeter and thus show increased staining. Anti type I collagen immunohistochemical antibody staining demonstrated weak positive staining in lesions with 19.4 ± 1.7 % staining seen in ApoE$^{-/-}$ and 18.0 ± 1.6 % staining in ApoE$^{-/-}$.CD151$^{-/-}$ lesions with no significant difference observed between the mouse genotypes investigated (Table 5.2). Early plaque lesions are typically collagen rich as opposed to advanced unstable atherosclerotic plaques which are collagen poor.(370,371) The Masson's trichrome and Verhoeff Van Gieson stains identified the prevalent presence of collagen. It is important to take note that these staining techniques do not discriminate between types of collagen in comparison to the anti type I collagen rabbit polyclonal primary antibody and peroxidase conjugated affini-pure goat anti rabbit secondary antibody used in immunohistochemistry staining which stain specific for type I collagen. Furthermore, as IHC staining for type I collagen, macrophages and smooth muscle actin did not present significant data to identify the component responsible for an increased plaque size in the ApoE$^{-/-}$ strain, it is suggested that the increased presence of fatty streaks, lipid deposits and ongoing intimal thickening to be associated in the larger plaque size and burden in the ApoE$^{-/-}$ strain.

Immunohistochemical staining for CD151 demonstrated CD151 expression in the lesions of ApoE$^{-/-}$ mice. The absence of CD151 in the ApoE$^{-/-}$.CD151$^{-/-}$ mouse model was void of significant positive staining though did show unspecific staining which was negligible as shown in Table 5.1. As it is a broadly expressed tetraspanin, its precise area in which it is most highly expressed was not isolated however is known to be associated with plaque lesions. This data suggests the involvement of CD151 in atherosclerosis plaque development and its expression in early and intermediate stages of the disease. On the contrary, macrophages, collagen and smooth muscle actin composition were unaffected in the absence of CD151 as demonstrated by the insignificant alterations to the plaque composition between ApoE$^{-/-}$ and ApoE$^{-/-}$.CD151$^{-/-}$ mouse strains.

5.4 Conclusion

This chapter has demonstrated that at 16 weeks of age, ApoE$^{-/-}$ and ApoE$^{-/-}$.CD151$^{-/-}$ mice developed plaque lesions that had similar type I collagen, F4/80 macrophages and smooth muscle actin composition. The absence of CD151 absence does not appear to influence type I collagen, F4/80 macrophages and smooth muscle actin presence in plaque lesions. CD151 expression was significantly in higher in ApoE$^{-/-}$.CD151$^{-/-}$ mice and demonstrates the presence of CD151 in atherosclerotic plaque lesions at 16 weeks.

5.5 Limitations

As discussed in section 5.5 on the limitations in the examination of plaque burden, similarly it is important to examine plaque composition in intermediate to advanced lesions, as well as in vulnerable plaques that are prone to rupture, to observe whether CD151 absence may provide protection in advanced atherosclerosis in mice older than 16 weeks. Due to antibody incompatibility, T lymphocytes were unable to be examined in ApoE$^{-/-}$ and ApoE$^{-/-}$.CD151$^{-/-}$ plaque lesions thus it justifies examination of plaques with an effective antibody.

6 CHAPTER 6: INVESTIGATION OF THROMBUS GROWTH STABILITY AND DEVELOPMENT IN THE ApoE$^{-/-}$.CD151$^{-/-}$ STRAIN

6.1 Introduction

Platelets are implicated in the strict regulation of haemostasis by managing thrombosis and the integrity of the vascular system. Platelet responses are regulated by positive feedback loops, which rapidly amplify initial activation signals to facilitate the recruitment of platelets and thrombus stability.(372) The rapid contact adhesion of platelets to proteins such as vWF, or collagen through GP Ib-IX-V complex and GPVI/FcR γ-chain induces platelet activation, spreading and platelet aggregation.(373, 374)

This can also occur in the presence of soluble agonists released from platelets such as ADP, thrombin and thromboxane A_2. Platelet shape change and secretion of granules occur in response to receptor-specific platelet activation signalling events. This leads to induction of the inside-out signalling pathway and transformation of integrin $\alpha_{IIb}\beta_3$ from its low-affinity inactive state to a high-affinity activated state.(375,376) Binding of integrin $\alpha_{IIb}\beta_3$ to its ligands in turn activates the outside-in signalling pathway which ultimately leads to the stable adhesion and aggregation of platelets, secretion of granules, thrombus formation as well as clot retraction.(376) The stability of thrombus formed is influenced not only by the active confirmation of integrin $\alpha_{IIb}\beta_3$ and induction of outside-in signalling events but also the involvement of Src family kinases, protein tyrosine phosphatase 1B, α_2-adrenergic receptor as well as secondary wave mediators such as ADP, thrombin and thromboxane A_2.(138, 377)

Increasing evidence points towards the influence of CD151 in atherothrombosis and plaque stability. Previous *in vivo* studies reveal that CD151$^{-/-}$ mice have an unstable haemostasis phenotype shown by an increased tendency to re-bleeds and prolonged tail bleeding times.(102) CD151$^{-/-}$ platelets displayed an abnormality in haemostasis *in vitro* with delayed kinetics of clot retraction, impaired cytoskeletal reorganisation in platelet spreading on fibrinogen and decreased platelet aggregation, which are all integrin $\alpha_{IIb}\beta_3$ dependent events.(4) These studies highlighted that integrin $\alpha_{IIb}\beta_3$ requires CD151 for optimal stabilisation of platelet-platelet interactions.

As activated platelets are a feature in the development and progression of atherosclerosis, there is potential for a prothrombotic state. This is particularly evident in plaque rupture where type I collagen is exposed potentiating ECM platelet interactions. Being a novel genotype it is unknown as to whether the $ApoE^{-/-}.CD151^{-/-}$ atherosclerotic mouse exhibits a prothrombotic phenotype compared to the $ApoE^{-/-}$ or $CD151^{-/-}$ mouse. To investigate this, *in vivo* and *in vitro* platelet thrombus formation studies comparing $ApoE^{-/-}$ and $ApoE^{-/-}.CD151^{-/-}$ were performed. Specifically, $FeCl_3$ was used *in vivo* to induce oxidative injury to the carotid arteries and mesenteric arterioles. This caused endothelial cell denudation and exposure of resting circulating platelets to the sub endothelium, allowing for the examination of arteriolar and microvascular thrombosis.(378, 379)

Also, agonists such as ADP, collagen and PAR-4 were used in platelet aggregation studies to prompt the formation of platelet aggregates to compare $ApoE^{-/-}$ and $ApoE^{-/-}.CD151^{-/-}$ PRP responses to agonists. PAR-4 is one of four isoforms of PARs expressed on platelets which is common in both human and mouse species, and is the major PAR receptor in mice. It is a thrombin receptor wherein thrombin is a very effective activator of platelets.(380,381) ADP release from the dense granules of platelets results in platelet cytoskeletal shape change, further granule secretion, aggregation of platelets and in addition, the generation of TXA_2. ADP induced platelet activation involves purinergic G-coupled receptors, $P2Y_1$ and $P2Y_{12}$.(382-385) The complementary activation of both receptors are required for platelet aggregation.(385) In humans, the formation of platelet aggregates on exposed lesions in a vessel may lead to the occlusion of the arterial lumen with the development of a large occlusive thrombi.(386) Meanwhile, collagen has also been established to be a potent thrombogenic component in the subendothelium of vessels and is an agonist with capabilities in platelet adhesion and triggering both platelet activation and aggregation.(387) *In vitro* studies involved the perfusion of $ApoE^{-/-}$ and $ApoE^{-/-}.CD151^{-/-}$ platelets at high shear rates resembling arterial blood flow to type I fibrillar collagen immobilised in a flow chamber. Collagen has been established to be a potent thrombogenic component in the subendothelium of vessels and is an agonist with capabilities in platelet adhesion and triggering both platelet activation and aggregation.(387)

Studying thrombus formation *in vivo and in vitro* would permit observations into the influence of the absence of CD151 has in atherosclerosis and whether the unstable phenotype it

exhibits as observed in previous studies imparts a protective effect in an atherosclerosis setting. In the 16 week old ApoE$^{-/-}$ and ApoE$^{-/-}$.CD151$^{-/-}$ mouse, the atherosclerotic plaques formed are early in nature and thus is unclear if platelet activaton and thrombus formation would be potentiated under these conditions. In addition, as CD151 is polygenic and broadly expressed in a variety of cell types, its involvement in the development and progression of atherosclerosis is not clear. Likewise the features of atherothrombosis in ApoE$^{-/-}$ and ApoE$^{-/-}$.CD151$^{-/-}$ in mice have not been investigated.

6.2 Results

6.2.1 Influence of agonist induced platelet aggregation on ApoE$^{-/-}$ and ApoE$^{-/-}$.CD151$^{-/-}$ mice

Platelet activation involves a series of events of which one is the remodelling of the cytoskeletal structure of platelets. This is followed by the formation of platelet aggregates and subsequent formation of a stable platelet plug. Outside-in integrin $\alpha IIb\beta_3$ signalling events leads to this cytoskeletal reorganisation and is hence paramount in the eventuation of platelet aggregation.(4) Previous studies have also established that integrin $\alpha IIb\beta_3$ to be associated both physically and functionally with CD151.(4) As such, investigating platelet aggregation in the absence of CD151 is important.

Furthermore, platelet function is also influenced by lipoprotein interactions with platelets, where in humans, hypercholesterolaemic subjects are observed to have increased platelet aggregability *in vitro* and simultaneously also having increased activity *in vivo*.(218,221, 388) Therefore, as platelet activation and aggregation pathways play a pivotal role in cardiovascular development, new therapies to target platelets is warranted. Platelet adhesion and aggregation is initiated upon plaque disruption and triggers the coagulation clotting pathways as well as the atherothrombotic process. It is thus of value to investigate CD151 as a potential target in managing hyperaggregability in an atherosclerotic setting as previous studies have indicated its importance and key role in platelet aggregation. Lau et al. (4) observed impaired outside in integrin signalling and defective platelet aggregation responses to PAR-4, collagen and ADP in CD151 deficient mice.

We have assessed this in an atherosclerotic diseased setting by using the novel ApoE$^{-/-}$.CD151$^{-/-}$ mouse genotype strain and compared it to the ApoE$^{-/-}$ mouse strain examining platelet aggregation responses to selected agonists. ADP and PAR-4 agonists were used as these are G-protein coupled agonists. Type I collagen was also used as an agonist. A significant difference was observed between ApoE$^{-/-}$ and ApoE$^{-/-}$.CD151$^{-/-}$ mouse PRP in response to 3.75 µg/ml type I collagen where inhibition of aggregation occurred minimally in the ApoE$^{-/-}$.CD151$^{-/-}$ group. In addition, a significant difference in platelet aggregation was observed in response to PAR-4 300 µM with the ApoE$^{-/-}$.CD151$^{-/-}$ mice displaying a heightened response and increased aggregation compared to the ApoE$^{-/-}$ strain (Figure 6.1). Platelet response to other respective agonists in an atherosclerotic setting was unchanged in

the absence of CD151. Representative images of the responses to PRP agonists is observed in Figure 6.2 and Figure 6.3.

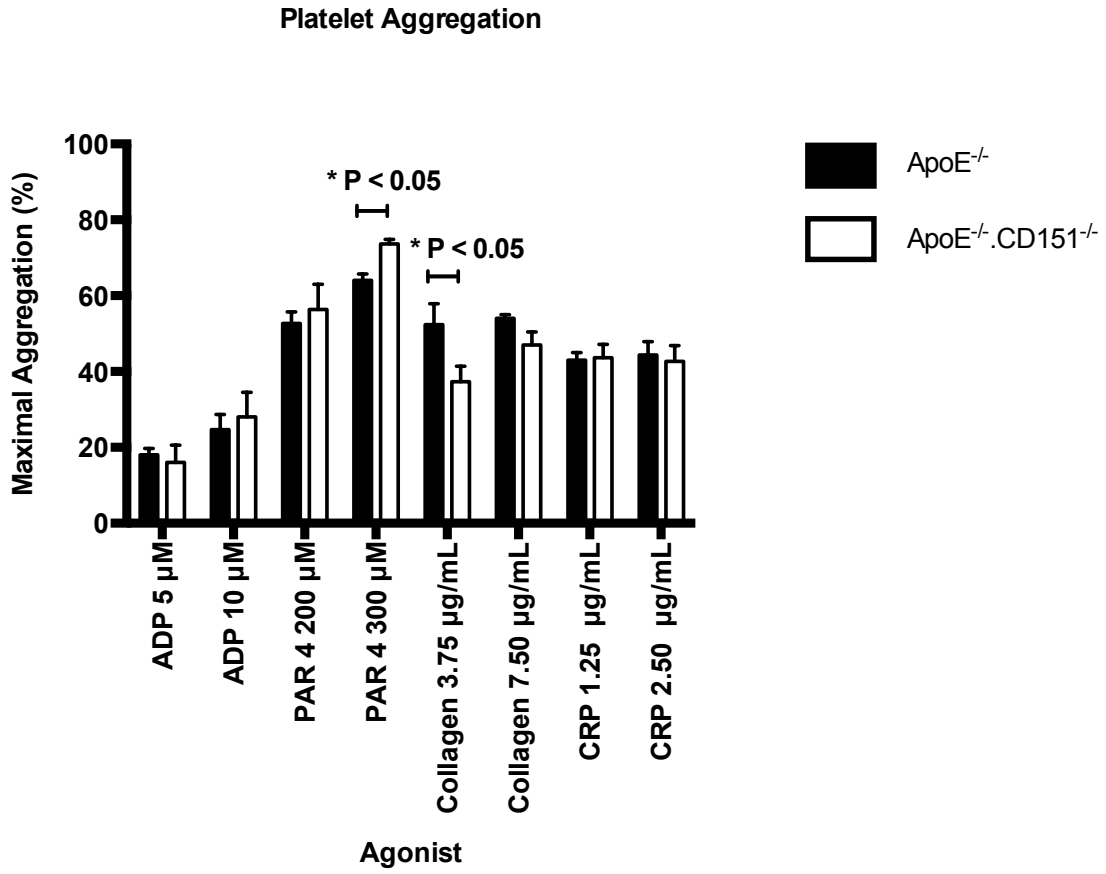

Figure 6.1. ApoE$^{-/-}$ and ApoE$^{-/-}$.CD151$^{-/-}$ platelet aggregation responses of platelet rich plasma (platelet count adjusted to 100 x 10^9/L) to agonists: ADP (5 µm and 10 µm), PAR-4 (200 µm and 300 µm), collagen (3.75 µg/ml and 7.50 µg/ml) and CRP (1.25 µg/ml and 2.50 µg/ml). Aggregation response to PAR-4 at 300 µm ApoE$^{-/-}$.CD151$^{-/-}$ was significantly higher compared to the ApoE$^{-/-}$ mouse group (* P < 0.05), whilst the ApoE$^{-/-}$.CD151$^{-/-}$ platelet aggregation response was significantly decreased (* P < 0.05). No significant differences were observed in aggregation responses between the strains for the remaining agonists (P > 0.05, unpaired Student's t-test; n=3 per group).

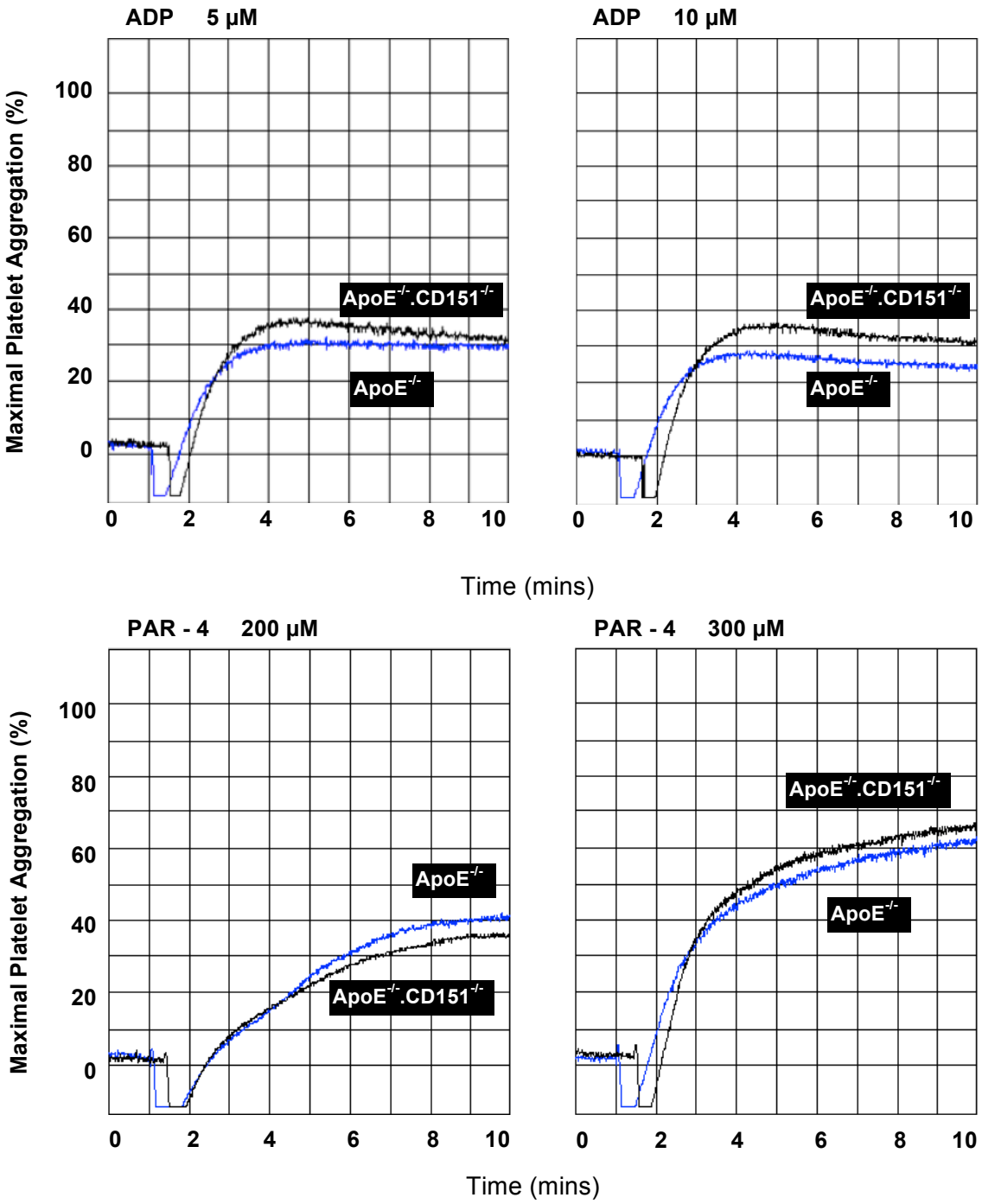

Figure 6.2 Representative images of $ApoE^{-/-}$ and $ApoE^{-/-}.CD151^{-/-}$ platelet aggregation responses of platelet rich plasma (platelet count adjusted to 100 x 10^9/L) to 5 µm ADP and 10 µm ADP; 200 µm PAR-4 and 300 µm PAR-4. Only platelet aggregation response to PAR-4 300 µm showed significant differences ($P < 0.05$, unpaired Student's t-test, n=3 per group). No significant differences were observed in the amplitude and maximal platelet aggregation responses (%) between the strains for 5 µm ADP and 10 µm ADP ($P > 0.05$, unpaired Student's t-test; n=3 per group).

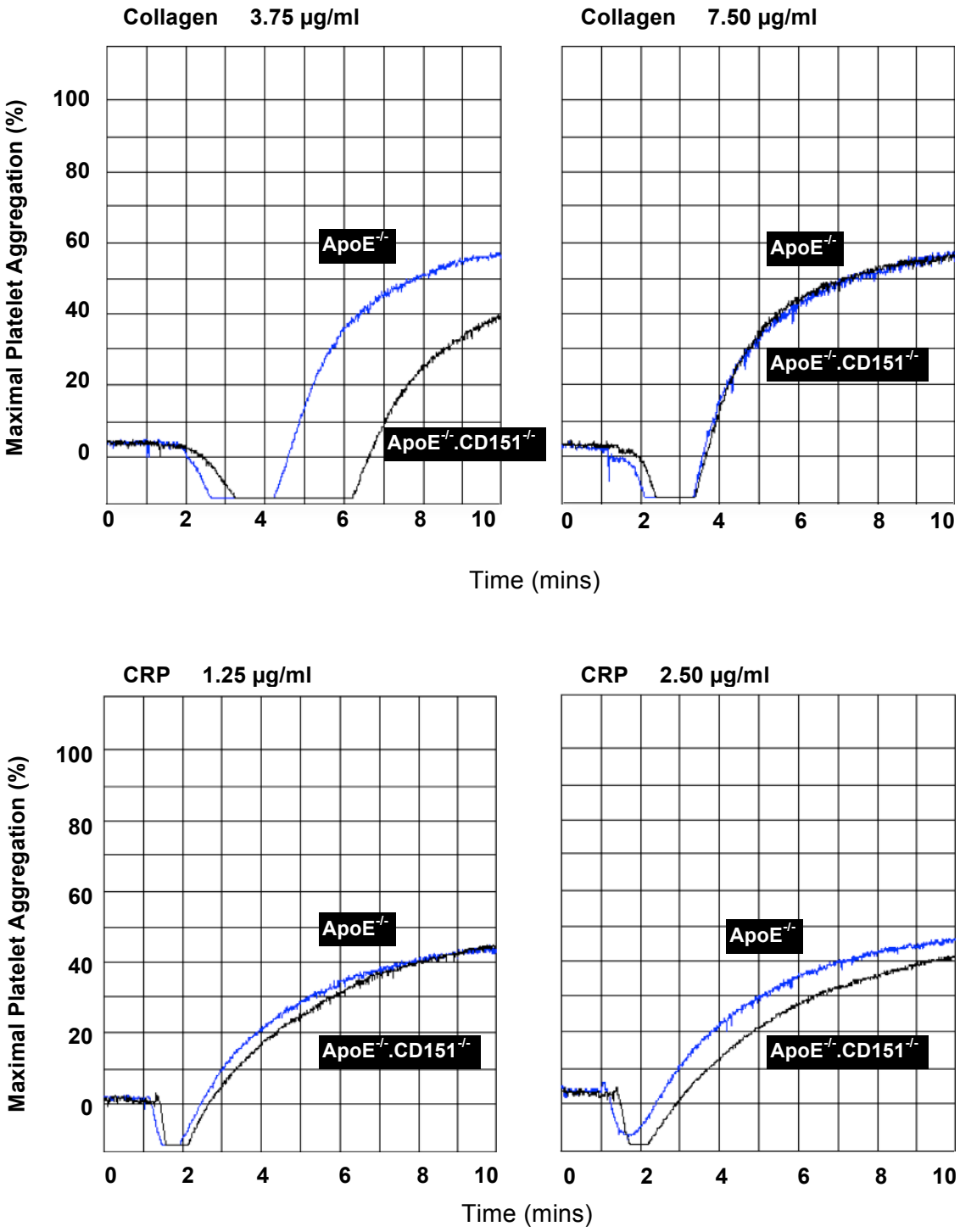

Figure 6.3. Representative images of ApoE$^{-/-}$ and ApoE$^{-/-}$.CD151$^{-/-}$ platelet aggregation responses of platelet rich plasma (platelet count adjusted to 100 x 10^9/L) to type I fibrillar collagen; 1.25 µg/ml CRP and 2.50 µg/ml CRP. Only platelet aggregation response to collagen at 3.75 µg/ml showed significant differences ($P < 0.05$, unpaired Student's t-test, n=3 per group). No statistical significance was observed in other respective agonists and concentrations in the amplitude and maximal platelet aggregation responses (%) between the strains ($P > 0.05$, unpaired Student's t-test, n=3 per group).

6.2.2 Shear induced platelet activation and collagen adhesion *in vitro* monitored via IVM

In normal circulation, platelets flow freely in a resting state and do not interact with vessel walls however in atherosclerotic arteries, thrombus formation can lead to myocardial infarction (MI) and stroke. The rupturing of plaque caps in atherosclerotic arteries exposes collagen in the sub-endothelium in areas of the vessel where blood shear rates are high.(389) Under these conditions, platelet adhesion to type I collagen is dependent on vWF. The stable adhesion of platelets to collagen also requires GPVI and integrin $\alpha_2\beta_1$. These receptors are also known to be involved in signalling pathways intracellularly which promotes platelet activation and for improved stability of platelet aggregates.(390)

In order to examine the formation of platelet aggregates and growth of a thrombus upon exposure to type I collagen we developed an *in vitro* model to mimic human pathology and high shear rates within an arterial vessel. The $CD151^{-/-}$ mouse phenotype has been shown *in vivo* to generate smaller and less stable thrombi.(197) In our investigation, we have adapted this into an atherosclerotic setting with the use of $ApoE^{-/-}$ and $ApoE^{-/-}.CD151^{-/-}$ mouse blood *in vitro.*

The procedure is as described in Section 2.1.14. Briefly, citrated whole blood from $ApoE^{-/-}$ and $ApoE^{-/-}$. $CD151^{-/-}$ mice was labeled with 0.05% (w/v) rhodamine and perfused through a three channel µ-slide III flow chamber (0.1×1.0×45 mm, IBIDI, Martinsried, Germany) coated with type I collagen. A wall shear rate of 1800 $seconds^{-1}$ was induced using a Harvard Apparatus syringe pump. Six cycles of real time images were recorded per minute and analysed via deconvolution of z-stack images to obtain thrombus area, height and volume over time.

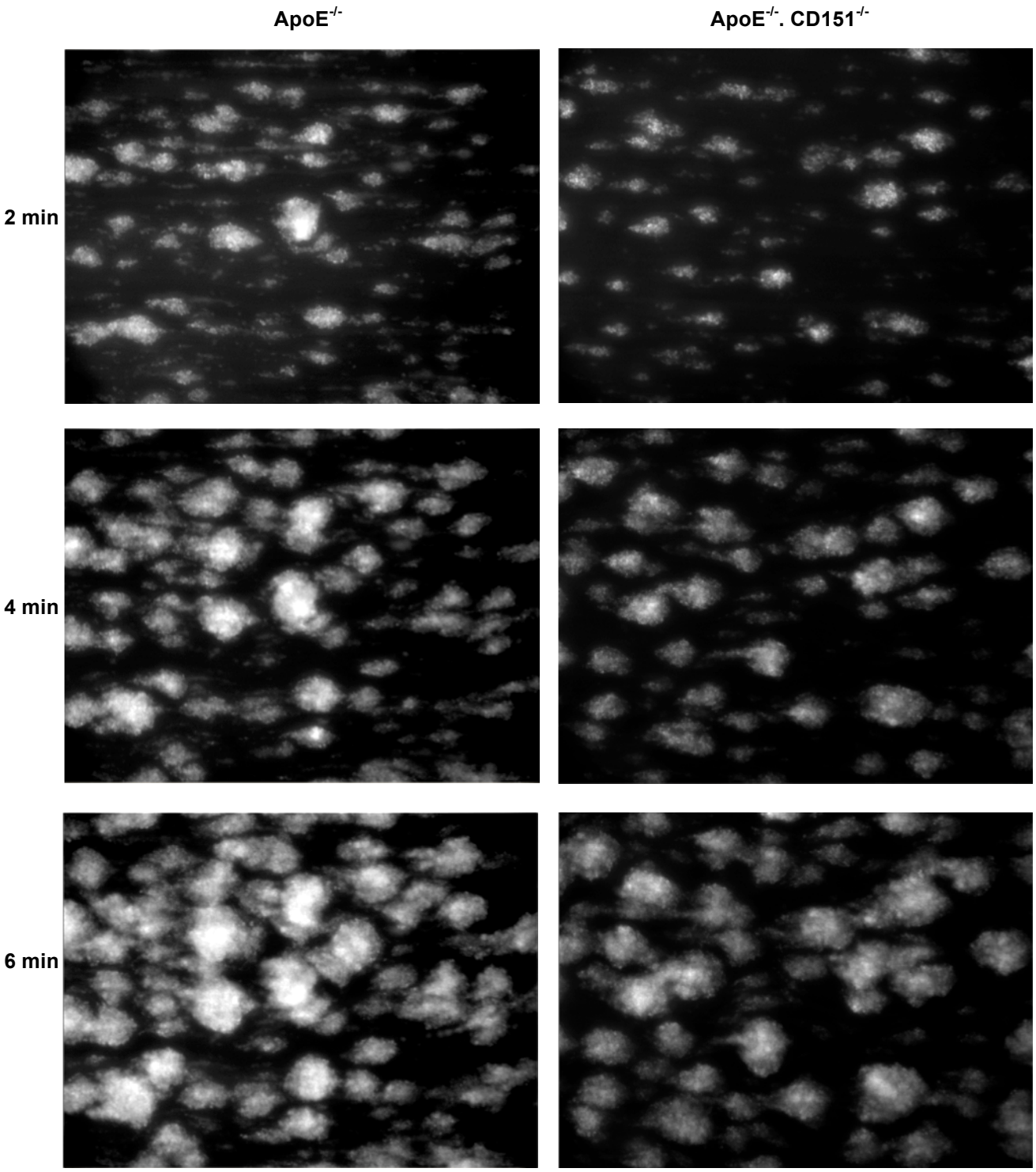

Figure 6.4. Representative images of thrombus formation in the presence of type I collagen *in vitro* under arterial shear rates. The left column displays thrombus development in the $ApoE^{-/-}$ mouse strain over time versus the right column which is representative of the $ApoE^{-/-}$. $CD151^{-/-}$ mouse strain. The citrated whole blood samples were subjected to a high shear rate of $1800s^{-1}$ induced by a Harvard syringe pump. The real time images were captured over 6 cycles of 1 minute duration each with a digital Axiocam mRm camera (Carl Zeiss) with a 1280 x 1024 pixel array using Axiovision Rel4.6 version software attached to an Axiovert 135 M1 microscope (Carl Zeiss). The images above highlight the significantly larger thrombi forming in the $ApoE^{-/-}$ mouse strain in comparison to the $ApoE^{-/-}$.$CD151^{-/-}$ mouse strain.

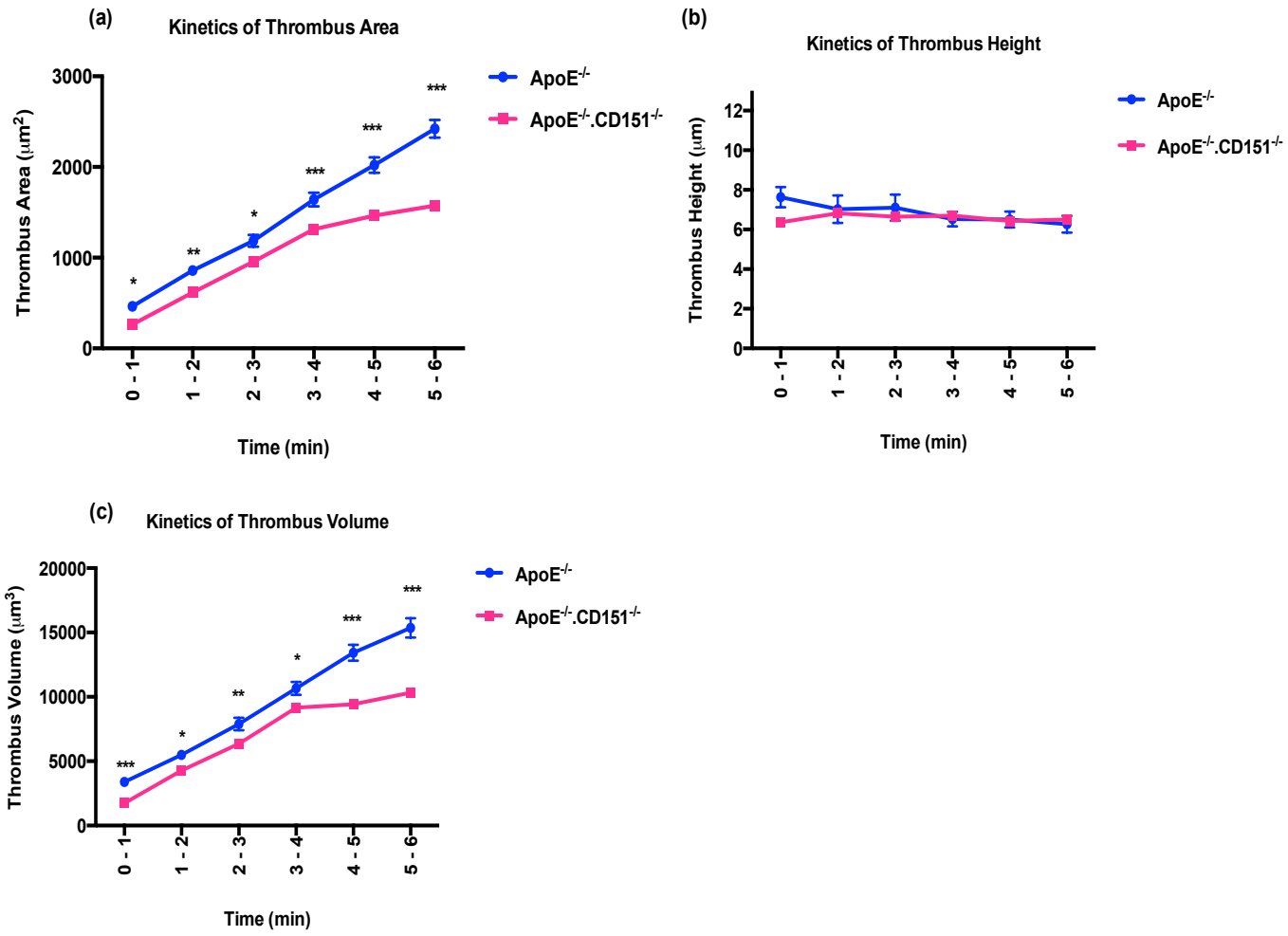

Figure 6.5. The kinetics of thrombus area, height and volume were determined for thrombi formed in type I fibrillar collagen immobilised flow chambers perfused with ApoE$^{-/-}$ and ApoE$^{-/-}$.CD151$^{-/-}$ citrated whole blood. The kinetics of thrombus height is unchanged between ApoE$^{-/-}$ and ApoE$^{-/-}$.CD151$^{-/-}$ mouse strains. In comparison, the kinetics of thrombus area and volume in ApoE$^{-/-}$. CD151$^{-/-}$ mice is significantly lower at each time point over 6 minutes compared to ApoE$^{-/-}$ mice (n= 7 in each group). Results represent the mean ± SEM. * P < 0.05; ** P < 0.005 ; *** P < 0.0005, unpaired Student's t-test.

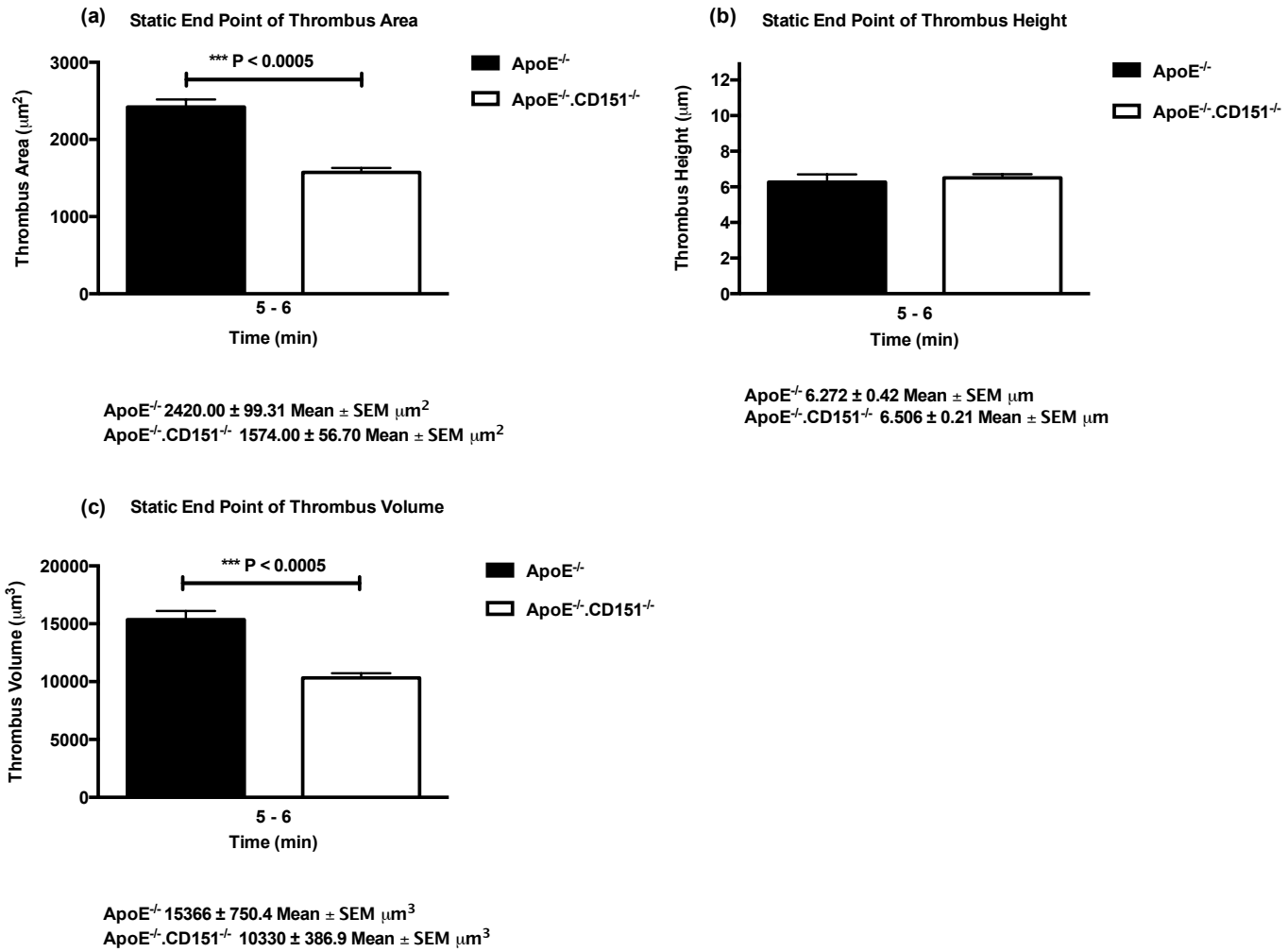

Figure 6.6. Defective thrombus formation and adhesion to type I collagen is observed in ApoE$^{-/-}$. CD151$^{-/-}$ mice. (a-c) The static end point of thrombi area, height and volume at 6 minutes was determined in ApoE$^{-/-}$ and ApoE$^{-/-}$. CD151$^{-/-}$ mice (n=7). (a) and (c) The thrombi formed at 6 minutes were significantly smaller in area and volume in ApoE$^{-/-}$. CD151$^{-/-}$ mice compared to ApoE$^{-/-}$ mice (*** P < 0.0005, unpaired Student's t-test). Thrombus height at 6 min was unchanged between the strains. Results represent mean ± standard error of the mean.

We have established through this specific investigation that thrombus area and volume in atherosclerotic mice is reduced significantly in the absence of CD151. At each time point over the 6 minutes in which the kinetics of thrombus formation was recorded, we observed the development of smaller thrombi in the ApoE$^{-/-}$.CD151$^{-/-}$ mice in contrast to ApoE$^{-/-}$ mice (Figure 6.5). Static end point data shown in Figure 6.6 demonstrates significantly smaller thrombi formed in the ApoE$^{-/-}$.CD151$^{-/-}$ mouse strain compared to ApoE$^{-/-}$ mice at the conclusion of testing at 6 minutes. Representative real time images at time points 2, 4 and 6 min as shown in Figure 6.4 supports this in illustrating a clear distinction in the size as well as the number of thrombi formed over time at high shear rates in the presence of type I collagen. These results are consistent with previous findings where CD151$^{-/-}$ is reported to produce smaller and less stable thrombi.(197)

6.2.3 Assessment of microvascular thrombosis in ApoE$^{-/-}$ and ApoE$^{-/-}$.CD151$^{-/-}$ mice via $FeCl_3$ induced vascular injury of mesenteric arterioles

Atherosclerotic plaques differ in their composition compared to that of a normal healthy arterial wall. Upon disruption or rupture to an atherosclerotic plaque, the thrombogenic sub endothelial matrix components which have potent thrombogenic potential is exposed.(391, 392) These platelet activating components include type I collagen, vWF, fibrinogen, thrombospondin, vitronectin, fibronectin, oxidised low density lipoproteins, cholesterols and stromal cell derived factor-1.(392) Platelet tethering and activation occurs subsequently leading to the formation of an arterial thrombus which could be occlusive and thus lead to acute myocardial infarction and/or cerebral ischaemic stroke.(391,392) CD151 is necessary in thrombus formation and regulation *in vivo*. Intravital microscope studies inducing injury with ferric chloride have shown that CD151$^{+/-}$ and CD151$^{-/-}$ mice form smaller and less stable thrombi than CD151$^{+/+}$ mice.

In order to assess if the ApoE$^{-/-}$.CD151$^{-/-}$ genotype carries the same characteristics as the CD151$^{-/-}$ mouse genotype, we have used the ferric chloride injury model to induce oxidative damage to the vascular wall and endothelium of mesenteric arterioles.(379) As CD151$^{-/-}$ mice form smaller thrombi *in vivo*, we hypothesised that in an atherosclerotic diseased setting, the absence of CD151 may have a protective effect in reducing the incidence in the formation of occlusive thrombi. Thrombus formation was examined and compared between ApoE$^{-/-}$ and ApoE$^{-/-}$.CD151$^{-/-}$ mice that are 4 – 6 weeks old in real time *in vivo* via intravital microscopy. Z-stack images were deconvolved to allow for three dimensional analysis and determination of thrombus characteristics such as area, height and volume.

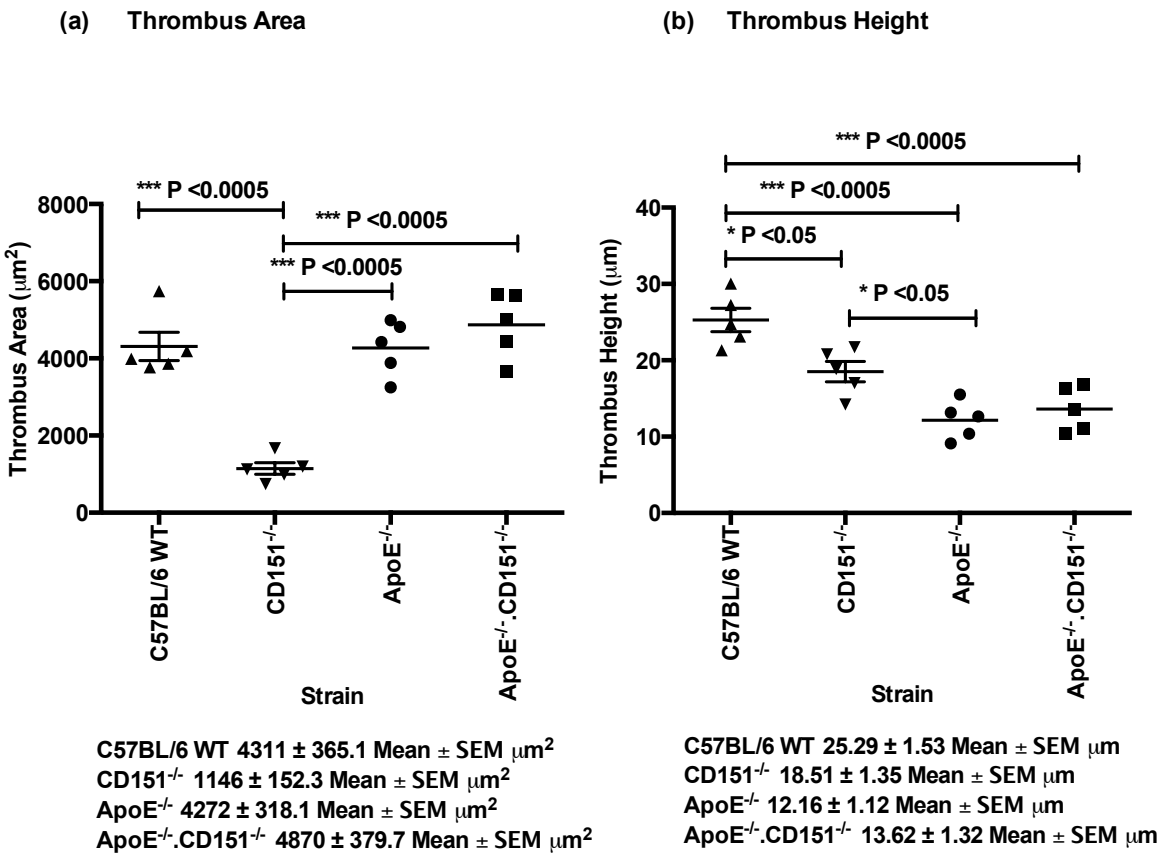

Figure 6.7. Observation of microvascular thrombosis via intravital microscopy of the mesenteric arterioles of ApoE$^{-/-}$ and ApoE$^{-/-}$.CD151$^{-/-}$ mice at 4 weeks of age. Preliminary data on C57BL/6 WT and CD151$^{-/-}$ was previously generated and included here for background data. Injury was induced with 7.5% (w/v) $FeCl_3$ immersed grade 1 Whatman filter paper which was placed on the exposed mesenteric artery of 80-100 μm for 4 minutes. Z-stack images were captured in 2 minute intervals over 5 cycles with a digital Axiocam mRm camera (Carl Zeiss) with a 1280 x 1024 pixel array using Axiovision Rel4.6 version software attached to an Axiovert 135 M1 microscope (Carl Zeiss). Rhodamine 6G dye was infused through a cannula inserted into the jugular vein for visualisation of thrombi. No significant difference is observed in (a) Thrombus Area and (b) Thrombus height developed in the arterioles between ApoE$^{-/-}$ and ApoE$^{-/-}$.CD151$^{-/-}$ mice. (a) Thrombus area was significantly higher in ApoE$^{-/-}$ and ApoE$^{-/-}$.CD151$^{-/-}$ in comparison to CD151$^{-/-}$ mice (*** P < 0.0005); Thrombus area was also significantly higher in the C57BL/6WT mice group compared to CD151$^{-/-}$ (*** P < 0.0005). (b) Thrombus height was significantly lower in CD151$^{-/-}$, ApoE$^{-/-}$ and ApoE$^{-/-}$.CD151$^{-/-}$ mice in comparison to C57BL/6 WT mice (* P < 0.05, *** P < 0.0005 and *** P < 0.0005) whilst thrombus height in CD151$^{-/-}$ mice was raised compared to ApoE$^{-/-}$ (* P < 0.05). Each data point represents an average of 3 vessels per mouse (P < 0.05, ANOVA post test; n=5 examined).

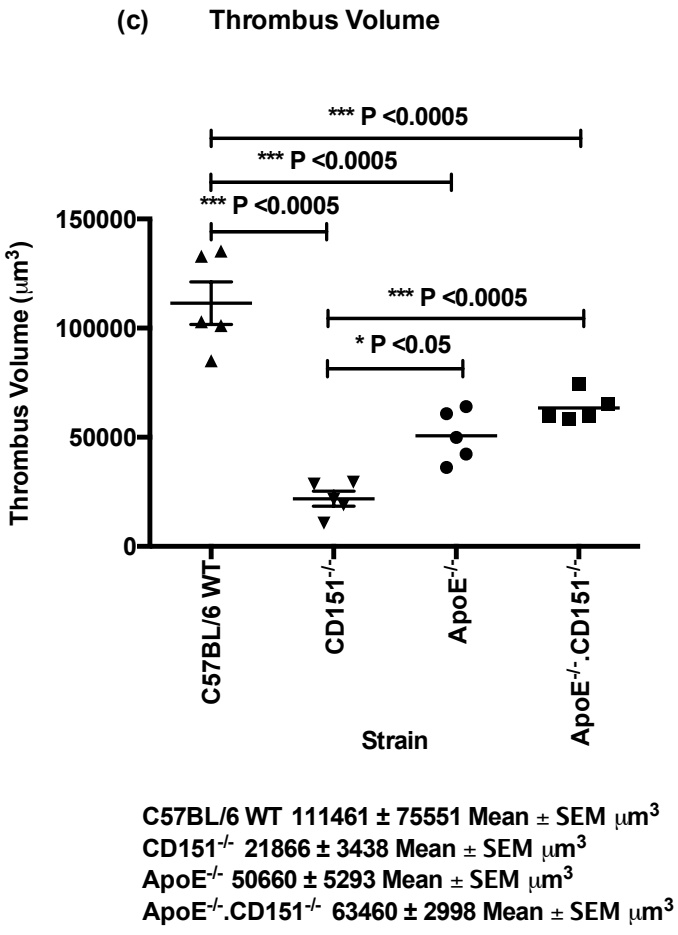

Figure 6.8. Observation of microvascular thrombosis via intravital microscopy of the mesenteric arterioles of ApoE$^{-/-}$ and ApoE$^{-/-}$.CD151$^{-/-}$ mice at 4 weeks of age. Preliminary data on C57BL/6 WT and CD151$^{-/-}$ was previously generated in our laboratory and included here for background data. Injury was induced with 7.5% (w/v) $FeCl_3$ immersed grade 1 Whatman filter paper which was placed on the exposed mesenteric artery of 80-100 μm for 4 minutes. Z-stack images were captured in 2 minute intervals over 5 cycles with a digital Axiocam mRm camera (Carl Zeiss) with a 1280 x 1024 pixel array using Axiovision Rel4.6 version software attached to an Axiovert 135 M1 microscope (Carl Zeiss). Rhodamine 6G dye was infused through a cannula inserted in to the jugular vein for visualisation of thrombi. The thrombus volume (c) is unchanged and does not seem to have been affected by the absence of CD151$^{-/-}$ in atherosclerosis. ApoE$^{-/-}$ and ApoE$^{-/-}$.CD151$^{-/-}$ mice both demonstrated significantly larger thrombus volumes compared to CD151$^{-/-}$ mice (* $P < 0.05$ and *** $P < 0.0005$). C57BL6/WT mice developed thrombi with significantly greater volumes than CD151$^{-/-}$, ApoE$^{-/-}$ and ApoE$^{-/-}$.CD151$^{-/-}$ mice (all *** $P < 0.0005$). Each data point represents an average of 3 vessels per mouse ($P < 0.05$, ANOVA post test; n=5 examined).

The thrombus area, thrombus height and thrombus volume does not appear to be influenced by the absence of CD151 in atherosclerotic disease as no statistically significant differences are observed within these parameters. When comparing our findings with previous studies, there are inconsistencies. Note however the previous studies by Orlowski et al. (197) observed the absence of CD151 in a normal C57BL6 mouse and not in a diseased atherosclerotic mouse. At 10 minutes, we report a thrombus area for $ApoE^{-/-}$ and $ApoE^{-/-}.CD151^{-/-}$ of 4272 ± 318.1 μm^2 versus 4870 ± 379.7 μm^2 which is approximately four fold compared to the thrombus area produced in $CD151^{-/-}$ arterioles. $ApoE^{-/-}$ and $ApoE^{-/-}.CD151^{-/-}$ produced thrombi with similar height (12.2 ± 1.1 μm^2 versus 13.6 ± 1.3 μm^2) when compared with each other, however is slightly reduced when compared to Orlowski et al.(197) and their findings for thrombus heights in $CD151^{-/-}$ mice. As for thrombus volume no significant differences are observed between $ApoE^{-/-}$ and $ApoE^{-/-}.CD151^{-/-}$ genotypes. In contrast to Orlowski et al. (197), the authors reported that the thrombus volume generated in both $ApoE^{-/-}$ and $ApoE^{-/-}.CD151^{-/-}$ were approximately 3-4 fold larger in area. Our observed thrombus volumes however were almost half of their reported values for C57BL/6 WT mice.

6.2.4 Thrombus stability in $ApoE^{-/-}$ and $ApoE^{-/-}.CD151^{-/-}$ mice following $FeCl_3$ induced injury of the mesenteric arterioles

For the examination of thrombus stability, 4 – 6 week old $ApoE^{-/-}$ and $ApoE^{-/-}.CD151^{-/-}$ mice mesenteric arterioles were compared. 7.5% (w/v) Ferric chloride injury was induced on mesenteric arterioles of 80 – 100 µm in length to trigger thrombus formation *in vivo.* This was recorded over time with a digital Axiocam mRm camera (Carl Zeiss) with a 1280 x 1024 pixel array using Axiovision Rel4.6 version software attached to an Axiovert 135 M1 microscope (Carl Zeiss). The percentage of the vessel occupied by the thrombus was first calculated and later scored from 1 – 10 with 1 being 1-10% occupancy or occlusion and 10 being 91-100% occupancy or complete occlusion. Our findings show that the $ApoE^{-/-}.CD151^{-/-}$ mouse has increased thrombus stability compared to the $ApoE^{-/-}$ mouse (Figure 6.9). Preliminary data from the Jackson laboratory reported a less stable thrombi phenotype for mice lacking the CD151 tetraspanin which corresponds to reduced occupancy of the vessel or less occlusion. We report a stability score of 2.9 ± 0.2 for $ApoE^{-/-}$ and 3.4 ± 0.2 for $ApoE^{-/-}.CD151^{-/-}$ mice. Although not statisically significantly higher the latter does indicate and suggest more stability which is directly conflicting previous preliminary data as well as findings by Orlowski et al. which is indicative of the $ApoE^{-/-}$ and $ApoE^{-/-}.CD151^{-/-}$ mouse strain

possessing a similar phenotype to a CD151$^{+/+}$ mouse and not that of a CD151$^{-/-}$ mouse.(197) Increasing the study population and furthering this investigation will help confirm if there is in fact more or less stability in the absence of CD151 in atherosclerosis. Figure 6.10 illustrates the presence of $FeCl_3$ deposits on mesenteric arterioles and provides visual confirmation of effective oxidative injury to the arterioles to induce platelet activation.

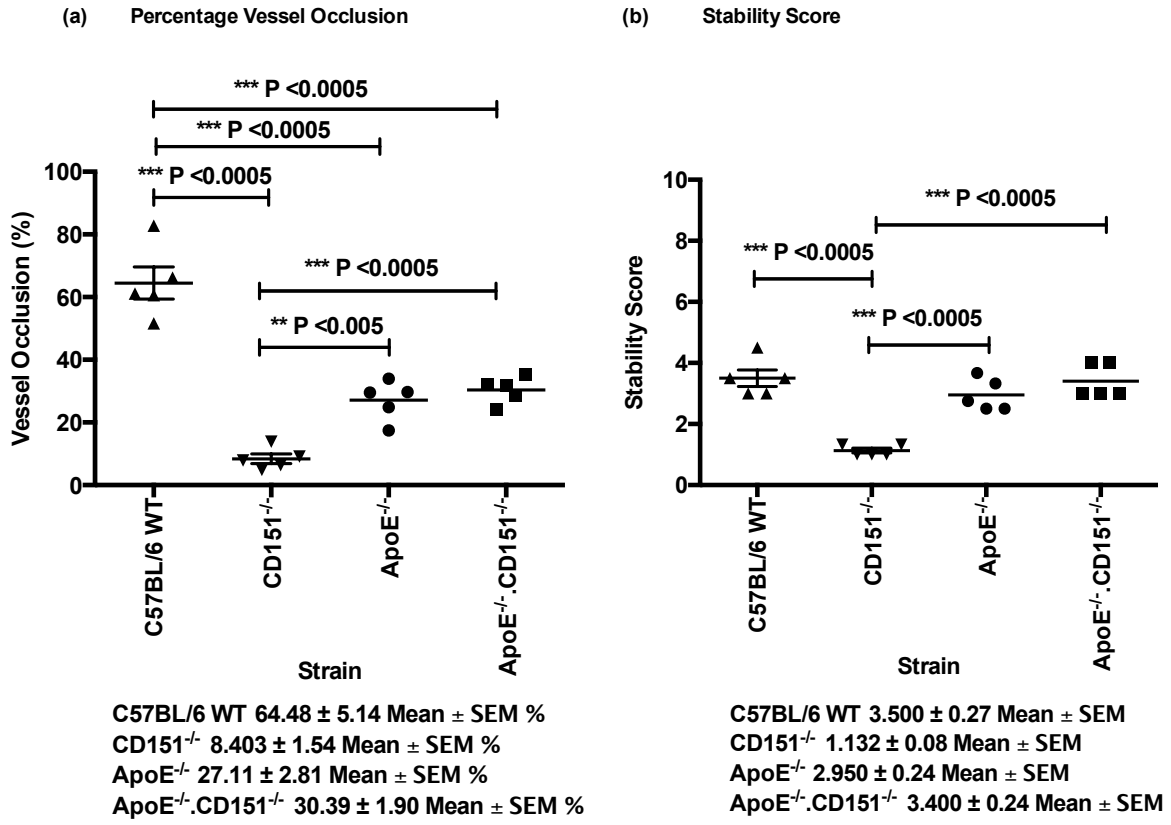

C57BL/6 WT 64.48 ± 5.14 Mean ± SEM %
CD151$^{-/-}$ 8.403 ± 1.54 Mean ± SEM %
ApoE$^{-/-}$ 27.11 ± 2.81 Mean ± SEM %
ApoE$^{-/-}$.CD151$^{-/-}$ 30.39 ± 1.90 Mean ± SEM %

C57BL/6 WT 3.500 ± 0.27 Mean ± SEM
CD151$^{-/-}$ 1.132 ± 0.08 Mean ± SEM
ApoE$^{-/-}$ 2.950 ± 0.24 Mean ± SEM
ApoE$^{-/-}$.CD151$^{-/-}$ 3.400 ± 0.24 Mean ± SEM

Figure 6.9. Observation of microvascular thrombosis via intravital microscopy of the mesenteric arterioles of ApoE$^{-/-}$ and ApoE$^{-/-}$.CD151$^{-/-}$ mice at 4 weeks of age. Preliminary data on C57BL/6 WT and CD151$^{-/-}$ was previously generated and included here for background data. Injury was induced with 7.5% (w/v) $FeCl_3$ immersed grade 1 Whatman filter paper which was placed on the exposed mesenteric artery of 80-100 µm for 4 minutes. Z-stack images were captured in 2 minute intervals over 5 cycles with a digital Axiocam mRm camera (Carl Zeiss) with a 1280 x 1024 pixel array using Axiovision Rel4.6 version software attached to an Axiovert 135 M1 microscope (Carl Zeiss). Rhodamine G6 dye was infused through a cannula inserted in to the jugular vein for visualisation of thrombi. The percentage of vessel occlusion (a) ApoE$^{-/-}$ and ApoE$^{-/-}$.CD151$^{-/-}$ mice is unchanged between strains and does not seem to have been affected by the absence of CD151 in atherosclerosis. Both ApoE$^{-/-}$ and ApoE$^{-/-}$.CD151$^{-/-}$ mice display increased percentages of Vessel occlusion in comparison to CD151$^{-/-}$ mice (** P < 0.005 and *** P < 0.0005); C57BL/6 WT mice also are observed to have raised vessel occlusion in the mesenteric arteries compared to CD151$^{-/-}$, ApoE$^{-/-}$ and ApoE$^{-/-}$.CD151$^{-/-}$ mice (all *** P < 0.0005). (b) ApoE$^{-/-}$ and ApoE$^{-/-}$.CD151$^{-/-}$ mice appeared to have greater stability compared to CD151$^{-/-}$ mice (*** P < 0.0005). C57BL/6 WT mice were also observed to have a significantly greater stability score compared to CD151$^{-/-}$ mice (*** P < 0.0005), demonstrating increased occupancy of the vessel by the thrombi developed in C57BL/6 and

thus increased stability. Each data point represents an average of 3 vessels per mouse. ($P < 0.05$, ANOVA post test; n=5 examined).

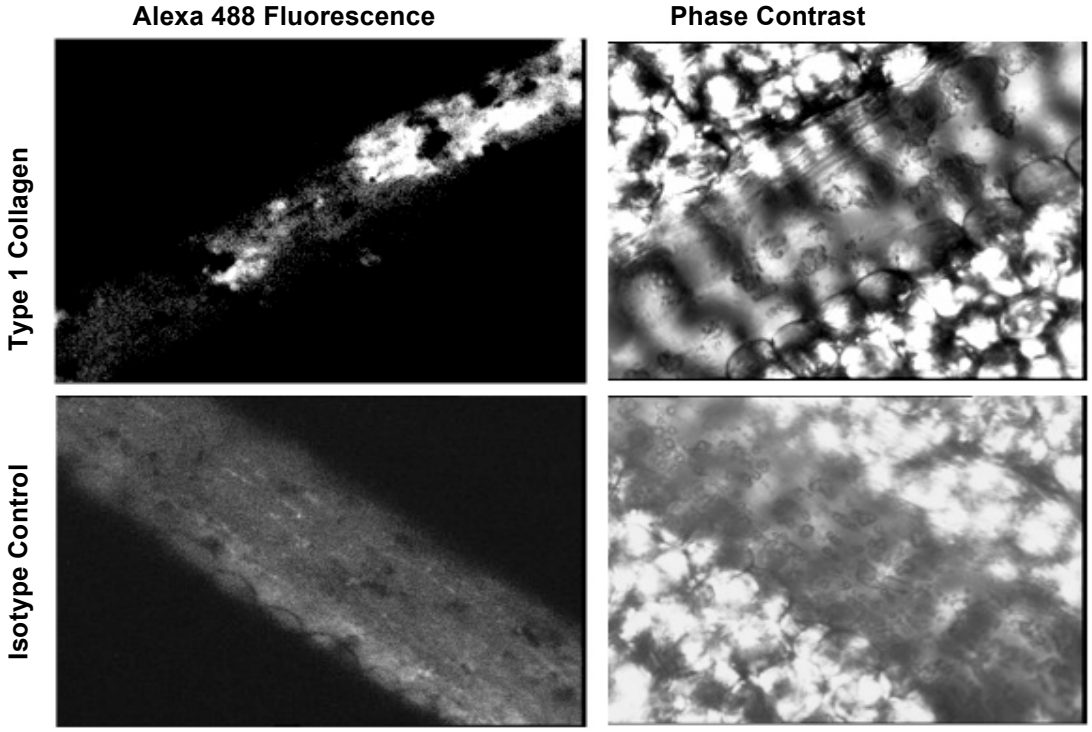

Figure 6.10. Type I Collagen exposure upon $FeCl_3$ injury. The phase contrast images shows the presence of $FeCl_3$ deposits whilst Alexa 488 Fluorescence images demonstrates for Type I Collagen exposure and staining after being subjected to effective $FeCl_3$ injury.

6.2.5 Examination of arteriolar thrombosis and time to vessel occlusion with $FeCl_3$ induced injury of the carotid arteries

Previous studies report a significant prolongation in time to > 95% occlusion of carotid arteries in $CD151^{-/-}$ mice compared to $CD151^{+/+}$ mice (*** $P < 0.001$, 835.80 ± 57.10 s versus 477.20 ± 39.15 s).(197) To investigate whether this defect in thrombus formation is also applicable in an atherosclerosis diseased setting, we monitored the blood flow and time to > 95 % occlusion in 16 week old $ApoE^{-/-}$ and $ApoE^{-/-}.CD151^{-/-}$ mice. The carotid arteries were subjected to 7.5% (w/v) $FeCl_3$ injury which induces redox endothelial damage and exposes the sub endothelial components that are thrombogenic to the blood. Recent studies found that $FeCl_3$ induced vascular injury is erythrocyte dependent and requires both haemolysis and oxidation of haemoglobin for endothelial denudation to occur.(378, 393)

This experiment allows us to observe rapid platelet recruitment and adhesion to the site of injury in response to type 1 collagen exposure and the formation of a thrombus with the use of a laser doppler perfusion monitor and probe.

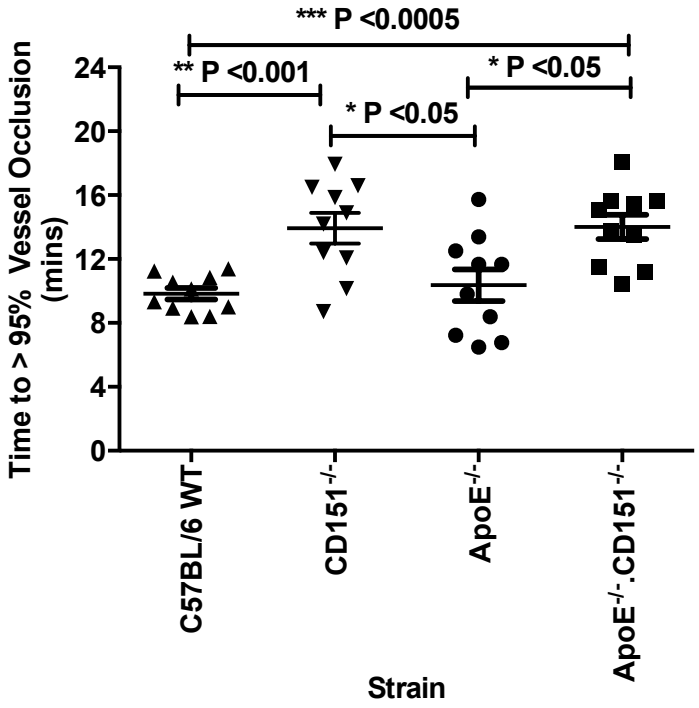

C57BL6 WT 9.83 ± 0.36 Mean ± SEM mins
CD151$^{-/-}$ 13.93 ± 0.95 Mean ± SEM mins
ApoE$^{-/-}$ 10.36 ± 0.99 Mean ± SEM mins
ApoE$^{-/-}$.CD151$^{-/-}$ 14.02 ± 0.76 Mean ± SEM mins

Figure 6.11. Folts Carotid Artery Injury Model for time to > 95% Vessel Occlusion (minutes). The time to > 95% vessel occlusion was observed in ApoE$^{-/-}$ and ApoE$^{-/-}$.CD151$^{-/-}$ mice of 16 weeks of age. Injury was induced with 20% (w/v) $FeCl_3$ immersed grade 1 Whatman filter paper which was placed on the exposed carotid artery for 4 minutes. No significant difference was observed in the time to > 95% occlusion between C57BL/6 wild-type (WT) and ApoE$^{-/-}$ mice. In contrast, a significantly prolonged time to occlusion is observed between C57BL/6 WT and ApoE$^{-/-}$.CD151$^{-/-}$ mice (*** P < 0.0005). A significant prolongation in time to 95% blood vessel occlusion between ApoE$^{-/-}$ and ApoE$^{-/-}$.CD151$^{-/-}$ mouse genotypes was also observed (* P < 0.05) (P < 0.05, ANOVA post test; n=10 examined).

A defect in thrombus formation following $FeCl_3$ induced injury in the carotid artery is also observed in our study (Figure 6.11) where a significantly prolonged time to > 95% occlusion is observed between C57BL/6 wild-type and ApoE$^{-/-}$.CD151$^{-/-}$ mice (*** P < 0.0005, 9.83 ± 0.36 minutes versus 14.02 ± 0.76 minutes), as well as between ApoE$^{-/-}$ and ApoE$^{-/-}$.CD151$^{-/-}$ mice (* P < 0.05, 10.4 ± 1.0 minutes versus 14.02 ± 0.76 minutes). Figure 6.12 illustrates a significantly prolonged time to occlusion in the ApoE$^{-/-}$.CD151$^{-/-}$ versue ApoE$^{-/-}$ and C57BL/6 WT mice.

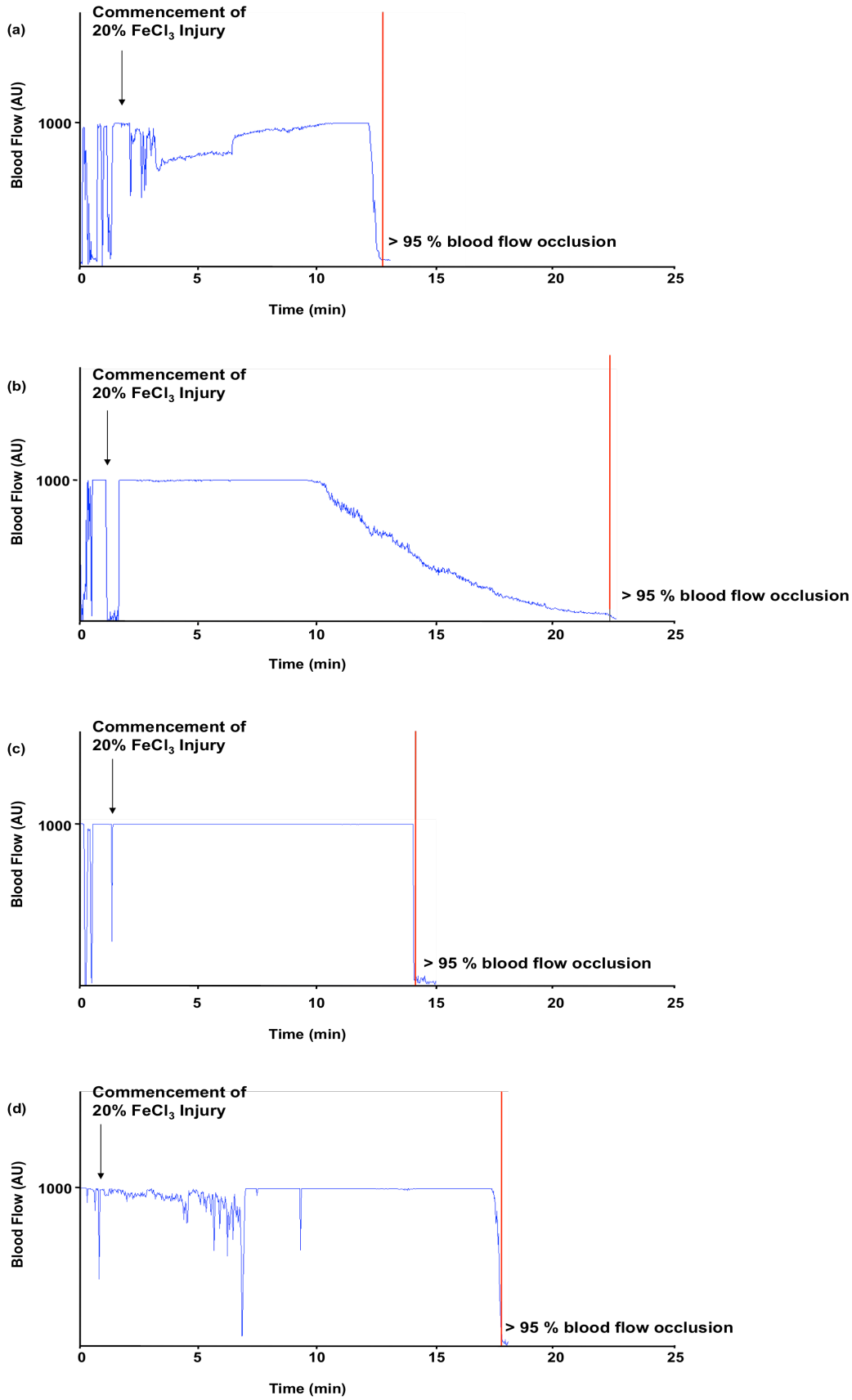

Figure 6.12. Representative graphs of blood flow occlusion in mouse carotid arteries subjected to 20% w/v $FeCl_3$ injury. (a) C57BL/6 WT 9.83 min (b) $CD151^{-/-}$ 13.93 min (c) $ApoE^{-/-}$ 10.36 mins and (b) $ApoE^{-/-}.CD151^{-/-}$ 14.02 mins. (b) and (c) A prolongation in the time to > 95% blood vessel occlusion suggests a defect in thrombus formation in the injured carotid arteries in atherosclerosis. Results are represented as mean ± SEM and are representative of n=10 replicates for each genotype.

6.2.6 Investigation of haemostasis through an *in vivo* mouse tail bleeding assay conducted in ApoE$^{-/-}$ and ApoE$^{-/-}$.CD151$^{-/-}$ mice.

The tail bleeding assay was conducted on ApoE$^{-/-}$ and ApoE$^{-/-}$.CD151$^{-/-}$ mice to investigate for abnormalities in platelet or endothelial function and thus as a measure of haemostasis stability. The tail bleeding time in Figure 6.13 (a) in the ApoE$^{-/-}$.CD151$^{-/-}$ model showed prolonged periods of bleeding compared to the ApoE$^{-/-}$ group (11.70 ± 0.10 mins versus 7.20 ± 0.31 mins, ** $P < 0.005$, unpaired Student's t-test). A similar pattern was observed in the volume of blood lost, which was significantly higher in ApoE$^{-/-}$.CD151$^{-/-}$ mice versus blood lost in the ApoE$^{-/-}$ mice group examined (81.75 ± 5.19 µl versus 58.50 ± 4.03 µl, * $P < 0.05$, unpaired Student's t-test). Haemostasis was quantitated by calculating the occurrence of positive rebleeds as a percentage of the specific genotype group tested. Rebleeds were significantly more pronounced in the ApoE$^{-/-}$.CD151$^{-/-}$ mouse group examined (*** $P < 0.0005$ n=4, unpaired Student's t-test). These findings show that the absence of CD151 in atherosclerosis through examination of the ApoE$^{-/-}$.CD151$^{-/-}$ model versus the ApoE$^{-/-}$ model has an *in vivo* platelet or vascular defect and thus indicating unstable haemostasis. This abnormality and state of unstable haemostasis observed in the absence of CD151 may be a result of defects associated with platelet to platelet interactions or platelet with the endothelium as CD151 is expressed on platelet surface as well as on endothelial cells.(102)

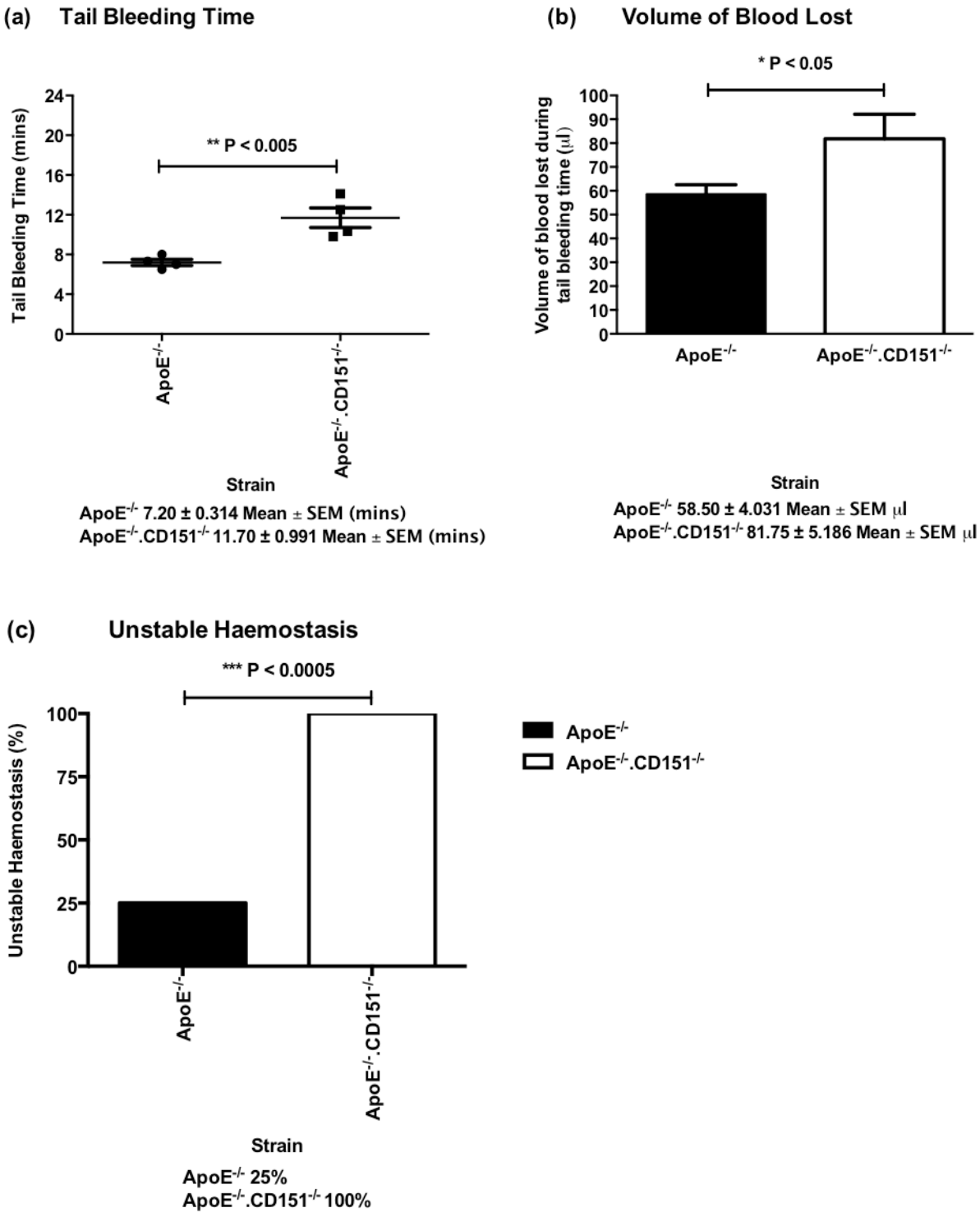

Figure 6.13. (a) – (c) A tail bleeding assay conducted on 6-8 week old ApoE$^{-/-}$ and ApoE$^{-/-}$.CD151$^{-/-}$ mice showed an *in vivo* bleeding defect present in ApoE$^{-/-}$.CD151$^{-/-}$ mice. (a) The time taken for initial cessation of bleeding to occur was significantly prolonged in ApoE$^{-/-}$.CD151$^{-/-}$ mice compared to ApoE$^{-/-}$ mice. (b) The volume of blood lost (µl) in the ApoE$^{-/-}$.CD151$^{-/-}$ mice group showed an *in vivo* bleeding defect present with a significantly higher volume of blood lost compared to the ApoE$^{-/-}$ group. (c) Unstable haemostasis was demonstated with significantly occurrence of rebleeds in the ApoE$^{-/-}$.CD151$^{-/-}$ group compared to the ApoE$^{-/-}$ group (n=4 in each group, * P < 0.05, unpaired Student's t-test).

6.3 Discussion

In this study, a variety of techniques were employed to examine the formation and stability of platelet thrombi generated between ApoE$^{-/-}$ and ApoE$^{-/-}$.CD151$^{-/-}$ mice. Whilst CD151$^{-/-}$ mice have been studied and shown to possess an unstable phenotype in haemostasis *in vivo* and *in vitro*, the lack of the CD151 gene and knowledge of its clinical implications specifically in atherosclerosis is rare.(4,197) All but one study has been found in the literature to have investigated protein expression and distribution of the tetraspanin in atherosclerotic tissues in humans.(128) This however was performed strictly *in vitro* and only gives a brief review seeing the complexities in the processes of haemostasis and thrombosis.(394-396) Given the insight into the involvement of CD151 in atherosclerosis, we were interested into furthering this investigation with our ApoE$^{-/-}$.CD151$^{-/-}$ novel strain.

The eventual formation of platelet aggregates follows the events accompanying platelet activation such as reorganisation of the platelet cytoskeleton, granule release and integrin clustering. We examined the platelet aggregation response to various platelet agonists as the processes involved in the formation of platelet aggregates require integrin $\alpha_{IIb}\beta_3$ involvement. Representative platelet aggregation responses to the agonists for ApoE$^{-/-}$ and ApoE$^{-/-}$.CD151$^{-/-}$ are shown in Figure 6.2 and 6.3. The absence of CD151 caused selective but significant perturbations to agonist induced platelet aggregation. Figure 6.1 shows the maximal aggregation percentages between the mouse genotypes for each agonist ($P > 0.05$, unpaired student's t-test). The PAR-4 (300 μM) agonist induced greater aggregation in ApoE$^{-/-}$.CD151$^{-/-}$ mice compared to ApoE$^{-/-}$ mice. A significant difference in aggregation was also observed between ApoE$^{-/-}$ and ApoE$^{-/-}$.CD151$^{-/-}$ mouse PRP in response to 3.75 μg/ml type I collagen where inhibition of aggregation was impeded in the ApoE$^{-/-}$.CD151$^{-/-}$ group.

From these results, it appears the absence of CD151 in an atherosclerosis setting differs to the observed responses in healthy non-atherosclerotic mice also deficient in CD151.(4) CD151$^{-/-}$ mice display a 50% to 70% reduction in platelet aggregation in response to ADP, PAR-4 and collagen, compared to wild-type mice.(4) If we compare the ApoE$^{-/-}$ and ApoE$^{-/-}$.CD151$^{-/-}$ agonist induced aggregation responses to the response observed by CD151$^{-/-}$ mice, it appears that although no difference is seen in response to ADP (5 μm and 10 μm) agonist induced aggregation responses in atherosclerosis, but compared to the CD151$^{-/-}$ profile, there is a marked reduction in aggregation responses in the ApoE$^{-/-}$ and ApoE$^{-/-}$.CD151$^{-/-}$ mouse strains. CD151 in this instance may not be as integral in platelet

aggregation as compared to a non-atherosclerotic setting and perhaps the similarities seen in aggregation profiles between our current study for ADP response and previous wild-type responses are in part contributed by atherosclerosis influence possibly on the outside-in and/or inside-out integrin $\alpha_{IIb}\beta_3$ signalling pathways. The results expected in PAR-4 agonist induced aggregation would to some degree be similar to ADP response as both are G protein coupled receptors. Our findings however showed that PAR-4 (300 μm) agonist induced aggregation displayed an aggregation response between 60% - 70% maximal platelet aggregation which is similar to a wild-type aggregation response to PAR-4 (500 μm).(4) For PAR-4, neither CD151 absence and/or atherosclerosis has had an effect as shown in Figure 61. Likewise collagen induced aggregation response was similar to a wild-type aggregation profile when compared to the literature (Figure 6.3).(4) Note that in these previous studies, higher concentrations of collagen were used. At 3.75 μg/ml and 7.50 μg/ml type I fibrillar collagen concentrations in our study, we observed approximately 60% maximal aggregation whilst the Lau et al.(4) reported an aggregation response of approximately 80%. For all three agonists used, our results suggest that the amplitude and slope of platelet aggregation responses specifically in atherosclerosis is not affected by the deficiency of CD151 and thus not influencing the inside out and/or outside in integrin $\alpha_{IIb}\beta_3$ signalling pathways.

In vitro platelet adhesion under high shear conditions (1800 s^{-1}) was examined by perfusing rhodamine labelled whole blood from $ApoE^{-/-}$ and $ApoE^{-/-}.CD151^{-/-}$ mice over a type I fibrillar collagen coated flow chamber in independent experiments. This was performed to question if CD151 absence in atherosclerosis alters thrombus formation under flow on type I collagen. After deconvolution of the images captured over the 6 minute recording period, platelet adhesion and thrombi which formed appeared smaller in size and number in the $ApoE^{-/-}.CD151^{-/-}$ platelets compared to the $ApoE^{-/-}$ platelets (Figure 6.4). Static end point results of thrombus area and volume at 6 minutes supports this with significantly smaller area and volume observed for thrombi formed (Figure 6.6). This suggests that the absence of CD151 has an effect on platelet adhesive properties and the collagen receptors namely integrin $\alpha_2\beta_1$ and GPVI to its ligand, type I fibrillar collagen which was immobilised and coated on the flow chamber.

For our *in vivo* study, ferric chloride was used to induce oxidative damage and denudation of the endothelium to the mesenteric arterioles, exposing circulating platelets to sub-endothelium collagen. Real time imaging and analysis revealed a similar and unchanged

platelet response between ApoE$^{-/-}$ and ApoE$^{-/-}$.CD151$^{-/-}$ mice whereby thrombus area, height and volume were unchanged between the strains. These preliminary findings suggest the absence of CD151 in atherosclerosis does not affect the development of thrombi for the parameters measured. Compared to previous findings in the literature, thrombus height (Figure 6.7) of ApoE$^{-/-}$ and ApoE$^{-/-}$.CD151$^{-/-}$ mice were lower than the thrombus heights measured at 8-10 minutes in CD151$^{-/-}$ mice (12.16 ± 1.12 μm and 13.62 ± 1.32 μm versus 18.56 ± 1.03 μm).(197) Secondly, thrombus area were approximately four fold larger in ApoE$^{-/-}$ and ApoE$^{-/-}$.CD151$^{-/-}$ compared to CD151$^{-/-}$ mice (4272 ± 318.10 μm^2 and 4870 ± 379.70 μm^2 versus 1101 ± 81.24 μm^2). Figure 6.8 similarly shows thrombus volumes were larger by approximately three fold in ApoE$^{-/-}$ and ApoE$^{-/-}$.CD151$^{-/-}$ mice compared to CD151$^{-/-}$ (50660 ± 5293 μm^3 and 63460 ± 2998 μm^3 versus 21680 ± 2363 μm^3) and was closer in volume to the CD151$^{+/-}$ and wild type phenotypes (38740 ±3815 and 10800 ± 5554 μm^3). These parameters were used to calculate the percentage of the vessel, which was occupied by a thrombus and subsequently to determine the stability score of the thrombi formed. Figure 6.9 showed that the stability of the thrombus was similar between ApoE$^{-/-}$ and ApoE$^{-/-}$.CD151$^{-/-}$ mice with no significant difference between the genotypes (2.95 ± 0.24 and 3.40 ± 0.24). Compared to preliminary data from our laboratory on the stability scores for CD151$^{+/-}$, CD151$^{-/-}$ and CD151$^{+/+}$ (2.57 ± 0.21, 1.12 ± 0.06 and 3.60 ± 0.21), our latest findings report higher stability scores than expected in a CD151$^{-/-}$ phenotype and is more comparable to the stability score of a CD151$^{+/-}$ mouse.

Our study has examined the effect of the absence of CD151 in an atherosclerotic setting on thrombus formation. Whilst previous studies show that CD151 presence is essential in thrombus formation *in vivo*, where in its absence thrombi are smaller and less stable, we have not observed this in our study.(197) Our reported findings are more similar to that of a CD151$^{+/+}$ or wild-type phenotype and appears that the hypothesised protective effect of CD151 absence on healthy mice and thrombosis does not carry over in an atherosclerotic setting or that the data obtained in $FeCl_3$ induced injury of mesenteric arterioles in the presence of fat tissue may obscure the phenotype.

Lau et al. (4) specifically highlighted the critical role of CD151 in modulating integrin $\alpha_{IIb}\beta_3$ outside in signalling and its involvement in transmembrane signalling pathways. Adhesion strengthening in platelets is influenced by this signalling pathway and is critical in maintaining platelet to platelet interactions and thrombus stability. The authors also suggest that the recruitment of cytoskeletal proteins or signalling molecules may occur with phosphorylation or non-phosphorylation events as the amino acid sequences do not

demonstrate enzymatic activity.(4) As discussed before, like CD151, integrin $\alpha_3\beta_1$ and $\alpha_6\beta_1$ is associated functionally with protein kinase C. Phosphorylation of α_3 and α_6 is protein kinase C dependent however it has not been confirmed if this occurs with the N or C terminus of CD151. $\alpha_6\beta_1$ adhesion strengthening though, is modulated by the C-terminus of CD151. In the context of mice with a β_3 deficiency, which in humans manifests as Glanzmann thrombasthenia, platelet function is defective with the occurrence of spontaneous bleeding.(397,398) This manifests differently with the CD151 deficient phenotype. There appears to be a compensatory effect as the CD151 deficient mouse does not present with bleeding problems and is only partially affected by this deficiency as the outside-in integrin $\alpha_{IIb}\beta_3$ signalling pathway is only selectively impaired. It is not possible at this stage to attribute the differences observed in thrombus formation between the phenotype of the CD151 deficient mouse to the $ApoE^{-/-}.CD151^{-/-}$ observed. We cannot conclude and pinpoint a particular pathway responsible in reverting the CD151 deficient phenotype in an atherosclerotic model to manifest to that of a wild-type mouse. There certainly are limitations with the $ApoE^{-/-}.CD151^{-/-}$ model as these mice present with more fat deposition on their mesenteric arteries and potentially obscuring the accurate acquisition of Z-stack images. Given the close physical and functional associations of tetraspanins, a compensatory mechanism occurring in the outside-in integrin $\alpha_{IIb}\beta_3$ signalling pathway cannot be excluded. Despite this insignificant finding, our study investigates the functional importance of tetraspanin CD151 in atherosclerosis and thrombus formation *in vivo* in that in its absence, thrombus formation is not any different in an atherosclerotic mouse.

For our second *in vivo* experimental model, we examined the time to vessel occlusion in $ApoE^{-/-}$ and $ApoE^{-/-}.CD151^{-/-}$ mice by isolating the carotid arteries and inducing injury with ferric chloride as detailed in Section 2.1.12. The time to taken to reach > 95% vessel occlusion was monitored with a laser doppler probe which revealed a significantly prolonged time to occlusion in the $ApoE^{-/-}.CD151^{-/-}$ compared to the $ApoE^{-/-}$ and wild-type mice genotype (14.02 ± 0.76 min versus 10.36 ± 0.99 min and 9.83 ± 0.36 min) (Figure 6.11 and Figure 6.12). These results suggest the presence of a defect in arterial thrombus formation in $ApoE^{-/-}.CD151^{-/-}$. Furthermore, these observations are consistent with previous studies which have reported defects in outside-in integrin $\alpha_{IIb}\beta_3$ signalling and thus resulting in defective platelet aggregation.(4,197) Recruitment of platelets to the site of ferric chloride injury was delayed in atherosclerosis and is likely to be dependant on this signalling pathway and CD151.

To further support these findings, a tail bleeding assay was performed on ApoE$^{-/-}$ and ApoE$^{-/-}$.CD151$^{-/-}$ mice *in vivo* to investigate for abnormalities in platelet or endothelial function. CD151 has been shown in the literature to be expressed on platelets as well as on the vascular endothelium in humans. Studies have also shown platelet agonist activity in studies on monoclonal antibodies on CD151.(6, 399) Across all parameters being tested, tail bleeding time, volume of blood lost and percentage of rebleeds, the ApoE$^{-/-}$.CD151$^{-/-}$ model demonstrated statistically significant results which suggested an impairment in haemostasis in atherosclerotic disease (Figure 6.13). The prolonged bleeding times and higher volumes of blood lost (11.70 ± 0.10 mins versus 7.20 ± 0.31 mins, ** $P < 0.005$ and 81.75 ± 5.19 µl versus 58.50 ± 4.03 µl, * $P < 0.05$) as well as increased tendency to rebleeds (100% versus 25%, *** $P < 0.0005$) in the absence of CD151 proposes the presence of an *in vivo* bleeding defect in either platelet to platelet interactions or platelet to endothelium interactions.

Overall, our *in vivo* and *in vitro* studies have presented us with some conflicting findings within our own study as well as compared with the literature. Our *in vitro* studies which examined agonist induced platelet aggregation and platelet adhesion to type I fibrillar collagen under high shear were also opposing in its validation of CD151 contribution to thrombus adhesion and aggregation. The latter experiment supports our *in vivo* carotid artery results in confirming that CD151 deficiency in atherosclerosis provides a protective effect as thrombi formed are smaller and less stable, thus suggesting a defect in the outside-in integrin $\alpha_{IIb}\beta_3$ signalling pathway. As mentioned before, the discrepancy in results from our study for the mesenteric model and aggregation studies versus the literature may also be influenced by atherosclerosis and the accompanying clinical presentations such as hypercholesterolaemia and insulin sensitivity. Orlowski et al. (197) have determined that CD151 functioning is unlikely to be compensated by other tetraspanins and as such in the context of the mesenteric model and aggregation studies, there could also be an underlying involvement of other tetraspanins with platelet glycoproteins with an influence in thrombus formation which has not been established. The *in vivo* models of the carotid arteries and mesenteric arteries were used to examine microvascular and arterial thrombosis involving the recruitment of platelets and formation of thrombus at areas of arterial vessel injury in ApoE$^{-/-}$ and ApoE$^{-/-}$.CD151$^{-/-}$ mouse strains. In the carotid model, the prolongation in time to vessel occlusion highlights the fundamental influence that CD151 has for thrombus growth and stability. This however was not observed in the mesenteric model. Furthermore, *in vivo* tail bleeding assays performed also showed unstable haemostasis in the ApoE$^{-/-}$.CD151$^{-/-}$ mouse characterised by the increased tendency to rebleeds, volume of blood lost and time to cessation of bleeding. This suggests that although CD151 is required and important in the

positive regulation of platelet to platelet interactions and ultimately primary haemostasis and thrombosis in the carotid arteries, its involvement may not apply in other vascular beds and injury models as a critical regulator for outside-in integrin $\alpha_{IIb}\beta_3$ signalling. As such, it is imperative that this experimental model be applied to the cremaster arterioles of $ApoE^{-/-}$ and $ApoE^{-/-}.CD151^{-/-}$ mice to confirm these findings. The data supports that overall CD151 absence in atherosclerosis, may confer a protective role in the development of this disease through its regulation of thrombus growth and stability.

6.4 Conclusion

The absence of CD151 in the setting of atherosclerotic disease in this chapter has shown to provide a protective effect. Prolongation to 95% vessel occlusion promotes improved arterial blood flow in the $ApoE^{-/-}.CD151^{-/-}$ compared to $ApoE^{-/-}$ mice. A decrease in platelet adhesion to immobilised type I collagen under high shear rates as well as reduced haemostasis stability in the $ApoE^{-/-}.CD151^{-/-}$ model further supports the working hypothesis as thrombi formed are smaller, less stable and are thus less likely to propagate and result in an occlusive thrombus.

6.5 Limitations

Results generated from the *in vivo* study of arterial thrombosis in the mesenteric arterioles did not provide conclusive data. It is likely that the presence of fat on the mesenteric arterioles obscured results, and may have influenced the effectiveness of oxidative injury induced by application of $FeCl_3$ to the arterioles. As such, further studies are warranted to investigate arterial thrombosis in a different vascular bed. It is imperative that these studies be applied to the cremaster arterioles with injury induced by laser, as there is less fat present on the cremaster arterioles. PRP aggregation responses may differ if fasting conditions are implemented prior to cardiac puncture. Therefore, it would be appropriate to investigate platelet aggregation responses in these conditions using washed platelets.

7 CHAPTER 7: GENERAL DISCUSSION

7.1 General Discussion

A complex interplay of endothelial, haematopoietic and stromal cells are involved in the pathogenesis of atherosclerotic disease.(400) Platelets are known to circulate in the blood in a quiescent state within close proximity to the endothelium under physiological conditions, exerting their haemostatic and prothrombotic functions in the advent of vascular injury. (18, 134,401-404) Platelets are also now acknowledged to be a key player in the propagation of atherosclerosis with its ability to facilitate the recruitment of inflammatory cells to sites of inflammation and vascular injury.(144,381) Studies have also noted that vascular injury or disruption to the endothelium is not essential to elicit platelet activation and adherence to arterial walls.(405) A myriad of cytokines and chemokines are released from the α granules upon platelet activation establishing a localised inflammatory response. These include interleukin-1β (IL-1β), CD40L, platelet factor 4, and RANTES (regulated upon activation normal T-cell expressed and secreted, also known as chemokine CC motif ligand 5). (144, 406) Increasing lines of evidence supports this where findings have shown that the deposition of RANTES and platelet factor 4 for instance induces monocyte adhesion and leads to the infiltration of macrophages in the vascular wall (35,407,408) whilst secretion of CD40L and IL-1β can activate endothelial nuclear factor-B and subsequent transmigration and attachment of monocytes.(409,410) Platelet-leukocyte interactions are involved in plaque formation and occur through the adhesion of leukocytes to the endothelium or platelets attached to the endothelium. These interactions are made possible by the binding of fibrinogen with $\alpha_{IIb}\beta_3$, P-selectin with P-selectin glycoprotein-1 and/or Mac-1 with glycoprotein 1β.(411-414) The release of platelet derived growth factors from platelets are reported to also have a stimulatory role in the proliferation of cells, particularly smooth muscle cells, as well as in promoting angiogenesis within an atherosclerotic plaque.(147)

Platelets are integral in the development of cardiovascular diseases.(415) In its active conformation, integrin $\alpha_{IIb}\beta_3$ binds to fibrinogen and vWF thus allowing for outside-in integrin $\alpha_{IIb}\beta_3$ signalling events to occur, followed by the reorganisation of the platelet cytoskeleton and postoccupancy events such as platelet tethering and aggregation and clot retraction. Studies have demonstrated the distinct association both functionally as well as physically of CD151 with $\alpha_{IIb}\beta_3$. This is further supported by studies performed in murine models which have demonstrated defective platelet outside-in integrin $\alpha_{IIb}\beta_3$ signalling in CD151 deficiency which ultimately manifests as dysregulation in platelet thrombus formation.(4,197) The

development *in vivo* of smaller and unstable thrombi in the absence of CD151 postulates a protective role of CD151 deletion in atherosclerosis.

The focus of this thesis was to investigate the effect of CD151 deficiency in the context of atherosclerosis, atherothrombosis and plaque stability, and ultimately to identify tetraspanin CD151 as a target for therapeutic strategies in this disease. The main findings of this thesis have improved the understanding of CD151 influence in atherosclerotic disease and have validated its critical role as a regulator for outside-in integrin $\alpha_{IIb}\beta_3$ signalling of which events occurring downstream involve platelet growth and stability. Having developed a novel ApoE$^{-/-}$.CD151$^{-/-}$ model it was critical to characterise this model and the effect of CD151 deficiency on Mendelian inheritance, haematological parameters, lipid profiles, non-fasting glucose levels and mouse body weights. This study is the first to identify altered Mendelian inheritance frequencies in murine models lacking tetraspanin CD151 in an atherosclerotic setting (Section 3.2.2, Table 3.1). Platelet counts in the ApoE$^{-/-}$.CD151$^{-/-}$ model were significantly higher than ApoE$^{-/-}$ as well as C57BL/6 WT mice (Section 3.2.5, Table 3.3), whilst lipid profiles (Section 3.2.7, Figure 3.8) were altered though postulated to be more likely a consequence of lipid metabolism associated with ApoE$^{-/-}$ deficiency rather than the lack of CD151.

Histological analysis on the liver, lungs and kidneys of mice did not identify any remarkable changes in the absence of CD151$^{-/-}$. Analysis of plaque burden through histology studies presented the first evidence of reduced plaque burden in the ApoE$^{-/-}$.CD151$^{-/-}$ model compared to ApoE$^{-/-}$, suggesting a protective role of CD151 deficiency on atherosclerotic plaque lesion progression (Section 4.2.6, Figure 4.6 and Figure 4.7). More significantly, plaque burden in females was found to be significantly reduced compared to males of the ApoE$^{-/-}$.CD151$^{-/-}$ genotype postulating that CD151 absence has a greater protective potential in females whilst male mice may be more resistant. As alluded to earlier in Chapter 4 (Section 4.3), male humans are reported to have a predisposition to atherosclerosis.(292) Females develop atherosclerosis later in life compared to males which is said to be reflective of their hormonal state where a lack of oestrogen in menopause contributes to this development of atherosclerosis.(295) Furthermore, mice studies have also shown that oestrogen supplementation in female mice has a protective effect on the progression of atherosclerosis.(306) Immune states have also been suggested to have an effect on atherosclerosis development, however no significant differences between male and female mice were observed in atherosclerosis progression.(309) The mechanism in which CD151

absence attenuates the development of atherosclerosis in females is unknown, however given the statistical significant results observed in the reduction of plaque burden incidence compared to males it raises CD151 as a valuable tetraspanin to consider as a therapeutic target for atherosclerosis.

The composition of atherosclerotic plaque lesions between the ApoE$^{-/-}$ and ApoE$^{-/-}$.CD151$^{-/-}$ mice were unchanged and together with plaque burden analysis reported that at 16 weeks, the plaques developed were that of early to intermediate lesion types (Section 5.2). Furthermore, immunohistochemical staining shown in Section 5.2.1 for CD151 expression demonstrated the presence and expression of CD151 in atherosclerotic plaques as statistical significance was observed for negative, positive, strong positive staining (Table 5.1). In support of this, *in vitro* and *in vivo* platelet function studies performed in this thesis proposes the protective role of CD151 deficiency in atherosclerotic disease. Firstly, *in vitro* studies investigating platelet adhesion to immobilised type I collagen found platelet aggregates formed were smaller in size and fewer in number as shown in Section 6.2.2, Figure 6.4 to Figure 6.6. *In vivo* examination of time to vessel occlusion showed significantly prolonged times in carotid artery occlusion in the ApoE$^{-/-}$.CD151$^{-/-}$ mouse (Section 6.2.5, Figure 6.11 and Figure 6.12) and increased haemostasis instability determined through mouse tail bleed assays demonstrated in Figure 6.13. These results suggest the antithrombotic therapeutic potential of CD151 deficiency in atherosclerosis, a disease of which its etiology is multifactorial involving genetic and environmental risk factors.

Tetraspanins are described to have the ability to form lateral associations with other tetraspanins and membrane proteins, resulting in the subsequent formation of tetraspanin enriched microdomains. These microdomains mediate cell and membrane compartmentalisation and are involved in numerous cellular processes such as fusion, adhesion, and trafficking.(416-418) The interactions of tetraspanins with specific proteins maintains the effective function and trafficking of these proteins in their pathological processes, such as CD151 in its lateral associations with integrin $\alpha_{IIb}\beta_3$. Tetraspanin CD151 is highly expressed in numerous cell types as discussed and associates with many proteins, primarily the laminin binding integrins, $\alpha_3\beta_1$ and $\alpha_6\beta_4$.(258) Characterisation of the novel ApoE$^{-/-}$.CD151$^{-/-}$ model in Chapter 3 of this thesis found Mendelian inheritance frequencies to be severely altered with deletion of tetraspanin CD151.

It was previously found that the deficiency of CD151 generated mice of normal Mendelian inheritance, that were healthy and fertile.(102) The present study found CD151$^{-/-}$ mice to breed poorly, generating less than half the percentage of expected values as detailed in Table 3.1. Impairment to Mendelian inheritance frequencies also affected the ApoE$^{-/-}$.CD151$^{-/-}$ model in similar proportions, severely limiting the number of mice available for experimental investigation.

The close physical associations of CD151 with laminin binding integrins led to previous speculation that CD151$^{-/-}$ would generate mice with impairments in kidney and lung development.(102) Macroscopic examinations of the kidneys, lungs and liver of ApoE$^{-/-}$ and ApoE$^{-/-}$.CD151$^{-/-}$ mice in Chapter 3 and histological analysis of the tissue structure and morphology in Chapter 4 did not reveal any remarkable findings to suggest that the deficiency of CD151 in the context of atherosclerosis affects the development of the kidney, lung, or liver. CD151 deletion and its implication on disease is discussed extensively in the literature. CD151$^{-/-}$ mice on a C57BL/6 WT background have been reported by Sachs et al.(270) to present with renal pathologies, however is observed to vary extensively between litters. Proteinuria, which is indicative of kidney dysfunction, varied considerably in the time of onset and extent of the condition.(270) On a similar note, Wright and colleagues predicted that based on the strong associations of α_3 and α_6 with CD151, deletion of the tetraspanin would result in neonatal lethality which is observed in mice lacking these subunits.(102) In humans, binding of α_3 and α_6 with CD151 is essential for integrity of the epithelium where mutations result in hereditary nephritis manifesting as blistering of the skin, sensorineural deafness and β-thalassaemia minor.(93,124,125,240,261, 265,271,272,419) Mutations to the YRSL sequence in the C terminal cytoplasmic domain of CD151 disrupts trafficking of CD151 highlighting the importance of CD151 for the regulation of cell motility and integrin trafficking.(175) CD151 has also been reported to regulate the glycosylation of α_3 where alterations to glycosylation patterns influences cell migration towards laminin.(420) *In vitro* studies have similarly noted of the involvement of CD151 in adhesion strengthening and consequently proposing the importance of the $\alpha_3\beta_1$ and CD151 for *in vivo* function.(272)

With extensive variability known to occur between litters, in firstly the reduced Mendelian inheritance frequencies and secondly, the absence of disease apart from atherosclerosis, it can be proposed that there are underlying genetic conditions, not exclusive to CD151 deletion, that are contributing to the ApoE$^{-/-}$.CD151$^{-/-}$ phenotype displayed. It is important to note that differences in the genetic background of CD151 deficient mice used by other

research groups may explain why conditions such as renal failure and associated proteinuria were not observed in the present study.(102,270)

Lipid profiles in humans differ to the murine species as humans predominantly carry their plasma cholesterols in LDL form whereas mice carry plasma cholesterols in HDL form.(245, 246) It appears that the absence of CD151 has had a beneficial influence on cholesterol levels as total cholesterol and HDL is significantly decreased in the $ApoE^{-/-}.CD151^{-/-}$ model as demonstrated in Figure 3.8. This reduction may also be a result of the natural atheroprotective role which mice are proposed to have, given the reversed lipid profiles observed compared to human.(225) Furthermore, mice in this study were fed ad libitum chow diets which may account for the altered lipid profiles as diets were not controlled prior to time of culling and experimentation at 16 weeks. In saying that, the absence of changes in plaque composition in the $ApoE^{-/-}$ and the $ApoE^{-/-}.CD151^{-/-}$ model may likely be associated with the reduced cholesterol levels observed. Despite being a mouse model prone to the development of atherosclerosis, the lipid profiles we observed were substantially lower than typically observed in the literature (Chapter 3). Studies have reported cholesterol levels in mice to reach 400mg/dl even on a low fat diet.(225) In characterising the $ApoE^{-/-}$ and $ApoE^{-/-}.CD151^{-/-}$ lipid profiles, we observed cholesterol levels to be near that of wild type mice values in both strains, and were less than half of the expected total cholesterol levels in ApoE deficient mice observed in the literature.(225) It is likely that the lack of hypercholesterolaemia contributed to the delay in atherosclerosis progression as depicted by the lack of positive staining for F4/80 macrophages, collagen, and smooth muscle actin in $ApoE^{-/-}$ as well as $ApoE^{-/-}.CD151^{-/-}$ mice investigated detailed in Chapter 5.

The internalisation of LDLs by macrophages and formation of foam cells would thus be hampered, also resulting in a lesser pro-inflammatory state. The proliferation of smooth muscle cells and plaque development, followed by the production of extracellular matrix molecules namely collagen and elastin would similarly be impeded and thus a delay in the formation of a necrotic core.(421,422) In humans, the expression of CD151 in atherosclerotic arteries was up-regulated versus expression in normal healthy arteries. Expression of CD151 was most abundant in endothelial cells and vascular smooth muscle cells (VSMCs), more so in the former cell type.(128) The authors believed that CD151 complexed with integrins $\alpha_3\beta_1$, $\alpha_5\beta_1$ and $\alpha_7\beta_1$ were necessary for the regulation and proliferation of vascular smooth cells to potentiate the progression of atherosclerosis.(128) Chapter 5 of this thesis discusses CD151 expression identified through

immunohistochemical antibody staining in ApoE$^{-/-}$ mice, highlighting the presence and expression of CD151 in early atherosclerotic plaque lesions. The absence of staining in ApoE$^{-/-}$. CD151$^{-/-}$ plaque lesions validate these results acting as a negative control and in demonstrating specificity of CD151 H80 antibody staining (Figure 5.2, Table 5.1). Given only early to intermediate lesion types were observed in ApoE$^{-/-}$ and ApoE$^{-/-}$. CD151$^{-/-}$ mice examined in Chapter 4 and Chapter 5 of this thesis, it further elucidates the lack of smooth muscle proliferation and subsequent changes in plaque composition observed between ApoE$^{-/-}$ and ApoE$^{-/-}$. CD151$^{-/-}$ mice. Further investigations are warranted to extend the study and observing the progression of atherosclerosis in intermediate to advanced plaques in ApoE$^{-/-}$ and ApoE$^{-/-}$. CD151$^{-/-}$ so as to identify if in fact CD151 expression is upregulated in atherosclerotic plaques versus healthy arteries. This would also allow observations into plaque composition and assess if in an atherosclerotic model, CD151 has a protective role inhibiting progression towards advanced lesion types. As discussed a limiting factor in this thesis was the age of mice studied, in that prolonging the age at which mice were culled would potentially raise issues pertaining to animal welfare that needed to be considered as cutaneous xanthomas and skin lesions are known to develop in ApoE$^{-/-}$ mice. Feeding a high fat diet for prolonged periods similarly increases this risk and would as such require close monitoring, however it is a valid consideration for advanced studies in the future.(228)

On the contrary, the haematological parameters demonstrated that ApoE$^{-/-}$.CD151$^{-/-}$ mice had significantly higher platelet counts than C57BL/6 WT and ApoE$^{-/-}$ mice (Table 3.3). As it is a novel model, the influence of atherosclerosis on CD151 deficiency is unknown in its effect if any on platelet counts. At least in humans, a high platelet count is associated with coronary disease. This is based on an assumption that the authors have made whereby an increase in platelet number represents an increased tendency in non resolving platelet thrombi or presence of reactive platelets resulting in an increase in vulnerable plaques.(423) Note however the authors did not conduct an investigation on atherosclerotic lesions to observe this but drew the conclusion based on associations.(423) To corroborate this, mouse studies reported hypercholesterolaemia to result in increased neutrophil and monocyte circulation, as well as platelet counts. Increased production of these cells were stimulated by ABC4G, a cholesterol efflux transporter on megakaryocyte progenitors and subsequently thrompoietin receptor c-mpl signalling.(424) Although a raised platelet count was observed in the ApoE$^{-/-}$.CD151$^{-/-}$, this was not observed to occur in conjunction with hypercholesterolaemia. Note also, the literature reports that in ApoE$^{-/-}$ mice, the predominant lipoprotein fractions are VLDL/LDL with HDL lipoprotein fractions approximating 8 mg/dl only.(230) The HDL profile of ApoE$^{-/-}$ mice in this study was comparable more so to

a wild-type mouse HDL lipoprotein profile instead of an ApoE$^{-/-}$ mouse lipoprotein profile, which has in the past been found to be consistently ranging 8 mg/dl.(230) Triglycerides, LDL levels were also observed to have discrepancies compared to published references with the current study reporting low ranges compared to said previous findings.(230) Factors such as blood collection and fasting modes, as well as specimen handling needs to be re-evaluated to overcome errors that may be influential in determining an accurate lipoprotein profile. Again however, as the ApoE$^{-/-}$.CD151$^{-/-}$ mouse strain is a novel model, there are no references in the literature which one may compare results to and this proves novel and an advantage for the current study.

Chapter 6 of this thesis investigates the role of CD151 as a master regulator of laminin binding integrins specifically in platelet thrombus formation *in vitro* and *in vivo.* The functional and physical association of $\alpha_{IIb}\beta_3$ with CD151 reported by Wright et al. (102) provided a foundation for this thesis to investigate the outcome of CD151 absence in the context of atherosclerosis disease.(102) CD151 deficiency as discussed extensively throughout this thesis results in an *in vivo* bleeding defect, impaired outside-in $\alpha_{IIb}\beta_3$ signalling, and the formation of smaller and unstable thrombi. Reiterating the strong associations and complementary roles of CD151 with $\alpha_{IIb}\beta_3$ for effective cellular functioning, it is crucial to note studies which have similarly investigated the effects of $\alpha_{IIb}\beta_3$ deficiencies. Whilst studies have not been performed to investigate CD151 absence in atherosclerosis, the literature has found that the adhesion of platelets to damaged or activated endothelium in mice lacking $\alpha_{IIb}\beta_3$ in an ApoE$^{-/-}$ model of atherosclerosis, is void. Either a genetic deficiency or inhibition of $\alpha_{IIb}\beta_3$ has been found to result in significant decreases in atherosclerosis progression marked by a reduction in the recruitment of monocytes.(145,425) Conflicting findings have been reported in the literature as to whether the use of $\alpha_{IIb}\beta_3$ inhibitors can decrease platelet leukocyte complexes involved in propagation of atherosclerotic plaque formation.(426) Human studies of Glanzmann thrombasthenia characterised by a deficiency of $\alpha_{IIb}\beta_3$ did not demonstrate complete reduction of atherosclerosis as plaque lesions persisted in the carotid bifurcations of patients.(427) The authors proposed that it is likely atherosclerosis development in this case may not require integrin $\alpha_{IIb}\beta_3$ for platelet to endothelium adhesion and is compensated for by other platelet receptors.(427)

The results in Chapter 6 presented some conflicting findings where *in vitro* aggregation studies showed aggregation responses to be unchanged in the absence of CD151 in atherosclerosis in ApoE$^{-/-}$.CD151$^{-/-}$ mice compared to ApoE$^{-/-}$ mice tested. Aggregation

response to CRP and ADP did not demonstrate significant reductions in the amplitude and slope of aggregation responses. Minimal reduction was observed in ApoE$^{-/-}$.CD151$^{-/-}$ aggregation response to collagen 3.75µg/ml whilst the aggregation response to PAR 4-300 µM was heightened significantly compared to ApoE$^{-/-}$ mouse PRP (Figure 6.1). Previous studies reported CD151$^{-/-}$ mice with defective outside in integrin $\alpha_{IIb}\beta_3$ signalling to demonstrate a defective aggregation response to PAR-4, collagen and ADP which translates as reduced aggregability and thus a reduction in the formation of platelet aggregates and ultimately formation of a stable thrombus.(4) Another negative result we observed in this chapter was in the *in vivo* studies examining thrombus formation in the mesenteric arterioles which induced oxidative injury to arterioles mimicking human atherosclerotic plaque rupture and exposure of type I collagen leading to platelet activation and adherence of platelets to the localised area of vascular injury (Figure 6.7). As previously discussed, fat accumulation on mesenteric arterioles was likely to be the reason results were unfavourable which thus suggests the need to conduct further studies into monitoring thrombus formation in other vascular beds such as the cremaster arterioles. Unlike the literature which reported CD151$^{-/-}$ deficient mice develop smaller thrombi, display increased thrombus instability and tendency to embolise, the current findings found the thrombi developed were larger, more stable and occupied a larger area of the vessel in the ApoE$^{-/-}$.CD151$^{-/-}$ compared to thrombi formed in ApoE$^{-/-}$ and CD151$^{-/-}$ mice (Figure 6.9). Despite these negative findings which are in disagreement with the literature, the extensive positive results detailed in Chapter 6 as well as the significantly reduced plaque burden in ApoE$^{-/-}$.CD151$^{-/-}$ mice documented in Chapter 4 supports the hypothesis that CD151 absence in atherosclerosis promotes a protective effect. *In vitro* platelet adhesion of ApoE$^{-/-}$.CD151$^{-/-}$ mice blood to immobilised type I collagen under high shear rates shown in Figure 6.4 to Figure 6.6 developed significantly smaller and fewer thrombi compared to ApoE$^{-/-}$ mice. Furthermore, time to 95% vessel occlusion in the carotid arteries of ApoE$^{-/-}$.CD151$^{-/-}$ mice were prolonged and haemostatic instability characterised by increased volumes of blood lost, prolonged bleeding times and tendency to rebleed in the ApoE$^{-/-}$.CD151$^{-/-}$ mice compared to ApoE$^{-/-}$ mice (Section 6.2.5, Figure 6.12). Plaque burden was significantly reduced in ApoE$^{-/-}$.CD151$^{-/-}$ mice and provides further support of the protective effect of CD151 in atherosclerosis (Figure 4.7). Collectively these *in vitro* and *in vivo* results demonstrates improved carotid artery blood flow in the ApoE$^{-/-}$.CD151$^{-/-}$ mice and both a delay in thrombus formation as well as smaller and few thrombi were formed.

The formation of atherosclerotic plaques on endothelium at high shear rates increases platelet recruitment and tethering to these areas of inflammation and injury. GPIbα interaction with vWF mediates tethering and exposure of binding sites on GPIbα for

leukocytes and macrophages.(428) GPVI and integrin $\alpha_2\beta_1$ maintains stable platelet adhesion, potentiating the activation and aggregation of platelets. Calcium mobilisation by phospholipase C activation leads to $\alpha_{IIb}\beta_3$ activation, secretion of granules, stimulating increased activation and aggregation.(392, 428) Integrin $\alpha_2\beta_1$ interacts with collagen binding sites to maintain platelet adhesion. Deletion of CD151 affects the integrins which the tetraspanin complexes with as it as been suggested to be involved in transmembrane signalling pathways, and therefore altering integrin function *in vivo*. The β_1 subunit has recently been associated with renal pathologies as discussed in Chapter 3 and Chapter 4 in comparison to earlier studies, which focussed primarily on CD151 associations with the α_3 and α_6 subunits. Platelet adhesive ligand interactions together with defective outside-in $\alpha_{IIb}\beta_3$ signalling retards the development of platelet thrombi formation and occlusion which puts forward that CD151 absence confers a protective role in Chapter 4. Plaque burden may have benefited from this where defective platelet thrombus formation and instability has contributed significantly in conferring a reduced plaque burden in the $ApoE^{-/-}.CD151^{-/-}$ mouse model. As mentioned previously, platelet activation and tethering to arterial walls does not always require vascular injury and exposure of the sub endothelial matrix as cytokine and chemokine release from platelets encourages a localised inflammatory response.(405) The involvement of platelets in the earlier stages of atherosclerosis is now more widely acknowledged where interaction of platelets with leucocytes as well as endothelial cells are capable of initating autocrine and paracrine pathways encouraging leucocyte infiltration towards vascular walls.(162) The release of inflammatory mediators stimulates endothelial cells which promotes inflammation and consequently increasing the proatherogenic nature of the endothelium.(162) Smaller and instable thrombi reduces the risk of luminal obstructions which culminate in debilitating cardiovascular ischaemic events. Cosemans et al. (429) proposed that clinically, the presence of smaller thrombi with a greater propensity to disintegration are clinically silent in comparison to large emboli which when it sheds may be more damaging in leading to increased vessel occlusion.(429)

7.2 Conclusion

This thesis has been successful in developing a novel ApoE$^{-/-}$.CD151$^{-/-}$ mouse model which allowed for advances in the investigation of CD151 deficiency and its influence in atherosclerotic disease. It has provided insight into the anti-thrombotic potential of CD151 in this disease in that the absence of CD151 conferred a protective role demonstrated by the reduction in size of thrombi formed, the delay in time to thrombus formation, improved carotid blood flow and significant reduction in plaque burden. The results have further demonstrated the critical role of tetraspanin CD151 in stable platelet aggregates involving integrin $\alpha_{IIb}\beta_3$ outside-in signalling and unstable thrombi in murine platelets. The significance of the results obtained in this thesis on the essential role of CD151 in thrombus formation and progression of an atherosclerotic plaque has improved our understanding of CD151 in the mechanisms of atherothrombosis and atherosclerosis which poses as a valuable therapeutic target for cardiovascular disease.

7.3 Future directions

The studies carried out in this thesis demonstrate that deletion of CD151 confers a protective role by delaying time to 95% vessel occlusion, reduced platelet adhesion to immobilised type I collagen, unstable haemostasis and reduced plaque burden. Hypercholesterolaemia is known to influence the progression of atherosclerosis and thus influence the efficiency of CD151 protection in the advent of disease. Thus, further studies are warranted involving the controlled feeding of ApoE$^{-/-}$ and ApoE$^{-/-}$.CD151$^{-/-}$ mice to ensure variables pertaining to fat and caloric intake are excluded and verify the protective effect of CD151 deficiency on plaque burden, haematological profiles, thrombus formation and platelet aggregation.

As fat accumulation on the mesenteric arterioles limited the efficacy of *in vivo* intravital microscopy experiments which simulated human rupture of atherosclerotic plaques and exposure of type I collagen, studying thrombus formation in a different vascular bed is imperative. *In vivo* intravital microscopy studies on the cremaster arterioles of male mice, induced with thermal laser injury will allow for better visual quantitative analysis and thrombus formation as there is less fat present on these arterioles. P-selectin is known to

promote atherosclerosis and plaque lesion formation through the recruitment of monocytes and leukocytes in forming platelet leukocyte aggregates. This therefore warrants further studies to investigate circulating P-selectin positive platelet levels in $ApoE^{-/-}$ and $ApoE^{-/-}$.$CD151^{-/-}$ through flow cytometry and the quantification of soluble P-selectin levels by ELISA. Lastly, although Haematoxylin and Eosin staining of aortic valve cusps were sufficient in identifying plaques and quantitating plaque burden, the gold standard of lesion size quantification is reported to be with Oil Red O or Sudan Dye staining. These methods however are not without limitations where they both lack specificity. Being a broadly expressed protein and found not just in platelets but also on endothelial cells, smooth muscles, megakaryocytes, cardiac muscle, the immune system and epithelia, it would be insightful to conduct studies to further investigate whether the deficiency of CD151 in cells other than platelets have an influence on the size of thrombi, formation of thrombi and carotid blood flow *in vivo*. Studying the cardiovascular physiology and haemodynamics by using the Doppler ultrasound to monitor aortic and mitral blood velocities and aortic pulse-waves of CD151 deficient mice may supplement our understanding of CD151 absence in cardiac muscle, smooth muscle and its influence on changes in haemodynamics and its influence on atherosclerosis. Furthermore, as atherosclerosis is also known to be influenced by inflammation, studying proinflammatory cytokines, inflammatory phospholipids, heat shock proteins for instance, will widen our understanding of inflammation and its contribution to the results we have observed in the current study *in vivo* and the plaque rupture and thrombosis which ensues.

8 REFERENCES

8.1 References

1. National Heart Foundation of Australia. Data and statistics Australia: Heart Foundation [Internet]. 2011 [updated 2014; cited 2014 July 25]. Available from: http://www.heartfoundation.org.au/information-for-professionals/data-and-statistics/Pages/default.aspx

2. Australian Bureau of Statistics. 3303.0 - Causes of death, Australia, 2011: Australian bureau of statistics. 2013 [updated 2014 March 24; cited 2014 July 23]. Available from: http://www.abs.gov.au/ausstats/abs@.nsf/Lookup/3303.0Chapter42011.

3. Charrin S, Manie S, Oualid M, Billard M, Boucheix C, Rubinstein E. Differential stability of tetraspanin-tetraspanin intereactions: role of palmitoylation. Federation of the societies of biochemistry and molecular biology. 2002;516:139 - 144.

4. Lau LM, Wee JL, Wright MD, Moseley G, Hogarth PM, Ashman LK, et al. The tetraspanin superfamily member CD 151 regulates outside-in integrin $\alpha_{IIb}\beta_3$ signaling and platelet function. Blood. 2004;104:2368 - 2375.

5. Ashman LK. CD151. Journal of biological regulators and homeostatic agents. 2002;16: 223 - 226.

6. Sincock P, Mayrhofer G, Ashman LK. Localisation of the transmembrane 4 superfamily (TM4SF) member PETA-3 (CD 151) in normal human tissues: comparison with CD 9, CD 63, and α5β1 integrin. Journal of histochemistry and cytochemistry. 1997;45:515 - 525.

7. Sincock P, Fitter S, Parton R, Berndt MC, Gamble J, Ashman LK. PETA-3/CD151, a member of the transmembrane 4 superfamily, is localised to the plasma membrane and endocytic system of endothelial cells, associates with multiple integrins and modulates cell function. Journal of cell science. 1999;112:833 - 844.

8. Goschnick MW, Jackson DE. Tetraspanins-structural and signalling scaffolds that regulate platelet function. Mini reviews in medical chemistry. 2007;7(12):1248-1254.

9. Australian Institute of Health and Welfare. Healthcare expenditure on cardiovascular diseases 2004-2005 [Internet]. 2008. [updated 2008 December 4; Cited 2013 February 5]. Available from: http://www.aihw.gov.au/publication-detail/?id=6442468190

10. Pavelka M, Roth J. Functional ultrastructure. Vienna, Zurich: Springer Vienna; 2010.

11. White J. Interaction of membrane systems in blood platelets. The American journal of pathology. 1972;66(2):295 - 312.

12. Hartwig J. The platelet cytoskeleton. In: Michelson AD, editor. Platelets. 3rd ed. San Diego, CA.: Academic press; 2013. p. 145 - 168.

13. Gerrard J, White J, Peterson D. The platelet dense tubular system: its relationship to prostaglandin synthesis and calcium flux. Journal of thrombosis and haemostasis. 1978;40(2):224-231.
14. Gonzalez U, Sanzhez A, Hidalgo J. Cytochemical localisation of K+ dependent p-nitrophenyl phosphatase and adenylate cyclase by using one-step method in human washed platelets. Histochemistry and cell biology. 1992;97(6):503 - 507.
15. White J. Platelet structure. In: Michelson AD, editor. Platelets. San Diego, CA.: Academic press; 2013. p. 117 - 144.
16. Thon J, Italiano J. Antiplatelet agents. Berlin Heidelberg: Springer Berlin Heidelberg; 2012.
17. White J. Platelets in thrombotic and non-thrombotic disorders: Cambridge University Press; 2010.
18. Varga-Szabo D, Pleines I, Nieswandt B. Cell adhesion mechanisms in platelets. Arteriosclerosis, thrombosis, and vascular biology. 2008;28(3):403-412.
19. Hartwig J, Italiano J. The birth of the platelet. Journal of thrombosis and haemostasis. 2003;1:1580 - 1586.
20. Kaushansky K. Thrombopoietin. The New England journal of medicine. 1998;339(11):746 - 754.
21. Kaushansky K. Lineage specific haematopoietic growth factors. The New England journal of medicine. 2006;354(19):2034 - 2045.
22. Gregg D, Goldschmidt-Clermont PJ. Cardiology patient page. Platelets and cardiovascular disease. Circulation. 2003;108(13):e88-90.
23. Haglund, L. Finding better targets for the treatment of atherothrombosis [Internet]. 2009. [updated 2009 June 25; cited 2013 May 10]. Available from: https://www.ifm.liu.se/edu/biology/master_projects/2009/presentation-of-master-th/student-web-presentations/haglund-linda/?__printable=1
24. Patrono C, Rocca B. The future of antiplatelet therapy in cardiovascular disease. Annual review of medicine. 2010;61:49-61.
25. Gardiner EE, Arthur JF, Shen Y, Karunakaran D, Moore LA, Am Esch JS, 2nd, et al. GPIbalpha-selective activation of platelets induces platelet signaling events comparable to GPVI activation events. Platelets. 2010;21(4):244 - 252.
26. King S, Reed G. Development of platelet secretory granules. Seminars in cell & developmental biology. 2002;13:293 - 302.
27. Flaumenhaft R, Dilks J, Rozenvayn N, Monahan-Early R, Feng D, Dvorak A. The actin cytoskeleton differentially regulates platelet α-granule and dense-granule secretion. Arteriosclerosis, thrombosis, and vascular biology. 2005;10:3879 - 3887.

28. Reed G. Platelet secretory mechanisms. Seminars in thrombosis and haemostasis. 2004;30:441 - 450.

29. Frojmovic M, Milton J. Human platelet size, shape, and related functions in heath and disease. Physiological reviews. 1982;62(1):185 - 261.

30. Flaumenhaft R. Platelet secretion [internet]. Saint Louis, MO: Academic press; 2012. Chapter 18.[cited 2014 February 20].Available from:http://books.google.com.au/books?id=xB4rgPR6lagC&pg=PA343&lpg=PA343&dq=flaumenhaft+platelet+secretion+2013+platelets&source=bl&ots=IyJr_LJQTY&sig=rVaH1l1378fBJIyqcwJ7-HL_ffU&hl=en&sa=X&ei=CDYSVIWzPMfjuQSXlIH4BA&ved=0CD8Q6AEwBA#v=onepage&q=flaumenhaft%20platelet%20secretion%202013%20platelets&f=false

31. Maynard D, Heijnen H, Horne M, White J, Gahl W. Proteomic analysis of platelet alpha granules using mass spectrometry. Journal of thrombosis and haemostasis. 2007;5(9):1945 - 1955.

32. Zarbock A, Singbartl K, Ley K. Complete reversal of acid induced lung injury by blocking of platelet-neutrophil aggregation. Journal of clinical investigation. 2006;116(12):3211 - 3219.

33. Smith M, Cramer E, Savidge G. Megakaryocytes and platelets in alpha-granule disorders. Bailliere's clinical haematology. 1997;10:125 - 148.

34. Karshovka E, Weber C, von Hundelshausen P. Platelet chemokines in health and disease. Journal of thrombosis and haemostasis. 2013;110:894 - 902.

35. Pitsilos S, Hunt JR, Mohler E, Prabhakar A, Poncz M, Dawicki J, et al. Platelet factor 4 localization in carotid atherosclerotic plaques: correlation with clinical parameters. Journal of thrombosis and haemostasis. 2003;90(6):1112 - 1120.

36. Suzuki H, Murasakai K, Kodama K, Takayama H. Intracellular localisation of glycoprotein VI in human platelets and its surface expression upon activation. British journal of haematology. 2003;121(6):904 - 912.

37. Blair R, Flaumenhaft R. Platelet alpha-granules: Basic biology and cllnical correlates. Blood reviews. 2009;23:177 - 189.

38. McNicol A, Israels S. Platelet dense granules: structure, function, and implications for haemostasis. Thrombosis research. 1999;95:1 - 18.

39. Ruiz F, Lea C, Oldfield E, Docampo R. Human platelet dense granules contain polyphosphate and are similar to acidocalcisomes of bacteria and unicellular eukaryotes. Journal of biological chemistry. 2004;279(43):44250 - 44257.

40. Harper A, Mason M, Sage S. A key role for the dense granule secretion in potentiation of the Ca2+ signal arising from store-operated calcium entry in human platelets. Cell calcium. 2009;45:413 - 420.

41. Jin J, Mao Y, Thomas D, Kim S, Daniel J, Kunapuli S. RhoA downstream of Gq and G12/13 pathways regulates protease-activated receptor mediated dense granule release in platelets. Biochemical pharmacology. 2009;77:835 - 844.

42. Cattaneo M. The platelet P2 receptors. In: Michelson AD, editor. Platelets. San Diego, CA: Academic press; 2006, p. 261 - 282.

43. Hernandez-Ruiz L, Valverde F, Jimenez-Nunez M, Ocana, Saez-Benito A, Rodriguez-Martorell J. Organellar proteomics of human platelet dense granules reveals that 14-3-3zeta is a granule protein related to atherosclerosis. Journal of proteome research. 2007;6:4449 - 4457.

44. King S, Mcnamee R, Houng A, Patel R, Brands M, Reed G. Platelet dense-granule secretion plays a critical role in thrombosis and subsequent vascular remodeling in atherosclerotic mice. Circulation. 2009;120:785 - 791.

45. Menard M, Meyers K, Prieur D. Demonstration of secondary lysosomes in bovine megakaryocytes and platelets using acid phosphatase cytochemistry with cerium as a trapping agent. Journal of thrombosis and haemostasis. 1990;63(1):127 - 132.

46. Guy L. Platelet Secretion. In: Michelson AD, Barry S, editors. Platelets. Burlington: Academic press; 2012. p. 309 - 318.

47. Gillian G. What's special about secretory lysosomes? Seminars in cell & developmental biology. 2002;13:279 - 284.

48. Reed G. Platelet secretion. In: Michelson AD, editor. Platelets. San Diego, CA: Academic oress; 2002. p. 181 - 195.

49. Heemskerk J, Bevers E, Lindhout T. Platelet activation and blood coagulation. Journal of thrombosis and haemostasis. 2002;88:186 - 193.

50. Doolittle R. Step by step evolution of vertebrae blood coagulation. Cold Spring Harbor symposia on quantitative biology. 2009;74:35 - 40.

51. Mackman N, Tilley R, Key N. Role of the extrinsic pathway of blood coagulation in haemostasis and thrombosis. Arteriosclerosis, thrombosis and Vvscular biology. 2007;27:1687 - 1693.

52. Muller F, Mutch N, Schenk W, Smith S, Esterl L, Spronk H, et al. Platelet polyphosphates are proinflammatory and procoagulant mediators. Cell. 2009;139(6):1143 - 1156.

53. van der Mejiden PE, Munnix IC, Auger JM, Govers-Riemslag JW, Cosemans JM, Kulipers MJ, et al. Dual role of collagen in factor XII-dependent thrombus and clot formation. Blood. 2009;114(4):881 - 890.

54. Reininger A, Bernlochner I, Penz S, Ravanat C, Smethurst PA, Farndale R, et al. A 2-step mechanism of arterial thrombus formation induced by human atherosclerotic plaques. Journal of the American college of cardiology. 2010;55(11):1147 - 1158.

55. Cosemans JM, Schols S, Stefanini L, de Witt S, Feijge M, Hamulyak K, et al. Key role of glycoprotein Ib/V/IX and von Willebrand factor in platelet activation-dependent fibrin formation at low shear flow. Blood. 2011;117(2):651 - 660.

56. Davie E, Fujikawa K, Kurachi K, Kisiel W. The role of serine proteases in the blood coagulation cascade. Advances in enzymology and related subjects to biochemistry. 2009;38:277 - 318.

57. White T, Berny M, Tucker E, Urbanus R, de Groot P, Fernandez J, et al. Protein C supports platelet binding and activation under flow: role of glycoprotein Ib and apolipoprotein E receptor 2. Journal of thrombosis and haemostasis. 2008;6(6):995 - 1002.

68. Osterud B, Bjorklid E. Sources of tissue factor. Seminars in thrombosis and haemostasis. 2006;32(1):11 - 23.

59. Kasthuri R, Roberts H, Monahan P. Factor IX deficiency or hemophilia B: clinical manifestations and management, in hemostasis and thrombosis. In: Saba H, Roberts H, editors. Haemostasis and thrombosis. Oxford, UK: John Wiley & Sons; 2014.

60. Radcliffe R, Nemerson Y. Activation and control of factor VII by activated factor X and thrombin. Isolation and characterisation of a single chain form of factor VII. Journal of biological chemistry. 1975;250(2):388 - 395.

61. Seligsohn U, Osterud B, Brown S, Griffin J, Rapaport S. Activation of human factor VII in plasma and in purified systems- roles of activated factor IX, Kallikrein and activated factor XII. Journal of clinical investigation. 1979;64(4):1056 - 1065.

62. Morrissey J. Tissue factor and factor VII initiation of coagulation, in haemostasis and thrombosis. Basic principles and clinical practice. Philadelphia, USA: Lippincott Williams and Wilkins; 2001. p. 89 - 101.

63. Arun B, Kesler C. Clinical manifestations and therapy of the haemophilias, in haemostasis and thrombosis. Basic principles and clinical practice. Philadelphia, USA: Lippincott Williams and Wilkins; 2001. p. 815 - 824.

64. Mackman N. New targets for atherothrombosis. Arteriosclerosis, thrombosis and vascular biology. 2014;34:1607 - 1608.

65. Colman R. Inflammatory, fibrinolytic, anti-coagulant, anti-adhesive and anti-angiogenic activities. Haemostasis and thrombosis: Basic principles and clinical practice. Philadelphia , USA: Lippicott WIlliams and Wilkins; 2001. p. 103 - 121.

66. Scott C, Silver L, Purdon A, Colman R. Cleavage of human high molecular weight kininogen by factor XIa in vitro. Effect on structure and function. Journal of biological chemistry. 1985;260(196):10856 - 10863.

67. Renne T, Pozgajova M, Gruner S, Schuh K, Pauer HU, Burfeind P, et al. Defective thrombus formation in mice lacking coagulation factor XII. Journal of experimental medicine. 2005;202(2):271-281.

68. Kleinschnitz C, Stoll G, Bendszus M, Schuh K, Pauer HU, Burfeind P, et al. Targeting coagulation factor XII provides protection from pathological thrombosis in cerebral ischemia without interfering with hemostasis. Journal of experimental medicine. 2006;203(3):513-518.
69. Rallapalli P, Orengo C, Studer R, Perkins S. Positive selection during the evolution of the blood coagulation factors in the context of their disease causing mutations. Molecular biology and evolution. 2014:1 - 39.
70. Mann K, Nesheim M, Church W, Haley P, Krishnaswamy S. Surface dependent reactions of the vitamin dependent enzyme complexes. Blood. 1990;76(1):1 - 16.
71. Bachmann F. Plasminogen-plasmin enzyme system. Haemostasis and thrombosis. Philadelphia, USA: Lippincott Williams and Wilkins; 2001. p. 275 - 320.
72. Gaffney P, Edgell T, Creighton-Kempsford L, Wheeler S, Tarelli E. Fibrin degradation product (FnDP) assays: analysis of standardization issues and target antigens in plasma. British Journal of Haematology. 1995;90(1):187 - 194.
73. Wiman B, Collen D. On the mechanism of the reaction between human a2-antiplasmin and plasmin. Journal of biological chemistry. 1979;254(18):9291 - 9297.
74. Rivera J, Lozano ML, Navarro-Nunez L, Vicente V. Platelet receptors and signaling in the dynamics of thrombus formation. Haematologica. 2009;94(5):700-711.
75. Luo SZ, Mo X, Lopez JA, Li R. Role of the transmembrane domain of glycoprotein IX in assembly of the glycoprotein Ib-IX complex. Journal of thrombosis and haemostasis. 2007;5(12):2494-2502.
76. Stoll G, Kleinschnitz C, Nieswandt B. The role of glycoprotein Ibalpha and von Willebrand factor interaction in stroke development. Hamostaseologie. 2010;30(3):136-138.
77. Stoll G, Kleinschnitz C, Nieswandt B. Combating innate inflammation: a new paradigm for acute treatment of stroke? Annals of the New York academy of sciences. 2010;1207:149 - 154.
78. Pugh N, Simpson AM, Smethurst PA, de Groot PG, Raynal N, Farndale RW. Synergism between platelet collagen receptors defined using receptor-specific collagen-mimetic peptide substrata in flowing blood. Blood. 2010;115(24):5069-5079.
79. Marjoram R, Voss B, Pan Y, Dickeson K, Zutter M, Hamm H, et al. Suboptimal activation of protease-activated Receptors enhances α2β1 integrin-mediated platelet adhesion to collagen. Journal of biological chemistry. 2009;284:34640 - 34647.
80. Herr A, Farndale R. Structural insights into the interactions between platelet receptors and fibrillar collagen. Journal of biological chemistry. 2009;284:19781 - 19785.
81. Tao L, Zhang Y, Xi X, Kieffer N. Recent advances in the understanding of the molecular mechanisms regulating platelet integrin αIIbβ3 activation. Protein & cell. 2010(1):627 - 667.

82. Srichai M, Zent R. Integrin structure and function. 1st ed. USA: Springer science; 2010.
83. Cosemans JM, Iserbyt B, Deckmyn H, Heemskerk J. Multiple ways to switch platelet integrins on and off. Journal of thrombosis and haemostasis. 2008(6):1253 - 1261.
84. Wagner C, Mascelli M, Neblock D, Weisman H, Coller B, Jordan R. Analysis of GPIIb/IIIa receptor number by quantitation of 7E3 binding to human platelets. Blood. 1996;88(3):907 - 914.
85. Duperray A, Berthier R, Chagnon E, Ryckewaert J, Ginsberg M, Plow E, et al. Biosynthesis and processing of platelet GPIIb-IIIa in human megakaryocytes. Journal of cell biology. 1987;104(6):1665 - 1673.
86. Ill C, Engvall E, Ruoslahti E. Adhesion of platelets to laminin in the absence of activation. Journal of cell biology. 1984;99:2140 - 2145.
87. Choi W, Rice W, Stokes D, Coller B. Three dimensional reconstruction of intact human integrin aIIbb3: new implications for activation dependent ligand binding. Blood. 2013;122(26):4165 - 4171.
88. Adair B, Yeager M. Three-dimensional model of the human platelet integrin alpha IIbbeta 3 based on electron cryomicroscopy and x-ray crystallography. Proceedings of the national academy of sciences USA. 2002;99(22):14059 - 14064.
89. Hughes P, Diaz-Gonzalez F, Leong L, Wu C, McDonald J, Shattil S, et al. Breaking the integrin hinge. A defined structural constraint regulates integrin singalling. Journal of biological chemistry. 1996;271(12):6571 - 6574.
90. Peterson J, Visentin G, Newman P, Aster P. A recombinant soluble form of the integrin alpha IIb beta 3 (GPIIb-IIIa) assumes an active, ligand-binding conformation and is recognized by GPIIb-IIIa-specific monoclonal, allo-, auto-, and drug-dependent platelet antibodies. Blood. 1998;92(6):2053 - 2063.
91. Xu Z, Chen X, Zhi H, Gao J, Bialkowska K, Byzova T, et al. Direct Interaction of kindlin-3 with integrin αIIbβ3 in platelets is required for supporting arterial thrombosis in mice. Arteriosclerosis, thrombosis and vascular biology. 2014;34:1961 - 1967.
92. Kasirer-Friede A, Kang J, Kahner B, Ye F, Ginsberg M, Shattil S. ADAP interactions with talin and kindlin promote platelet integrin αIIbβ3 activation and stable fibrinogen binding. Blood. 2014;123(20):3156 - 3165.
93. Nishiuchi R, Sanzen N, Nada S, Sumida Y, Wada W, Okada M, et al. Potentiation of the ligand-binding activity of integrin α3β1 via association with tetraspanin CD151. Proceedings of the national academy of sciences USA. 2005;102:1939 - 1944.
94. Jackson D, White M, Jennings L, Newman P. A Ser162-->Leu mutation within glycoprotein (GP) IIIa (integrin beta3) results in an unstable alphaIIbbeta3 complex that

retains partial function in a novel form of type II Glanzmann thrombasthenia. Journal of thrombosis and haemostasis. 1998;80(1):42 - 48.

95. Kitadokoro K, Borod D, Galli G, Petracca, Galugi F, Abrignani S, et al. CD 81 extracellular domain 3D: insight into the tetraspanin uperfamily structural motifs. The EMBO Journal. 2001;20:12 - 18.

96. Seigneruret M, Delaguillaumie A, Lagaudriere-Gesbert C, Conjeaud H. Structure of the tetraspanin main extracellular domain. A partially conserved fold with a structurally variable domain insertion. Journal of biological chemistry. 2001;276:40055 - 40054.

97. Levy S, Shoham T. Protein-protein interactions in the tetraspanin web. American physiological society: Physiology. 2005;20:218 - 224.

98. Hemler M. Tetraspanin proteins mediate cellular penetration, invasion and fusion events and define a novel type of membrane microdomain. Annual review of cell and developmental biology. 2003(19):397 - 422.

99. Hemler M. Specific tetraspanin function. Journal of cell biology. 2001;155:1103 - 1107.

100. Hemler M. Tetraspanin function and associated microdomains. Nature reviews molecular cell biology. 2005;6:801 - 811.

101. Israels SJ, McMillan-Ward E. Palmitoylation supports the association of tetraspanin CD63 and CD9 and integrin αIIbβ3 in activated platelets. Thrombosis research 2009;125:152 - 158.

102. Wright MD, Geary SM, Fitter S, Moseley G, Lau L, Sheng K, et al. Characterisation of mice lacking the tetraspanin superamily member CD 151. Molecular and cellular biology. 2004;24:5978 - 5988.

103. Tomlinson M. Platelet tetraspanins: small but interesting. Haemostasis. 2009;7:2070 - 2073.

104. Boucheix C, Eunenstein R. Tetraspanins. Cellular and molecular life sciences. 2001(58):1189 - 1205.

105. Yanez-Mo M, Mittelbrunn M, Sanchez-Madrid F. Tetraspanins and intercellular interactions. Microcirculation. 2001;8:153 - 168.

106. Maecker H, Todd S, Levy S. The tetraspanin superfamily: molecular facilitators. The journal of the federation of American societies for experimental biology. 1997;11:428 - 442.

107. Berditchevski F. Complexes of tetraspanins with integrins: more than meets the eye. Journal of cell science. 2001;114:4143 - 4151.

108. Gartland K, Belz G, Tarrant J, Minigo G, Katsara M, Sheng K, et al. The journal of immunology. 2010(185):3158 - 3166.

109. Protty M, Watkins N, Colombo D, Thomas S, VL. H, Herbert J, et al. Identification of Tspan9 as a novel platelet tetraspanin and the collagen receptor GPVI as a component of tetraspanin microdomains. Biochemical journal.2009;17(1):391 - 400.
110. Roberts J, Rodgers S, Drury K, Ashman LK, Lloyd J. Platelet activation induced by a murine monoclonal antibody directed against a novel tetraspanin antigen. British journal of haematology. 1995;102:1939 - 1944.
111. Chattopadhyay N, Wang Z, Ashman LK, Brady-Kalnay S, Kreidberg J. α3β1 integrin-CD 151, a component of the cadherin-catenin complex, regulates PTP μ expression and cell-cell adhesion. Journal of cell biology. 2003;163:1351 - 1362.
112. Sawada S, Yoshimoto M, Odintsova E, Hotchin H, Berditchevski F. The tetraspanin CD151 functions as a negative regulator in the adhesion-dependent activation of Ras. Journal of biological chemistry. 2003;278:26323 - 26326.
113. Shigeta M, Sanzen N, Ozawa M, Gu J, Hasegawa H, Sekiguchi K. CD 151 regulates epithelial cell-cell adhesion through PKC and Cdc42 dependent actin cytoskeletal reorganisation. Journal of cell biology. 2003;163:165 - 176.
114. Johnson J, Winterwood N, DeMali K, Stipp C. Tetraspanin CD 151 regulates RhoA activation and the dynamic stability of carcinoma cell-cell contacts. Journal of cell biology. 2009;122:2263 - 2273.
115. Nishimoto S, Nishida E. MAPK signaling: ERK4 versus ERK1/2. European molecular biology organisation. 2006;7:782 - 786.
116. Avruch J, Khoklatchev A, Kyriakis JM, Luo ZJ, Tzivion G, Vavvas D, et al. Ras activation of the Raf kinase: Tyrosine kinase recruitment of the MAP kinase cascade. Recent progress in hormone research. 2001;56:127 - 155.
117. Palmer T, Zijlstra A. CD 151. University of California San Diego Nature Molecule Pages [Internet]. 2011. [updated 2011 January 10; cited 2013 February 5]. Available from: http://www.signaling-gateway.org/molecule/query;jsessionid=c6ca4b34229c5f416906d9484b26b48c9669c87aa303?afcsid=A004123&type=abstract.
118. Belcheva M, Szucs M, Wang D, Sadee W, Coscia C. μ-Opioid receptor-mediated ERK activation involves calmodulin-dependent epidermal growth factor receptor transactivation. Journal of biological chemistry. 2011;276:33847 - 33853.
119. Testa J, Brooks P, Lin J, Quigley J. Eukaryotic expression cloning with an antimetastatic monoclonal antibody identifies a tetraspanin (PETA-3/CD 1510 as an effector of human tumor cell migration and metastasis. Cancer research. 1999;59:3812 - 3820.
120. Hong I, Jin Y, Byun H, Jeoung D, Kim Y, Lee H. Homophilic interactions of tetraspanin CD151 up-regulate motility and matrix metalloproteinase-9 expression of human melanoma cells through adhesion-dependent c-Jun activation signaling pathways. Journal of biological chemistry. 2006;281:24279 - 24292.

121. Kohno M, Hasegawa H, Miyake M, Yamamoto N, Fujita S. CD151 enhances cell motility and metastasis of cancer cells in the presence of focal adhesion kinase. International journal of cancer. 2002;97(3):336 - 343.
122. Lammerding J, Kazarov A, Huang H, Lee R, Hemler M. Tetraspanin CD151 regulates α6β1 integrin adhesion strengthening. Proceedings of the national academy of sciences USA. 2003;100:7616 - 7621.
123. Zhang F, Kotha J, Jennings LK, Zhang X. Tetraspanins and vascular functions. Cardiovascular research. 2009;83:7 - 15.
124. Karamatic Crew V, Burton A, Kagan A, Green C, Levene C, Flinter F, et al. CD151, the first member of the tetraspanin (TM4) superfamily detected on erythrocytes, is essential for the correct assembly of human basement membranes in kidney and skin. Blood. 2004;104:2217 - 2223.
125. Yauch R, Berditchevski F, Harler M, Reichner J, Hemler M. Highly stoichiometric, stable, and specific association of integrin α3β1 with CD151 provides a major link to phosphatidylinositol 4-kinase, and may regulate cell migration. Molecular biology of the cell. 1998;9:2751 - 2765.
126. Crew V, Burton N, Kagan A, Green C, Levene C, Flinter F, et al. CD151, the first member of the tetraspanin (TM4) superfamily detected on erythrocytes, is essential for the correct assembly of human basement membranes in kidney and skin. Journal of the American society of haematology: Blood. 2004;204:2217 - 2223.
127. Whittock N, McLean W. Genomic organisation, amplification, fine mapping, and intragenic polymorphisms of the human hemidesmosomal tetraspanin CD 151 gene. Biochemical and biophysical research communications. 2001;281:425 - 430.
128. Yang J, Liu Z, Shen X, Yao W, Qu H, Yang M, et al. Expression of CD151 in human atherosclerotic artery and its implication. Journal of Huazhong university of science and technology. 2005;25(6):629 - 631.
129. Moseley G, Jackson DE. The multiple functions of PECAM-1. Australia biochemist. 2004;2:9 - 12.
130. Wong M, Harbour S, Wee JL, Lau LM, Andrews RK, Jackson DE. Proteolytic cleavage of platelet endothelial cell adhesion molecule-1 (PECAM-1/CD41) is regulated by a calmodulin-binding motif. Journal of federation of European biochemical societies. 2004;568:70 - 78.
131. Jackson DE. The unfolding tale of PECAM-1. Journal of federation of European biochemical societies. 2003;540:7 - 14.
132. Mamdouh Z, Chen Z, Pierini L, Maxfield F, Muller W. Targeted recycling of PECAM from endothelial surface-connected compartments during diapedesis. Nature. 2003;421:748 - 753.

133. Ferrero E, Ferrero M, Pardi R, Zocchi M. The platelet endothelial cell adhesion molecule-1 (PECAM1) contributes to endothelial barrier function. Journal of federation of European biochemical societies. 1995;374:323 - 326.

134. Denis C, Wagner D. Platelet adhesion receptors and their ligands in mouse models of thrombosis. Arteriosclerosis, thrombosis and vascular Biology. 2007;27(4):728 - 739.

135. Falati S, Liu Q, Gross P, Merrill-Skoloff G, Chou J, Vandendries E, et al. Accumulation of tissue factor into developing thrombi in vivo is dependent upon microparticle P-selectin glycoprotein ligand 1 and platelet P-selectin. Journal of experimental medicine. 2003;197(11):1585 - 1598.

136. Celi A, Merrill-Skoloff G, Gross P, Falati S, SIm D, Flaumenhaft R, et al. Thrombus formation: direct real-time observation and digital analysis of thrombus assembly in a living mouse by confocal and widefield intravital microscopy. Journal of thrombosis and haemostasis. 2003;1(1):60 - 68.

137. Ni H, Denise C, Subbarao S, Degen J, Sato T, Hynes R, et al. Persistence of platelet thrombus formation in arterioles of mice lacking both von Willebrand factor and fibrinogen. Journal of clinical investigation. 2000;106(3):385 - 392.

138. Bergmeier W, Piffath C, George T, Cifuni S, Ruggeri Z, Ware J, et al. The role of platelet adhesion receptor GPIb far exceeds that of its main ligand, von Willebrand factor, in arterial thrombosis. Proceedings of the national academy of sciences USA. 2006;103(45):16900 - 16905.

139. Brass L, Jiang H, Wu J, Stalker T, Zhu L. Contact-dependent signaling events that promote thrombus formation. Blood cells molecules and diseases. 2006;36(1):157 - 161.

140. Getz G, Reardon C. Animal models of atherosclerosis. Arteriosclerosis, thrombosis, and vascular biology. 2012;32:1104 - 1115.

141. Hamilton J, Cornelissem I, Mountford J, Coughlin S. Atherosclerosis proceeds independently of thrombin-induced platelet activation in $ApoE^{-/-}$ mice. Atherosclerosis. 2009;205:427 - 432.

142. Andersson J, Libby G, Hansson K. Adaptive immunity and atherosclerosis. Clinical immunology. 2010;134: 33 - 46.

143. Sadik C, Sies H, Schewe T. Inhibition of 15-lipoxygenases by flavonoids: structure activity relations and mode of action. Biochemical pharmacology. 2003;65:773 - 781.

144. Gawaz M, Langer H, May A. Platelets in inflammation and atherogenesis. Journal of clinical investigation. 2005;115(12):3378 - 3384.

145. Massberg S. A critical role of platelet adhesion in the initiation of atherosclerotic lesion formation. Journal of experimental medicine. 2002;196(7):887 - 896.

146. Jackson SP. Arterial thrombosis - insidious, unpredictable and deadly. Nature. 2011;17(11):1423 - 1436.

147. Boucher P, Gotthardt M. LRP and PDGF signaling: a pathway to atherosclerosis. Trends cardiovascular medicine. 2004;14:55 - 60.
148. Evangelista V, Smyth SS. Interactions between platelets, leukocytes, and endothelium. Platelets. In: Michelson AD, editor. Platelets. London: Elsevier; 2013, p. 295 - 312.
149. Schwertz H, Weyrich AS, ZImmerman GA. Platelets, atherosclerosis and immunity. [press release]. in press: Encyclopedia of Medical Immunology; 2013.
150. van Gils J, Zwaginga J, Hordijjk P. Molecular and functional interactions among monocytes, platelets, and endothelial cells and their relevance for cardiovascular diseases. Journal of Leukocyte Biology. 2009;85:195 - 204.
151. Theilmeier G, Michiels C, Spaepen E, Vreys I, Collen D, Vermylen J, et al. Endothelial von Willerband factor recruits platelets to atherosclerosis prone sites in response to hypercholesterolaemia. Blood. 2002;99:4486 - 4493.
152. Davies M, Fulton W, Roberston W. The relation of coronary thrombosis to ischaemic myocardial necrosis. Journal of pathology. 1979;127:99 - 110.
153. Falk E. Plaque rupture with severe pre-existing stenosis precipitating coronary thrombosis. British heart Journal. 1983;50:127 - 134.
154. Burke A, Kolodgie F, Farb A, weber D, Malcom G, Smialek J, et al. Healed plaque ruptures and sudden coronary death: evidence that subclinical rupture has a role in plaque progression. Circulation. 2001;103:934 - 940.
155. Falk E. Unstable angina with fatal outcome: dynamic coronary thrombosis leading to infarction and/or sudden death. Autopsy evidence of recurrent mural thrombosis with peripheral embolization culminating in total vascular occlusion. Circulation. 1985;71:699 - 708.
156. Davies M. A macro and micro view of coronary vascular insult in ischemic heart disease. Circulation. 1990;82:1138 - 1146.
157. Davi G, Patrono C. Platelet activation and atherothrombosis. New England journal of medicine. 1999;357:2482 - 2494.
158. Mann J, Davies M. Mechanisms of progression in native coronary artery disease: role of healed plaque disruption. Heart. 1999;82:265 - 268.
159. Libby P. Inflammation in atherosclerosis. Nature. 2002;420:868 - 874.
160. Langer H, Gawaz M. Platelet-vessel wall interactions in atherosclerotic disease. Journal of thrombosis and haemostasis. 2008;99:480 - 486.
161. Schneider D, Tracy P, Sobel B. Acute coronary syndromes: 1. The platelet's role. Hospital practice. 1998;33:171 - 185.
162. Manduteanu I, Simionescu M. Inflammation in atherosclerosis: a cause or a result of vascular disorders? Journal of cellular and molecular medicine. 2012;16(9):1978 - 1990.

163. Holmsen H. Platelet Secretion. 2nd Ed ed. Colman R, Hirsh I, Marder V, Salzman E, editors. Philadelphia, USA: Lippincott Williams and Wilkins; 1987.
164. Cha J, Jo W, Shin H, Bae H, Ho J, Kim J. Increased platelet CD63 and P-selectin expression persist in atherosclerotic ischemic stroke. Platelets. 2004;15(1):3 - 7.
165. Zeller J, Tschoepe D, Kessler C. Circulating platelets shows increased activation in patients with acute cerebral ischemia. Journal of thrombosis and haemostasis. 1999;81:373 - 377.
166. Lee K, Cho W, Jeong M, Lim Y, Park K, Cha J. Statin reduced the platelet CD63 and CD40L expression in atherosclerotic ischemic stroke with hyperlipidemia. Journal of the Korean neurological association. 2004;22(5):453 - 458.
167. van der Zee P, Biro E, Ko Y, de Winter R, Hack C, Sturk A, et al. P-Selectin and CD63 exposing platelet microparticles reflect platelet activation in peripheral arterial disease and myocardial infarction. Clinical chemistry. 2006;52(4):657 - 664.
168. Maecker H, Do M, Levy S. CD81 on B cells promotes interleukin 4 secretion and antibody production during T helper type 2 immune responses. Proceedings of the national academy of sciences USA. 1998;95:2458 - 2462.
169. Deng J, DeKryuff R, Freeman M, Umetsu D, Levy S. Critical role of CD81 in cognate T-B cell interactions leading to Th2 responses. International immunology. 2002;14(5):513 - 523.
170. Deng J, Yeung V, Tsitoura D, DeKryuff R, Umetsu D, Levy S. Allergen-induced airway hyperreactivity is diminished in CD81deficient mice. Journal of immunology. 2000;165:5054 - 5061.
171. Kelic S, Levy S, Suarez C, Weinstein D. CD81 regulates neuron induced astrocyte cell cycle exit. Molecular and cellular neuroscience. 2001;17(3):551 - 560.
172. Geisert EJ, Williams R, Geisert G, Fan L, Asbury A, Maecker H, et al. Increased brain size and glial cell number in CD81 null mice. Journal of comparative neurology. 2002;453(1):22 - 32.
173. Rohlena J, Volger O, van Buul J, Hekking LHO, van Gils J, Bonta P, et al. Endothelial CD81 is a marker of early human atherosclerotic plaques and facilitates monocyte adhesion. Cardiovascular research. 2008;81:187 - 196.
174. Yan F, Li X, Jin Q, Chen J, Shandas R, Wu J, et al. Ultrasonic imaging of endothelial CD81 expression using CD81-targeted contrast agents in *in vitro* and *in vivo* studies. Ultrasound in medicine and biology. 2012;38(4):670 - 680.
175. Liu L, He B, Liu W, Zhou D, Cox J, Zhang X. Tetraspanin CD 151 promotes cell migration by regulating integrin trafficking. Journal of biological chemistry. 2007;282:31631 - 31642.

176. Berditchevski F, Odintsova E. Tetraspanins as regulators of protein trafficking. Traffic. 2007;8:89 - 96.
177. Kotha J, Longhurst C, Appling W, Jennings L. Tetraspanin CD9 regulates beta 1 integrin activation and enhances cell motility to fibronectin via a PI-3 kinase-dependent pathway. Experimental cell research. 2008;314(8):1811 - 1822.
178. Kersey J, LeBien T, Abramson C, Newman R, Sutherland R, Greaves M. P-24: a human leukemia associated and lymphohemopoietic progenitor cell surface structure identified with monoclonal antibody. Journal of experimental medicine. 1981;153(3):726 - 731.
179. Kaprielian Z, Cho K, Hadjiargyrou M, Patterson P. CD9, a major platelet cell surface glycoprotein, is a ROCA antigen and is expressed in the nervous system. Journal of neuroscience. 1995;15:562 - 573.
180. Nishida M, Miyagawa J, Yamashita S, Higashiyama S, Nakata A, Ouchi N, et al. Localization of CD9, an enhancer protein for proheparin binding epidermal growth factor−like growth factor, in human atherosclerotic plaques: Possible involvement of juxtacrine growth mechanism on smooth muscle cell proliferation. Arteriosclerosis, thrombosis and vascular biology. 2000;20:1236 - 1243.
181. Scherberich A, Moog S, Haan-Archipoff G, Azorsa D, Lanza F, Beretz A. Tetraspanin CD9 Is associated with very late acting integrins in human vascular smooth muscle cells and modulates collagen matrix reorganization. Arteriosclerosis, thrombosis and vascular biology. 1998;18:1691 - 1697.
182. Miao W, Vasile E, Lane W, Lawler J. CD36 associates with CD9 and integrins on human blood platelets. Haemostasis, thrombosis, and vascular biology. 2001;97:1689 - 1696.
183. Bond R, Jackson C. The fat-fed Apolipoprotein E knockout mouse brachiocephalic artery in the study of atherosclerotic plaque rupture. Journal of biomedicine and biotechnology. 2011;2011:1 - 10.
184. Zanotti I, Pedrelli M, Poti F, Stomeo G, Gomaraschi M, Calabresi L, et al. Macrophage, but not systemic, Apolipoprotein E is necessary for macrophage reverse cholesterol transport *in vivo*. Arteriosclerosis, thrombosis, and vascular biology. 2011(31):74 - 80.
185. Fuster JJ, Castillo AI, Zaragoza C, Ibanez B, Andres V. Animal models of atherosclerosis [internet]. San Diego, CA: Academic press; 2012. Chapter 1. [cited 2013 July 25]. Available from:Available from: http://books.google.com.au/books?id=oV7bZB2HBbYC&pg=PA1&dq=fuster+castillo+animal+models+of+atherosclerosis+progress+in+molecular+biology&hl=en&sa=X&ei=a0ISVKK_Bsb28QXP6IDIBg&ved=0CCoQ6AEwAA#v=onepage&

q=fuster%20castillo%20animal%20models%20of%20atherosclerosis%20progress%20in%20molecular%20biology&f=false

186. Mahley R. Apolipoprotein E: cholesterol transport protein with expanding role in cell biology. Science. 1988;240:622 - 630.

187. Krieger M. Structures and functions of multiligand lipoprotein receptors: macrophage scavenger receptors and LDL receptor-related protein (LRP). Annual review of biochemistry. 1994;40:1 - 16.

188. Mahley R, Ji Z. Remnant lipoprotein metabolism: key pathway involving cell-surface heparan sulfate proteoglycans and apolipoprotein E. Journal of lipid research. 1999;40:1 - 16.

189. Kwiterovich PO. The metabolic pathways of high-density lipoprotein, low-density lipoprotein, and triglycerides: a current review. The American journal of cardiology. 2000;86(12):5 - 10.

190. Allan CM WD, Segrest JP, Taylor JM. Identification of new human gene (APOC4) in the apolipoprotein E, C-I, and C-II gene locus. Genomics. 1995;28:291- 300.

191. Sharifov O, Nayyar G, BGarber D, Handattu S, Mishra V, Golberg D, et al. Apolipoprotein E mimetics and cholesterol-lowering properties. American journal of cardiovascular drugs. 2011;11(6):371 - 381.

192. Wetterau J, Aggerbeck L, Rall Jr S, Weisgraber K. Human apolipoprotein E3 in aqueous solution. I. Evidence for two strucural domains. The journal of biological chemistry. 1988;263:6240 - 6248.

193. Aggerbeck L, Wetterau J, Weisgraber K, Wu C, Lindgren F. Human apolipoprotein E3 in aqueous solution: II. Properties of the amino and carboxyl terminal domains. The journal of biological chemistry. 1988;263:6249 - 58.

194. Cardin A, Hirose N, Blankenship D, jackson R, Harmony J, Sparrow D, et al. Binding of a high reactive heparin to human apolipoprotein E: identification of two heparin binding domains. Biochemical biophysical research communications 1986;134(2):783 - 789.

195. Huang Y. Mechanisms linking apolipoprotein E isoforms with cardiovascular and neurological diseases. Current Opinion in Lipidology. 2010;21(4):337 - 345.

196. Gladstone Institutes. ApoE Research [internet]. 2013. [updated 2013; cited 2014 March 4]. Available from: http://labs.gladstone.ucsf.edu/huang/pages/apoe-research.

197. Orlowski E, Chand R, Yip J, Wong C, Goschnick MW, Wright MD, et al. A platelet tetraspanin superfamily member, CD 151, is required for regulation of thrombus growth and stability in vivo. Journal of thrombosis and haemostasis. 2009;6:2074 - 2084

198. Bio Rad. GAPDH PCR Module [internet]. 2014; Catalog #166-5010EDU. Available from: http://www.bio-rad.com/webroot/web/pdf/lse/literature/10011369A.PDF

199. Standards NCfCL. Approved Standard, H1 - A5. Fifth ed2003.
200. Hall J, Matthews G. Simple routine trichrome staining for epoxy resin embedded histological sections. Australian journal of medical technology. 1979;10:61 - 64.
196.
201. Cowin AJ, Adams D, Geary SM, Wright MD, Jones JC, Ashman LK. Wound healing is defective in mice lacking tetraspanin CD151. Journal of investigative dermatology. 2006;126:680 - 689.
202. Daugherty A, Whitman S. Quantification of atherosclerosis in mice. In: Hofker M, van Deursen J, editors. Methods in molecular biology: Transgenic mouse methods and Protocols. 209. USA: Humana Press Inc.; 2003 p. 293 - 309.
203. Whitman S. A practical approach to using mice in atherosclerosis research. Clinical biochemist reviews. 2004;25:81 - 93.
204. Shore B, Shore V. Heterogeneity of human plasma very low density lipoproteins. Separation of species differing in protein components. Biochemistry. 1973;12:502 - 507.
205. Saito H, Lund-Katz S, Phillips M. Contributions of domain structure and lipid interaction to the functionality of exhangeable human apolipoproteins. Progress in Lipid Research. 2004;43:350 - 380.
206. Raussens V, Slupsky C, Sykes B, Ryan R. Lipid-bound structure of an apolipoprotein E-derived peptide. Journal of Biological Chemistry. 2003;278:5998 - 6006.
207. Lund-Katz S, Zaiou M, Wehrli S, Dhansekaran P, Baldwin F, Weisgraber K, et al. Effects of lipid interaction on the lysine micro environments in apolipoprotein E. Journal of Biological Chemistry. 2000;275:24459 - 34464.
208. Mahley R, Rall SJ. Apolipoprotein E: far more than a lipid transport protein. Annual Review Genomics Human Genetics. 2000;1:507 - 537.
209. Kuipers F, Jong M, Lin Y, Eck M, Havinga R, Bloks V, et al. Impaired secretion of very low density lipoprotein-triglycerides by apolipoprotein E-deficient mouse hepatocytes. Journal of Clinical Investigation. 1997;100L:2915 - 2922.
210. Huang Y, Li X, Rall S, Taylor J, Von Eckardstein A, Assmann G, et al. Overexpression and accumulation of apolipoprotein E as a cause of hypertriglyceridemia. Journal of Biological Chemistry. 1998;273:26388 - 26393.
211. Schaefer E, Gregg R, Ghiselli G, Forte T, Ordovas J, Zech L, et al. Familial apolipoprotein E deficiency. Journal of Clinical Investigation. 1986;78:1206 - 1219.
212. Ghiselli G, Schaefer E, Gascon P, Brewer HJ. Type III hyperlipoproteinemia associated with apolipoprotein E deficiency. Science. 1981;78:1206 - 1219.
213. Greenow K, Pearce N, Ramji D. The key role of apolipoprotein E in atherosclerosis. Journal of Molecular Medicine. 2005;83:329 - 342.

214. Zhang S, Reddick R, Burkey B, Maeda N. Diet-induced atherosclerosis in mice heterozygous and homozygous for apolipoprotein E gene disruption. Journal of Clinical Investigation. 1994;94:937 - 945.

215. Plump A, Smith J, Hayek T, Aalto-Setala K, Walsh A, Verstuyft J, et al. Severe hypercholesterolemia and atherosclerosis in apolipoprotein E-deficient mice created by homologous recombination in ES cells. Cell. 1992;71:343 - 353.

216. Shimano H, Yamada N, Katsuki M, Shimada M, Gotoda T, Harada K, et al. Overexpression of apolipoprotein E in transgenic mice: marked reduction in plasma lipoproteins except high density lipoprotein and resistance against diet-induced hypercholesterolemia. Proceedings of the National Academy of Sciences USA. 1992;89:1750 - 1754.

217. Nikoulin I, Curtiss L. An apolipoprotein synthetic peptide targets to lipoproteins in plasma and mediates both cellular lipoprotein interactions in vitro and acute clearance of cholesterol-rich lipoproteins *in vivo*. Journal of Clinical Investigation. 1998;101:223 - 234

218. Ferroni P, Basili S, Santilli F, Davi G. Low-density lipoprotein-lowering medication and platelet function. Pathophysiology of Haemostasis and Thrombosis. 2006;35:346 - 354.

219. Elisaf M, Karabina S, Bairaktari E, Goudevenos J, Siamopoulous K, Tselepis A. Increased platelet reactivity to the aggregatory effect of platelet activating factor, in vitro, in patients with heterozygous familial hypercholesterolaemia. Platelets. 1999;10:124 - 131.

220. Betteridge D, Cooper M, Saggerson E, Prichard B, Tan K, Ling E. Platelet function in patients with hypercholesterolaemia. European Journal of Clinical Investigation. 1994;1:30 - 33.

221. Siegel-Axel D, Daub K, Seizer P, Lindemann S, Gawaz M. Platelet lipoprotein interplay: trigger of foam cell formation and driver of atherosclerosis. Cardiovascular Research. 2008;78:8 - 17.

222. Goschnick MW, Lau LM, Wee JL, Liu YS, Hogarth PM, Robb LM, et al. Impaired "outside-in" integrin alphaIIbbeta3 signaling and thrombus stability in TSSC6-deficient mice. Blood. 2006;108(6):1911- 1918.

223. Schreyer S, Vick S, Lystig T, Mystkowski P, LeBoeuf R. LDL receptor but not apolipoprotein E deficiency increases diet-induced obesity and diabetes in mice. Journal Physiology Endocrinology and Metabolism. 2002;282:E207 - E214.

224. Hofmann S, Perez-Tilve D, Greer T, Coburn B, Grant E, Basford J, et al. Defective lipid delivery modulates glucose tolerance and metabolic response to diet in apolipoprotein E-deficient mice. Diabetes. 2008;57:5 - 12.

225. Pendse A, Arbones-Mainar J, Johnson L, Altenburg M, Maeda N. Apolipoprotein E knock-out and knock-in mice: atherosclerosis, metabolic syndrome, and beyond. Journal of Lipid Research. 2009;50(Suppl):S178 - S182.

226. Services UoAP. Normal clinical chemistry and haematology reference values USA [cited 2013 5th April].
227. Fernandez I, Pena A, Del Teso N, Perez V, Rodiriguez-Cuesta J. Clinical biochemistry parameters in C57BL/6 mice after blood collection from the submandibular vein and retroorbital plexus. Journal of the American Association for Laboratory Animal Science. 2010;49(2):202 - 206.
228. Moghadasian M, McManus B, Nguyen L, Shefer S, Nadji M, Godin D, et al. Pathophysiology of apolipoprotein E deficiency in mice: relevance to apo E-related disorders in humans. The Journal of the Federation of American Societies for Experimental Biology. 2001;15:2623 - 2630.
229. Meir K, Leitersdorf E. Atherosclerosis in the Apolipoprotein E–deficient mouse a decade of progress. Arteriosclerosis, Thrombosis and Vascular Biology. 2004;24:1006 - 1014.
230. Yin W, Carballo-Jane E, McLaren D, Mendoza V, Gagen K, Geoghagen N, et al. Plasma lipid profiling across species for the identification of optimal animal models of human dyslipidemia. Journal of lipid research. 2012;53:51 - 65.
231. Fukuyama N, Homma K, Wakana N, Kudo K, Suyama A, Ohazama H, et al. Validation of the Friedewald equation for evaluation of plasma LDL cholesterol. Journal of Clinical Biochemistry and Nutrition. 2008;43(1):1 - 5.
232. Hartley C, Reddy A, Madala S, Martin-McNulty B, Vergona R, Sullivan M, et al. Hemodynamic changes in apolipoprotein E knockout mice. American journal of physiology heart circulation. 2000;279:2326 - 2334.
233. Watson A, Schumacher J, Gasparo M, Feng B, Thomas M, Allen T, et al. The endothelin receptor antagonist avosentan ameliorates nephropathy and atherosclerosis in diabetic apolipoprotein E knockout mice. Diabetologia. 2010;53(1):192 - 203.
234. Laboratory TJ. Malocclusion in the Laboratory Mouse USA2003 [cited 2013]. Issue 489, Spring 2003:[Available from: http://jaxmice.jax.org/jaxnotes/archive/489h.html.
235. Chiba T, Nakazawa T, Yui K, Kaneko E, Shimokado K. VLDL induces adipocyte differentiation in ApoE-dependent manner. Arteriosclerosis, Thrombosis and Vascular Biology. 2003;23:1423 - 1429.
236. Gao J, Katagiri H, Ishigaki Y, Yamada T, Ogihara T, Imai J, et al. Involvement of Apolipoprotein E in excess fat accumulation and insulin resistance. Diabetes. 2007;56(1):24 - 33.
237. Sterk L, Geuijen C, van den Berg J, Claessen N, Weening J, Sonnenberg A. Association of the tetraspanin CD151 with the laminin-binding integrins α3β1, α6β1, α6β4 and α7β1 in cells in culture and in vivo. Journal of Cell Science. 2002;115:1161 - 1173.

238. Borradori K, Sonnenberg A. Structure and function of hemidesmosomes: more than simple adhesion complexes. Journal of Investigative Dermatology. 1999;112: 411 - 418.

239. Uitto J, Pulkkinen L. Molecular genetics of heritable blistering disorders. Archives of Dermatology. 2001;137(11):1458 - 1461.

240. Kreidberg J, Donovan M, Goldstein S, Rennke H, Shepherd K, Jones R, et al. α3β1 integrin has a crucial role in kidney and lung organogenesis. Development. 1996;122:3537 - 3547.

241. DiPersio C, Hodivala-Dilke K, Jaenisch R, Kreidberg J, Hynes RO. α3β1 integrin is required for normal development of the epidermal basement membrane. Journal of cell biology. 1997;137:729 - 742.

242. Takeda Y, Kazarov A, Butterfield C, Hopkins B, Benjamin L, Kaipainen A, et al. Deletion of tetraspanin CD151 results in decreased pathologic angiogenesis in vivo and in vitro. Blood. 2007;109(4):1524 - 1532.

243. Takahashi S, Suzuki J, Kohno M, Oida K, Tamai T, Miyabo S. Enhancement of the binding of triglyceride-rich lipoproteins to the very low density lipoprotein receptor by apolipoprotein E and lipoprotein lipase. Journal of biological chemistry. 1995;270:15747 - 15754.

244. Karagiannides I, Abdou R, Tzortzopoulou A, Voshol P, Kypreos K. Apolipoprotein E predisposes to obesity and related metabolic dysfunctions in mice. The Federation of European biochemical sSocieties journal. 2008;275:4796 - 4809.

245. Miller N. Coronary atherosclerosis and plasma lipoproteins: epidemiology and pathophysiologic considerations. Journal of cardiovascular pharmacology. 1982;4:190 - 195.

246. Havel R, Kane J. Introduction: structure and metabolism of plasma lipoproteins. In: Scriver C, Beaudet A, Sly W, Valle D, editors. The Metabolic Basis of Inherited Disease. New York: McGraw-Hill; 1989. p. 1129 - 1138.

247. Reddick R, Zhang S, Maeda N. Atherosclerosis in mice lacking apo E: evaluation of lesional development and progression. Arteriosclerosis, thrombosis and vascular biology. 1994;14:141 - 147.

248. Nakashima Y, Plump A, Raines E, Breslow J, Ross R. ApoE-deficient mice develop lesions of all phases of atherosclerosis throughout the arterial tree. Arteriosclerosis, thrombosis and vascular biology. 1994;14:133 - 140.

249. Tani M, Matera R, Horvath K, Hasan T, Schaefer E, Asztalos B. The influence of apoE-deficiency and LDL-receptor-deficiency on the HDL subpopulation profile in mice and in humans. Atherosclerosis. 2014;233(1):39 - 44.

250. Australian Bureau of Statistics. 4364.0.55.005 - Australian Health Survey: Biomedical Results for Chronic Diseases, 2011-12 2013 [updated 2nd August 2013; cited 2014]. Available from: http://www.abs.gov.au/ausstats/abs@.nsf/Latestproducts/4A23558C8E59E015CA257BBB00121786?opendocument.

251. Hemler M. Targeting of tetraspanin proteins–potential benefits and strategies. Nature reviews drug discovery. 2008;7:747 - 758.

252. Lazo P. Functional implications of tetraspanin proteins in cancer biology. Journal of cancer science and therapy. 2007;98:1666 - 1677.

253. Sugiura T, Berditchevski F. Function of alpha3beta1-tetraspanin protein complexes in tumor cell invasion. Evidence for the role of the complexes in production of matrix metalloproteinase 2 (MMP-2). Journal of cellular biology. 1999;146:1375 - 1389.

254. Chien C, Lin S, Lai Y, Lin B, Lin S, Lee J, et al. Regulation of CD151 by hypoxia controls cell adhesion and metastasis in colorectal cancer. Clinical cancer research. 2008;14:8043 - 8051.

255. Yoo S, Lee KJ, Chae J, Moon K. CD151 expression can predict cancer progresion in clear cell renal cell carcinoma. Histopathology. 2011;58:191 - 197.

256. Wang H, Li Q, Sharma C, Knoblich K, Hemler M. Tetraspanin protein contributions to cancer. Biochemical society transactions. 2011;39:547 - 552.

257. Sadej R, Romanska H, Kavanagh D, Baldwin G, Takahashi T, Kalla N, et al. Tetraspanin CD151 regulates transforming growth factor beta signaling: implication in tumor metastasis. Cancer research. 2010;70(14):6059 - 6070.

258. Kazarov A, Yang X, Stipp C, Sehgal B, Hemler M. An extracellular site on tetraspanin CD 151 determines α3 and α6 integrin dependent cellular morphology. Journal of cellular biology. 2002;158:1299 - 1309.

259. Klosek S, Nakashiro K, Hara S, Shintani S, Hasegawa H, Hamakawa H. CD151 forms a functional complex with c-Met in human salivary gland cancer cells. Biochemical and biophysical research communication. 2005;336(2):408 - 416.

260. Yang X, Richardson A, Torres-Arzayus M, Zhou P, Sharma C, Kazarov A, et al. CD151 accelerates breast cancer by regulating alpha 6 integrin function, signaling, and molecular organization. Cancer research. 2008;68(9):3204 - 3213.

261. Sterk L, Geuijen C, Oomen L, Calafat J, Janssen H, Sonnenberg A. The tetraspan molecule CD151, a novel constituent of hemidesmosomes, associates with the integrin alpha6beta4 and may regulate the spatial organization of hemidesmosomes. Journal of cell biology. 2000;149:969 - 982.

262. Serru V, Le Naour F, Billard M, Azorsa D, Lanza F, Boucheiz C, et al. Selective tetraspan-integrin complexes (CD81/alpha4beta1, CD151/alpha3beta1,

CD151/alpha6beta1) under conditions disrupting tetraspan interactions. Biochemical journal. 1999;15(340):103 - 111.

263. Zevian S, Winterwood N, Stipp C. Structure-function analysis of tetraspanin CD151 reveals distinct requirements for tumor cell behaviors mediated by a3b1 versus a6b4 integrin. Journal ofbBiological chemistry. 2011;286:7496 - 7506.

264. Georges-Labouesse E, Messaddeq N, Yehia G, Cadalbert L, Dierich A, Le Meur M. Absence of integrin alpha 6 leads to epidermolysis bullosa and neonatal death in mice. Nature genetics. 1996;13:370 - 373.

265. van der Neut R, Krimpenfort P, Calafat J, Niessen CM, Sonnenberg A. Epithelial detachment due to absence of hemidesmosomes in integrin bold italic beta4 null mice. Nature genetics. 1996;13:366 - 369.

266. Pozzi A, Zent R. Hold tight or you'll fall off: CD151 helps podocytes stick in high-pressure situations. Journal of clinical investigation. 2012;122(1):13 - 16.

267. Mathew S, Chen X, Pozzi A, Zent R. Integrins in renal development. Pediatric nephrology. 2012;6:891 - 900.

268. El Aouni C, Herbach N, Blattner S, Henger A, Rastaldi M, Jarad G, et al. Podocyte-specific deletion of integrin linked kinase results in severe glomerular basement membrane alterations and progressive glomerulosclerosis. Journal of the American society of nephrology. 2006;17(5):1334 - 1344.

269. Kaplan J, Kim S, North K, Rennke H, Correia L, Tong H, et al. Mutations in ACTN4, encoding alpha-actinin-4 cause familial focal segmental glomerulosclerosis. Nature genetics. 2000;24(3):251 - 256.

270. Sachs N, Kreft M, van den Bergh J, Weerman M, Beynon A, Peters T, et al. Kidney failure in mice lacking the tetraspanin CD151. Journal of cellular biology. 2006;175(1):33 - 39.

271. Baleato R, Guthrie P, Gubler M, Ashman LK, Roselli S. Deletion of CD151 results in a strain dependent glomerular disease due to severe alterations of the glomerular basement membrane. Americna journal of pathology. 2008;174(4):927 - 937.

272. Sachs N, Claessen N, Aten J, Kreft M, Teske G, Koeman A, et al. Blood pressure influences end-stage renal disease of CD151 knockout mice. Journal of clinical investigation. 2012;22(1):348 - 358.

273. Tsujino K, Takeda Y, Arai T, Shintani Y, Inagaki R, Saiga H, et al. Tetraspanin CD151 Protects against pulmonary Fibrosis by maintaining epithelial integrity. American journal of respiratory and critical care medicine. 2012;186(2):170 - 180.

274. King T, Pardo A, Selman M. Idiopathic pulmonary fibrosis. Lancet. 2011;345:517 - 525.

275. Crosby L, Waters C. Epithelial repair mechanisms in the lung. American journal of physiology lung cellular and molecular physiology. 2010;298:L715 - L731.
276. Xia H, Diebold D, Nho R, Periman D, Kleidon J, Kahm J, et al. Pathological integrin signaling enhances proliferation of primary lung fibroblasts from patients with idiopathic pulmonary fibrosis. Journal of experimental medicine. 2008;205(7):1659 - 1672.
277. Kim K, Wei Y, Szekeres C, Kugler M, Wolters P, Hill M, et al. Epithelial cell alpha3beta1 integrin links beta-catenin and Smad signaling to promote myofibroblast formation and pulmonary fibrosis. Journal of clinical investigation. 2009;119(1):213 - 224.
278. Yanez-Mo M, Barreiro O, Gonzalo P, Batista A, Meglas D, Genis L, et al. MT1-MMP collagenolytic activity is regulated through association with tetraspanin CD151 in primary endothelial cells. Blood. 2008;112(8):3217 - 3226.
279. Kwon M, Seo J, Kim Y, Kwon M, Choi J, Kin T, et al. Prognostic significance of CD151 overexpression in non-small cell lung cancer. Lunc\g Cancer. 2013;81(1):109 - 116.
280. Tokuhara T, Hasegawa H, Hattori N, Ishida H, Taki T, Tachinana S, et al. Clinical significance of CD151 gene expression in non-small cell lung cancer. Clinical cancer research. 2001;7(12):4109 - 4114.
281. Ang J, Lijovic M, Ashman LK, Kan K, Frauman A. CD151 protein expression predicts the clinical outcome of low-grade primary prostate cancer better than histologic grading: a new prognostic indicator?. Cancer epidemiology, biomarkers & prevention. 2004;13(11):1717 - 1721.
282. Copeland B, Bowman M, Ashman LK. Genetic ablation of the tetraspanin CD151 reduces spontaneous metastatic spread of prostate cancer in the TRAMP model. Molecular cancer research. 2013;11:95 - 105.
283. Piedrahita J, Zhang S, Hagaman J, Oliver P, Maeda N. Spontaneous hypercholesterolemia and arterial lesions in mice lacking apolipoprotein E. Proceedings of the national academy of sciences USA. 1992;89:4471 - 4445.
284. Virmani R, Kolodogie F, Burke A, Farb A, Schwartz S. Lessons from sudden coronary death: a comprehensive morphological classification scheme for atherosclerotic lesions. Arteriosclerosis, thrombosis and vascular biology. 2000;20:1262 - 1272.
285. Shintani Y, Maeda M, Chaika N, Johnson K, Wheelock M. Collagen I promotes epithelial-to-mesenchymal transition in lung cancer cells via transforming growth factor-beta signaling. American journal of respiratory cell and molecular biology. 2008;38:95 - 104.
286. Kisseleva T, Brenner D. Fibrogenesis of parenchymal organs. Proceedings of the national academy of sciences USA. 2008;5:338 - 342.
287. Zijlstra A, Lewis J, Degryse B, Stuhlmann H, Quigley J. The inhibition of tumor cell intravasation and subsequent metastasis via regulation of in vivo tumor cell motility by the tetraspanin CD151. Cancer cell. 2008;13:221 - 234.

288. Paigen B, Ishida B, Verstuyft J, Winters R, Albee D. Atherosclerosis susceptibility differences among progenitors of recombinant inbred strains of mice. Arteriosclerosis. 1990;10:316 - 323.

289. Mehrabian M, Demer L, Lusis AJ. Differential accumulation of intimal monocyte-macrophages relative to lipoproteins and lipofuscin corresponds to hemodynamic forces on cardiac valves in mice. Arteriosclerosis, thrombosis and vascular biology. 1991;11:947 - 957.

290. Zhang S, Reddick R, Piedrahita J, Maeda N. Spontaneous hypercholesterolaemia and arterial lesions in mice lacking apolipoprotein E. Science. 1992;258:468 - 471.

291. Stary H, Chandler A, Glagov S, Guyton J, Insull W, Rosenfel M, et al. A definition of initial, fatty streak, and intermediate lesions of atherosclerosis: a report from the Committee on vascular lesions of the council on Arteriosclerosis, American heart association. Arteriosclerosis, thrombosis and vascular biology. 1994;14:840 - 856.

292. McCrohon J, Death A, Nakhla S, Jessup W, Handelsman D, Stanley K, et al. Androgen Receptor Expression Is Greater in Macrophages From Male Than From Female Donors: A Sex Difference With Implications for Atherogenesis. Circulation. 2000;101:224 - 226.

293. Bennet A, Di Angelantonio E, Yu Z, Wesley F, Dahlin A, Ahlbom A, et al. Association of medical association. 2007;298(11):1300 - 1311.

294. Song Y, Stampfer M, Liu S. Meta-analysis: apo- lipoprotein E genotypes and risk for coronary heart diseas. Annals of internal medicine. 2004;141(2):137 - 147.

2925 Mendelsohn M, Karas R. Molecular and Cellular Basis of Cardiovascular Gender Differences. Science. 2005;308:1583 - 1587.

296. Moroi M, Zhang L, Yasuda T, Virmani R, Gold H, Fishman M, et al. Interaction of Genetic Deficiency of Endothelial Nitric Oxide, Gender, and Pregnancy in Vascular Response to Injury in Mice. The journal of clinical investigation 1998;101(6):1225 - 1232.

297. Bairey C, Shaw L, Reis S, Bittner V, Kelsey S, Olson M, et al. Insights From the NHLBI-Sponsored Women's Ischemia Syndrome Evaluation (WISE) Study. Journal of the American college of cardiology. 2006;47(3):S21 - S29.

298. Vaccarino V, Parsons L, Every N, Barron H, Krumholz H. Sex-based differences in early mortality after myocardial infarction. National Registry of Myocardial Infarction 2 participants. New England journal of medicine. 1999;341:217 - 225.

299. Lagerqvist B, Safstrom K, Stahle E, Wallentin L, Swahn E. Is early invasive treatment of unstable coronary artery disease equally effective for both women and men? Journal of the American college of cardiology. 2001;38 41 - 48.

300. Nohria A, Vaccarino V, Krumholz H. Gender differences in mortality after myocardial infarction. Why women fare worse than men. Cardiology clinics. 1998;16:45 - 57.

301. Lerner D, Kanenl W. Patterns of coronary heart disease morbidity and mortality in the sexes: a 26-year follow-up of the Framingham population. American heart journal. 1986;111:383 - 390.

302. Smith SJ, Blair S, Bonow R, Brass L, Cerqueira M, Dracup K, et al. HA/ACC guidelines for preventing heart attack and death in patients with atherosclerotic cardiovascular disease: 2001 update: a statement for healthcare professionals from the American Heart Association and the American College of Cardiology. Journal of the American college of cardiology. 2001;38(5):1581 - 1583.

303. Jacobs A, Johnston J, Haviland A, Brooks M, Kelsey S, Holmes DJ, et al. Improved outcomes for women undergoing contemporary percutaneous coronary intervention: a report from the National Heart, Lung, and Blood Institute Dynamic registry. Journal of the AmericancCollege of cardiology. 2002;39(10):1680 - 1614.

304. Al Suwaidi J, Higano S, Hamasaki S, Holmes D, Lerman A. Association between obesity and coronary atherosclerosis and vascular remodeling. Journal of the American college of cardiology. 2001;88:1300 - 1303.

305. Mehili J, Kastrati A, Dirschinger J, Bollwein H, Neumann F, Schomig A. Differences in prognostic factors and outcomes between women and men undergoing coronary artery stenting. Journal of American medical association. 2000;284:1799 - 1805.

306. Hodgin J, Maeda N. Minireview: estrogen and mouse models of atherosclerosis. Endocrinology. 2002;143:4495 - 4501.

307. VanderLaan P, Reardon C, Getz G. Site Specificity of Atherosclerosis Site-Selective Responses to Atherosclerotic Modulators. Arteriosclerosis, thrombosis and vascular biology. 2004;24:12 - 22.

308. Tangirala R, Rubin E, Palinski W. Quantification of atherosclerosis in murine models: correlation between lesions in the aortic origin and in the entire aorta, and differences in the extent of lesion between sexes in the LDL receptor-deficient and apolipoprotein E-deficient mice. Journal of lipid research. 1995;36:2320 - 2328.

309. Whitman S, Ravisankar P, Daugherty A. IFN-y deficiency exerts gender specific effects on atherogenesis in apoE$^{-/-}$ mice. Journal of interferon & cytokine research. 2002;22:661 - 670.

310. Dowling J, Yu Q, Fuchs E. Beta4 integrin is required for hemidesmosome formation, cell adhesion and cell survival. Journal of cellular biology. 1996;134(2):559 - 572.

311. Ke A, Shi G, Shou J, Weu F, DIng Z, Hu M, et al. Role of overexpression of CD151 and/or c-Met in predicting prognosis of hepatocellular carcinoma. Hepatology. 2009;49(2):491 - 503.

312. Miller Baker AE. Mendelian inheritance of t haplotypes in house mouse (Mus musculus domesticus) field populations. Genetics research. 2008;90(04):331 - 339.

313. Webb N, Moore K. Macrophage-derived foam cells in atherosclerosis: lessons from murine models and implications for therapy. Current Drug Targets. 2007;8(12):1249 - 1263.
314. Bobryshev Y. Monocyte recruitment and foam cell formation in atherosclerosis. Micron Journal. 2006;37(3):208 - 222.
315. Hansson G, Robertson A, Soderberg-Naucler C. Inflammation and atherosclerosis. Annual review of pathology mechanisms of disease. 2006;1:297 - 329.
316. Hansson G. The immune response in atherosclerosis: a double-edged sword. Nature reviews immunology. 2006;6(7):508 - 519.
317. Ley K, Miller Y, Hendrick C. Monocyte and macrophage dynamics during atherogenesis. Arteriosclerosis, thrombosis and vascular biology. 2011;31(7):1506 - 1516.
318. Chawla A, Nguyen K, Goh Y. Macrophage-mediated inflammation in metabolic diseas. Nature reviews immunology. 2011;1:738 - 749.
319. Murray P, Wynn T. Protective and pathogenic functions of macrophage subsets. Nature reviews immunology. 2011;11(1):723 - 737.
320. Wrobel T, Mateuszuk L, Chlopicki S, Malek K, Baranska M. Imaging of lipids in atherosclerotic lesion in aorta from ApoE/LDLR$^{-/-}$ mice by FT-IR spectroscopy and Hierarchical Cluster Analysis. Analyst. 2011;136:5247 - 5255.
321. Burke A, Virmani R, Galis Z, Haudenschild C, Muller J. Task force #2—what is the pathologic basis for new atherosclerosis imaging techniques? Journal of the American college of cardiology. 2003;41:1874 - 1886.
322. Zhang X, Kazarov A, Yang X, Bontrager A, Stipp C, Hemler M. Function of the Tetraspanin CD151–α6β1 Integrin Complex during Cellular Morphogenesis. The American society for cell biology. 2002;13:1 - 11.
323. Hemler M. Integrin associated proteins. Current opinion in cell biology. 1998;10:578 - 585.
324. Zhang X, Bontrager A, Hemler M. Transmembrane-4 superfamily proteins associate with activated protein kinase C (PKC) and link PKC to specific beta(1) integrins. Journal of biological chemistry. 2001;276:25005 - 25013.
325. Berditchevski F, Gilbert E, Griffiths M, Fiter S, Ashman LK, Jenner S. Analysis of the CD151-alpha3beta1 integrin and CD151-tetraspanin interactions by mutagenesis. Journal of biological chemistry. 2001;276:4:1165 - 1174.
326. Yauch R, Kazarov A, Desai B, Lee R, Hemler M. Direct extracellular contact between integrin alpha(3)beta(1) and TM4SF protein CD151. Journal of biological chemistry. 2000;275:9230 - 9238.

327. Gesierich S, Paret C, Hildebrand D, Weitz J, Zgraggen K, Schmitz-Winnenthal F. Colocalization of the tetraspanins, CO-029 and CD151, with integrins in human pancreatic adenocarcinoma: impact on cell motility. Clinical cancer research. 2005;11:2840 - 2852.
328. Winterwood N, Varzavand A, Meland M, Ashman LK, Stipp C. A critical role for tetraspanin CD151 in alpha3beta1 and alpha6beta4 integrin-dependent tumor cell functions on laminin-5. Molecular biology of the cell journal. 2006;17:2707 - 2721.
329. Yanez-Mo M, Alfranca A, Cabanas C, Marazuela M, Etejedor R, Angeles Ursa M, et al. Regulation of endothelial cell motility by complexes of tetraspan molecules CD81/TAPA-1 and CD151/PETA-3 with α3β1 Integrin localized at endothelial lateral junctions. Journal of cell biology. 1998;141(3):791 - 804.
330. Jongstra-Bilen J, Haidari M, Zhu S, Chen M, Guha D, Cybulsky M. Low-grade chronic inflammation in regions of the normal mouse arterial intima predisposed to atherosclerosis. Journal of experimental medicine. 2006;203:2073 - 2083.
331. Liyama K, Hajra L, Liyama M, Li H, DiChiara M, Medoff B, et al. Patterns of vascular cell adhesion molecule-1 and intercellular adhesion molecule-1 expression in rabbit and mouse atherosclerotic lesions and at sites predisposed to lesion formation. Circulation research. 1999;85:199 - 207.
332. Cybulsky M, Gimbrone MJ. Endothelial expression of a mononuclear leukocyte adhesion molecule during atherogenesis. Science. 1991;251:788 - 791.
333. Nakashima Y, Raines E, Plump A, Breslow J, Ross R. Upregulation of VCAM-1 and ICAM-1 at atherosclerosis-prone sites on the endothelium in the ApoE-deficient mouse. Arteriosclerosis, thrombosis and vascular biology. 1998;18:842 - 851.
334. Sakai A, Kume N, Nishi E, Tanoue K, Miyasaka M, Kita T. P-selectin and vascular cell adhesion molecule-1 are focally expressed in aortas of hypercholesterolemic rabbits before intimal accumulation of macrophages and T lymphocytes. Arteriosclerosis, thrombosis and vascular biology. 1997;17:310 - 316.
335. Volger O, Fledderus J, Kisters N, Fontijn R, Moerland P, Kuiper J, et al. Distinctive expression of chemokines and transforming growth factor-beta signaling in human arterial endothelium during atherosclerosis. American journal of pathology. 2007;171(1):326 - 337.
336. Ross R. Atherosclerosis: an inflammatory disease. New England journal of medicine. 1999;340:115 - 126.
337. Huo Y, Schober A, Forlow S, Smith D, Hyman M, Hung S, et al. Circulating activated platelets exacerbate atherosclerosis in mice deficient in apolipoprotein E. Nature medicine. 2003;9(1):61 - 67.
338. Barreiro O, Yanez-Mo M, Sala-Valdes M, Gutierrez-Lopez M, Ovalle S, Higginbottom A, et al. Endothelial tetraspanin microdomains regulate leukocyte firm adhesion during extravasation. Blood. 2005;105(7):2852 - 2861.

339. Bretscher M, Aguado Velasco C. Membrane traffic during cell locomotion. Current opinions in cell bology. 1998;10:537 - 541.
340. Kobayashi T, Vischer U, Rosnoblet C, Lebrand C, Lindsay M, Parton R, et al. The tetraspanin CD63/lamp3 cycles between endocytic and secretory compartments in human endothelial cells. Molecular biology of the cell journal. 2000;11(5):1829 - 1843.
341. Duffield A, Kamsteeg E, Brown A, Pagel P, Caplan M. The tetraspanin CD63 enhances the internalization of the H,K-ATPase beta-subunit. Proceedings of the national academy of sciences USA. 2003;100:15560 - 15565.
342. Caswell P, Vadrevu S, Norman J. Integrins: masters and slaves of endocytic transport. Nature reviews molecular cell biology. 2009;10:843 - 853.
343. Pant S, Deshmukh A, Mehta J. Angiogenesis in Atherosclerosis: An Overview. Advances in biochemistry in health and disease. 2013;6:209 - 224.
344. Jaipersad A, Lip GYH, Silverman S, Shantsila E. The role of monocytes in angiogenesis and atherosclerosis journal of the American college of cardiology. 2014;63(1):1 - 11.
345. Kumar V, Abbas A, Fausto. Robbins and Cotran pathologic basis of disease. 7th Edition ed. Philadelphia: Elsevier and Saunders; 2005.
346. Nadkarni S, Bouma B, de Boer J, Tearner G. Evaluation of collagen in atherosclerotic plaques: the use of two coherent laser-based imaging methods. Lasers in medical science. 2009;24(3):439 - 445.
347. Plenz G, Deng M, Robenek H, Volker W. Vascular collagens: spotlight on the role of type VIII collagen in atherogenesis. Atherosclerosis. 2003;166(1):1 - 11.
348. Lee R, Libby P. The unstable atheroma. Arteriosclerosis, thrombosis and vascular biology. 1997;17:1859 - 18567.
349. Burleigh M, Briggs A, Lendon C, Davies M, Born G, Richardson P. Collagen Types I and III, collagen content, GAGs and mechanical strength of human atherosclerotic plaque caps span-wise variations. Atherosclerosis. 1992;96:71 - 81.
350. Sachs UJ, Nieswandt B. In vivo thrombus formation in murine models. Circulation research. 2007;100(7):979 - 991.
351. Lievens D, Zernecke A, Seijkens T, Soehnlein O, Beckers L, Munnix ICA, et al. Platelet CD40L mediates thrombotic and inflammatory processes in atherosclerosis. Blood. 2010;116(20):4317 - 4327.
352. Newby A, Zaltsman A. Fibrous cap formation or destruction - the critical importance of vascular smooth muscle cell proliferation, migration and matrix formation. Cardiovascular research. 1999;41:345 - 360.
353. Moore KJ, Sheedy FJ, Fisher EA. Macrophages in atherosclerosis: a dynamic balance. Nature. 2013;13:709 - 721.

354. Khallou-Laschet J, Varthaman A, Fornasa G, Compain C, Gaston A, Clement M, et al. Macrophage plasticity in experimental atherosclerosis. PLoS ONE. 2010;5(1):1 - 10.
355. Galvan Pena S, O'Neil LAJ. Metabolic reprogramming in macrophage polarisation. Frontiers in immunology. 2014;4(420):1 - 6.
356. Finn AV, Saed O, Virmani R. Macrophage subsets in human atherosclerosis. Circulation. 2012;110(e64):1-2.
357. Schroeder A, Falk E. Vulnerable and dangerous coronary plaques. Atherosclerosis. 1995(118):S141 - S149.
358. Deguchi J, Aiikawa E, Libby P, Vachon J, Inada M, Krane S, et al. Matrix metalloproteinase-13/collagenase-3 deletion promotes collagen accumulation and organization in mouse atherosclerotic plaques. Circulation. 2005;112:2708 - 2715.
359. Galis Z, Sukhova G, Lark M, Libby P. Increased expression of matrix metalloproteinases and matrix degrading activity in vulnerable regions of human atherosclerotic plaques. Journal of clinical investigation. 1994;94:2493 - 2503.
360. Shah P, Falk E, Badimon J, Fernandez O, Mailhac A, Villareal-Levy G, et al. Human monocyte derived macrophages induce collagen breakdown in fibrous caps of atherosclerotic plaques. Potential role of matrix-degrading metalloproteinases and implications for plaque rupture. Circulation. 1995;92(6):1565 - 1569.
361. Lee R, Schoen F, Loree H, Lark M, Libby P. Circumferential stress and matrix metalloproteinase 1 in human coronary atherosclerosis. Implications for plaque rupture. Arteriosclerosis, thrombosis and vascular biology. 1996;16:1070 - 1073.
362. Sukhova G, Schonbeck U, Rabkin E, Schoen F, Poole A, Bilinghurst R, et al. Evidence for increased collagenolysis by interstitial collagenases-1 and -3 in vulnerable human atheromatous plaques. Circulation. 1999;99:2503 - 2509.
363. Sadej R, Romanska H, Baldwin G, Gkirtzimanaki K, Novitskaya V, Filer A, et al. CD151 regulates tumorigenesis by modulating the communication between tumor cells and endothelium. Molecular cancer research. 2009;7(76):787 - 798.
364. Kwon M, Park SH, Choi J, Oh E, Kim Y, Park Y, et al. Clinical significance of CD151 over expression in subtypes of invasive breast cancer. British journal of cancer. 2012;5:923 - 930.
365. Hashida H, Takabayashi A, Tokuhara T, Hattori N, Taki T, Hasegawa H, et al. Clinical significance of transmembrane 4 superfamily in colon cancer. British journal of cancer. 2003;89(1):158 - 167.
366. Zhu G, Huang C, Qiu Z, Liu J, Zhang Z, Zhao N, et al. Expression and prognostic significance of CD151, c-Met, and integrin alpha3/alpha6 in pancreatic ductal adenocarcinoma. Digestive, diseases and sciences. 2011;56(4):1090 - 1098.

367. Huang X, Ke A, Shi G, Ding Z, Devbhandari R, Gu F, et al. Overexpression of CD151 as an adverse marker for intrahepatic cholangiocarcinoma patient. Cancer cell. 2010;116(23):5440 - 5451.
368. Lee D, Suh Y, Park T, Do I, Seol H, Nam D, et al. Prognostic significance of tetraspanin CD151 in newly diagnosed glioblastomas. Journal of surgical oncology. 2013;107(6):646 - 652.
369. Lutgens E, Tjwa M, de Frutos PG, Wijnands E, Beckers L, Dahlback B, et al. Genetic loss of Gas6 induces plaque stability in experimental atherosclerosis. Journal of pathology. 2008;216:55 - 63.
370. Robertson AK, Rudling M, Zhou X, Gorelik K, Flavell R, Hansson G. Disruption of TGFβ signaling in T cells accelerates atherosclerosis. Journal of clinical investigation. 2003;112:1342 - 1350.
371. Gojova A, Brun V, Esposito B, Cottrez F, Gourdy P, Ardouin P. Specific abrogation of transforming growth factor-beta signaling in T cells alters atherosclerotic lesion size and composition in mice. Blood. 2003;102:4052 - 4058.
372. Li Z, Delaney M, O'Brien K, Du X. Signaling During Platelet Adhesion and Activation. Arteriosclerosis, thrombosis and vascular biology. 2010;30:2341 - 2349.
373. Nieswandt B, Watson S. Platelet-collagen interaction is GPVI the central receptor? Blood. 2003;102:449 - 461.
374. Jackson SP, Nesbitt W, Kulkarni S. Signalling events underlying thrombus formation. Journal of thrombosis and haemostasis. 2003;1:1602 - 1612.
375. Coller B, Shattil S. The GPIIb/IIIa (integrin alphaIIbbeta3) odyssey: a technology driven saga of a receptor with twists, turns, and even a bend. Blood. 2008;112:3011 - 3025.
376. Shattil S, Kim C, Ginsberg M. The final steps of integrin activation: the end game. Nature reviews molecular cell biology. 2010;11:288 - 300.
377. Nesbitt W, Giuliano S, Kulkarni S, Dopheide S, Harper I, Jackson SP. Intercellular calcium communication regulates platelet aggregation and thrombus growth. Journal of cell biology. 2003;160:1151 - 1161.
378. Eckly A, Hechler B, Fruend M, Zerr M, Cazenave J, Lanza F, et al. Mechanisms underlying FeCl3-induced arterial thrombosis. Journal of thrombosis and haemostasis. 2011;9:779 - 789.
379. Li W, McIntyre T, SIlverstein R. Ferric chloride-induced murine carotid arterial injury: A model of redox pathology. Redox biology. 2013;1(1):50 - 55.
380. Voss B, McLaughlin J, Holinstat M, Zent R, Hamm H. PAR1, but Not PAR4, Activates Human Platelets through a Gi/o/Phosphoinositide-3 Kinase Signaling Axis. Molecular pharmacology. 2007;71:1399 - 1406.

381. Lievens D, von Hundelshausen P. Platelets in atherosclerosis. Journal of thrombosis and haemostasis. 2011;106:827 - 838.
382. Ohlmann P, Eckly A, Freund M, Cazenave J, Offermanns S, Gachet C. ADP induces partial platelet aggregation without shape change and potentiates collagen-induced aggregation in the absence of Gq. Haemostasis, thrombosis, and vascular biology. 2000;96:2134 - 2139.
383. Andrews R, Arthur J, Gardiner E. Targeting GPvi as a novel antithrombotic strategy. Journal of blood medicine. 2014;5:59 - 68.
384. Cattaneo M. Update on Antithrombotic Therapy. Circulation. 2010;121:171 - 179.
385. Jin J, Quinton T, Zhang J, Rittenhouse S, Kunapuli S. Adenosine diphosphate (ADP)–induced thromboxane A2generation in human platelets requires coordinated signaling through integrin αIIbβ3 and ADP receptors. Blood. 2002;99(1):193 - 198.
386. Etulain J, Schattner M. Glycobiology of platelet-endothelial cell interactions. Glycobiology [Internet]. 2014:1 - 29.
387. Riondino S, Lotti L, Cutini L, Pulcinelli F. Collagen-induced Platelet Shape Change Is Not Affected by Positive Feedback Pathway Inhibitors and cAMP-elevating Agents. The journal of biological chemistry. 2005;280(8):6504 - 6510.
388. Cipollone F, Mezzetti A, Porreca E. Association between enhanced soluble CD40L and prothrombotic state in hypercholesterolemia: effects of statin therapy. Circulation. 2002;106:399 - 402.
389. Para A, Ku D. A low-volume, single pass in-vitro system of high shear thrombosis in a stenosis. Thrombosis research. 2013;131(5):418 - 424.
390. Lenting P, Westerlaken G, Denis C, Akkerman J, Meyaard L. Efficient Inhibition of Collagen-Induced Platelet Activation and Adhesion by LAIR-2, a Soluble Ig-Like Receptor Family Member. PLoS ONE. 2010;5(8):1 - 8.
391. Schulz C, Massberg S. Antiplatelet agents. Berlin: Springer Berlin Heidelberg; 2012.
392. Penz S, Reininger AJ, Brandl R, Goyal P, Rabie T, Bernlochner I, et al. Human atheromatous plaques stimulate thrombus formation by activating platelet glycoprotein VI. The journal of the federation of american societies for experimental biology. 2005;19(8):898 - 909.
393. Woollard K, Sturgeon S, Chin Dusting J, Salem H, Jackson SP. Erythrocyte haemolysis and haemoglobin oxidation promote ferric chloride induced vascular injury. Journal of biochemistry. 2009;284(19):13110 - 13118.
394. Westrick R, Winn M, Eitzmann D. Murine models of vascular thrombosis. Arteriosclerosis, thrombosis, and vascular biology. 2007;27(10):2079 - 2093.
395. Vilahur G, Padro T, Badimon J. Atherosclerosis and thrombosis: insights from large animal models. Journal of biomedicine and biotechnology. 2011;20:1 - 12.

396. Thijs T, Deckmyn H, Broos K. Model systems of genetically modified platelets. Blood. 2012;119(7):1634 - 1642.
397. Poon M, Demers C, Jobin F, Wu J. Recombinant factor VIIa is effective for bleeding and surgery in patients with Glanzmann thrombasthaenia. Blood. 1999;94(11):3951 - 3953.
398. French D, Seligsohn U. Platelet glycoprotein IIb/IIIa receptors and Glanzmann's throbasthaenia. Arteriosclerosis, thrombosis and vascular biology. 2000;20(3):607 - 610.
399. Ashman LK, Aylett P, Hemrabani L, Bendall S, Niutta A, Cambareri C, et al. The murine monoclonal antibody, 14A2. H1, identified a novel platelet surface antigen. British journal of haematology. 1991;79:263 - 270
400. Koltsova E, Sundd P, Zarpellon A, Ouyang H, Mikulski Z, Zampolli A, et al. Genetic deletion of platelet glycoprotein Ib alpha but not its extracellular domain protects from atherosclerosis. Journal of thrombosis and haemostasis. 2013;112(5).
401. Ruggeri Z. Platelets in atherothrombosis. Nat Med. 2002;8:1227 - 1234.
394.
402. Jackson SP. The growing complexity of platelet aggregation. Blood. 2007;109:5087 - 5095.
403. Ruggeri Z. Platelet adhesion under flow. Microcirculation. 2009;16:58 - 83.
404. Kaplan Z, Jackson SP. The Role of Platelets in Atherothrombosis. American society of haematology. 2011;2011:51 - 61.
405. Nityanand S, Pande I, Bajpai V, Singh L, Chandra M, Singh B. Platelets in essential hypertension. Thrombosis research. 1993;72(5):447 - 454.
406. Li Z, Yang F, Dunn S, Gross A, Smyth S. Platelets as immune mediators: Their role in host defense responses and sepsis. Thrombosis research. 2011;127(3):184 - 188.
407. Mause S, von Hundelshausen P, Zernecke A, Koenan R, Weber C. Platelet microparticles: a transcellular delivery system for RANTES promoting monocyte recruitment on endothelium. Arteriosclerosis, thrombosis and vascular biology. 2005;25(7):1512 - 1518.
408. von Hundelshausen P, Weber K, Huo Y, Proudfoot A, Nelson P, Ley K, et al. RANTES deposition by platelets triggers monocyte arrest on inflamed and atherosclerotic endothelium. Circulation. 2001;103(13):1772 - 1777.
409. Gawaz M, Brand K, Dickfeld T, Pogatsa-Murray G, Page S, Bogner C, et al. Platelets induce alterations of chemotactic and adhesive properties of endothelial cells mediated through an interleukin- 1-dependent mechanism. Atherosclerosis. 2000;148(1):75 - 85.
410. Bavendiek U, Libby P, Kilbride M, Reynolds R, Mackman N, Schonbeck U. Induction of tissue factor expression in human endothelial cells by CD40 ligand is mediated via activator protein 1, nuclear factor kappa B, and Egr-1. Journal of biological chemistry. 2002;277(28):25032 - 25039.

411. Butt E, Gambaryan S, Gottfert N, Galler A, Marcus K, Meyer H. Actin binding of human LIM and SH3 protein is regulated by cGMP- and cAMP-dependent protein kinase phosphorylation on serine 146. Journal of biological chemistry. 2003;278(18):15601 - 15607.
412. Ramos C, Huo Y, Jung U, Ghosh S, Manka D, Sarembock I, et al. Direct demonstration of P-selectin and VCAM-1-dependent mononuclear cell rolling in early atherosclerotic lesions of apolipoprotein E-deficient mice. Circulation research. 1999;84(11):1237 - 1244.
413. Weber C, Springer T. Neutrophil accumulation on activated, surface adherent platelets in flow is mediated by interaction of Mac-1 with fibrinogen bound to alphaIIbbeta3 and stimulated by platelet activating factor. Journal of clinical investigation. 1997;100:2085 - 2093.
414. Diacovo T, Roth S, Buccola J, Bainton D, Springer T. Neutrophil rolling, arrest, and transmigration across activated, surface adherent platelets via sequential action of P-selectin and the beta 2-integrin CD11b/CD18. Blood. 1996;88(1):146 - 157.
415. Nieswandt B, Pleines I, Bender M. Platelet adhesion and activation mechanisms in arterial thrombosis and ischaemic stroke. Journal of thrombosis and haemostasis. 2011;9(1):S92 - S104.
416. Charrin S, Jouannet S, Boucheix C, Rubinstein E. Tetrspanins at a glance. Journal of cell science. 2014:127:3641 - 3648.
417. Rubinstein E, Charrin S, Tomlinson M. Organisation of the tetraspanin web. In: Berditchevski F, Rubinstein E, editors. Tetraspanins. Birmingham, UK: Springer Netherlands; 2013. p. 47- 90.
418. Monk P, Partridge L. Tetraspanins: gateways for infection. Infectious disorders drug targets. 2012;12(1):4 - 17.
419. Kagan A, Feld S, Chemke J, Bar-Khaylm Y. Occurrence of hereditary nephritis, pretibial epidermolysis bullosa and beta-thalassemia minor in two siblings with end-stage renal disease. Nephron journals. 1988;49(2):331 - 332.
420. Baldwin G, Novitskaya V, Sadej R, Pochec E, Litynska A, Hartmann C, et al. Tetraspanin CD 151 regulates glycosylation of α3β1 integrin. Journal of biological chemistry. 2008;283:35445 - 35454.
421. Weber C, Zernecke A, Libby P. The multifaceted contributions of leukocyte subsets to atherosclerosis: lessons from mouse models. NaturerReviews immunology. 2008;8:802 - 815.
422. Libby P, Ridker P, Hansson G. Progress and challenges in translating the biology of atherosclerosis. Nature. 2011;473:317 - 325.

423. Folsom A, Wu K, Rosamond W, Sharrett A, Chambless L. Prospective study of hemostatic factors and incidence of coronary heart disease: the Atherosclerosis Risk in Communities (ARIC) Study. Circulation. 1997;96:1102 - 1108.
424. Murphy A. Deficiency of ATP-binding cassette transporter B6 in megakaryocyte progenitors accelerates atherosclerosis in mice. Arteriosclerosis, thrombosis and vascular biology. 2014;34(4):751 - 758.
425. Massberg S, Schurzinger K, Lorenz M, Konrad I, Schulz C, Plesnila N, et al. Platelet adhesion via glycoprotein IIb integrin is critical for atheroprogression and focal cerebral ischemia: an in vivo study in mice lacking glycoprotein IIb. Circulation. 2005;112(8):1180 - 1188.
426. Klinkhardt U, Graff J, Harder S. Clopidogrel, but not abciximab, reduces platelet leukocyte conjugates and P-selectin expression in a human ex vivo in vitro model. Clinical pharmacology & therapeutics. 2002;71:176 - 185.
427. Shpilberg O, Rabi I, Schiller K, Walden R, Harats D, Tyrrell K, et al. Patients with Glanzmann thrombasthenia lacking platelet glycoprotein alpha(IIb)beta(3) (GPIIb/IIIa) and alpha(v)beta(3) receptors are not protected from atherosclerosis. Circulation. 2002;105(9):1044 - 1048.
428. Freynhofer M, Bruneo V, Wojta J, Huber K. The role of platelets in athero-thrombotic events. Current pharmaceutical design. 2012;18:5197 - 5214.
429. Cosemans JM, Angelillo-Scherrer A, Mattheij N, Heemskerk J. The effects of arterial flow on platelet activation, thrombus growth, and stabilization. Cardiovascular research. 2013;99:342 - 352.